

Copyright is owned by the Author of the thesis. Permission is given for a copy to be downloaded by an individual for the purpose of research and private study only. The thesis may not be reproduced elsewhere without the permission of the Author.

# Stabilisation of dried *Lactobacillus rhamnosus* against temperature-related storage stresses

---

A thesis presented in partial fulfilment of the  
requirements for the degree of

Doctor of Philosophy in Food Technology at  
Massey University, Manawatū, New Zealand

Sarah Priour

2019



# Abstract

---

In the past few years, research has established a link between gut health and overall health and wellbeing. A diverse microbiome is a major step towards a healthy gut. Probiotics could help by improving the gut microbiome diversity and thus, are being added to a wide range of food products. However, maintaining them in a viable state within these food products is a considerable challenge. In order to increase the shelf-life of probiotics, numerous encapsulation systems have been developed to help protect them. Techniques such as emulsification, coacervation, or drying methods have all been employed with varying levels of success. While the final encapsulated bacteria may have enhanced protection and stability, a range of stresses are imposed on the bacterial cells during the actual encapsulation process, including mechanical, physical and chemical. Drying is the technique that confers the most protection to the probiotics, potentially stabilising them for up to several years. However, water plays a structural role and upon its removal, forces appear between cell components leading to the denaturation of proteins or the phase transition of the phospholipids membrane. Thus, bacterial cells need to be dried in the presence protectants that can prevent detrimental events from occurring and damaging the cells.

It is thought that there are three main mechanisms by which protectants will confer superior stability. Firstly, the protective matrix can form a glassy system preventing further chemical reactions from happening, and thus protecting the bacteria. Secondly, if protectants are introduced for a period prior to drying, they can interact with the cellular biomolecules, replacing the structural role of the water, and maintaining the biomolecules in their native state when the water is removed from the system. Finally, the protectants can increase the free energy of water, maintaining it in the vicinity of the biomolecules,



so that when the water is removed, the biomolecules are still hydrated and in their native state. Therefore, it is obvious that the role of protectants during the drying step is critical. The question that has remained largely unanswered, however, is how long and under what conditions should the protectants be introduced, and what type of protectants work best? Once the probiotics are successfully dehydrated, storage stresses may impair their stability on the shelf. Among these stresses, high temperatures of the surrounding environment is one that has been well documented to be detrimental to the cells and generally leads to a rapid drop in shelf stability. These temperatures can be experienced not only during the life of the product on the supermarket shelves, but also during transport of these consumables around the globe. The effect of changes in temperature on bacterial cell viability is an area which has not been explored in great depth, and the impact that encapsulation may have on the viability under these conditions even less so. Once again, like in the case of the protectants, the materials used to encapsulate the bacteria will be critical to final stability. Materials such as ‘phase change materials’ (PCM), which can absorb and release heat over different temperature ranges could be the key to protecting bacteria under extreme conditions.

The aim of this thesis was thus to stabilise a model probiotic: *Lactobacillus rhamnosus* HN001 to high temperatures occurring during storage and transport.

In order to do so, the study was separated into four principal research questions. Firstly, can a pre-drying step (for example the uptake of protectants) help the stability/viability of the bacteria during storage? Secondly, what are the best protectants for long-term storage of *Lb. rhamnosus* HN001, and why? Thirdly, is it possible that combinations of the most suitable protectants act in synergy, bringing increased storage stability compared to either protectant on its own? Finally, can the inclusion of PCM in the encapsulation matrix give extra protection to the cells during storage? This question

would be of particular significance when examining the effect of the fluctuating temperatures experienced during the transport of the probiotics.

The first study, therefore, consisted of establishing a protocol to prepare the cells for drying, by finding the early stationary phase where cells are known to be most stable to stress, and then optimising the exposure of the cells to potentially protective solutions of glucose and sucrose at 4 and 20°C. The uptake of the solutes was explored using HPLC, before drying the cells and evaluating the effect that their uptake had on the shelf-life stability of freeze-dried cells. In order to try and understand any interactions between the intracellular biomolecules and the protectants, the Nano DSC was used. Results showed that when cells were exposed to glucose at 20°C, metabolisation took place, and the longer the exposure, the lower the stability of the cells after drying and over storage. Overall, the study revealed that cells exposed to sucrose at 20°C for 4 hours presented best stability indicating that both the type of protectant, and exposure settings are critical to a successful outcome. The results from the Nano DSC showed that sucrose interacted with some of the cell biomolecules, rendering them more stable. The exposure temperature for the rest of the experiments was thus set at 4°C to avoid metabolisation, and the time was set at one hour so that exposure settings would be adapted for both sugars.

In the second part of the study, a range of nine protectants (glucose, fructose, galactose, sucrose, lactose, trehalose, betaine, monosodium glutamate (MSG) and sorbitol) were compared for their ability to stabilise freeze-dried *Lb. rhamnosus* at 30°C for 6 months. Inulin was used as a carrier. The impact of galactose, sucrose, betaine, MSG and sorbitol was studied using a Nano DSC to again try and establish links between biomolecule interaction and stability during storage. Interestingly, MSG led to the best stability overall with a cell loss of 0.19 /month, even though it had the highest water

activity of all the samples following freeze-drying. This is contradictory to general thought on how water activity affects bacterial cell stability, with higher water activity generally resulting in increased cell death over time. It was shown, using the Nano DSC, that MSG interacted with most of the cell biomolecules rendering them more stable. MSG was thus selected for further study.

Three additional protectants were selected (galactose, sucrose and sorbitol) to look for potential synergistic effects with MSG in terms of protecting the bacteria during storage. The study followed a mixture design of experiment (DoE) in order to obtain an optimal protective matrix. The powder structure was also studied at this point by microscopy along with analysis using the DSC to try and comprehend the importance of the powder structure on the stability of the dried cells. Multivariate analysis was used to link all factors and their relative impact on the cell death rate together. Interestingly, it was found that neither a high glass transition temperature ( $T_g$ ) nor a low water activity helped to stabilise the bacteria. Instead, the amount of MSG was clearly shown to improve the shelf-life, and a synergy was found between sorbitol and MSG. Microscopy showed that this powder led to a unique structure that most likely collapsed during drying resulting in the shrinkage of the cake and the loss of the porous structure, thus lowering the exposure of the bacteria to oxygen. In addition, a small amount of the sorbitol present in the matrix seemed to help in stabilising additional biomolecules as shown by the Nano DSC. The slowest death rate results obtained were 0.04 /month when MSG alone was mixed with inulin, but the model predicted an even lower death rate due to the synergy occurring between MSG and sorbitol.

Finally, this optimised stabilisation matrix was used to study the impact of further protection, in the form of an encapsulate containing a PCM, on the stability of the bacteria. Powders with two different structures were compared using freeze-drying and

spray drying techniques. The viability of the resulting powders was assessed during two separate storage studies designed to test the cells against fluctuating temperatures (20 to 50°C) and at constant temperature (35°C). The results showed that PCM appeared to have little impact on the overall stability of the powder. However, it was confirmed that a dense and smooth powder structure helped to maintain the bacteria in a viable state for a longer time than a more porous structure. This was most likely due to the lower surface-area ratio decreasing the exposure with the environment and preventing detrimental reaction such as oxidation. The bacteria in the optimised stabilisation matrix had the best stability, with a death rate of 0.07 /month at 35°C and 0.18 /month under fluctuating temperature from 20 to 50°C.

In conclusion, it was found that the interaction of the protectants with cells is of paramount importance in maintaining the cells in a dried, viable state for longer periods at elevated temperatures. In addition, the structure of the powder should also be considered as one of the main mechanisms for protecting the bacteria, as it has a substantial impact on the shelf-life of the powder. Conversely, in this body of work it was shown that a high glass temperature did not enhance, or indeed help to maintain cell viability as has been suggested by many previous studies. A dense structure is, however, believed to protect the bacteria through preventing exchanges with the environment, especially with oxygen. If future work is to be done, it should follow the oxidation of the cells during storage and link it with measures of the powder porosity to gain further insight into the impact of the structure on oxidation stress.

# Acknowledgement

---

First of all, I would like to thank my main supervisor Dr. Ashling Ellis. Without her support, I am not sure I would have come this far, or at least not as smoothly. She always had the right words to calm me down and was a great listener. I have shared with her all the anger, frustration and joy that this PhD has brought over the years. And that is the best thing I could expect from a supervisor. Thank you for believing in me Ashling, and offering me the Post Doc, I wish I could stay a bit longer.

Another big thank you to my two co-supervisors Dr. Alan Welman and Dist. Prof. Harjinder Singh. Alan has always been here to challenge me a bit more, and get the best from me. He also coordinated help from Fonterra whenever it was needed. Dist. Prof. Harjinder always gives wise advice, and without his broad knowledge of the food community I would not be here. He also took the time to listen to me when I needed too. Thanks to him I was able to go to a few additional conferences in Singapore, Hangzhou and Hamilton.

I am thankful for the Riddet Institute scholarship, which made this journey possible. And of course, nothing would have been possible without the whole administration team from the Riddet Institute: Ansley Te Hiwi, Terri Palmer, John Henley-King, Sarah Golding, Hannah Hutchinson, Angela Gemmell and Rebecca Olsson. Ansley and Terri are two of the nicest, most efficient people I know, always smiling and willing to help. Thank you John, you have always been so nice, listening and helping when it was most needed. I hope that I will dream of flying when I submit this piece of work. Once again, thank you Sarah, you have always taken the time to help me find new opportunities, reassure me and get my confidence back up when it was at a low!

## *Acknowledgement*

I would like to warmly thank Ann-Marie Jackson, Kylie Evans and Haoran Wang for their support in the lab, the laughs we had, and their patience with me when I was upset because my bacteria did not grow, or when someone took a piece of equipment I had booked! You made this journey so much nicer! Without the three of you, I would not have had so much pleasure going to the lab.

Thank you to Yonatan Souid that came all the way here to work along with me. You have helped me a lot and for that, I am grateful. I want to also warmly thank Geoff Jameson and Mark Waterland. You always had some time for me and gave me wise advice. Geoff, your knowledge is incredibly powerful, you always see the big picture and played a very important role in not only my research, but in the research of so many students. I know that most of my work with you Mark was not so successful, but I did learn a lot from you, so thank you.

A huge thank for all the microscopy team: Matthew Savoian, Niki Minards, and Abraham Chawanji. I know some of my samples were tricky, but you have always looked for solutions. The beauty of this thesis is partly because of you. A big thank to Michelle Tamahena for all her help with the HPLC, and also for the friendship all through the years, as well as all the beer tastings! Thank you for Maggie Zou, Chris Hall and Janiene Gilliland for their help and support in the Riddet Institute lab. Thank you Chris especially for teaching me how to run most instruments used during my research, and for always helping me when I had issues with the spray-dryer.

I would also like to thank the people from Fonterra who took time to help me. Lisa Thomasen helped me a lot for all the statistical analysis. Alastair McGibbon was always here when I needed to have a fresh view on some of my data. Steve Holroyd and Elizabeth Nickless assisted me with all my FTIR analysis and Yvonne van der Does was always present when I needed help with the SFC NMR.

### *Acknowledgement*

Obviously, the time in the lab would not have been as bearable without all the other students. A special thanks to Roland who always had a great tip to share, you made my life easier a number of times. Another big thank to Paul, Max and David for their friendships all along. I also want to thank you all the PhD students from the Riddet Institute, especially Sewuese, Nan, Natasha, Marit and Laura for their friendship and support. I am also grateful for the Riddet Institute Student Society that started towards the end of my PhD, a great initiative started by the board, which made being a Riddet PhD student part of a family.

This journey would not have been so exciting, and interesting without the Nutri Sprinky team! This adventure started thanks to John Henley-King and thanks to our first mentor, Chris Kirk. Together with Feng Ming, Sewuese and Nicole, we learned a lot about innovation and business ideas. This adventure brought our time as a Riddet Student to the next level, and made us ready to take up new challenges.

Finally, I would like to thank all my friends from New Zealand, from home and around the world. There are too many names to mention here but they will recognise themselves: the ones with whom I laughed and I cried; the ones with whom I sweated out all the stress; the ones with whom I climbed mountains and hills over the weekends; the ones with whom I developed my left side of my brain; the ones that made delicious food over a barbeque or a potluck; the ones that were always there when I came back home over a drink, or for New Year's Eve celebrations; the ones that hosted me for a conference or a visit; and everyone who listened to me complaining when times were hard!

Un immense merci à ma famille, Maman, Papa, Yannou, Laure-Helene et Victoire. Ils ont tous pris sur eux-mêmes quand je suis partie à l'autre bout de la terre. Malgré cela ils m'ont supporté à chaque instant. Sans eux, rien n'aurait été possible !

### *Acknowledgement*

Y por fin, un gran gracias a mi chiquitito. Gracias por estar a mis lados cada día y suportarme hasta aquí. Me ayudaste mucho en los momentos difíciles, siempre apoyándome. Tu presencia hizo de ese PhD la historia más importante de mi vida. Te amo.



# Table of Contents

---

Abstract .....	I
Acknowledgement .....	VI
Table of Contents .....	X
List of Tables .....	XV
List of Figures .....	XVII
List of Abbreviation .....	XXIV
Chapter 1 – General introduction .....	1
1.1 Introduction.....	1
1.2 Outline of the thesis.....	4
Chapter 2 – Literature review .....	8
2.1 Probiotics .....	8
2.1.1 Definition of probiotics .....	8
2.1.2 Application of probiotics in the food industry.....	10
2.1.3 <i>Lactobacillus rhamnosus</i> HN001 .....	11
2.2 Drying related stresses and their responses in lactic acid bacteria.....	14
2.2.1 Stresses experienced prior to drying .....	14
2.2.2 Dehydration related stresses .....	27
2.2.3 Post-drying and storage stresses .....	37
2.3 Drying technologies for probiotics preservation.....	39
2.3.1 Main drying methods .....	39
2.3.2 Discussion of their limits and benefits .....	46

## Table of Contents

2.4	Protecting the probiotics in the dried state .....	49
2.4.1	Triggering stress responses for better stability .....	50
2.4.2	Preparing the cells prior to a dehydration stress .....	50
2.4.3	Finding the right protection .....	51
2.5	Techniques to further improve storage.....	53
2.5.1	Drying technique, powder structure and storage stability.....	53
2.5.2	Materials with higher thermal protection .....	56
2.6	Analysis techniques used for monitoring the stabilisation properties of protectants .....	58
2.6.1	Differential scanning calorimetry (DSC) .....	59
2.6.2	Fourier-Transform Infra Red (FTIR) .....	61
2.7	Concluding remark.....	62
Chapter 3	– Sugar uptake by <i>Lactobacillus rhamnosus</i> and its impact on shelf-life ..	64
3.1	Introduction.....	64
3.2	Materials and Methods .....	66
3.2.1	Materials .....	66
3.2.2	Growth curve of <i>Lb. rhamnosus</i> HN001 .....	67
3.2.3	Bacterial strain and growth.....	67
3.2.4	Harvesting of the cells.....	68
3.2.5	Study of the uptake and metabolism of the sugars .....	68
3.2.6	Shelf-life study.....	70
3.2.7	Calculation of the death rate.....	71
3.2.8	Nano differential scanning calorimetry.....	71
3.2.9	Data analysis and statistics .....	72

## Table of Contents

3.3	Results and discussion .....	73
3.3.1	Determination of the stationary phase .....	73
3.3.2	Uptake and metabolism of protectants prior to drying .....	75
3.3.3	Impact of the different exposure times on the stability of dried <i>Lb. rhamnosus</i> .....	79
3.3.4	Understanding the interaction between the sugars and <i>Lb. rhamnosus</i> .....	85
3.4	Conclusions .....	93
Chapter 4 – Effect of different protectants on the viability of <i>Lactobacillus rhamnosus</i> during storage .....		95
4.1	Introduction .....	95
4.2	Material and methods .....	96
4.2.1	Materials .....	96
4.2.2	Shelf-life study .....	97
4.2.3	Water activity measurement .....	97
4.2.4	Nano differential scanning calorimetry .....	97
4.2.5	Data analysis and statistics .....	98
4.3	Results and discussion .....	98
4.3.1	Effect of different protectants on bacterial viability .....	98
4.3.2	Nano differential scanning calorimetry results .....	102
4.3.3	Potential effect of the osmotic pressure on thermograms .....	110
4.4	Conclusions .....	111
Chapter 5 – Optimising the stabilisation matrix for protection of <i>Lactobacillus rhamnosus</i> .....		113

## Table of Contents

5.1	Introduction.....	113
5.2	Materials and methods.....	114
5.2.1	Materials.....	114
5.2.2	Design of experiments (DoE) – response surface methodology ...	114
5.2.3	Shelf-life study.....	115
5.2.4	Characterisation of the powder.....	117
5.2.5	Nano differential scanning calorimetry study of the synergy between MSG and sorbitol.....	118
5.2.6	Statistical analysis.....	118
5.3	Results and discussion.....	119
5.3.1	Characteristics of the powder .....	119
5.3.2	Stability of <i>Lb. rhamnosus</i> HN001 at 30°C .....	123
5.3.3	Powder structure .....	124
5.3.4	Multivariate analysis of the model.....	128
5.3.5	FTIR spectrum of the powders .....	131
5.3.6	Synergy between sorbitol and MSG .....	133
5.3.7	Cells dried in buffer .....	135
5.4	Conclusions.....	140
Chapter 6	– Phase change materials for the stabilisation of <i>Lactobacillus rhamnosus</i> ...	
	.....	141
6.1	Introduction.....	141
6.2	Materials and methods.....	143
6.2.1	Materials.....	143
6.2.2	Sample Preparation .....	143

## *Table of Contents*

6.2.3	Drying.....	145
6.2.4	Shelf-life study.....	146
6.2.5	Characterisation of the powder.....	147
6.2.6	Statistical analysis .....	149
6.3	Results and discussion.....	149
6.3.1	Emulsion characteristics.....	149
6.3.2	Characteristics of the powders.....	152
6.3.3	Viability after drying.....	164
6.3.4	Shelf-life studies .....	166
6.3.5	Correlations between the death rates.....	172
6.4	Conclusions.....	173
Chapter 7	– Overall discussion and conclusions .....	175
7.1	Summary and discussion .....	175
7.2	Recommendations for future work.....	183
References	.....	186
Appendix A -	FTIR study of the mixture powder.....	203

# List of Tables

---

Table 2.1: Examples of dried food products containing probiotics. ....	11
Table 2.2: Main characteristics, limitations and benefits of the three main drying methods use to stabilise probiotics. ....	49
Table 2.3: Some examples of phase change materials used in different application and their respective melting temperature.....	58
Table 3.1: Production of lactic acid in the cell supernatant after exposing <i>Lb. rhamnosus</i> to glucose or sucrose at 4 or 20°C. “Exp.” stands for exposure. Data are expressed as the mean of triplicates with their standard deviation.....	77
Table 3.2: Details of the protectant solution and the exposure settings for the shelf-life study of freeze-dried <i>Lb. rhamnosus</i> .....	80
Table 3.3: Viability after drying and over storage of <i>Lb. rhamnosus</i> exposed to glucose or sucrose at 4 or 20°C for up to 4 hours prior to drying. Values are expressed in their arithmetic mean with their standard deviation. ....	84
Table 3.4: Statistical analysis of the factorial design for the stability of <i>Lb. rhamnosus</i> after freeze-drying and over storage. ....	85
Table 3.5: Mean value of peak maxima ( $T_m$ ) and maximal heat flux ( $C_p^{T_m}$ ) of the cells exposed to phosphate buffer or sucrose solution at 4 or 20°C for 0 min or 240 min. ....	90
Table 4.1: Water activity of the powders after freeze-drying prepared with a range of protectants (detailed values of the triplicates).....	100
Table 4.2: Stability of <i>Lb. rhamnosus</i> HN001 in sugar powders after freeze-drying and over storage at 30°C. Data are expressed as the mean with the standard deviation of triplicates. Different superscript letters within the same column indicate significant differences ( $P < 0.05$ ).....	100
Table 4.3: Mean value of peak maxima ( $T_m$ ) and maximal heat capacity ( $C_p^{T_m}$ ) of <i>Lb. rhamnosus</i> exposed to solution of betaine, MSG, sorbitol or sucrose or buffer. n indicates the number of thermograms where the peaks were identified. Samples with different	

## List of Tables

superscripts letters means statistical difference of their T <sub>m</sub> or their maximum heat capacity (C <sub>p</sub> <sup>T<sub>m</sub></sup> ) (p-value<0.05). .....	109
Table 5.1: Composition of the protectant solutions for optimising the stabilisation matrix following the mixture DoE presented in section 5.2.2.....	116
Table 5.2: Powder characteristics of the samples – moisture content, water activity and glass transition temperature (T <sub>g</sub> ). Moisture content and T <sub>g</sub> are the mean of three true replicates, measured three times with their standard deviation. Water activity is the mean value of the three replicates measured at least five times over the storage period with the standard deviation. ....	121
Table 5.3: Characteristics of freeze-dried <i>Lb. rhamnosus</i> HN001 dried in phosphate buffer. Data are expressed as the mean value with the standard deviation of triplicates. ....	136
Table 6.1: Composition of the seven samples with or without PCM. The little cartoons represent the desired structure, with the stabilisation matrix in grey, the bacteria in blue, the protein in green, and the lipid in red. All samples contained 3.3% (w/w) of dried cells. ....	146
Table 6.2: Glass transition temperature and water activity of powders with and without PCM after drying. Data are shown as the mean values of triplicates with their standard deviation. ....	160
Table 6.3: Crystallisation behaviour of the samples with PCM. Data are expressed as the mean with the standard deviation of triplicates. ....	163
Table 6.4: Details of the storage of samples with and without PCM. Data are expressed as the mean with their standard deviation of triplicates. Samples with different superscripts letter are significantly different (P<0.05).....	169
Table 7.1: Death rate of bacteria dried in a 1:1 mix of protectant and inulin, comparison of results from Chapter 4 (samples were stored in closed container, but not aliquoted) and from Chapter 5 (where samples were mixed in skim milk powder and aliquoted in aluminium pouches). ....	178

# List of Figures

---

Figure 1.1: Outline of the thesis .....	7
Figure 2.1: Main stress responses of the bacterial cells following an acid stress. HSP stands for heat shock proteins.....	16
Figure 2.2: Main stress responses of the bacterial cells following a starvation stress....	18
Figure 2.3: Main stress responses of the bacterial cells following a cold stress. ....	21
Figure 2.4: Main stress responses of the bacterial cells following a hyperosmotic stress. ....	26
Figure 2.5: Main processes of freezing stress endured by the bacteria. ....	30
Figure 2.6: Thermograms of whole cells of <i>E. coli</i> (solid line) and <i>Lb. plantarum</i> (dotted line) obtained by DSC (heating rate of 3°C/min). Endothermic events are down, with the denaturation of the ribosome in a1, a2 and a3 with the 30S subunit suggested to be a1, the DNA melting in b, denaturation of cell wall components in c and d. Results are taken from Lee and Kaletunç (2002).....	32
Figure 2.7: Dehydration stresses endured by the bacterial cells in the absence of protectants (left) and the three protection mechanisms of protective solutes (on the right). ....	36
Figure 2.8: Spray dryer in a simplified form. Based on Jacobs (2014) .....	40
Figure 2.9: Diagram of the two-fluid nozzle (left) and three-fluid nozzle (right) set up of a spray drier. Adapted from Pabari et al. (2012). ....	42
Figure 2.10: Fluid-bed dryer principle, adapted from Frey (2014) .....	44
Figure 2.11: Examples of mixture design of experiment. The simplex centroid design is presented on the left, and a {3,3} simplex lattice design on the right. X1, X2 and X3 represent the three components. ....	53
Figure 3.1: <i>Lb. rhamnosus</i> HN001 growth curve, incubated at 37°C in MRS media, followed by plate counting and absorbance reading at 610 nm. Data are shown as the mean of triplicates and the error bars represent the standard error.....	74













## List of Figures

Figure 3.2: Relationship between the dry cell weight and the absorbance at 610 nm of <i>Lb. rhamnosus</i> HN001. $y = 1.26 + 1.92x$ with $R^2 = 0.978$ . Data are shown as the mean of triplicates and the error bars represent the standard error. ....	74
Figure 3.3: Comparison of lactic acid release in the supernatant from <i>Lb. rhamnosus</i> exposed to glucose (in blue) or sucrose (in black) solutions at 4°C (dashed line) or at 20°C (solid line). Data are shown as the mean of triplicates and the error bars represent the standard error. ....	76
Figure 3.4: Glucose (orange) and lactic acid (blue) concentrations in cell pellet after exposure to glucose at 4°C (dashed line) or at 20°C (solid line). Data are shown as the mean of triplicates and the error bars represent the standard error. ....	78
Figure 3.5: Sucrose (red) and lactic acid (blue) concentrations in cell pellet after exposure to sucrose at 4°C (dashed line) or at 20°C (solid line). Data are shown as the mean of triplicates and the error bars represent the standard error. ....	79
Figure 3.6: Shelf-life study conducted at 40°C (column a) and 30°C (column b) of <i>Lb. rhamnosus</i> exposed to glucose (row 1) or sucrose (row 2), at 20°C (in red) and 4°C (in blue) for 0 min up to 240 min. Data are shown as mean of triplicates and the error bars represent the standard error ....	82
Figure 3.7: Thermograms of cells exposed to phosphate buffer (control, in graphs a and b), to sucrose (graphs c and d) or to glucose (graphs e and f) at 4°C (a,c and e) or 20°C (b,c and f) for 0 min (in dashed line) or 240 min (in solid line). The curve is the mean value of triplicates, and the standard deviation is denoted as the ribbon. ....	87
Figure 3.8: First and second principal components explaining the variance between all the thermograms of cells exposed to the different solutions. The thermograms of cells exposed to the phosphate buffer, glucose or sucrose solution, before baseline removal, are presented on the left (a). Thermograms of cells exposed to sucrose and phosphate buffer, after removal of the baseline are presented on the right (b). ....	88
Figure 3.9: Thermograms of all samples exposed to phosphate buffer and to sucrose at 4 or 20°C for 0 min or 240 min after baseline removal. ....	92
Figure 4.1: Stability of <i>Lb. rhamnosus</i> HN001 at 30°C. Each powder contained the protectant and inulin in a 1:1 ratio. Control consisted of inulin only. Each point represents the mean of triplicates, and the error bar represents the standard error. ....	99

Figure 4.2: Thermograms of <i>Lb. rhamnosus</i> exposed to galactose, betaine, MSG, sorbitol or sucrose in phosphate buffer, or buffer alone. Data are shown as the mean of triplicates (in straight line) with their standard deviation (ribbon). .....	104
Figure 4.3: First two principal components of <i>Lb. rhamnosus</i> thermograms exposed to galactose, betaine, MSG, sorbitol or sucrose in phosphate buffer, or buffer alone. ....	104
Figure 4.4: Baseline corrected thermograms of <i>Lb. rhamnosus</i> exposed to betaine, MSG, sorbitol, sucrose in phosphate buffer, or buffer alone. Mean value of triplicates are presented as the straight lines with their standard deviation (ribbon). Thermograms have been offset for clarity. ....	105
Figure 4.5: First two principal components of <i>Lb. rhamnosus</i> baseline corrected thermograms exposed to betaine, MSG, sorbitol, sucrose in phosphate buffer, or buffer alone. “av” stands for averaged thermogram, and “r” replicate. ....	106
Figure 4.6: Temperature of peak maxima of four peaks identified from the thermograms, as a function of osmotic pressure of the protectants concentration. Peak S-4 and S-5 are respectively, the second to last and last peak of the s region. PB stands for phosphate buffer, Suc for sucrose, Sor for sorbitol and Bet for betaine.....	111
Figure 5.1: Four-component mixture DoE followed in this study: augmented simplex-lattice of degree 2 with the centroid (in red) and axial points (open circles). ....	115
Figure 5.2: Mixture contour plots of the glass transition of powders (graph A), the moisture content after drying (graph B) and the water activity after drying (graph C). Blocks were included in the model, as they presented a significant impact on the variables. ....	122
Figure 5.3: Mixture contour plots of the death rate based on the component amounts, bacteria were stored 8 months at 30°C. ....	124
Figure 5.4: SEM micrographs of the first block of samples from the mixture DoE (magnification 1 000 X). Numbers indicate the sample number (composition detailed in Table 5.2). ....	126
Figure 5.5: SEM micrographs of freeze-dried powder of inulin in phosphate buffer without bacteria (on the left), and a mix of inulin and MSG (1:1) in phosphate buffer (on the right). ....	127

## List of Figures

Figure 5.6: SEM micrographs of freeze-dried powder of mix of protectants without bacteria: 100% of inulin in buffer (A), inulin and galactose 1:1 (B), inulin and MSG (C), inulin and sucrose 1:1 (D), inulin and sorbitol 1:1 (E), and inulin with MSG, sorbitol galactose and sucrose 4:1:1:1:1 (F).....	127
Figure 5.7: Three-dimensional representation of the three first principal components explaining the relationship between the death rate, the composition and the characteristics of the powder. Higher death rate is denoted with red dots, while low death rates are in green.....	130
Figure 5.8: First four PC of the powders spectra with and without bacteria, with first two PC in a and b, and second two PC in c and d. Matrices are in black, bacteria are coloured as a function of their death rate in graph a and c (green, lower death rate and red higher death rate). Bacteria samples are coloured as a function of their amount of MSG in graph b and d, with light blue higher amount of MSG, darker blue lower amount of MSG and pink, no MSG.....	132
Figure 5.9: SEM micrographs of the freeze-dried mix 4:1 MSG:Sorbitol with inulin and without bacteria. Magnification 800 X. ....	134
Figure 5.10: Thermograms of <i>Lb. rhamnosus</i> HN001 run with a mix of MSG and sorbitol (4:1 ratio) compared with the cells exposed to MSG and sorbitol alone, obtained from Chapter 4. The straight line denotes the mean values of triplicates, and the ribbon shows the standard deviation. ....	134
Figure 5.11: SEM pictures of dried cells in phosphate buffer. Picture A shows the overall structure of the powder. Pictures B, C and D show characteristic details of the powder, location of these pictures are marked as black squares on picture A. Magnifications are indicated on the micrographs.....	136
Figure 5.12: Comparison of the viability of cells dried in phosphate buffer only to cells dried with inulin, a mix of MSG and inulin and a mix of sucrose and inulin, all mixed with buffer. Results from cells mixed with inulin are from previous study in Chapter 4. The error bars denotes the standard error.....	138
Figure 5.13: Viability of cells dried in phosphate buffer, compared with cells dried with MSG and sucrose. Data are shown as the mean values of triplicates and error bars show the standard error. ....	140

Figure 6.1: Particle size distribution of the emulsions before and after dilutions. The lines denote the mean value and the ribbon the standard deviation. Dilution was made before drying to match the concentration of the protein solution, i.e. 10.9% (w/w).....	150
Figure 6.2: Crystallisation pattern of Witocan® 42/44 in a pure state. ....	151
Figure 6.3: Crystallisation pattern of emulsions after dilution, which was made before drying to match the concentration of the protein solution, i.e. 10.9% (w/w).....	152
Figure 6.4: Confocal microscopy of the spray-dried samples: SD-P1-L0 (  ) in first row, SD-P1-L1 (  ) in second row and SD-P1-L3 (  ) in third row. Bacteria are in blue, protein in green, and lipid in red. The bar indicates 5 µm. ....	154
Figure 6.5: Confocal microscopy of the spray-dried powder using a two-fluid nozzle. Bacteria in the stabilisation matrix was mixed with the emulsion system (P1-L1) before spraying. Bacteria are in blue, protein in green, and lipid in red. The bar indicates 5 µm. ....	155
Figure 6.6: SEM micrographs of the spray-dried samples. SD-P1-L0 (  ), SD-P1-L1 (  ), and SD-P1-L3 (  ). Micrographs on the right presents the enlargement (6 000 X) of the micrograph on the left (1 500 X). The blue arrow show a black stain.....	157
Figure 6.7: SEM micrographs of the freeze-dried samples: FD-P0-L0 (  ), FD-P1-L0 (  ), FD-P1-L1 (  ) and FD-P1-L3 (  ). Micrographs on the right presents the enlargement (6 000 X, apart for FD-P0-L0, 800 X) of the micrograph on the left (400 X). Bacteria are denoted with a red arrow, crystallised fat with a green arrow and black stains with a blue arrow. ....	158
Figure 6.8: SEM micrograph of the FD-P1-L3 prepared without bacteria. Magnification 1500 X.....	159
Figure 6.9: Crystallisation pattern of the 4 samples containing Witocan® 42/44, with the details of their replicate. Freeze-dried samples are presented at the top, and spray-dried samples at the bottom. Samples with 1:1 lipid to protein are on the left, and samples with 3:1 lipid to protein are on the right. ....	161
Figure 6.10: Solid fat content change over two cycles of temperatures from 20 to 50°C of the 12 sample containing Witocan® 42/44. Freeze-dried samples are presented at the top,	

and spray-dried samples at the bottom. Samples with 1:1 lipid to protein are on the left, and samples with 3:1 lipid to protein are on the right.....	162
Figure 6.11: Viability after drying of PCM samples. Data are the mean values of triplicates and the error bar denotes de standard error. Samples with different letter are significantly different ( $P<0.05$ ). .....	165
Figure 6.12: Shelf-life study of the PCM powders under fluctuating versus constant temperature. Data are the mean values of triplicates and the error bar denotes the standard error.....	167
Figure 6.13: SEM micrographs of the freeze-dried and spray dried powder after 3 months under fluctuating temperature from 20 to 50°C. Magnification is of 6 000X for all micrographs. ....	171
Figure 6.14: Correlation between the death rate under fluctuating temperature and under constant temperature. ....	173
Figure A.1: Infra-Red spectra of the Mixture DoE samples (Chapter 5), with bacteria (in colour) or without bacteria (in black). Samples with bacteria are coloured as a function of their amount of MSG, with light blue being low amount of MSG, dark blue, lower amount of MSG and pink no MSG. After visualising the raw data (a, b), the treatment consisted in centre and scaling (c, d) and smoothing (e, f). For each treatment the spectra are shown in a, c and e, and the first two PC in b, d and f. ....	206
Figure A.2: Averaged spectra of the mixture DoE after centring, scaling and smoothing. Spectra are shown in a and b, and the first four PC of the PCA are shown in c and d. Samples with no bacteria are shown in black. In a, c and d samples with bacteria coloured as a function of their death rate, green being lower death rate and red being higher. In figure b samples are coloured as a function of their MSG content, in light blue higher amount of MSG, dark blue lower amount and pink no MSG. ....	208
Figure A.3: First derivative of the averaged and corrected spectra of the mixture DoE (a,b). The four first PC of the PCA are shown in c and d. Samples are shown as a function of their death rate in a, c and d (green low death rate, red high death rate) and as a function of the MSG amount in b (light blue higher amount of MSG, dark blue lower amount and pink no MSG). ....	209

Figure A.4: Vector corrected spectra of the mixture DoE (a,b). The four first PC of the PCA are shown in c and d. Samples are shown as a function of their death rate in a, c and d (green low death rate, red high death rate) and as a function of the MSG amount in b (light blue higher amount of MSG, dark blue lower amount and pink no MSG). .....	210
Figure A.5: IR spectra of Inulin, retrieved from Grube et al. (2002) .....	211
Figure A.6: Centred, scaled, smoothed and averaged spectra of the 15 mixes (a), isolation of the 900 – 1200 cm <sup>-1</sup> region, corresponding to the inulin signal. The PCA of this region is showed in b, and samples are coloured as a function of the MSG amount (light blue higher amount of MSG, dark blue lower amount and pink no MSG). .....	212
Figure A.7: Second derivative of centred, scaled, smoothed and averaged spectra of the 15 mixes (a), isolation of the 900 – 1200 cm <sup>-1</sup> region, corresponding to the inulin signal. The PCA of this region is showed in b, and samples are coloured as a function of the MSG amount (light blue higher amount of MSG, dark blue lower amount and pink no MSG).....	212
Figure A.8: Mixture contour plots of the four peaks associated with the signal of inulin. ....	214

# List of Abbreviation

---

A<sub>w</sub>: Water activity

CFU: Colony Forming Unit

CSLM: Confocal Scanning Laser Microscopy

DSC: Differential Scanning Calorimetry

DoE: Design of Experiment

FTIR: Fourier-Transform Infra Red

HPLC: High-Performance Liquid Chromatography

*Lb. Lactobacillus*

*Lc.: Lactococcus*

MSG: Monosodium Glutamate

PCA: Principal Component Analysis

PCM: Phase Change Material

PC: Principal Components

SEM: Scanning electron microscopy

SFC NMR: Solid fact content nuclear magnetic resonance

T<sub>g</sub>: Glass transition temperature

# Chapter 1 – General introduction

---

## 1.1 Introduction

Over the last decade, the fortified and functional packaged food market has grown by 32%, reaching USD 16.7 billion in 2018 (Euromonitor International, 2019). Consumers are now looking for nutritious food, which can also confer health effects with many now viewing food as medicine. Within this market share, probiotic products are also growing, with dairy-based products being the major format consumed with about USD 3.2 billion in 2018 (Oster, 2018). However, new types of products containing probiotics are entering the market such as chocolates, peanut butter and even crackers and chips. It was found that probiotic supplements growth had declined steeply in the US since 2016 (Oster, 2018). According to this report, the main reason being that people are becoming fatigued with taking pills every day and prefer food-based nutrition more befitting of a busy lifestyle, e.g. the snack option. In addition, scientific reports often show that lower numbers of viable bacteria are actually present compared to those stated on the label (Chen et al., 2017; Drago, Rodighiero, Celeste, Rovetto, & de Vecchi, 2010; Kolaček et al., 2017; Zawistowska-Rojek, Zareba, Mrowka, & Tyski, 2016). This could be due to the stresses that the bacteria undergo during the shelf-life of the product, leading to significant decreases in viability. An example of such a stress would be changes in the temperature of the surrounding environment. It could also be due to insufficient protection of the bacterial strain prior to drying or incorporation into the food product. Therefore, it would seem that there is still a need to improve the stability of probiotics both in supplements and in food products. It is imperative that the food industries find new methods to maintain probiotics in a live state as these microorganisms face new stressful production processes and environments.



There are four main techniques used by the industry to improve probiotic stability.

1. Genetic selection of resistant strains. One of the criterion for being recognised as a probiotic is for the strain to be able to survive transit through the digestive tract, with or without a protective matrix (FAO/WHO, 2006). Therefore, a specific strain may be chosen by the industry because of its natural resistance to stresses (Prasad, Gill, Smart, & Gopal, 1998).
2. Pre-stressing the cells to develop their protection mechanisms (Nag & Das, 2013), optimisation of the growth medium (Carvalho et al., 2004; Chen, Chen, Chen, Wu, & Shu, 2014) and harvesting time (Saarela et al., 2005), can all impact viability in the long term as the bacterial cells develop general stress response mechanisms.
3. Encapsulating bacterial cells by techniques including emulsion (Zhang, Lin, & Zhong, 2015), extrusion (Doherty et al., 2011) or complex coacervation (Zhao et al., 2018)
4. Drying the cells in a protective matrix using methods such as freeze-drying, spray drying, fluid-bed drying or vacuum drying (Broeckx, Vandenhevel, Claes, Lebeer, & Kiekens, 2016).

These techniques are sometimes combined in a bid to optimise the cell resistance to stresses. For instance, Oliveira et al. (2007) used complex coacervation followed by spray drying to stabilise *B. lactis* and *Lb. acidophilus*, with a log reduction of 6 log (CFU/g) and 1.9 log (CFU/g), respectively at 37°C for 120 days. However, it is pivotal to first understand the stresses endured by the cells during the encapsulation process and/or the drying, as well as during the storage, to efficiently stabilise them. For instance, in the study by Oliveira et al. (2007), a casein and pectin complex was used as wall

material as it can form a coacervate, and because it can resist acid stress therefore protecting the cells from the passage through the stomach. However, as the encapsulation system was not designed to protect from dehydration and storage stresses, it could have been foretold that the bacteria would not be very stable during storage in the dried state, and adequate protectants should have been included in the system to protect the cells from these added stresses. When properly controlled, drying is an efficient way of stabilising the bacterial cells and it allows the cells to be kept in a stable format for months and even years depending on the storage conditions. Pre-stressing the cells and optimising their growth conditions have a direct impact on the cells resistance to drying because of the stress response of the cells. Understanding the response mechanisms can help in targeting the stress location and in turn designing an adequate system to protect the cells. However, studies often look either at the drying mechanisms itself, to try to develop a gentle or efficient encapsulation method (Zhang, Li, Park, & Zhao, 2013), at pre-stressing the cells, and/or at drying them in the presence protectants (Carvalho et al., 2002). Few studies try to go further and integrate these different factors to optimise stabilisation of the bacteria. For instance, studies that have looked at the synergistic effects of different protectants generally focus on mixing protectants in a defined ratio (Jofré, Aymerich, & Garriga, 2015; Miao et al., 2008; Roos & Pehkonen, 2010). The use of surface response analysis, and more specifically mixture design of experiment, allows the optimisation of the protective mixture to achieve high stability of the bacteria (Bustamante, Villarroel, Rubilar, & Shene, 2015). This technique could also be used to optimise the drying settings (Gomez-Mascaraque, Morfin, Pérez-Masiá, Sanchez, & Lopez-Rubio, 2016), however to date it has not been used in this context. There is thus a real need to have a more integrated view of the protection of bacterial cells, by first understanding the stresses endured by the

cells during stabilisation and over storage, and to then design a protective system which is suited to the cell and specific to the bacterial strain.

Another challenge is to be able to maintain the stability of bacterial cells to harsh conditions during storage. For instance, when the temperature goes above room temperature, the viability of cells drastically drop, even in the dried state. Albadran, Chatzifragkou, Khutoryanskiy, and Charalampopoulos (2015) managed to stabilise *Lb. plantarum* at 30°C for 45 days with 1 log (CFU/g) reduction, but when the temperature was increased to 37°C the cell viability dropped by 3 log (CFU/g) over the same period of time. This is a major issue for countries with warmer climates where products can face high storage temperatures. As an example, the New Zealand economy relies heavily on exports to Asia, and during transportation temperatures can fluctuates to between 30-35°C and can go as high as 60°C depending on the zone (Rodríguez-Bermejo, Barreiro, Robla, & Ruiz-García, 2007; Singh, Saha, Singh, & Sandhu, 2012).

Thus, this thesis aims to stabilise *Lactobacillus rhamnosus* HN001 at 30°C and above for an extended period of time. The study focuses on the preparation of the cells to drying from the harvesting point by optimising the interactions of the protectants with the cells and finding the optimal protection matrix that lead to long-term storage at high temperatures. In addition, this work aims to look at novel materials that have the potential to absorb heat in order to improve the stability of bacteria when stored at temperatures above 30°C.

## 1.2 Outline of the thesis

The research was structured from the bacteria upwards, by exploring ways of preparing the cells prior to drying, and then adding further protection by using encapsulation techniques and materials known to absorb heat. The full scope of the research and indeed the thesis is outlined visually in Figure 1.1.

The first step of the present work was to gain further insight and a better understanding of the cells and how to prepare them for the drying and subsequent storage (Chapter 3). This included finding the start of the stationary phase, which is known to be the point at which the bacteria are most stable. Then, the impact of cells exposure to protectants before drying (in terms of cell viability) was studied. Previous studies have mentioned the importance of this step for optimising the uptake of protective solutes and hence optimising overall protection (Hubálek, 2003) in the longer term. The previous studies published in this area, however, are inconsistent regarding the method of exposure, especially in terms of temperature and time. Thus, the overall aim from this part of the work was to establish a protocol for preparing the cells prior to the drying step. This protocol would then be applied in the following studies.

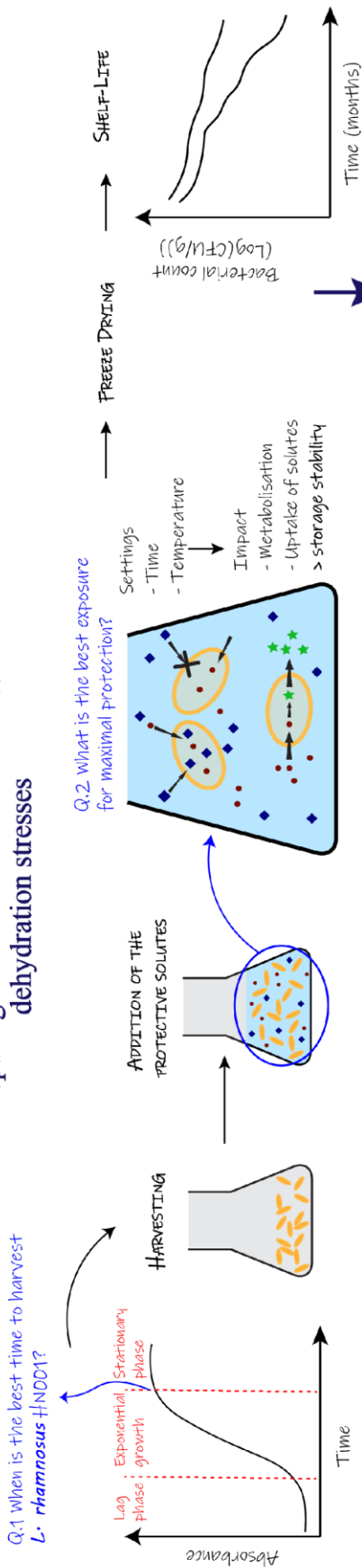
The second step of the thesis was to develop a stabilisation matrix that could protect *Lb. rhamnosus* at a minimum of 30°C for at least 6 months. Numerous protective solutes are referenced in the literature but not all may be effective with the *Lb. rhamnosus* HN001 given many seem to be strain dependent. Therefore, on review of the literature, nine protectants were screened for their ability to stabilise freeze-dried *Lb. rhamnosus* HN001 (Chapter 4). In addition, the interaction between the protectants and cells were studied using a Nano DSC to understand their influence on the stability of the dried cells. Studies have long focused on the interactions of the protectants with the membranes, but this technique allowed examination of all the cell components, including cytoplasmic biomolecules.

The next study looked at possible synergies between the various protectants rather than on an individual basis in order to find an optimal stabilisation matrix (Chapter 5). This study also examined the differences in the structure of the final powders, depending

on their composition and how this may impact the final viability of the cells using multivariate analysis.

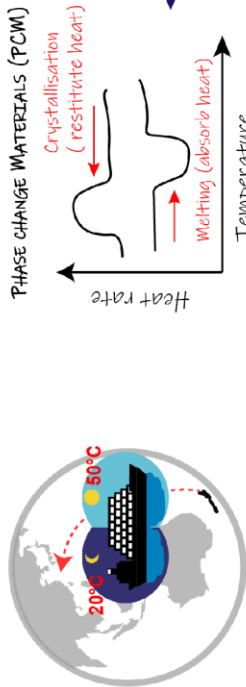
Finally, Chapter 6 takes the research to another level, by examining a new stress, which has to our knowledge not been explored before in the literature in relation to bacterial stability: temperature fluctuation. The conditions for this study were set out to mimic the type of transportation conditions that a dried product may go through during its shelf-life. Phase change materials (PCM) were proposed as a protective material due to their ability to absorb heat during phase transition. In addition, a core-and-layer structure – composed of the stabilisation matrix obtained in the former chapter as core, and encapsulated PCM in the outer layer – was compared to the structure obtained by freeze-drying. This helped to shed further light on the importance of powder structure in stabilising bacterial cells.

### Chapter 3 Preparing *Lactobacillus rhamnosus* to dehydration stresses

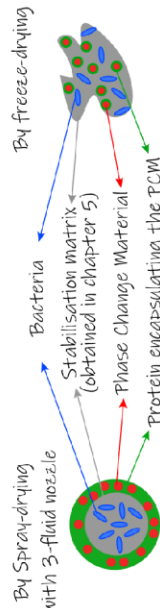


### Chapter 6 Addition of Phase Change Materials (PCM)

Q.5 Can Phase Change Materials protect from temperature fluctuation occurring during transportation?

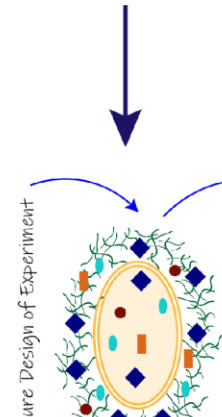


Q.6 Can the structure impact the cell viability?

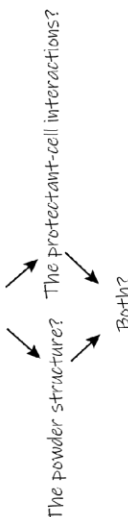


### Chapter 5 Optimising the stabilisation matrix

Q.4 What is the optimal mix of the best protectants?



Q.5 where is the protection coming from?



### Chapter 4 Selection of the right protectants

Q.3 What are the best protectant for *L. rhamnosus* HND01?

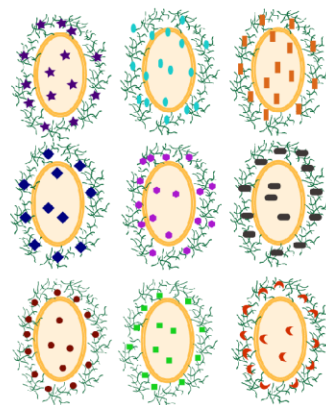


Figure 1.1: Outline of the thesis

## Chapter 2 – Literature review

---

### 2.1 Probiotics

#### 2.1.1 Definition of probiotics

The term “probiotic” has been derived from the Greek language and means “for life”. It was first mentioned in 1965 to identify a growth-promoting factor produced by microorganisms which promotes the growth of other microorganisms (Lilly & Stillwell, 1965). Today, probiotics are internationally defined as live microorganisms that, when administered in adequate amounts, confer a health benefit on the host (Hill et al., 2014).

Probiotics are often sourced from the microflora, i.e. fungi, bacteria and yeast, inhabiting humans, where the number of bacteria is of the same order as the number of human cells (Sender, Fuchs, & Milo, 2016). The typical concentration of bacteria in the intestinal tract varies between  $10^3$  CFU/mL, in the stomach, the duodenum and jejunum, and  $10^{11}$  CFU/mL, in the large intestine. Colonisation of the intestinal tract starts at birth and evolves throughout life, with notable age-specific changes (Mitsuoka, 1992). The gut microflora has been recognised to have beneficial roles to the host, notably by protecting from colonization of ingested pathogens (van der Waaij, Berghuis-de Vries, & Lekkerkerk, 1971; Vollaard & Clasener, 1994). Thus, there is an opportunity to increase the number of beneficial microorganisms such as probiotics, to improve the health and general well-being of the host.

To date, the health benefits reported by probiotics are quite diverse. They have been shown to generally modulate and improve the immune system. For instance, they can enhance the natural killer cells cytotoxicity in the elderly and can induce the production of mucus or macrophage activation (Gill, Rutherford, & Cross, 2001). They can also prevent the appearance of allergic diseases (Kalliomäki et al., 2001). In addition,

probiotics can inhibit the growth and adhesion of some enteropathogens, and thus protect from diseases such as diarrhoea, urogenital tract disorder and urinary tract infections (Allonsius et al., 2017; Praselia & Kesetyaningsih, 2015). They can also help to alleviate inflammatory conditions in the gut such as the Crohn's disease and irritable bowel disease (Shen et al., 2017). Finally, probiotics could potentially protect the body from various forms of cancer by preventing the production of carcinogens (Wang et al., 2017).

The amount of bacteria that can be termed a “beneficial” dose of probiotics is strain dependent and can vary between  $10^8$  and  $10^{10}$  colony forming unit (CFU) per day (Tamime, Marshall, & Robinson, 1995; Wickens et al., 2012). It has been suggested that the ingestion of probiotics only confers a transient effect, as they do not stay longer than days or weeks in the host (Tannock et al., 2000). However, probiotics could have a more long-term benefit in new-born where the commensal flora has not been established yet. They could also help repopulate the gut after the administration of antibiotics.

To summarise, the FAO and WHO organisations, give some guidelines for the assessment of probiotics in foods (FAO/WHO, 2006). Firstly, probiotics should be able to survive the passage through the digestive tract and to proliferate in the gut. This means probiotics should be resistant to gastric juices or be consumed in a matrix that allows them to survive. Secondly, probiotics should exert defined health benefits on the host through growth and/or activity in the human body. This means that they need to reach the body in a viable format in order for them to have a beneficial effect. Finally, as it is recognised that probiotic properties are strain specific, the strain must be identified with phenotypic test and genetic identification, and be named according the International Code of Nomenclature.



### **2.1.2 Application of probiotics in the food industry**

It is now generally accepted that probiotics are important to maintain health. Probiotics are naturally present in fermented foods such as yoghurts, which were one of the first processed foods consumed by humans (Marco et al., 2017). This eating habit, however, has been lost in some communities. The health benefits of these foods are thought to be so important that it has been advised to add a fermented foods group to the dietary guidelines to improve general health (Coulson, 2018).

In addition, in order to meet consumer demands, the food industry is looking to develop more functional food products, and are thus adding probiotics to a wider range of new processed food, such as chocolate, cereals, beverages or infant formulas (Kent & Doherty, 2014; Saarela, Virkajarvi, Nohynek, Vaari, & Matto, 2006). Table 2.1 presents a few products containing probiotics that are currently available in retail outlets. With new products, come new challenges, and to keep these microorganisms in a viable state in a complex food system is a significant one. Probiotics will endure numerous stresses before reaching the intestine (where they will then have to exert a beneficial effect) such as temperature changes, desiccation, mechanical disruption, oxidation, freezing, and finally, strong acids in the stomach. The main stresses endured by probiotics will be discussed in greater detail later.

For food industries, the cost of probiotic storage has to be considered as well. In the short term (up to 2 months), storage of probiotics would be more economical, and more environmental-friendly when frozen. In the longer term (more than 7 months), freeze-drying would be a better option (Pénicaud, Monclus, Perret, Passot, & Fonseca, 2018). Undoubtedly, the more efficient the preservation method, the more economical and the better for the environment. There is thus, a real need to protect these living cells effectively.

**Table 2.1:** Examples of dried food products containing probiotics.

Product	Probiotic strain	Bacterial count	Brand	Country of Origin
Raspberry porridge - Cereals	<i>Bacillus coagulans</i> GBI-30 6086	>5 billion CFU per 100 g	Blue Frog™	New Zealand
Mixed berry probiotic ball – Energy ball	<i>Bacillus coagulans</i>	5 billion CFU per 100 g	Health Lab™	Australia
Probiotic paleo breakfast - Cereals	<i>Bacillus coagulans</i> GBI-30 6086	1 billion CFU per 100 g	Something to crow about	New Zealand
Healtheries digestion tea - Tea	<i>Bacillus coagulans</i>	100 million CFU per serve	Healtheries	New Zealand
Potato, rice and pumpkin SNAPS - Chips	<i>Bacillus coagulans</i>	4 billion CFU per 100 g	Piranha®	Australia
Dark Belgian chocolate - Confectionary	<i>Bifidobacterium</i> BB536	1 billion CFU per serve	Bouchard	Belgium
Annum™ - Infant formula	<i>Bifidobacterium lactis</i> (DR10™)	1.4*10 <sup>7</sup> CFU per 100 mL	Fonterra™	New Zealand
THRIVE®™ PLUS - Lollipops	<i>Bacillus coagulans</i> GBI-30 6086	1 billion CFU per serve	Dr John's Candies®	USA

### 2.1.3 *Lactobacillus rhamnosus* HN001

*Lb. rhamnosus* HN001 is a gram positive bacterium from the Lactobacillales order. It is recognised as a probiotic as it has all of the prerequisite properties, that is: acid and bile resistance, adherence to intestinal cells, transient colonisation and lack of toxicity or other detrimental effects (Gopal, Prasad, Smart, & Gill, 2001; Tannock et al., 2000; Zhou, Gopal, & Gill, 2001; Zhou, Shu, Rutherford, Prasad, Birtles, et al., 2000; Zhou, Shu, Rutherford, Prasad, Gopal, et al., 2000). The strain has been shown to give effective protection against eczema in infants (Wickens et al., 2012) and other allergic diseases

such as hay fever (Wickens et al., 2018). It has also been shown to inhibit the growth of *Clostridium difficile* in the digestive tract (Lahtinen et al., 2012). The strain exerts immunostimulating effects, including in foetuses as it increases the cytotoxicity of natural killer cells (Ibrahim et al., 2010). A study has shown that *Lb. rhamnosus* HN001 could improve bone mineral density and mineral content, in female rats (Kruger, Fear, Chua, Plimmer, & Schollum, 2009). Finally, oral administration of *Lb. rhamnosus* HN001 can help overcome vaginal infection in women (Jang et al., 2017; Russo, Superti, Karadja, & De Seta, 2019).

The bacteria is a facultative anaerobe and its genome has been fully sequenced (Klaenhammer et al., 2002; Suharja, Henriksson, & Liu, 2014). It can grow efficiently on 26 carbon sources and is capable of utilising 53 different carbon sources in total (Ceapa et al., 2015). More specifically, Gopal, Sullivan, and Smart (2001) have shown that *Lb. rhamnosus* HN001 preferentially utilises disaccharides and monosaccharides from galacto-oligosaccharides and could grow on disaccharides fractions from galacto-oligosaccharides.

*Lb. rhamnosus* HN001 is a common non-starter lactic acid bacteria found in New Zealand cheddar cheese and presents flavour enhancing attributes, in addition to its probiotic properties (Klaenhammer et al., 2002). The strain has also been successfully added to low lactose yoghurt by modifying the processing conditions, in order to improve the beneficial effect of the product (Ibarra, Acha, Calleja, Chiralt-Boix, & Wittig, 2012). Apart from dairy products, fruit juices have also been supplemented with *Lb. rhamnosus* HN001 (Shah, Ding, Fallourd, & Leyer, 2010). The presence of green tea extract, grape fruit seed extract or vitamin C maintained the bacteria between 5 and 7 log (CFU/g) during 6 weeks of storage at 4°C. Interestingly, *Saccharomyces cerevisiae* and inactivated yeast derivatives have been shown to improve the stability of *Lb. rhamnosus* HN001

towards acid stress (Lim, Toh, & Liu, 2015; Toh & Liu, 2017). The protection from the yeast extract was attributed to its composition, most specifically to the presence of low molecular weight polysaccharides, free amino acids and/or the antioxidants that it contained.

However, maintaining viable bacteria in the dried state is another challenge, as dehydration of the cell can be fatal. To the best of our knowledge, only one study can be found in the literature that has looked at the stability of this strain in the dried state (Prasad, McJarrow, & Gopal, 2003). The study showed that heat and osmotically shocked bacteria showed better survival than unstressed bacteria during the storage period. Cells were simply harvested at the end of each treatment, reconstituted in chilled phosphate buffer (0.1 M, pH 7.5) before being fluid-bed dried. The number of previously stressed bacteria reduced by 2 log (CFU/g) after 14 weeks of storage at 30°C, while unstressed bacteria presented a reduction of approximately 8 log (CFU/g) over the same storage period. The increased stability was related to the synthesis of shock proteins, as well as modifications of saccharides improving interactions with cellular biomolecules. The response of the cells to both stresses are further developed in their corresponding sections (sections 2.2.1.3 and 2.2.2.2).

*Lb. rhamnosus* HN001 has thus several recognised health effects. However, little is known on its stability during storage, and more specifically in the dried state with a maximum stability of 2 log reduction over 3.5 months at 30°C. Therefore, there is a real potential to improve its shelf-life and to render it more stable, so it can be accessible to a higher number of people.

## **2.2 Drying related stresses and their responses in lactic acid bacteria**

Drying of the bacteria comes with different stresses depending on the method used. Water can be removed by direct heating and evaporation of the water, or by freezing and sublimation of the water. In addition to the drying stresses, numerous stresses are associated with the preparation, drying and storage of the probiotics, and knowledge of these will help target the sites that need protection and allow exploitation of natural stress responses. Different stresses endured by probiotics can be sorted depending on when they occur i.e. before the drying, during the drying or during the storage.

### **2.2.1 Stresses experienced prior to drying**

Before the drying step, bacterial cells will endure various stresses while still being in their original, viable or active biological state. The response to the stresses will hence also be active. Bacteria can change their metabolism, upregulate or downregulate genes, uptake components from the media, and even change the composition of their cell wall to protect themselves.

The first stresses occurring are mostly related to the growth of the bacteria, such as a drop in the pH of the culture, or the lack of various nutrients in the media. These stresses will lead to the start of the stationary phase where the cell growth will slow down and reach a plateau following the different stresses. However, the cells will gain resistance as the stress response mechanism will take place within the cells, and this is why the start of the stationary phase is known to lead to more resistant bacteria.

In the next section, the main stress responses will be described to try and understand what type of response can improve the overall resistance of stresses. Oxygen stress will not be considered as *Lb. rhamnosus* HN001 is a facultative aerobe and can thus handle some level of oxygen.

### 2.2.1.1 Acid stress

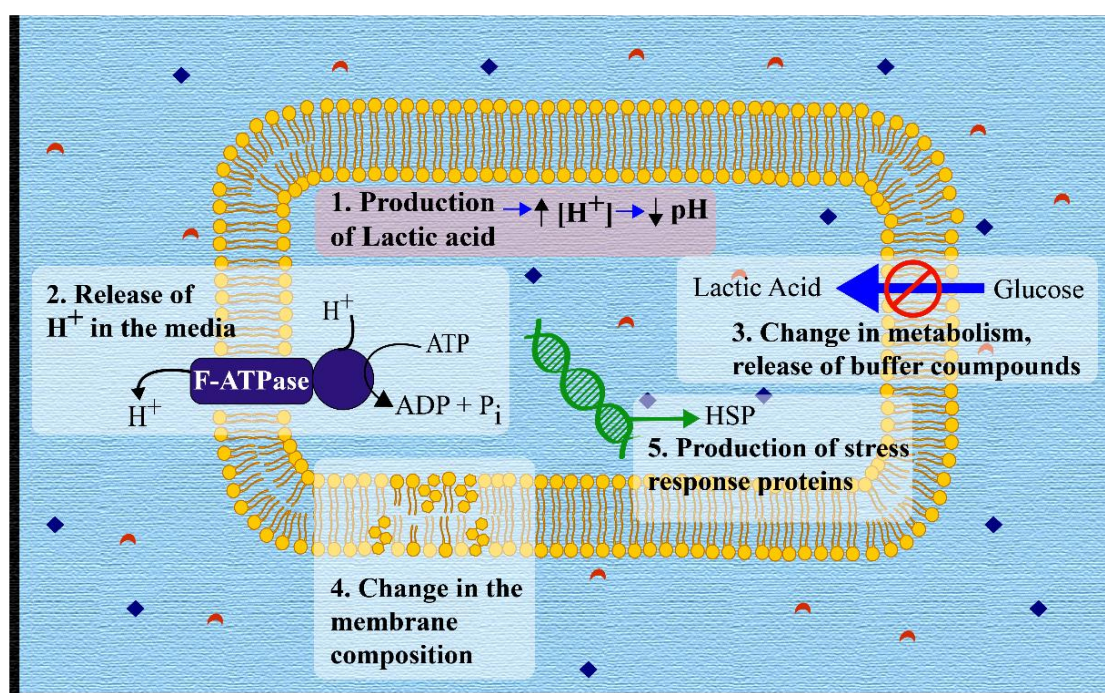
Lactic acid production from the fermentation of lactic acid bacteria is very rapid. For instance, *S. mutans* can decrease the pH by 2 or 3 in just a few minutes (Kajfasz & Quivey, 2011). As the pH is on a log scale a difference of 1 in pH is the result of the production of 10 times more lactic acid. This stress is thus self-imposed, and the overall tolerance of lactic acid bacteria in lower pH environment gives them a significant advantage against other bacteria. The overall stress response mechanism of the bacterial cells is summarised in Figure 2.1.

As a first response the F-ATPase will pump the proton out of the cytoplasm, at the expense of ATP, in order to maintain internal homeostasis. The amount of F-ATPase is directly related to the acid tolerance of the cells (Kajfasz & Quivey, 2011). The higher the amount of F-ATPase in the cell indicates that the bacteria have a lower optimum pH for growth. Therefore, if bacteria are grown at a pH that is lower than optimum, they will tend to have a higher amount of F-ATPase. Alternatively, the cells will change their metabolism in order to release molecules to buffer the media, such as ammonia (Tsakalidou & Papadimitriou, 2011).

If the stress is continuously imposed, bacteria will change their cell membrane composition. Cyclisation, saturation and chain shortening of the membrane fatty acids has been found in several *Lactobacillus* (*Lb. casei*, *Lb. helveticus*, *Lb. reuteri* and *Lb. sanfranciscensis*; Broadbent, Larsen, Deibel, & Steele, 2010; Liu, Hou, Zhang, Zeng, & Qiao, 2014; Montanari, Sado Kamdem, Serrazanetti, Etoa, & Guerzoni, 2010). The change in composition will affect both the fluidity of the membrane and its permeability (Wu, Zhang, Wang, Du, & Chen, 2012).

The response to acidic stress can in turn improve the tolerance toward other stresses such as heat, oxidation and freezing. Indeed, when facing acid stress the cells

have been shown to produce some heat shock proteins (van de Guchte et al., 2002). These proteins are mostly chaperones, helping to ensure the proper folding of proteins, and proteases to help remove damaged proteins. In addition, the response of acid stress has been found to be overlapping with oxidative stress response: stressed cells were putting in place DNA repairs normally associated with oxidation (Cappa, Cattivelli, & Cocconcelli, 2005; Hanna, Ferguson, Li, & Cvitkovitch, 2001). Finally, Streit, Delettre, Corrieu, and Béal (2008) showed that *Lactobacillus delbrueckii* subs. *Bulgaricus* were more resistant to freezing after facing an acid stress.



**Figure 2.1:** Main stress responses of the bacterial cells following an acid stress. HSP stands for heat shock proteins.

Extreme acidic conditions may decrease the activity of some transporters, thereby diminishing the availability of essential substrates (Papadimitriou et al., 2016). Acid stress and starvation are thus interrelated.

### 2.2.1.2 Starvation stress

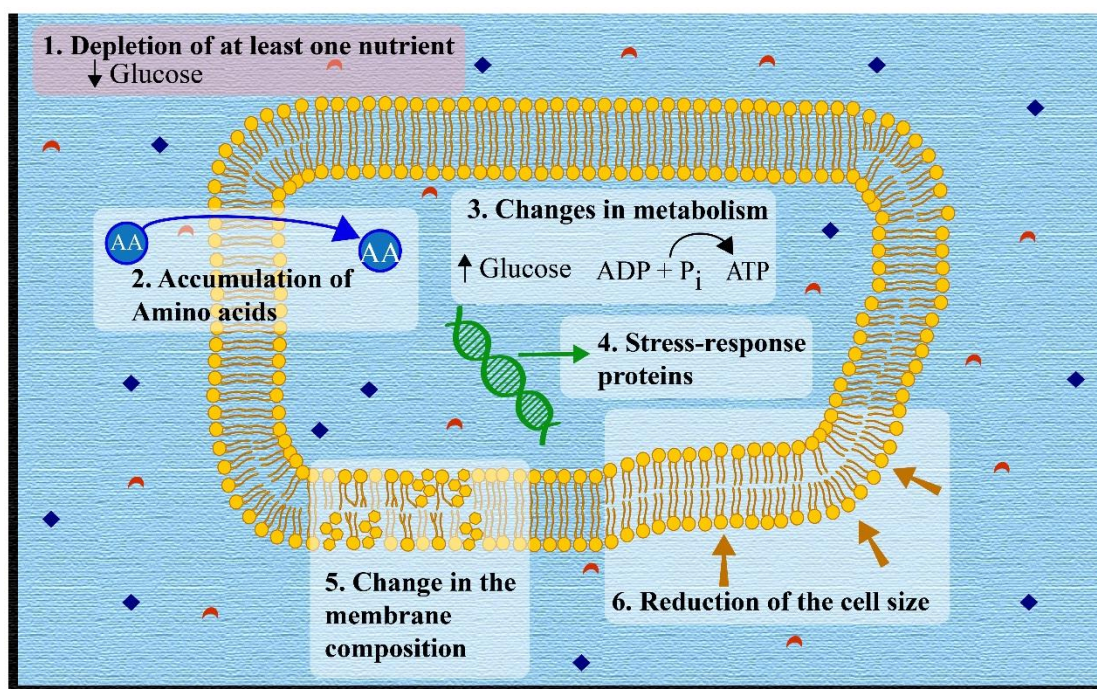
Starvation is defined as the depletion of at least one nutrient and the main mechanisms of response are presented below (Figure 2.2). As just mentioned, it can be provoked by other stresses such as acid stress, preventing the entry or use of nutrients into the cell.

When glucose is depleted from the media, the cells will start accumulating and consuming amino-acids, as found in *Lb. plantarum* (He et al., 2018). In this study, it was also shown that the cells started to produce glucose, and increase their production of ATP. Under lactose starvation, independent from the growth phase, *Lactobacillus acidophilus* RD758 increased the production of proteins involved in carbohydrate and energy metabolism as well as in pH homeostasis (Wang, Delettre, Corrieu, & Béal, 2011). This production of stress response proteins was one of the proposed reasons why this strain gained cryotolerance after facing the starvation stress. A second stress response was also identified in this study as a potential explanation for the enhanced cryotolerance. This was the change in membrane fluidity: *Lactobacillus acidophilus* increased the synthesis of unsaturated, cyclic and branched fatty acids to the detriment of saturated fatty acids. Similarly, the increase in the ratio of unsaturated fatty acids to saturated fatty acids in *Lactobacillus reuteri* was correlated to higher survival after freeze-drying (Liu et al., 2014).

Another factor which will change following starvation is the cell size (Giard, Rince, Capiiaux, Auffray, & Hartke, 2000; Hartke, Giard, Laplace, & Auffray, 1998). Under depletion of glucose or Tween 80, *Lb. plantarum* cells varied in size and shape. Although the membrane was still intact, its structure was rough with dense, fibre like protrusions. In the absence of glucose the shape of the cells changed from rod-shape to coccoid (Parlindungan, Dekiwadia, Tran, Jones, & May, 2018). He et al. (2018) also



found the cell envelope of *Lb. plantarum* was altered when the media was depleted of glucose. Senz, van Lengerich, Bader, and Stahl (2015) showed a correlation between the cellular morphology of *Lb. acidophilus* and the nutrients present in the growth medium. The morphology of the cells could also be correlated to their stability during freeze-drying, extrusion and the subsequent storage period. Overall, shorter cells were more stable than longer cells. In a study by Erlebach, Illmer, and Schinner (2000), the cell size was followed during the growth of the bacteria. The size of the cells decreased as the number of cells increased. The stationary phase was marked by a plateau in cell number as well as in cell size. This emphasises the observation that cells which are allowed to enter into the stationary phase develop better overall stress resistance.



**Figure 2.2:** Main stress responses of the bacterial cells following a starvation stress.

After bacteria have been grown, and during the handling prior to the drying, two other stresses often occur: the change in the osmotic pressure and a drop in temperature.

### 2.2.1.3 Cold stress

Cold stress is defined as a decrease in temperature below that which is optimal for growth of the bacteria. This stress can be divided into two parts: cold but positive temperatures, or sub-zero temperatures. Sub-zero temperatures, leading to freezing stress, will be covered in the following section (2.2.2.1), as it is related to storage, and to freeze-drying.

The lower the temperature, the longer it will take for the cell to actively respond. The time the cell needs to respond to the cold stress is in the order of hours, contrary to the acid, starvation or even osmotic and heat stresses where the cells generally respond within a matter of minutes (Derzelle et al., 2000).

The first major change that occurs is the change in membrane fluidity (Meneghel, Passot, Dupont, & Fonseca, 2017). As the temperature lowers to a certain point, the membrane lipids go through phase transition: from a liquid-crystalline state to a solid-like state. The phase transition of *Lb. helveticus* was found to be at 15.5 and 37.5, while for *E. coli* and *B. thuringiensis* it was around 10°C (Leslie, Israeli, Lighthart, Crowe, & Crowe, 1995; Santivarangkna, Naumann, Kulozik, & Foerst, 2010). It is not unusual to measure different phase transition of the membrane within a single organism, as the membrane is heterogeneous. As a result of the phase transition, the function associated with the membrane, such as transport of metabolites, will be affected. The change in membrane fluidity might be the first cold sensor of the cells. Second, the DNA and RNA topology will evolve toward the supercoil structure (López-García & Forterre, 2000). This will lead to a decrease in mRNA translation and transcription, with protein folding being slowed down or inefficient.

The metabolism will also be disturbed. In *Lb. plantarum*, the ATPase activity was significantly reduced after 1 hour at 5°C. However, the ATPase activity increased above

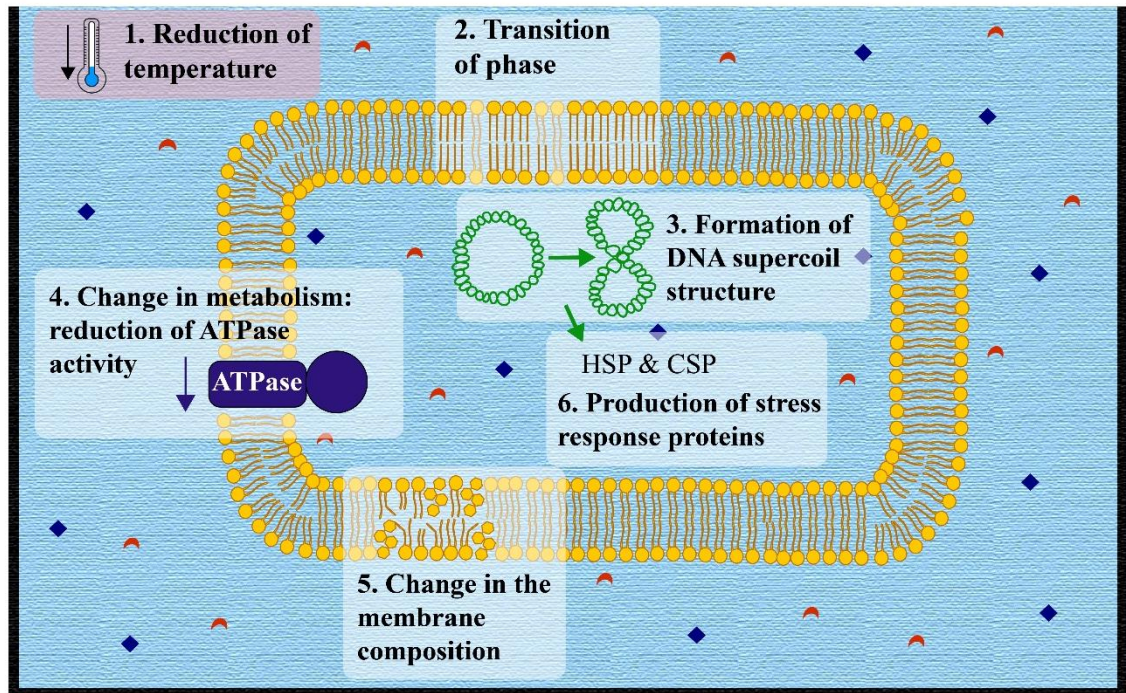
its standard value after 4 hours under the cold stress, before returning to a normal level after 6 hours (Song, Bae, Lim, Griffiths, & Oh, 2014). In this study it was postulated that the ATPase activity was involved in trying to maintain membrane fluidity. Overall, it would seem that all the cell mechanisms (and as a consequence cell growth) are slowed down or stopped in response to cold stress.

Eventually, the cells will adapt to the stress. *Lactobacillus reuteri* reduced the ratio of unsaturated fatty acids to saturated fatty acids in the membrane, from 1.45 for the control to 1.36 when grown at 27°C and 1.29 when grown at 4°C (Liu et al., 2014). A study following *Lb. helveticus* and *Lb. sanfranciscensis* under cold shock (2 hours at 10°C) suggested that the strategies used by the cells to maintain the membrane fluidity and functionality are strain dependent (Montanari et al., 2010). In this study, it was found that *Lb. helveticus* increased the proportion of cyclopropane fatty acids, while *Lb. sanfranciscensis* shortened the carbon chain length of membrane fatty acids.

Interestingly, the synthesis of cold shock proteins is not only found as a result of a cold shock, but also during specific stages of the bacterial growth (Derzelle et al., 2000). Although, the overall mechanism of these cold shock proteins are not fully understood, it is obvious that they act as transcriptional and translational regulators, and as molecular chaperones (Tsakalidou & Papadimitriou, 2011).

Finally, the synthesis of some heat shock proteins have also been found to be triggered by cold stresses (Song et al., 2014; Tsakalidou & Papadimitriou, 2011). These proteins are responsible for removing any improperly folded proteins. This observation is interesting as the heat shock proteins and cold shock proteins are normally regulated antagonistically, but it would very much depend on the strain and the protein in question.

The overall stress response to cold stress is presented below, in Figure 2.3.



**Figure 2.3:** Main stress responses of the bacterial cells following a cold stress.

Cold shock responses are thus not independent and seem to have a cross-linked effect with other stresses, such as the synthesis of heat shock proteins or the increase in unsaturated fatty acids observed after acid or osmotic stresses.

#### 2.2.1.4 Osmotic pressure

A change in osmotic pressure is very common in the handling and production of lactic acid bacteria. It happens every time the external osmolarity changes, i.e. the molar concentrations of solutes around the cells increases (hyperosmotic stress) or decreases (hypoosmotic stress). As a first response, the cell will try to re-establish the pressure inside the cells. This pressure, also called Turgor pressure, is maintained in normal conditions by the accumulation of solutes in the cytoplasm, more than the required concentration for metabolism. This ensures the water is flowing into the cells during the growth of the bacteria. When facing a hyperosmotic stress (Figure 2.4) the cell will take

up solutes from the surrounding environment and will release water. This stress is, therefore, often the predominant one in the manufacturing of lactic acid bacteria, and will be thus covered in this section.

The cells can sense the change in osmotic pressure thanks to their mechanosensitive channel, which responds to tension in the membrane usually created by a rapid change in the cell volume (Poolman, Spitzer, & Wood, 2004; Wood et al., 2001). In addition, the voltage-gated ion channel also helps the cells respond to the stress. A study from Lorca et al. (2007) showed that the genes of 11 lactic acid bacteria encode for more transport proteins than other bacteria (between 13 and 18% of their genes). This figure gives an idea of the importance of solute and water transport in the resistance of osmotic stress by lactic acid bacteria. Water is released from the cells by diffusion or thanks to aquaporins. If the hyperosmotic stress is maintained, the synthesis of aquaporins can increase as was shown for *Brucella abortus* (Hernandez-Castro, Rodriguez, Seoane, & Garcia Lobo, 2003).

In parallel, the cells will uptake some solute from the media. Here again bacteria can speed up the uptake of solutes by upregulating the expression of some transporters (Prasad et al., 2003; Xie, Chou, Cutler, & Weimer, 2004). This latter study on *Lc. lactis*, showed a preference in the solutes as the betaine ABC transporters were upregulated, whereas other transporters were unchanged or downregulated. Glycine betaine has been shown in a number of studies to be a preferred osmoprotectant i.e. a solute protecting from osmotic shock (Glaasker, Konings, & Poolman, 1996; Glaasker, Tjan, Ter Steeg, Konings, & Poolman, 1998; Hutkins, Ellefson, & Kashket, 1987; Sheehan, Sleator, Fitzgerald, & Hill, 2006; Zhao et al., 2014).

It is also important to note here the difference between an ionic and non-ionic osmotic stress. In the case of a non-ionic stress, cells are able to accumulate the osmolytes



present in the system, which is not the case for an ionic stress (Glaasker et al., 1996; Glaasker et al., 1998; Molina-Höppner, Doster, Vogel, & Gänzle, 2004). For instance, sugars can enter the cells through facilitated diffusion, following the concentration gradient (Glaasker et al., 1998), and thus the stress imposed by sugars would be less harsh on the cell than when imposed by ionic solutes. In this study, *Lb. plantarum* did not take up a significant amount of glycine betaine when faced with a lactose or sucrose hyperosmotic stress. However, when the cells were exposed to a KCl stress, glycine betaine uptake was increased. The addition of this osmoprotectant could alleviate the growth inhibition caused by KCl or NaCl. On the other hand, sugar could enter the cells following the gradient concentration, and thus relieve the hyperosmotic stress imposed by them. The researchers postulated that the increase in the intracellular concentration of salts might inhibit growth by binding to macromolecules. Therefore, glycine betaine could alleviate the growth inhibition by stabilising macromolecules (Glaasker et al., 1996). Thus, a non-ionic stress would be only momentous, as the cell can adapt quickly, and thus be less harsh compared to an ionic stress. Similar results were found for *Lb. rhamnosus* and *Lc. lactis* (Molina-Höppner et al., 2004; Prasad et al., 2003). In both studies, the osmotic shock had a protective effect toward drying and high-pressure treatment, respectively. In the study from Molina-Höppner et al. (2004), the protective effect of ionic solutes was indirect, as it caused the accumulation of disaccharides, whereas cells exposed to high concentration of sucrose were directly protected by the presence of sucrose in the system as well as in the cytoplasm. In a study, by Prasad et al. (2003), osmotically shocked cells presented with lower levels of free glycerol, and higher levels of modified oligosaccharides than the control. They postulated that the glycerol was reacting with the reducing terminus of the saccharides. The resulting solutes would present an increase in the number of hydroxyl groups which would then improve the

interaction with cellular macromolecules (via hydrogen bonding) and hence protect them from dehydration.

As a result of the movements of water and solutes in and out the cells, the cell size and morphology are constantly changing. As shown by Gong, Yu, Chen, and Han (2012) *Lb. salivarius* cells shrunk following their growth under hyperosmotic conditions, and their cells surface properties changed. Morphological changes have also been found in *Listeria monocytogenes* (Bereksi, Gavini, Bénézech, & Faille, 2002) and *Lb. plantarum* (Pieterse, Leer, Schuren, & van der Werf, 2005). It was also shown that cells could change their metabolism activity in response to an osmotic shock (Xie et al., 2004). For instance, *Lb. bulgaricus* increased the level of glycolytic enzymes when facing NaCl stress (Li, Sun, Qi, & Liu, 2015).

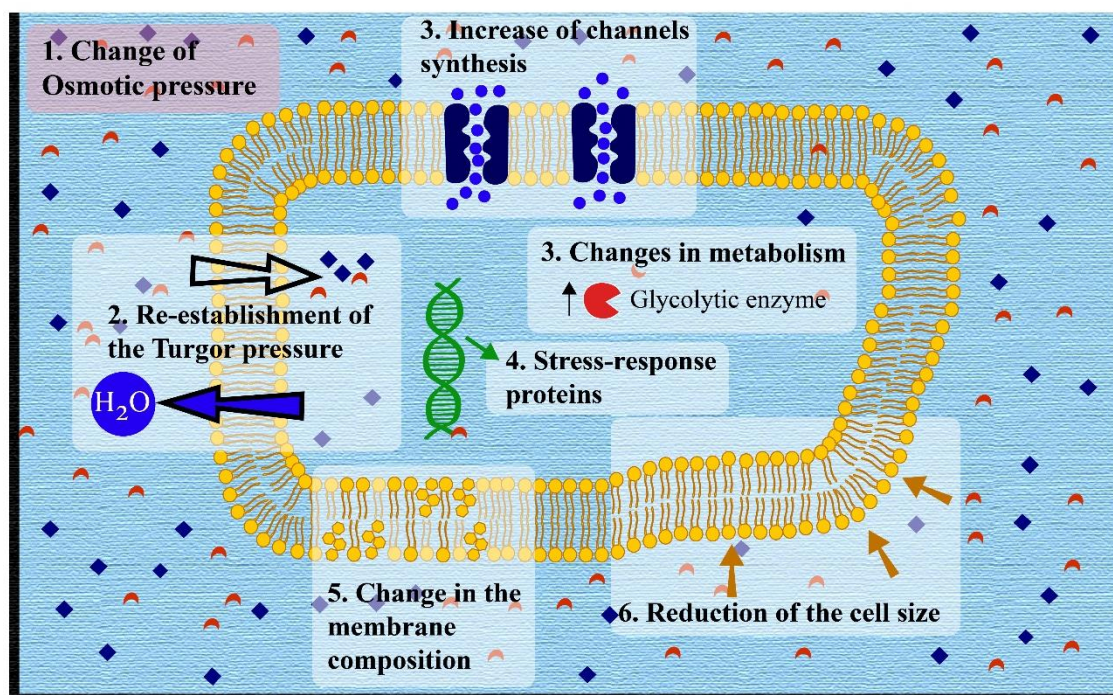
The membrane is another main location of the stress response. The fluidity, and the composition of the cell membrane can change. It was reported that when *Lb. salivarius* was facing an osmotic stress induced by NaCl, the ratio of saturated to unsaturated fatty acids increased, as well as the amount of cyclopropaneoctanoic acid (Gong et al., 2012). When *Lb. bulgaricus* faced a hyperosmotic stress, induced by polyethylene glycol, its membrane became more rigid (Tymczyszyn, Gómez-Zavaglia, & Disalvo, 2005). However, other studies have shown that membrane fluidity can remain unchanged, as was the case with *Lactococcus lactis*, but the number of cyclopropane fatty acids in the membrane clearly increased (Guillot, Obis, & Mistou, 2000). A similar stress response was found against cold and acid stresses for *Lb. bulgaricus* and *Lb. sanfranciscensis* (Montanari et al., 2010). In this study they discussed that the presence of cyclopropane fatty acids could improve the chemical properties and protect from oxidative stresses by acting as a barrier to protons or other chemicals. Conversely, *Lb. casei* presented altered proton permeability and packing of lipids when grown under hyperosmotic conditions

(Machado, López, Heras, & Rivas, 2004). These changes in the membrane can also affect the movement of water in and out of the cells, as well as the mechanical resistance of the cells resulting from the change in pressure. Mechanical strength could be induced by a change in the thickness of the membrane and the cell. When *Lb. acidophilus* was facing a high salt concentration in the stationary phase the S-layers proteins increased. This could be compensating for the cell wall and peptidoglycan reduction (Palomino et al., 2016).

Change in the membrane can also be due to the direct interaction between the membrane and the solutes in the environment. In a study, by Meneghel et al. (2017) they compared two different *Lb. bulgaricus* strains facing osmotic stress before freeze-drying, and found a major disorganisation of phospholipid head groups for the more sensitive strain, *Lb. bulgaricus* CFL1. It was postulated that sucrose was replacing water to form hydrogen bonds with the phospholipid head groups leading to the aforementioned membrane disruption. This finding is interesting, as it goes against some former theories which indicated that the replacement of water by osmoprotectants could protect from dehydration (Albertorio, Chapa, Chen, Diaz, & Cremer, 2007; Crowe et al., 1988; Leslie et al., 1995).

When facing an increase in osmotic pressure, cells will prepare themselves for dehydration, which could explain why pre-stressing the cells with osmotic shock can give more resistance towards dehydration than other type of stresses (Molina-Höppner et al., 2004; Nag & Das, 2013; Prasad et al., 2003). The response to this stress is complex but fast, for instance 30 min with 4% of NaCl was enough for *Lc. lactis* to up or downregulate 68 genes (Xie et al., 2004). Interestingly, *Lc. lactis* altered the expression of less genes when it was faced with a heat or acid stress (64 and 50 genes respectively). This could be because osmotic stress is a more frequent stress for lactic acid bacteria.





**Figure 2.4:** Main stress responses of the bacterial cells following a hyperosmotic stress.

### 2.2.1.5 Analogies between the different stresses

The cells membrane is the first cell location affected by the stresses. Changes are numerous: transporters can change in numbers or in affinity, the fluidity of the membrane can evolve, the composition can also change, as well as the thickness of the different layers constituting the membrane. Most of the cell responses are similar in different stresses, and various stress response proteins are found to be expressed in different stress environments. For instance in *Lactococcus lactis* ten genes were expressed similarly for both heat and osmotic treatments, six genes for acid and heat, and eight genes for osmotic and acid stresses (Xie et al., 2004). As a result, sub-lethal stresses can often lead to the overall resistance of the cells.

Finally the size and shape of the cell can also change. This will impact the volume to surface ratio, and can also give extra resistance to the cells (Senz et al., 2015).

Overall, the cells protect themselves from cell membrane and intracellular biomolecule damage. Later if the cells are dried, they will endure additional stresses, but the response in place can help them survive.

## **2.2.2 Dehydration related stresses**

As introduced earlier, drying of probiotics often involves a heating or freezing step. Thus, drying of bacteria can be divided into three individual stresses: heating, freezing and dehydration.

### **2.2.2.1 Freezing**

As the temperature goes down, the membrane will go through a phase transition: from a liquid-crystalline to a solid-like and ordered state. Membranes become more rigid and less fluid. The phase transition temperature generally ranges from -8°C to 38°C, and is dependent on the strain, the growth conditions and any potential stress previously endured (Gautier et al., 2013; Leslie et al., 1995; Santivarangkna et al., 2010). A lower phase transition temperature is correlated with a higher ratio of unsaturated or cyclic fatty acids in the membrane (Gautier et al., 2013; Meneghel et al., 2017), and means the membrane will be more fluid. Cells with a lower phase transition temperature have been shown to be more resistant to the freezing (Gautier et al., 2013; Meneghel et al., 2017). As previously mentioned, cells can change the composition of their membrane, to make it more fluid, following a cold shock (Liu et al., 2014; Montanari et al., 2010), an acid stress (Broadbent et al., 2010; Liu et al., 2014; Montanari et al., 2010) or an osmotic shock (Montanari et al., 2010; Tymoczyszyn et al., 2005).

The composition of the environment also has an impact on the membrane phase transition temperature. *Lc. lactis* phase transition lowered from 21.4°C in buffer, to 16.8°C in the presence of sucrose and 16.6°C in presence of NaCl (Molina-Höppner et

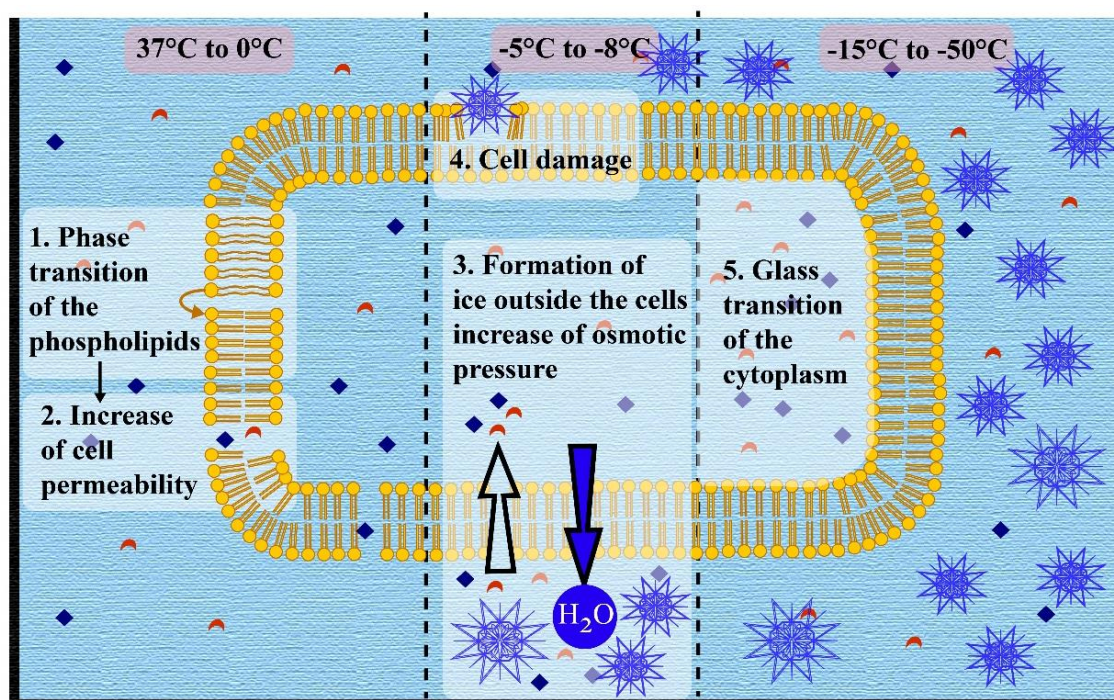
al., 2004). Interestingly, when comparing two *Lb. bulgaricus* strains, Meneghel et al. (2017) found that sucrose was directly interacting with the membrane of the cryo-sensitive strain. As a result, sucrose could replace water in the surrounding area of the phospholipid head group, and altered the membrane integrity. On the other hand, a more cryoresistant strain could keep its membrane hydrated. They postulated that sucrose was preferentially excluded from the vicinity of the membrane, and was thus helping the cell to maintain its integrity.

As a result of phase change, the membrane becomes more permeable and solutes can easily flow down their concentration gradient. This permeability can be useful if the cells are put in a protectant solution. For instance, Leslie et al. (1995) showed that trehalose was entering *B. thuringiensis* cells only at temperatures below 15°C, which could help protect the bacteria in the dried state, by interacting with the biomolecules in the cytoplasm.

Between -5°C to -8°C, ice will form outside the cells. The presence of ice crystals can cause damage to the cell tissues, and can cause cell loss (Venketesh & Dayananda, 2008). The bigger the crystals are, the more damage they cause to the cells (Schoug, Olsson, Carlfors, Schnürer, & Håkansson, 2006). However, cryoprotectant compounds can prevent the growth of ice crystals. As the water goes from liquid to solid state, the solutes are becoming more concentrated in the remaining liquid. This can lead to an increase in the osmotic pressure. The water will flow out of the cells, and the solutes will flow into the cells. As the osmotic pressure increases, the cells will release water and the concentration of the intracellular solutes will increase. As a result, intracellular glass transition would be induced before ice nucleation, between -15°C and -50°C, depending on the growth stage of the bacteria, and the environment (Fonseca, Meneghel, Cenard, Passot, & Morris, 2016). Compared to eukaryote cells, ice nucleation is less likely to

occur, as the intracellular concentration is higher in prokaryotes (Mika & Poolman, 2011). However, it may still happen when the cells are frozen in distilled water (Fonseca, Marin, & Morris, 2006), and if the cooling occurs faster than the outer flow of water (Dumont, Marechal, & Gervais, 2004). Formation of intracellular ice may disrupt the cells, and is thus to be avoided. Once the intracellular medium goes through glass transition, all molecular movements are stopped and the cells become osmotically inactive. It has been showed that the addition of penetrating cryoprotectants can lower the intracellular glass transition, and protect the cell from the freezing stress (Fonseca et al., 2016). However, it is not clear if it is the presence of protectants themselves or the decrease in the glass transition temperature that results in an increase in the survival of the cells. In addition, the cell morphology might also affect the survivability of the cells to the freezing process by facilitating the exchange with the surrounding environment when increasing the surface to volume ratio of the cells (Fonseca, Béal, & Corrieu, 2000; Mazur, 1984).

More recently, it has been shown that the osmotic stress can be more detrimental than cold stress, during freezing (Meneghel et al., 2017). Ultimately, we understand the importance for the cells to adapt to this osmotic stress, and thus to maintain their membrane in an optimum state to be able to exchange solute and water with the surrounding environment. On the other hand, the impact of freezing on proteins and nucleic acids has been less studied than the membrane. It is known that the DNA and RNA will form a supercoil structure when the temperature goes down (López-García & Forterre, 2000). Recently it has been shown that freezing can also affect the secondary structure of proteins, but some protectants (e.g. sucrose) can preserve the native form of the proteins (Passot et al., 2015). The overall process of cell freezing is summarised below in Figure 2.5.



**Figure 2.5:** Main processes of freezing stress endured by the bacteria.

#### 2.2.2.2 Heat

Heat shock is qualified as a sudden increase in the temperature. It implies conformational changes of the cell macromolecules, as well as the expression of several heat shock proteins. The cell response is relatively rapid, and occurs in the order of minutes. This section will focus on the conformational changes occurring in the cells, relative to the heat occurring during drying.

Heat shock proteins have been widely described and reviewed (Papadimitriou et al., 2016; Prasad et al., 2003; van de Guchte et al., 2002). Their function is indicative of the physical changes occurring in the cell when the temperature increases above the optimum growth temperature. These proteins mostly consist of chaperones or proteases, meaning that temperature increase would mostly affect proteins and nucleic acid. It was

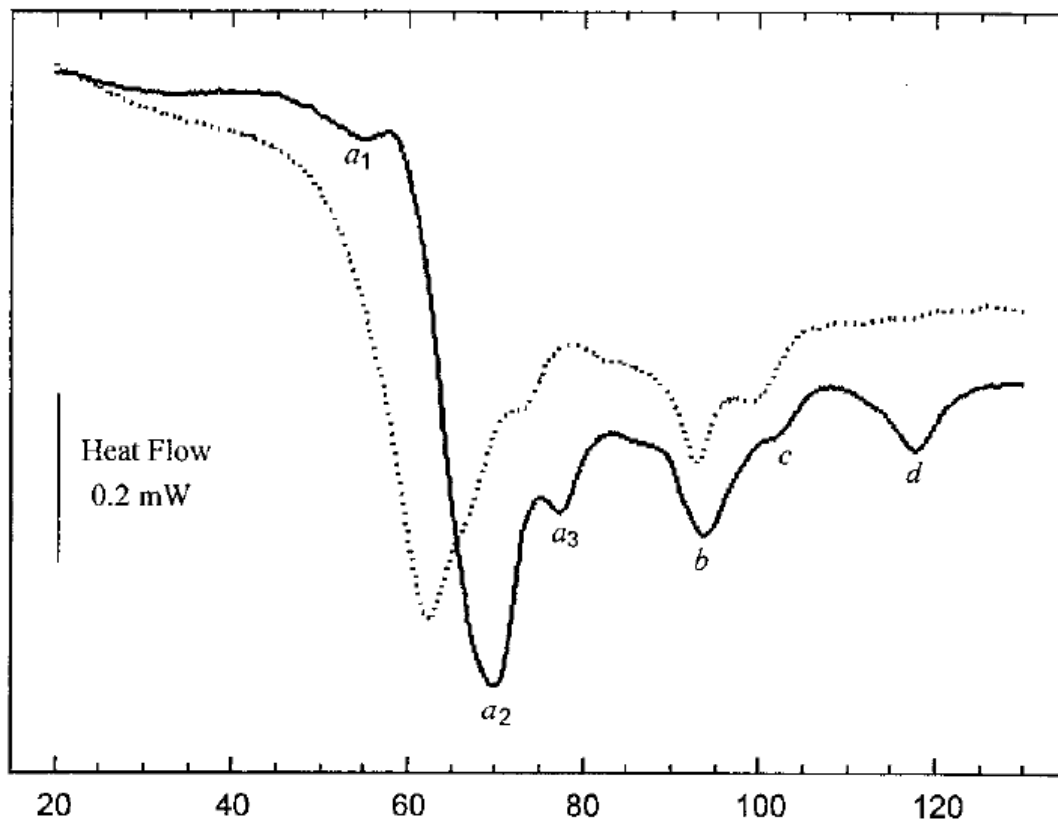


also shown with *Lb. plantarum* that a heat shock protein can lower membrane fluidity in order to protect the membrane from heat treatment (Capozzi et al., 2011).

Indeed, heat will firstly impact the cell membrane (Teixeira, Castro, Mohácsi-Farkas, & Kirby, 1997). When *Lb. bulgaricus* was facing a heat treatment from 62 to 66°C, there was a clear drop in the survival of cells treated at 65°C and above. The cells treated below 65°C presented an altered cytoplasmic membrane, the first cell location to be damaged. When heated to 65°C or above the cell wall and proteins seemed to have been altered, explaining the drop in survivability. Their findings were confirmed using calorimetry. Freshly harvested bacteria were run on a DSC from 10 to 120°C at 10°C/min. Ten major denaturation events were found and the main events were identified. Melting of lipids occurred at 45°C and 51°C, the denaturation of ribosome happened between 61°C and 80°C, and the melting of DNA took place around 90°C. Similar thermogram were found for other bacteria, including from the *Lactobacillus* genus (Brannan, Whelan, Cole, & Booth, 2015; Lee & Kaletunç, 2002; Mackey, Miles, Parsons, & Seymour, 1991; Miles, Mackey, & Parsons, 1986; Mohácsi-Farkas, Farkas, Mészáros, Reichart, & Andrassy, 1999; Tunick, Novak, Bayles, Lee, & Kaletunç, 2009). One of those thermogram is shown in Figure 2.6. It has been shown that the higher the denaturation temperatures of biomolecules are, the more thermally stable the cells are overall (Anderson, Hedges, Jones, & Cole, 1991; Miles et al., 1986). In addition, it was shown that presence of NaCl or polyamines could increase the melting temperature of DNA (Esposito, Del Vecchio, & Barone, 1997; Miles et al., 1986). This confirms that drying the cells within a protective matrix is one of the best ways of preserving the viability of probiotics.

The drying method for bacteria using the highest temperature is spray drying (see section 2.3.1.1), with inlet temperatures ranging from 100°C to 150°C. However, the

actual droplet temperature, or wet-bulb temperature, ranges from 20 to 60°C lower than the inlet temperature because of the cooling effect of water vaporisation (Lisboa, Duarte, & Cavalcanti-Mata, 2018). Thus, the temperature does not often exceed 100°C. It is, thus, unlikely to see DNA melting during heat-induced drying. Nevertheless, Hlaing et al. (2017) showed that there was more structural alteration in the backbone of the DNA when *Lb. rhamnosus* GG was spray-dried, with an inlet temperature of 160°C and an outlet temperature of 65°C, than when the bacteria were freeze-dried.



**Figure 2.6:** Thermograms of whole cells of *E. coli* (solid line) and *Lb. plantarum* (dotted line) obtained by DSC (heating rate of 3°C/min). Endothermic events are down, with the denaturation of the ribosome in a1, a2 and a3 with the 30S subunit suggested to be a1, the DNA melting in b, denaturation of cell wall components in c and d. Results are taken from Lee and Kaletunç (2002).

### 2.2.2.3 Dehydration

Dehydration stress is triggered by an increase in osmotic pressure. The water is either removed from the system, or frozen. When water is frozen, ice crystals will take most of the space and concentrate solutes, thus the cell will release water into the media, and dehydrate the cells.

In the hydrated state, the cell membrane's phospholipids exhibit a two-dimensional fluidity. Water acts as a stabiliser as it interacts with the phospholipids by forming hydrogen bonds with the polar groups. Removal of water decreases the area occupied by each of the head groups, resulting in the increase of Van der Waal's forces (Crowe et al., 1988). This causes large compressive stresses in the plane of the membrane and increases the phase transition temperature ( $T_m$ ). For instance, Linders, Wolkers, Hoekstra, and van 't Riet (1997) showed that the membrane phase transition temperature ( $T_m$ ) of hydrated *Lactobacillus plantarum* was 4°C, but this increased to 20°C when dried. Ultimately, the membrane phospholipids would supposedly undergo a phase transition, from liquid crystalline to gel (Wolfe, 1987). As bio-membranes are heterogeneous and possess different classes of lipids they are most likely to go through phase transition at different temperatures. For instance, Santivarangkna et al. (2010) showed that *Lb. helveticus* possessed two clear phase transitions: at 15.5°C and at 37.5°C. Liquid and gel domains will thus coexist over this temperature range (Crowe, Hoekstra, & Crowe, 1989). Leakage would then result from the packing defect caused by the inhomogeneity between liquid- and solid-like domains.

Similarly, drying can be highly detrimental to protein. In the aqueous state, the tertiary and quaternary structure of the protein is maintained. Dehydration causes unfolding of the protein, leading to the protein becoming inactivated (Crowe, Crowe, Carpenter, & Wistrom, 1987). When *Lb. rhamnosus* GG was freeze-dried or spray-dried,



protein, fatty acids and DNA presented with alterations or conformational changes (Hlaing et al., 2017). Main changes were observed in the DNA and RNA. More specifically, there was a change in conformation from B-DNA (the native form) to A-DNA. It has been shown that A-DNA is a generally more resistant form of DNA, notably, the ability for a cell to change from B-DNA to A-DNA upon dehydration, and back to B-DNA upon re-hydration could be associated with the cells survival (Whelan et al., 2014). The presence of a protective matrix (composed of whey protein isolate, maltodextrin and glucose) was clearly shown to diminish these conformational changes, and maintain the cells in a viable state.

The protection of cells by solutes during dehydration has been attributed to the ability to maintain the protein structure in their native state, and to maintain the membrane integrity. Three main protection mechanisms have been proposed, and are summarised in Figure 2.7. First, solutes could directly interact with the cells macromolecules and replace the water. For instance Prasad et al. (2003) analysed the carbohydrates in the cytoplasm of osmotically stressed *Lb. rhamnosus* HN001. In addition to the usual mono-, di-, tri- and tetrasaccharides they found saccharides modified by glycerol. They concluded that the modification could increase the number of hydroxyl groups for interaction with cellular macromolecules, via hydrogen bonding, under conditions of dehydration. Thus, the macromolecules would be protected against desiccation and improve the storage stability of the bacteria. Replacement of water theory has also been proposed as a mechanism explaining the depression of the phase transition temperature in phospholipid membrane (Leslie et al., 1995; Santivarangkna et al., 2010). Solutes would interact with the phosphate groups of the membrane phospholipids, thus decreasing the Van der Waal's forces between the head group. It has been proposed that the deeper a solute penetrates

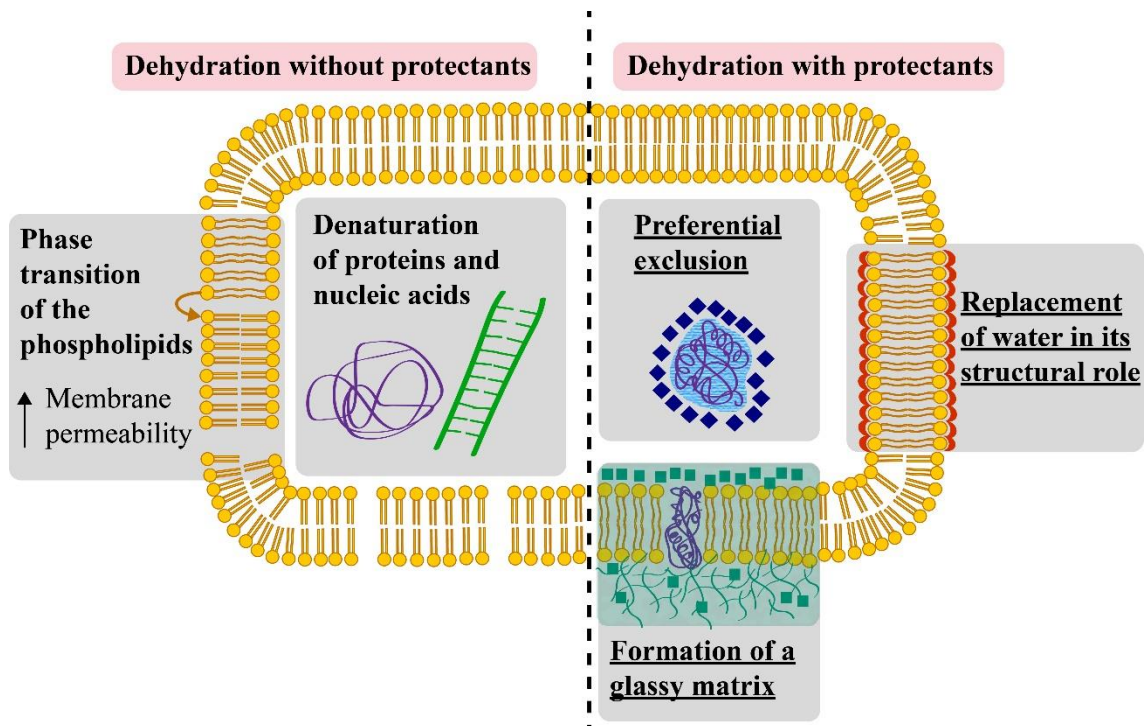
the membrane, or the stronger solutes bond with phospholipids, the better is the protection (Albertorio et al., 2007; Santivarangkna, Higl, & Foerst, 2008).

However, other studies looking at different strains, and different solutes, did not show any depression of the membrane  $T_m$ , or even an increase in the phase transition temperature in the presence of solutes (Linders et al., 1997; Oldenhof, Wolkers, Fonseca, Passot, & Marin, 2005). These differences could be due to the ability of the solute to enter the cells, and interact more directly with the membrane. *Lb. bulgaricus* subs *bulgaricus* CFL1 strain, studied by Oldenhof et al. (2005), was further studied by Meneghel et al. (2017). They found that the sensitivity of this strain toward freezing, was caused by the sucrose interaction with the phospholipids head group that would alter the membrane integrity (see section 2.2.2.1). Instead, the preferential exclusion of sugars from the vicinity of the membrane was the potential protection mechanism. This theory stated that the presence of solutes increases the surface free energy of water, and thus the surface tension of water. As a result, the molecule will be excluded from the water-macromolecule interface. As this is a thermodynamically unfavourable situation, the system will tend to reduce the effect by minimising the area of the water-protein interface, resulting in the stabilisation of the native structure (Arakawa & Timasheff, 1985; Bolen & Baskakov, 2001; Liu & Bolen, 1995). As a result, macromolecules are maintained in a hydrated state, and in their native form, even though the system is dried.

Finally, protective solutes such as sugars, can increase the glass transition temperature ( $T_g$ ) of a dried matrix. The highly viscous matrix can act as a cocoon protecting proteins and lipids from denaturation and slowing down the reaction rates (Jain & Roy, 2009). Oldenhof et al. (2005) showed that a strong glass composed of a mix of sucrose and maltodextrin helped to improve *Lb. bulgaricus* stability compared to a matrix composed of sucrose only. However, cells dried without protectants also presented a

relatively high glass transition temperature, showing that while glass transition improves protection, it is not sufficient on its own.

Overall, this would indicate that these three mechanisms often occur in parallel, and one of them alone is not sufficient to protect the cells. Similarly, different solutes will have different protection mechanisms (such as small sugars compared to a bigger carrier), and might interact differently depending on the strain. A summary of the main stresses occurring during dehydration and the three mechanisms of protection is presented below (Figure 2.7).



**Figure 2.7:** Dehydration stresses endured by the bacterial cells in the absence of protectants (left) and the three protection mechanisms of protective solutes (on the right).

### 2.2.3 Post-drying and storage stresses

Once probiotics are dried, they are still prone to protein denaturation, oxidation, and ultimately, viability loss. The main storage stress is the high temperature of the environment speeding up any chemical or physical reactions, which may be detrimental for the cells. The bacteria death rate ( $k$ ) can be described by the Arrhenius equation:

$$k = a \times e^{-\frac{E_a}{RT}} \quad (2.1)$$

Where  $a$  is the pre-exponential factor,  $E_a$  is the energy of activation,  $R$  the gas constant, and  $T$  the temperature. However, temperature is not the only factor impacting the bacteria. Oxygen and water activity have also been shown to have a significant impact on the viability of the bacteria (Kurtmann, Carlsen, Risbo, & Skibsted, 2009; Teixeira, Castro, & Kirby, 1996; Ying et al., 2010).

#### 2.2.3.1 Oxygen

The presence of oxygen in the environment of dried probiotic is very common, and even if the product is flushed with nitrogen, packaging is not completely impermeable and oxygen will diffuse to some extent over time. In itself, oxygen is mostly detrimental to bifidobacteria, and less so to lactobacillae. However, the reduction of oxygen generates free radicals which can then damage lipids, proteins and DNA (França, Panek, & Eleutherio, 2007). Presence of oxygen has been directly linked to bacterial loss, with the addition of an antioxidant reducing this detrimental effect (Kurtmann, Carlsen, Risbo, et al., 2009). Some protective agents, e.g. sorbitol, mannitol, myo-inositol and proline, have been shown to be effective hydroxyl radical scavengers (Smirnoff & Cumbes, 1989).

#### 2.2.3.2 Water activity

Water activity is the partial vapour pressure of water in the sample divided by the partial pressure of pure water, at the same temperature. It is generally considered as the

amount of water that is not bound to other substances, and that is “free” to chemically react. Water activity values range from 0 for a completely dry material to 1 (100% RH) for pure distilled water. A number of studies have shown that the higher the water activity of the system, the faster the probiotic dies off (Albadran et al., 2015; Harel & Tang, 2014; Kurtmann, Carlsen, Risbo, et al., 2009; Kurtmann, Carlsen, Skibsted, & Risbo, 2009; Tymczyszyn et al., 2012). However, a few studies have shown that extreme desiccation did not improve the stability of dried probiotic, and that an optimum value stands between 0.1 and 0.2, but may depend on the strain (Castro, Teixeira, & Kirby, 1995; Scott, 1959). As water is absorbed onto the matrix, from the dry state toward the monolayer, metal ions are being hydrated, decreasing their catalytic activity, and thus reducing formation of free radicals (Barbosa-Cánovas, Fontana, Schmidt, & Labuza, 2008). Water can also directly quench the free radicals. Finally, water replaces air in the small pores of the powder, and reduces the rate of oxygen diffusion. As a result, the oxidation rate is slowed down. However, if water is absorbed beyond this point, oxygen and metal ion mobility is increased, thus enhancing lipid oxidation (Barbosa-Cánovas et al., 2008).

Similarly, water activity will affect other chemical reactions such as crystallisation, plasticisation of glassy structures or non-enzymatic browning reactions, which in turn, can affect the bacteria stability (Crowe, Carpenter, & Crowe, 1998; Foerst, Kulozik, Schmitt, Bauer, & Santivarangkna, 2012; Kurtmann, Skibsted, & Carlsen, 2009; Miao et al., 2008; Santivarangkna, Aschenbrenner, Kulozik, & Foerst, 2011).

### ***2.2.3.3 Temperature fluctuation***

A final storage stress that has not yet been studied in the literature is the effect that fluctuating temperatures (which can occur during storage or transportation) can have on the viability of dried probiotic products. It has been shown that the temperature can fluctuate between 15 and 60°C in a container travelling over the summer or during periods

of warm weather (Accorsi, Manzini, & Ferrari, 2014; Rodríguez-Bermejo et al., 2007; Singh et al., 2012). Studies looking at the shelf-life of probiotics are generally undertaken at constant temperatures, but never under fluctuating temperatures. A few models have been proposed to follow reaction rates, of any chemical or biochemical change, under fluctuating temperatures (Labuza, 1979; Nunes & Swartzel, 1990). These models predict that the rate of a reaction undergoing fluctuation is greater than under the mean temperature, maintained constant. This was confirmed for reactions such as browning or protein loss (Chen, Bohnsack, & Labuza, 1983; Labuza & Saltmarch, 1982). Similar results could be expected for probiotic stability.

## **2.3 Drying technologies for probiotics preservation**

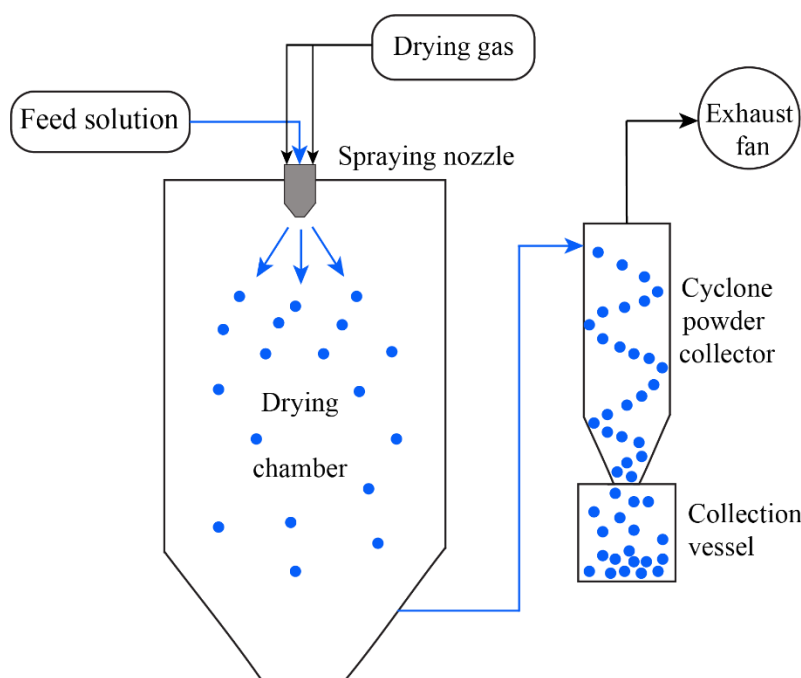
Drying technologies used for the preservation of probiotics range from freeze-drying, vacuum drying, spray drying, fluid-bed drying, drum drying and air-drying to electrospraying. The three main drying methods currently used by the food industry are spray drying, fluid-bed drying and freeze-drying. Each of them comes with numerous benefits and disadvantages as will be discussed in the next section.

### **2.3.1 Main drying methods**

#### ***2.3.1.1 Spray drying***

Spray drying consists of atomising a slurry into a flowing stream of hot gas, usually air. The liquid is sprayed through a small nozzle to form a mist of fine droplets with the drying gas. The atomisation creates high surface-to-volume ratio drops, allowing the particles to dry quickly (Matalanis, Jones, & McClements, 2011). As the drops dry and solidify, they are driven with the gas flow and move to a cyclonic flow chamber, where they drop in the collecting vessel (Figure 2.8). The gas is exhausted to the atmosphere. Inlet temperatures often vary between 100 and 300°C, while outlet

temperatures are often maintained above 70-80°C to favour rapid water vaporisation, even if some studies succeed in maintaining them as low as 45°C (Meng, Stanton, Fitzgerald, Daly, & Ross, 2008; Poddar et al., 2014).



**Figure 2.8:** Spray dryer in a simplified form. Based on Jacobs (2014)

A spray dryer is often used because of its low cost, easiness to scale up, and the good particle size distribution of the final powder (Dormer, Berkland, & Singh, 2014; Oxley, 2014; Yonekura, Sun, Soukoulis, & Fisk, 2014). In addition, formation of an outside coat often occurs when the polymers, acting as surfactants, migrate to the surface and lower the surface tension between air and water (Jayasundera, Adhikari, Aldred, & Ghandi, 2009). This creates a barrier between the bioactives in the core and the environment, which could potentially increase stability during storage (Yonekura et al., 2014).

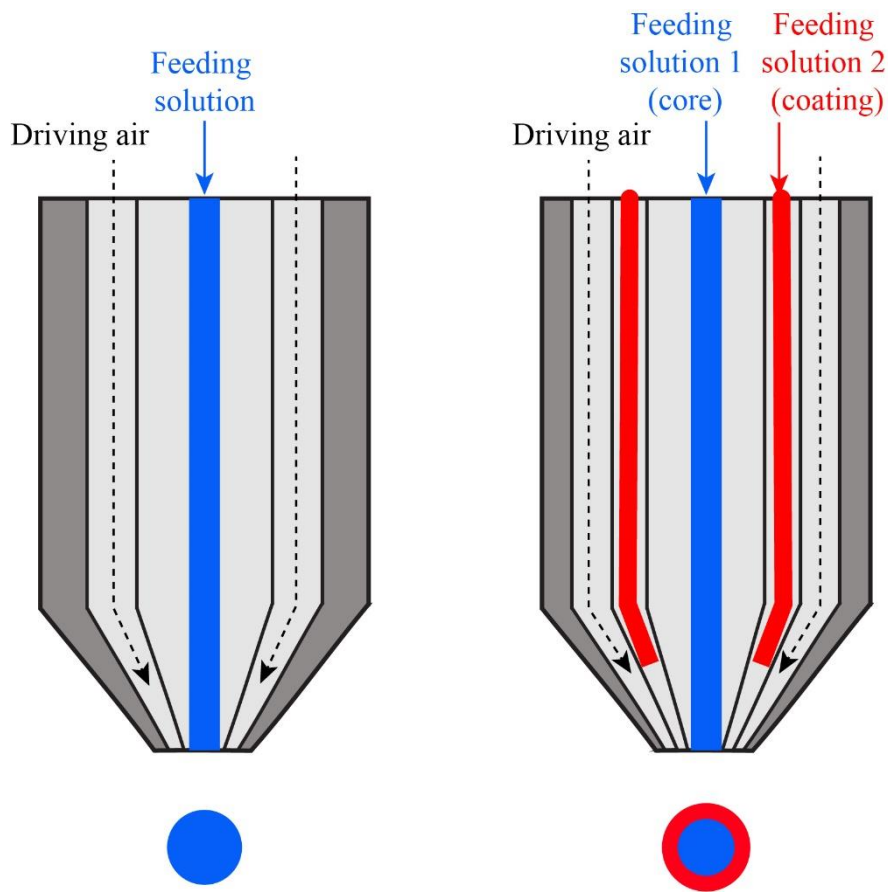
However, spray drying comes with some drawbacks. Firstly, because of the use of elevated temperature, this method is generally not appropriate for drying thermolabile compounds, even if the droplet temperature does not go above the wet-bulb temperature (Jacobs, 2014) as mentioned in section 2.2.2.2. In other words, as the water evaporates, the core is cooled, because of the energy lost during the phase change of water. The wet-bulb temperature, and thus the droplet temperature, is generally between 20 and 60°C lower than the inlet temperature, depending on the initial moisture content (Lisboa et al., 2018). Secondly, the feed solution greatly impacts the drying efficiency. A viscous feeding solution will lead to the formation of elongated and large droplets that negatively impact the drying rate (Rosenberg, Kopelman, & Talmon, 1990).

*Lb. rhamnosus* GG was successfully spray-dried and stored for 28 weeks at room temperature (Broeckx et al., 2017). Inlet temperature was 135°C and outlet was of -60°C. There was a clear improvement in the viability after drying when the protective media was prepared in phosphate buffer. Best storage stability was obtained with lactose and trehalose in phosphate buffer saline, with a loss rate of 0.83 log (CFU/g) and 1.07 log (CFU/g) reduction respectively over the 28 weeks at room temperature.

The common spray nozzle consists of a two-fluid nozzle where the polymer solution to be dried is pumped through the inner channel and the outer channel comprise of the driving gas (e.g. air or nitrogen). More recently new nozzles have been designed to increase the use of spray driers for encapsulating a range of bioactives. For example a three-fluid nozzle allows to spray two immiscible fluid together, e.g. fish oil and whey protein solution (Legako & Dunford, 2010), leading to multi-layer microparticles (Pabari, Sunderland, & Ramtoola, 2012) (Figure 2.9). This nozzle has been used to encapsulate a few thermolabile compounds, such as  $\alpha$ -amylase (Jiang, Zhang, McKnight, & Adhikari, 2013). The nozzle was used to simultaneously form a coacervate of calcium alginate and



chitosan while drying the powder. As a comparison point, the enzyme was dried in a two-step process by first forming the coacervate, then freeze-drying. The spray-dried enzyme was more stable when spray-dried with the three-fluid nozzle and the process was faster than in a two-step encapsulation. However, as far as we know, no bacteria have been dried using this equipment to date.



**Figure 2.9:** Diagram of the two-fluid nozzle (left) and three-fluid nozzle (right) set up of a spray drier.

Adapted from Pabari et al. (2012).

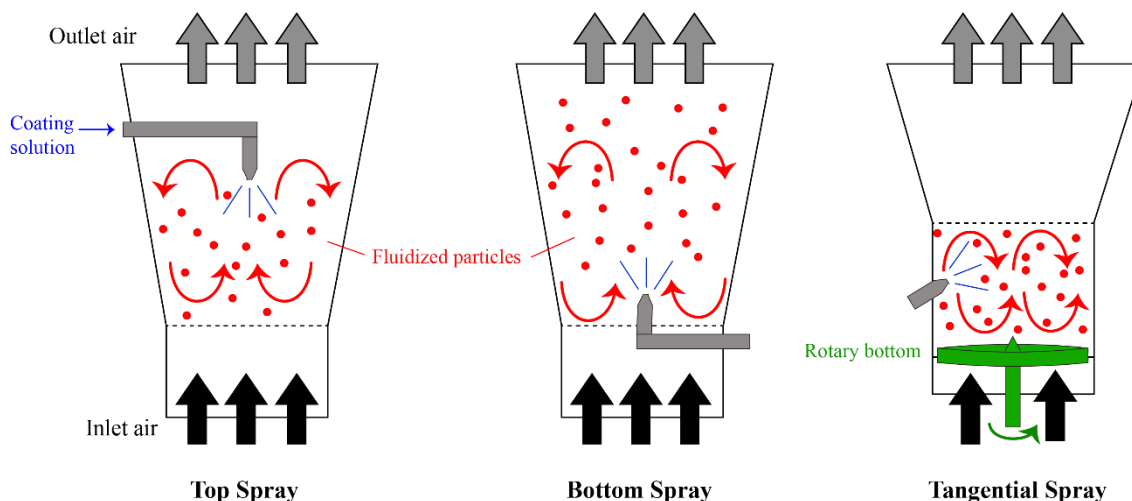
### 2.3.1.2 Fluid-bed Drying

Fluid-bed is a common technique used in the food industry to coat or agglomerate particles. The particles are lifted and suspended due to an airflow pushed or drawn upward. These particles are free to move and act as a fluid. When used for probiotic protection, fluidized bed can be a way to create either dry microcapsules, or coat probiotics by spraying a polymer onto the dispersed probiotics (Mazeaud et al., 2014). The solution can be sprayed through a bottom, top or tangential spray (Figure 2.10). A bottom spray is the most adapted solution for coating particles, while top and tangential sprays are more suited to granulation (Frey, 2014).

Fluid-bed drying has a major advantage for probiotics in that it uses lower temperatures than spray drying, however the exposure tends to be for a longer time. Another advantage is the possibility to coat particles with several layers of different polymers, by feeding the spray with successive solutions. Obviously, the end particles are often much bigger than spray-dried particles - 5 to 7 times bigger (Poddar et al., 2014), and this can be an issue in terms of incorporation into a food product.

*Lb. plantarum* was fluid-bed dried and stored at high temperature (37°C, with water activity between 0.11 and 0.70). Compared to freeze-dried bacteria, fluid-bed dried *Lb. plantarum* was generally more stable over the 45 days of storage, with about 4 log (CFU/g) reduction with an  $a_w$  of 0.11. At 30°C the storage stability was substantially improved with about 0.5 log (CFU/g) reduction for water activity of 0.11, 0.23 and 0.40, while freeze-dried bacteria led to 1 log (CFU/g) reduction over storage. However, when the water activity was raised to 0.70, freeze-dried bacteria demonstrated higher viable stability. Penhasi (2013) patented a technique to layer probiotic with heat absorbing material of increasing melting point (phase change materials), to progressively absorb

heat and protect the core. The methodology used a top spray fluid-bed dryer, and is described further in section 2.5.2.



**Figure 2.10:** Fluid-bed dryer principle, adapted from Frey (2014)

### 2.3.1.3 Freeze-drying

Freeze-drying relies on the sublimation of the water to dry a matrix, and has three major steps: freezing, primary drying and secondary drying (Oetjen & Haseley, 2004).

The rate at which the product is frozen will directly influence the size of the ice crystals as well as the amount of amorphous water present in the system. A minimum of water crystallisation is needed for efficient drying but the growth of ice crystals may lead to cell lysis (see section 2.2.1.3 for details). These freeze injuries may be avoided by the use of cryoprotectants, e.g. sugars, which prevent ice crystal formation. Schoug et al. (2006) showed that freezing rates, cell density and sucrose concentration interacted and influenced the viability of *Lb. coryniformis* Si3, as well as the drying efficiency. They postulated that the higher cell density and sucrose concentration reduced both the relative amount of water and the water crystallisation, therefore improving cell survival.

The primary drying stage consists of the sublimation of the ice into water vapour. It is followed by the secondary stage which involves desorption of the unfrozen water. This stage is usually carried out at higher temperature. If the drying occurs at a temperature above the collapse temperature, the structure of the cake will collapse. This event occurs when the viscosity of the product decreases to a point beyond which it cannot support its own structure (To & Flink, 1978). The resulting cake is characterised as a loss of physical structure with reduced volume and decreased solubility as the pore structure is lost. It also has a higher moisture content, as water cannot properly move out from the system (Rey & May, 2004).

Because of the use of low temperatures, this technique is often preferred over spray and fluid-bed drying, especially for thermolabile bioactives. It is also an adequate technique for highly viscous or structured product such as sourdough (Stefanello et al., 2018). However, freeze-drying is highly energy demanding, hence costly, and can last for up to 72 hours. In addition, the dried cake obtained is very porous, because of ice crystal formation (Harnkarnsujarit, Charoenrein, & Roos, 2012; Poddar et al., 2014). The resulting powder will therefore tend to absorb more water and the high surface-area ratio will increase the exposure to oxygen, both being detrimental for the viability of the bacteria during its shelf-life, see section 2.2.3 for a more in depth explanation. Finally, to obtain a powder, the cake needs to be grinded, an additional stress to the bacteria and the powder obtained presents a sheet-like morphology leading to poor flowability (Poddar et al., 2014).

Even though it would seem that the additional stresses imposed by freeze-drying might result in increased losses of viable bacteria, it would seem that the low temperatures used are in fact the critical factor to the survival of the cells. For instance, Jofré et al. (2015) managed to stabilise freeze-dried *Lb. rhamnosus* over 39 weeks at 22°C, i.e. about

10 months, with a reduction of only 2 log (CFU/g). On the other hand Carvalho et al. (2002) only managed to obtain a 4 log (CFU/g) reduction of freeze-dried *Lb. rhamnosus* over 10 month at 20°C. This difference in results may come down to the strain of bacterial cell as well as the protectants used, and will be further discussed in section 2.4.3.

### 2.3.2 Discussion of their limits and benefits

As mentioned above, freeze-drying is generally preferred over the other types of drying because it does not utilise heat, and is hence less detrimental for the cells. For instance, Hlaing et al. (2017) have used FTIR in order to compare the effect of spray-drying and freeze-drying on molecular changes of *Lb. rhamnosus* GG in lipids, fatty acid content, proteins and DNA conformation. Overall, freeze-drying led to less structural changes in the cell than spray-drying. These structural changes corresponded to changes in the secondary structure of the proteins, with the  $\alpha$ -helices shifting to  $\beta$ -sheets or  $\beta$ -turns which could impact the function of the protein, as well as conformational changes in the DNA shifting from B-DNA to A-DNA, corresponding to the DNA form in dormant cells.

Freeze-drying has also been shown to conserve the functionalities of *B. bifidum* and *Lb. plantarum* compared to spray drying and air-drying (Iaconelli et al., 2015). Overall, freeze-drying led to better cultivability, residual enzymatic activity and cell integrity. However, this type of drying led to the greatest growth retardation, which, according to the researchers, means that the repair of viable bacteria was longer than spray-dried ones when rewetting. On the other hand, spray drying, which is a shorter process is also a more heterogeneous process. This means that the cells which undergo spray drying are actually generally in a better state than the freeze-dried cells. By better state it is meant that even if the viability after drying is better for freeze-dried cells, the bacterial cells are overall more damaged than spray-dried cells, and might thus die-off

quicker over storage. Besides, this study by Iaconelli et al. (2015) showed that the effect of drying might be strain dependant as there was not significant difference for *Lb. zaea*.

None of these studies linked their results with the stability of the bacteria over storage. Moayyedi et al. (2018) compared freeze-drying, spray drying and electrospraying for the stabilisation of *Lb. rhamnosus* ATCC 7469 over storage at 25°C at 11% relative humidity. They found that the freeze-dried sample had higher viability than spray-dried cells, with about 10.5 log (CFU/g) after 24 weeks for freeze-dried samples, compared to 9.5 log (CFU/g). Similarly, *Lb. paracasei* stability was followed at different water activity after spray drying, fluid-bed drying and freeze-drying by Poddar et al. (2014). Freeze-dried samples had a higher survivability when stored at a  $a_w$  of 0.11 over 120 days at 25°C. However, when the water activity was increased fluid-bed drying led to the best survivability, closely followed by spray drying. Both of them led to a less porous powder, compared to freeze-drying, while fluid-bed drying gave bigger particle size, which could explain the better survivability. It is worth highlighting here that the drying does not only affect the bacteria itself, but also the structure of the dried powder. As previously mentioned, freeze-drying leads to a very porous structure, while more compact powder particles are obtained by spray drying and fluid-bed drying. On the other hand, freeze-drying is often a more efficient drying leading to a lower moisture content of the resulting powder and thus, lower water activity after drying which tends to be optimal for the bacteria survival. Barbosa et al. (2015) found that *Lb. plantarum* and *Pedococcus acidilactici* were more sensitive to water activity increases when freeze-dried than when spray-dried or air-dried. Ying et al. (2010) compared spray drying and freeze-drying, and found a stronger water-binding energy in the case of spray-dried sample. The researchers proposed that this difference could explain the better survivability of spray-dried bacteria.

Fluid-bed drying and spray drying can, hence, protect bacteria from storage-related stresses such as water activity, because of the formation of a less porous powder. However, fluid-bed drying comes with a few disadvantages as the media to be dried need to be granulated, or the slurry needs to be dried onto a powder. In addition, this process result in substantially bigger particle compared to those prepared by spray drying. On the other hand, the particle size distribution is better controlled with spray drying but the use of elevated temperatures can causes damage to the membrane and has been accounted to the main reason of cell loss (Ananta, Volkert, & Knorr, 2005; Sunny-Roberts & Knorr, 2011). Knowing this, Quintana, Gerbino, and Gómez-Zavaglia (2017) managed to improve the survival of *Lb. rhamnosus* GG to spray-drying and to resulting storage by growing the bacteria onto different growing media than MRS, leading to changes in lipid composition of the membrane. The resulting stabilised bacteria were even more stable than when freeze-dried, highlighting that both drying stresses lead to different location of the cell damages. However, the growing media was also used as drying media and it cannot be ascertained if the change in membrane composition accounted for the longer shelf-life, or if it was the composition of the drying media. Overall, the choice of the drying method will depend on the probiotic strain, the ability to recover after drying, the effect on the matrix and the storage conditions. The main limitations and benefits of the three drying methods are summarised below, in Table 2.2.

**Table 2.2:** Main characteristics, limitations and benefits of the three main drying methods use to stabilise probiotics.

<b>Drying method</b>	<b>Structure of the obtained powder</b>	<b>Main benefits</b>	<b>Main limitations</b>
<b>Freeze-drying</b>	<ul style="list-style-type: none"> <li>- Sheet-like particles</li> <li>- Porous powder</li> <li>- Low flowability</li> <li>- Large particles, depending on the grinding step (100 - 1000 <math>\mu\text{m}</math>)</li> </ul>	<ul style="list-style-type: none"> <li>- No use of heat</li> <li>- All drying media can be dried</li> <li>- Efficient drying</li> </ul>	<ul style="list-style-type: none"> <li>- Freezing stress</li> <li>- Long and expensive</li> <li>- Resulting powder absorbs water</li> <li>- Additional grinding step</li> </ul>
<b>Spray drying</b>	<ul style="list-style-type: none"> <li>- Controlled particle size distribution (20 – 100 <math>\mu\text{m}</math>)</li> </ul>	<ul style="list-style-type: none"> <li>- Narrow particle size distribution of the resulting powder</li> <li>- Different nozzles can lead to core-and-shell structures</li> <li>- Rapid drying</li> <li>- Relatively inexpensive process</li> </ul>	<ul style="list-style-type: none"> <li>- Heating above 100°C</li> <li>- Viscous media cannot be dried</li> </ul>
<b>Fluid-bed drying</b>	<ul style="list-style-type: none"> <li>- Large particles (100 - 700 <math>\mu\text{m}</math>)</li> </ul>	<ul style="list-style-type: none"> <li>- Mild heat</li> <li>- Possibility to obtain particles with several layer</li> </ul>	<ul style="list-style-type: none"> <li>- Drying media needs to be granulated first</li> <li>- Large particle size of the resulting powder</li> </ul>

## 2.4 Protecting the probiotics in the dried state

As introduced in the stress section 2.2 protecting bacterial cells in the dried state starts as early as in the fermentation batch, by using of the cell stress responses. The way in which bacteria are grown will influence their resistance to the upcoming stress. Following this, exposure to protectants before drying will also affect their stability. Finally, when designing a protection matrix, the end storage conditions must be known in advance to include protection to moisture or to oxidation or other potentially detrimental chemical and physical reactions.



### **2.4.1 Triggering stress responses for better stability**

As previously discussed, bacterial cells have natural stress responses that make them more resistant to different stresses, including dehydration. Pre-stressing the cells is a common technique to give additional protection. As discussed by Liu et al. (2014), the optimal growth conditions are not always the conditions leading to better viability after freeze-drying. Instead, they found that a slightly higher pH or higher temperature was leading to the best survival to freeze-drying. Osmotic stress has also shown to confer resistance to drying, and better stability over storage (Desmond, Ross, O'Callaghan, Fitzgerald, & Stanton, 2002; Prasad et al., 2003).

### **2.4.2 Preparing the cells prior to a dehydration stress**

From paragraph 2.2.2, it can be understood that all biomolecules can undergo denaturation upon drying and thus, the presence of a protectant in the cytoplasm, as well as in the surrounding environment is important for optimal protection. It has been advised to expose bacteria to protectants for a certain period of time in order to equilibrate before freezing or drying (Hubálek, 2003; Leslie et al., 1995). This would allow the protectant to be taken up by the cells, therefore protecting the biomolecules both inside and outside of the cells. Time, temperature and even the washing step, can have an impact on the uptake of protective solutes (Bolten & Wittmann, 2008; Hubálek, 2003; Leslie et al., 1995). These exposure settings will also depend on the bacterial strain and protective solute used.

This may explain why there is no consensus in the time and temperature of exposure of protectants before drying. Time generally varies between 1 and 2 hours, and temperature between 4°C and 37°C (Carvalho et al., 2002; Chen, Wang, Luo, & Shu, 2013; Giulio et al., 2005). It was proposed that at cold temperatures, the lipid membrane goes through phase transition, and become leakier (Leslie et al., 1995). Thus, solutes

could flow freely through the concentration gradient. On the other hand, at higher temperature, the cells might still be active and may be able to use active transporters to uptake solutes. However, if solutes are metabolisable, the cells might use the available solutes and start a new growth phase. For instance Strasser, Neureiter, Geppl, Braun, and Danner (2009) exposed *E. faecium* and *Lb. plantarum* to protectants for 1 hour at room temperature, after growing them on MRS. Cells dried with glucose showed much lower stability than dried with trehalose, sucrose and maltodextrin: there was no viable cells after 1 month at 35°C, whereas for the other protectants, cells were still viable after at least 6 months. This could be due to the fact that after exposure at room temperature for one hour, the cells being still active they produced lactic acid in the protectant solution and started a new growth phase. This could be detrimental to the viability over storage.

### 2.4.3 Finding the right protection

Finding the right protection for a certain probiotic strain is challenging. Numerous studies have looked at different protective solutes to maintain bacterial viability in the dried state. However, the protective effect of a solute is species and strain specific. For example, De Valdez, De Giori, De Ruiz Holgado, and Oliver (1983) compared the survivability of 12 different strains of lactic acid bacteria to freeze-drying in the presence of different protectants. They found that *Lb. leichmanii* ATCC 4797 would better respond to the freeze-drying in presence of glycerol (90% of survivability), while *Lb. bulgaricus* would present a very low survivability (2.5%). In another study on *Lb. delbrueckii*, the strain CFL1 was more sensitive than the strain ATCC 11842 to freezing, and sucrose was only efficient on the latest strain (Meneghel et al., 2017).

There is thus, a better chance to find a good protectant from a study conducted on the same strain, or at least the same species. For *Lactobacillus rhamnosus*, sorbitol, MSG and fructose (Carvalho et al., 2002; Sunny-Roberts & Knorr, 2009), glycerine (Savini et

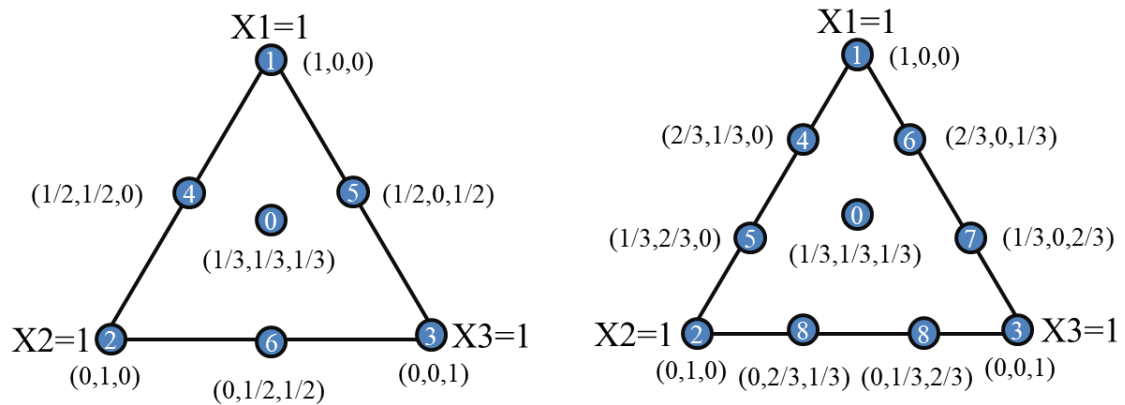
al., 2010), glucose (Zhu, Ying, Sanguansri, Tang, & Augustin, 2013), lactose (Jofré et al., 2015) or a combination of lactose and trehalose (Roos & Pehkonen, 2010) and sucrose (Saarela et al., 2006; Siaterlis, Deepika, & Charalampopoulos, 2009) have shown protective effect over drying and storage. In addition, more complex matrices such as reconstituted skim milk powder also protected *Lb. rhamnosus* in the dried state (Ananta et al., 2005; Jofré et al., 2015). A mix of different protectants, or a complex matrix such as the skim milk, is sometimes the best way to offer better protection to bacteria (Jofré et al., 2015; Roos & Pehkonen, 2010). Hubálek (2003) explained that a mix of penetrating (e.g. small sugars) and non-penetrating (e.g. polysaccharides) agents is needed to act both intra and extracellularly and, thus, efficiently protect the cell.

Synergy between protectants may also improve the stability of dried bacteria. Khorasani and Shojaosadati (2017) used a mixture design of experiment (DoE) to find the best formulation of protectant between bacterial nanocellulose, nanochitin and nanolignocellulose on survivability of *Bacillus coagulans*. They managed to improve the stability of the bacteria in fruit juice for 21 days by 15%.

A mixture DoE is a type of response surface designs, which allows the determination of the relationship between one or more response variables, and a set of quantitative experimental variables or factors. The mixture DoE is used when the sum of the proportion of each factor must be fixed, e.g. 100%, and has been introduced by Scheffe (1963). Thus, the response of the experiment, that is the death rate of the bacteria, will depend upon the relative proportions of the protectants.

There exist two types of mixture DoE: simplex-lattice and simplex-centroid, presented on Figure 2.11. Both designs include samples with only one component and the centroid, which corresponds to an equal mix of all components. The simplex-centroid compares mixtures of one components only to a mix of two, three or four components in

equal proportions. A  $\{q,m\}$  simplex lattice considers all combinations of each components (q) of  $m+1$  equally spaced proportions from 0 to 1 for each component, m being the degree of lattice.



**Figure 2.11:** Examples of mixture design of experiment. The simplex centroid design is presented on the left, and a  $\{3,3\}$  simplex lattice design on the right. X1, X2 and X3 represent the three components.

## 2.5 Techniques to further improve storage

In addition to usual protection techniques, studies have looked at additional ways of improving the stability of bacteria in the dried state. This includes designing microcapsules insulating the bacteria from environmental stresses, or looking for new materials with advanced protection mechanisms.

### 2.5.1 Drying technique, powder structure and storage stability

As mentioned earlier, oxygen and water activity, thus water absorption, are detrimental for the long term storage of bacterial cells. It has been proposed that the reduction of the surface-area ratio of the dried powder could protect from those stresses, and improve shelf-life of dried cells (Poddar et al., 2014). Encapsulating the bacteria prior

or during drying might also give extra protection to the cells by creating a barrier between the bacteria and the environment.

A new technique, named “oil induced biphasic hydrogel particle formations” was proposed to encapsulate the bacteria before drying them (Alehosseini, Gomez del Pulgar, et al., 2019). It consists in dropping bacteria dispersed in an agarose and whey protein concentrate mix, into a biphasic solution consisting of an upper oil phase as the particle-forming antisolvent, and a lower aqueous phase where particles are collected. The particles obtained, were then freeze-dried, and compared to sample with similar composition, but directly freeze-dried. A more compact, dense and smooth particle was obtained and linked with a higher storage stability. The influence of the morphology on the probiotic stability was accredited to the creation of a barrier between the environment and the bacteria. The authors also attributed the gain of cell stability to the oxygen barrier properties of the agarose, but this attribute is questionable as it was not clearly demonstrated.

Simultaneous encapsulation and drying is also possible for example by either electrospraying or spray drying. These techniques generally create an outer skin on the microparticles during drying as polymers contained in the solution, acting as surfactants, migrate to the droplet surface to reduce surface tension between water and air. Electrospraying is a gentle method that consists of the atomisation of a polymer solution through an electric field applied between two electrodes. This technique does not require the use of heat, and the solvent can be water. Alehosseini, Sarabi-Jamab, Ghorani, and Kadkhodae (2019) compared whey protein microcapsules obtained by electrospraying versus freeze-dried. There was no significant difference after drying, but after 3 months of storage at 25°C, there was a higher viability for electrosprayed cells, with about 1 log (CFU/g) difference. This increase in stability was accredited to the structure of the

powders. While the freeze-dried samples was very porous, electrosprayed capsules presented with a more compact rounded shape. In addition, the protection could also be due in part to the presence of whey protein, which has been proposed in the past to form an oxygen barrier around the core of the capsule, containing the bacteria (Hong & Krochta, 2006; López-Rubio, Sanchez, Wilkanowicz, Sanz, & Lagaron, 2012).

The use of a spray dryer mounted with a three-fluid nozzle has also shown to create a capsule like structure in the same time as the drying. This method was used for the encapsulation of  $\alpha$ -amylase (Jiang et al., 2013). The three-fluid nozzle improved the stability of the enzyme with less porous microcapsules, compared to the  $\alpha$ -amylase encapsulated by coacervation, followed by spray drying. However, this technique has not been yet applied to the preservation of probiotics to our knowledge.

Other studies looked at the potential of coacervation followed by freeze-drying for storage of probiotics (Zhang et al., 2013; Zhao et al., 2018). However, there was no comparison of different techniques with similar matrices composition to be able to conclude if the coacervation step was in fact an asset.

Overall, the technology used to encapsulate and dry probiotics can lead to a certain structure, dense and compact, and improve the stability over storage. The structure of powder obtained by freeze-drying, i.e. very porous, can thus be detrimental in the long term. Harnkarnsujarit et al. (2012) followed the stability of  $\beta$ -carotene over storage at room temperature after freeze-drying in different mixtures, and with different structures obtained by two different freezing rates. They found that overall, a collapsed structure, i.e. a denser powder, led to a higher stability. Similarly, the smaller the pore size, and the thinner the walls between the pores, led to a lower stability, as the contact with the environment was increased. Finally, the absorption of water increased the stability of the  $\beta$ -carotene when the water activity was low. There was thus an optimal water activity

sitting between 0.18 and 0.28, depending on the composition of the powder. This was accounted to the lower oxidation rate, as there is an optimal water activity for each product, leading to low oxidation rate (see section 2.2.3.1). Interestingly, no such study have been conducted on the stabilisation of probiotics. It would be thus interesting to be able to look at the potential synergistic effect between the composition of a stabilisation matrix and the creation of a protective wall or a dense powder structure.

### 2.5.2 Materials with higher thermal protection

As mentioned earlier (section 2.2.2.3) materials with a high glass transition temperature can slow down reaction rates and protect from storage injuries. It has been suggested that amorphous pharmaceutical solids should be stored 50°C below their T<sub>g</sub> in order to render molecular movements negligible over several years of storage (Hancock, Shamblin, & Zografi, 1995). Liu et al. (2018) showed that the improved storage stability of *Lb. zeae* at 25°C was related to the higher glass transition temperature of the protective matrix, especially for higher water activities (0.54 and 0.76). These results were in line with previous studies from their group (Liu et al., 2016). However, their findings also suggested that a high glass transition was not sufficient for proper protection, and confirmed previous studies on stabilisation of cells during dehydration (Crowe, Hoekstra, Nguyen, & Crowe, 1996). Not all studies on storage stability of probiotics measure the glass transition temperature of matrices, though many note that it can be a critical factor. It is thus challenging to conclude if it is one of the necessary conditions for probiotic preservation.

Insulating materials have also been proposed to delay heat transfer toward encapsulated bacteria. For instance, *B. animalis* was encapsulated with hydroxypropylmethyl cellulose (HPMC) and with a mix of HPMC and polyethylene glycol to protect them from reconstitution heat (about 70°C; Penhasi, 2015). HPMC is a

thermosensible material that swells in solution and forms a gel when the temperature increases. The study showed that this encapsulation formulation could protect the probiotic from heat stress occurring during reconstitution. The solid gel layers would then dissolve after cooling allowing the bacteria to be released in the solution. However, this technology can only be applied to short heat treatment – in the order of minutes. Thus, this encapsulation system will not protect bacteria during storage, but a similar design could be developed to target storage stresses.

Finally, instead of delaying heat transfer, materials can be used to absorb heat, under fluctuating temperatures for instance. This is the case of phase change materials (PCM), e.g. water, lipids or polyethylene glycol. During melting of a PCM, heat is absorbed and is redistributed later when the material is crystallising. Such technology is used for fire fighter clothing (Rossi & Bolli, 2005), energy storage (Sharma, Sharma, & Buddhi, 2002) or smart packaging (e.g. to keep a product cool; Espeau, Mondieig, Haget, & Cuevas-Diarte, 1997). A few examples of PCM used with their application are presented in Table 2.3. However, the temperature range in which PCM absorb temperature is narrow: to within a few degrees around their melting temperature ( $T_m$ ). To overcome this challenge, Penhasi (2013) patented a coating for probiotics covered with PCM (polyethylene glycols) of increasing  $T_m$ , using fluid-bed coating. As the temperature of the environment increases, the layers are progressively melting, delaying the temperature increase to the core where the bacteria were located. However, this patent does not show any viability studies. Pitigraisorn, Srichaisupakit, Wongpadungkiat, and Wongsasulak (2017) proposed a multi-layered particle obtained by combination of electrospinning and fluid-bed coating containing stearic acid ( $T_m = 66-69^\circ\text{C}$ ; Sharma et al., 2002) for protection of moist-heat treatment. Protection was efficiently gained in the presence of stearic acid when the probiotic was treated at  $70^\circ\text{C}$  and 100% relative



humidity for 30 min. Nevertheless, PCM have not been yet studied for the storage stability of probiotics.

**Table 2.3:** Some examples of phase change materials used in different application and their respective melting temperature

PCM	Application	Melting temperature	Reference
Mix galactitol and mannitol (30:70)	None specific – potential use in thermal energy storage	153°C	(Paul, Shi, & Bielawski, 2015)
Polyethylene glycol	Energy storage	Between 44°C and 70°C depending on the molecular weight	(Pielichowski & Flejtuch, 2002)
	Drug release		(Craig, 1990)
n-Eicosane	Drug release	36.8°C	(Ren & Zhang, 2015)
Fatty acids	Energy storage	Between 16.7°C and 102°C	(Sharma, Tyagi, Chen, & Buddhi, 2009)
e.g. Stearic acid	Protection of <i>Lb. acidophilus</i> from moist-heat treatment	63°C	(Pitigraisorn et al., 2017)
Paraffin	Fire fighter clothing	$\geq 37^\circ\text{C}$	(Rossi & Bolli, 2005)

## 2.6 Analysis techniques used for monitoring the stabilisation properties of protectants

Understanding the behaviour of the bacteria within the drying mix, as well as the impact of the properties of the matrix on the bacteria, is important to understand and improve the stability of probiotics in the dried state.

A general understanding of the protective matrix can be obtained with microscopy. For instance, Poddar et al. (2014) used Scanning Electron Microscopy

(SEM) to look at the structure of powder obtained by fluid-bed drying, spray drying and freeze-drying. The study showed that the porosity of the freeze-dried powder could affect the stability of the bacteria, which was then confirmed by pycnometry. A later study also used SEM to link the morphology of the powder with the stability of the bacteria (Alehosseini, Gomez del Pulgar, et al., 2019). Transmission Electron Microscopy (TEM) can be applied to look at the inner structure of a microencapsulation system, and to study the morphological change of the bacteria after a certain stress (Ann et al., 2007; Tabanelli et al., 2015).

However, additional techniques are needed to understand the protection mechanisms of a protective matrix. As introduced earlier, these mechanisms are either due to a direct interaction with the biomolecules helping to maintain them in their native or hydrated form or through the formation of a glassy matrix. Among the different techniques used to understand these properties, two are of most interest. Firstly, differential scanning calorimetry (DSC) has been extensively used to measure the glass transition temperature of the protective matrix. Denaturation of biomolecules can also be studied by DSC, and its potential application for the study of probiotic stability will be further discussed in the section below. Secondly, molecular spectroscopy, and specifically infra-red spectroscopy could allow further insight into the interactions between the protectants and the cells.

### **2.6.1 Differential scanning calorimetry (DSC)**

Calorimetry is the study of heat transfer which occurs during physical or chemical changes. DSC is the technique that follows the amount of heat needed to increase the temperature of a sample against an inert reference. In brief, a sample and a reference are heated up at a constant rate while maintained at the same temperature. The DSC measures the energy required to maintain the same temperature between the sample and the

reference ( $d\Delta q/dt$ ). If the sample goes through a phase transition it will either require more energy to increase its temperature (endothermic event), or produce energy (exothermic event). In the biology field, an exothermic event would be the crystallisation of lipids or metabolism of a solute and an endothermic event would be the melting of lipids or the denaturation of proteins.

In the preservation of probiotics, DSC can be used to measure the properties of the protectant system or could even look at the cells in themselves. In the first case, DSC is used mostly to measure the glass transition temperature of the powder. It can also follow the melting or crystallisation of the material. Finally, DSC has been used to measure the stability of cells, and their resistance to heat or antimicrobial agents (Brannan et al., 2015; Mackey et al., 1991; Miles et al., 1986; Tunick et al., 2009). Cells present a thermogram, with specific denaturation or melting peaks for each biomolecules. The DSC can measure the impact of the environment on the stability of the cells by looking at changes of peak location (melting or denaturation temperature) and peak area (enthalpy of the event). However, conventional DSC comes with a couple of limitations for this application. First, sample pans are made for dried sample, and are not always closing hermetically. One solution is to dry the sample first. Second, the sensitivity of a conventional DSC is often not sufficient for a biological sample. Because the composition of a cell is very complex, it might not be possible to see all the components denaturing or melting. MicroCal MC-DSC is a first alternative (Duguid, Bloomfield, Benevides, & Thomas, 1996). Nano DSC is another alternative as it is designed to follow protein denaturation in liquid system with low viscosity. It has not been used for complex biological systems, yet.

### 2.6.2 Fourier-Transform Infra Red (FTIR)

FTIR is part of molecular spectroscopy in that it gives information on chemical bonding between atoms or groups of atoms. Infra-red spectrum informs on the vibration and rotation of atoms and functional groups. These are influenced by their chemical environment. For instance, an increase in the frequency is a sign of an increase in the force constant of the bond, therefore, if the frequency decrease, the group is interacting with the environment. The Fourier-transform is a mathematical process to convert the data measure into a spectrum that can be interpreted and analysed. The great advantages of FTIR is that it does not require chemicals, it is non-destructive and it can perform measurement on different type of samples, e.g. gases, powders or liquids.

In the study of probiotic stability, FTIR has been used to study the lipids, proteins and nucleic acids of cells. One application is to follow their conformational changes, e.g. phase transition of the membrane, or loss of the proteins secondary structure, during heating, freezing or drying (Kilimann, Doster, Vogel, Hartmann, & Gänzle, 2006; Meneghel et al., 2017; Wolkers & Oldenhof, 2015). More specifically, FTIR has been broadly used to understand the role of protectants in the depression of phase transition of the membrane (Leslie et al., 1995; Oldenhof et al., 2005; Santivarangkna et al., 2010). It has been discussed that the protectant can interact with the phospholipid headgroup and help maintain them in a liquid crystalline form. Generally, in these studies, cells, or membrane and protein models, are mixed with protectant in a 1:1 to 1:5 weight ratio, allowing to obtain a good signal for the cells spectrum (Linders et al., 1997; Meneghel et al., 2017; Oldenhof et al., 2005). The percentage of bacteria is thus, much higher than in a conventional dried mix where they represent between 0.5 to 5% of the total weight. Hlaing et al. (2017) overcome this limitation by removing the spectrum of the protective matrix to the dried mix with bacteria using the non-subjective vector correction (Berger,

Koo, Itzkan, & Feld, 1998). They managed to look at the bacteria spectrum even if they were as little as 0.4% of the final mix, for both spray-dried and freeze-dried method.

## **2.7 Concluding remark**

Nowadays, consumers are looking for healthier foods that do not only nourish but can also heal. With this, the demands for probiotics is increasing, and industries are adding them to new ranges of food products. The most efficient way to keep probiotics alive in the long term (several months to years) is to dry them. However, this implies severe stresses on the microorganisms, before, during and after drying them. It is the role of the producer to ensure the probiotics will still be viable when arriving to the consumers.

Studies on the stability of probiotics are numerous, with extensive research going into this area for the past decade. The various mechanisms by which solutes can protect the cells and indeed the stress response from the cells are also better understood. However, the strain specificity of each studies makes it difficult to apply findings to other bacteria. In addition, not all studies are working in a systematic way by firstly understanding the bacteria and the stresses that will be imposed in order to efficiently stabilise them in the dried state and then, adding appropriate further protection as needed. For instance, studies are still lacking any clear explanation on how to prepare the cells to drying or to storage. It is proposed that loading the cells with protectants can improve their stability, but it is unclear on how to proceed, and what the exact effects on the cells stability are. Protection mechanisms of solutes are multifactorial and spectroscopy techniques managed to show the importance of the interaction between cells and protectants. However, some work is still needed to understand the relative importance of each factors, between the cell-protectant interactions, the protectant-protectant interactions as well as the physical properties of the matrix. Finally, a few studies have looked at layering bacteria with different protective layers. This reminds the conformation

of spores, which are stable in adverse conditions for years, and could be promising in this field.

# Chapter 3 – Sugar uptake by *Lactobacillus rhamnosus* and its impact on shelf-life

---

## 3.1 Introduction

In the past few years, probiotics have been added to a wide range of food products with research focused on improving their shelf-life. Drying is one technique used to improve the stability of probiotics. The bacteria are dried in a protective matrix with the intention of maintaining their viability and functionality. Three potential mechanisms of protection have been described in the literature (Santivarangkna et al., 2008). Firstly, the added protectants can replace the water in its structural role. In the hydrated state, biomolecules, such as lipids, protein and DNA, are in their native form, but when the water is removed, forces appear within and between biomolecules which can cause their denaturation. Protectants can fill these spaces and maintain these biomolecules in their native form (Santivarangkna et al., 2010). Secondly, the protectants increase the free energy of water, thus maintaining water in the surrounding area of the biomolecules (Meneghel et al., 2017). Finally, protectants may form a glassy matrix, protecting the whole cells by immobilisation (Santivarangkna et al., 2011). These mechanisms imply that protectants should be present both inside and outside the cells in order to impart their protective effect.

Numerous studies have shown that incubation of the bacterial cells with a solution containing protectants can improve the solute penetration into the cell (Chen, Chen, Chen, Wu, & Shu, 2015; Saarela et al., 2005). Studies related to determining the optimal conditions under which this incubation should take place, however, vary significantly. Leslie et al. (1995) showed that trehalose would not enter *B. thuringiensis* at temperatures

above 15°C. They suggested that the cell membrane becomes leakier in cold solutions as it goes through a phase transition; thus, carbohydrates can passively diffuse through the membrane, down their concentration gradient. However, contrary to this a number of stability studies have involved solute equilibration at room temperature (Carvalho et al., 2002; Conrad, Miller, Cielenski, & de Pablo, 2000; Strasser et al., 2009), or even higher (Chen et al., 2013). At these temperatures, cells are still active, and may actively take up solutes as well as metabolise them. In the study by Strasser et al. (2009) the protective effects of glucose, maltodextrin, trehalose and sucrose were compared. Interestingly, glucose elicited the least protection in both the strains studied. One could argue that at room temperature, sugars would be taken up actively; however, cells may catabolise glucose, leading to a lower cell stability. In his review on cryoprotectants, Hubálek (2003) explained that the ideal protectant equilibration time and temperature depend on the actual protective agent (e.g. its molecular weight and electrical charge) as well as on the organism. However, even though the *Lactobacillus* species has been at the forefront of the probiotic studies for at least a decade now, to the best of our knowledge no study has looked at optimisation of the temperature and time of exposure for the cells prior to drying.

Therefore, this initial study examined the solute uptake by *Lb. rhamnosus* HN001 at 4 and 20°C over 240 min. Glucose and sucrose were chosen as model sugars as they have been shown previously to have a protective effect on dried *Lb. rhamnosus* species (Saarela et al., 2006; Zhu et al., 2013). In addition, they can be utilised by *Lb. rhamnosus* HN001 (Ceapa et al., 2015), with the cells possessing active transport systems for both sugars (Kankainen et al., 2009). The sugars are of different molecular weights, and therefore may diffuse through the membrane at varying rates when exposed to cold conditions.



Initially, the uptake and catabolism of the sugars was assessed, before studying how the stability of the freeze-dried cells was affected by the different exposure conditions during storage at 30 and 40°C. Finally, in order to try to understand the nature of the interactions between the protectants and the cell biomolecules, the stability of the biomolecules was followed by Nano differential scanning calorimetry (DSC). Calorimetry is used to study the heat transfer occurring during physical or chemical change, such as protein denaturation, lipid melting or crystallisation. Conventional DSC has been used to measure the stability of cells and their resistance to heat or antimicrobial agents (Brannan et al., 2015; Mackey et al., 1991; Miles et al., 1986; Tunick et al., 2009). However, the sensitivity of a conventional DSC is relatively low. Thus, it may be difficult to distinguish all thermal events occurring when heating up a cell sample. MicroCal MC-DSC is an alternative that has been used to follow melting of DNA (Duguid et al., 1996). Nano DSC has also been used to study protein denaturation, but has not been applied to complex biological system such as cells. Interaction of the biomolecule with sugars will be seen as a shift in the melting or denaturation peak, or as a change in the enthalpy of the event, relative to the values for the sugar-free environment.

## 3.2 Materials and Methods

### 3.2.1 Materials

Analytical grade glucose and sucrose were obtained from Thermo Fisher Scientific (Waltham, MA). MRS broth and MRS agar were bought from Fort Richard (Fort Richard Laboratories Ltd., Auckland, New Zealand). Inulin (Frutafit TEX, degree of polymerisation (DP)  $\geq 22$ ) was obtained from IMCD New Zealand Ltd., Auckland, New Zealand. Frozen stock of *Lb. rhamnosus* HN001 was provided by Fonterra Ltd., Palmerston North, New Zealand.

### 3.2.2 Growth curve of *Lb. rhamnosus* HN001

First, three 10-mL MRS bottles were inoculated from a slope. After 18 hours at 37°C, the cultures were used to inoculate in 990-mL MRS broths. This marked time 0. The triplicate culture were placed in an incubator at 37°C under gentle agitation (110 rpm) to avoid sedimentation. At each time point four 1-mL samples were withdrawn; one for plating; one to measure the absorbance, and two samples for the dry cell weight. Plating the bacteria was done by serial dilution in sterile, salted peptone water. MRS agar plates were inoculated and placed at 37°C for 72 hours prior to counting. Each serial dilution was plated in duplicates.

The samples for the absorbance measurement was diluted 1 in 7 in a sterilised MRS broth. The absorbance was measured in duplicate for each sample, at 610 nm on a SPECTROstar® Nano (BMG Labtech). MRS broth was used as blank.

The last 2-mL aliquots were frozen, until performing further analysis. Prior to the dry cell weight measurement, aluminium pans were placed in a 105°C oven, for at least 12 hours. They were then placed in a desiccator to allow them to cool down before weighing them. The culture solution was centrifuged at 10,000g for 5 min, the broth discarded and cell pellet re-suspended in MilliQ water. The cell solution was then placed in the pans and dried overnight at 105°C.

### 3.2.3 Bacterial strain and growth

MRS broth was initially inoculated from the slopes and incubated for 18h at 37°C. This culture was then inoculated into a new MRS broth (1:9 ratio). The culture was grown for 16 hours at 37°C and under slow agitation (110 rpm). At this stage, the bacterial culture had reached its stationary phase (see Figure 3.1), determined by reading the absorbance (OD<sub>610</sub>) on a SPECTROstar® Nano (BMG Labtech).

### **3.2.4 Harvesting of the cells**

Bacteria were maintained by monthly inoculation on agar slopes, and stored at 4°C. Bacteria were grown as mentioned above and harvested at the start of the stationary phase by centrifugation (4,000 g for 5 min). Two different exposure temperatures were investigated throughout the study: 4°C and room temperature (20°C). Centrifugation prior to the addition of sugar was performed at the temperature under study.

Bacterial cells were washed twice with phosphate buffer (0.1 M, pH7.4, prepared in MilliQ water with potassium phosphate buffer) and maintained at the temperature of the study. For the HPLC analysis, the second washing was done with one tenth of the volume in order to concentrate the cells and thus increase the accuracy of the study. The sugar solution was added to the cell pellets and were then kept either on ice or at room temperature.

### **3.2.5 Study of the uptake and metabolism of the sugars**

The sugars solutions were prepared by first dissolving glucose or sucrose in 0.1 M phosphate buffer to reach a sugar concentration of 0.3 M (about 580 mOsmol/L). Phosphate buffer and glassware were autoclaved with an Astell chamber steriliser (model AVS490D) at 121°C for 15 min. The sugar solutions were then filtered through a sterile 0.45 µm filter. Solutions were freshly prepared prior to each experiment and maintained either at 4°C or 20°C depending upon the temperature of the study.

The time of exposure varied between 1 min and 90 min. The control sample was homogenized with phosphate buffer. At each time point, a cold (-20°C) quenching solution was added in a 1:3 ratio with samples being treated in triplicate. The samples were then centrifuged at 0°C, supernatants were collected, and cells were washed with the same volume of quenching solution.

Cell pellets were placed at -80°C prior to extraction, while collecting the remaining samples. Bacteria were extracted by first adding cold (-80°C) absolute methanol and glass beads (diameter 300-355 µm). Homogenisation was not efficient at these cell concentrations, and so the same volume of MilliQ water was added and samples were vortexed for 2 min. Four freeze-thaw cycles were performed to improve cell lysis (from -80°C to 4°C). The suspension was vortexed for at least 30 s after each thawing. Cell extracts were centrifuged for 10 min at 16,000 g and 0°C to remove any cell fragments.

The quenching solution consisted of 60% (v/v) methanol with 1.7% (w/v) ammonium carbonate in MilliQ water. This was adapted from the solutions proposed by Faijes, Mars, and Smid (2007): ammonium carbonate concentration was increased in order to match the osmotic pressure applied by the sucrose solution (580 mOsmol/L) and to avoid leakage of the cells.

Concentrations of sugars and lactic acid in supernatants and cell extracts were analysed by HPLC using the Shimadzu Prominence LC-20AD HPLC system. 10µL samples were injected using the 20A HT prominence autosampler, pumped at 0.5ml/min through the Bio-Rad Aminex HPX-87H column in the oven CTO-20AC at 25°C using 5mM H<sub>2</sub>SO<sub>4</sub> solvent. Detectors used were the SPD-20AV (UV/VIS Detector) set at 210nm and 254nm for acid analysis and the RID-20A (Refractive Index Detector) for sugar analysis. Software used to analyse the peaks was Shimadzu LabSolutions Lite. The runs were performed at 25°C to prevent sucrose inversion

All samples were filtered through a 0.22 µm filter prior to analysis. Serial dilutions of L-lactic acid, sucrose and glucose were used to calculate concentrations in samples. Standards were freshly run prior to each set of analyses.

### 3.2.6 Shelf-life study

The sugar solutions for the study of the bacterial stability after drying were similarly prepared prior to harvesting the cells. The composition of the solutions was adjusted in order to obtain a constant concentration of bacterial cells after drying. They consisted of 12.5% (w/v) of glucose or sucrose and 12.5% (w/v) of inulin in phosphate buffer. Inulin was used as a carrier, to ensure proper drying of the slurry. The inulin was first added to the phosphate buffer under stirring and low heat until complete dissolution (about 10 minutes). Then, the sucrose or glucose was added to the mix while still stirring. Solutions were then either placed at 4°C or maintained at room temperature (20°C), depending upon the temperature under study.

After harvesting the cells, they were exposed to the solution. The exposure time varied between 1 min and 240 min. The time was increased to obtain greater variation between the results. At each time point, the slurry was placed at -40°C and left overnight until freeze-drying.

Samples were subsequently freeze-dried in a Cuddon FD18 Freeze Drier (Cuddon FreezeDry, Blenheim, New Zealand) for approximately 72 hours, under vacuum of approximately 1 mbar and shelf temperature reaching 20°C. The condenser was set at -30°C. Once dried, the *Lb. rhamnosus* powders were ground using a pestle and a mortar. They were then mixed with skim milk powder at 10% (w/w) to stabilise the water activity. Final water activity was of  $0.16 \pm 0.1$ . The powder was split in individual three side seal foil pouches from Casp-Pak (Cas-Pak, Auckland, NZ), sealed, and stored in an incubator. Two shelf-life temperature were under study: 30 and 40°C.

The viability of the cells was followed over 8 months using the plate count method. One gram of powder was rehydrated in 9 mL sterile salted peptone water, and vortexed for at least 30 seconds at maximal speed. Decimal serial dilutions were made in

salted peptone water. Appropriate dilutions were plated on MRS agar plates and incubated at 37°C for 72 h in aerobic conditions. Two series of serial dilutions were done for each sample, and each dilution was plated onto two plates.

### 3.2.7 Calculation of the death rate

The loss of bacteria over time usually follows a first order kinetics, expressed as follows:

$$\frac{dN}{dt} = -kN \quad (3.1)$$

Where  $N$  stands for the number of bacteria still alive at time  $t$  and  $k$  is the death rate constant.  $k$  can be calculating by integrating the equation between time 0 and time  $t$ :

$$N = N_0 \exp(-kt) \quad (3.2)$$

Which is equivalent to:

$$\ln\left(\frac{N}{N_0}\right) = -kt \quad (3.3)$$

As the number of bacteria is usually expressed in log10,  $k$  is calculated as such:

$$k = \frac{\log_{10}\left(\frac{N_0}{N}\right)}{t} \quad (3.4)$$

For each sample  $k$  was determined as the sloped of the linear regression of  $\log_{10}\left(\frac{N_0}{N}\right)$  as a function of  $t$ , and is expressed as per unit of time.

### 3.2.8 Nano differential scanning calorimetry

For the calorimetry study, sugar solution were the same as for the shelf-life study, but without inulin. Control consisted in phosphate buffer only. Cells were harvested as described, and put in contact with the sugar solution at 4 or 20°C. Exposure time consisted of only 0 and 240 min, as the duration of the measurement did not allow to run another

sample with an intermediate exposure time. The control consisted of cells suspended in phosphate buffer.

The Nano DSC (TA instruments, USA) cells were conditioned prior to the experiment by running degassed potassium phosphate buffer in both the sample and reference cells.

After the bacteria were harvested and exposed to the sugar solution, as previously described, they were centrifuged and re-suspended in 1/10<sup>th</sup> of the same solution in order to increase the sensitivity of the measurement. The slurry was then degassed for 10 min at 4 or 20°C before being added to the sample cell of the Nano DSC. The sample and the reference sample were heated from either 4 or 20°C up to 130°C at 1°C/min. After each run, the sample cell was flushed with 1 L of MilliQ water. A blank thermogram, obtained by running the protectant solution without bacteria, was subtracted from the sample thermogram before further analysis. In addition, thermograms were normalised based on the amount of cells (g/L) present in the sample, calculated from the absorbance of the sample.

### 3.2.9 Data analysis and statistics

The correlation between the absorbance and the dry cell weight of the cell growth was obtained by Origin 2017© (version b9.4.1.354 (Academic), OriginLab Corporation, USA). The linear correlation was obtained by instrumental weighting, i.e. each point was weighted ( $w_i$ ) with the inverse of the measurement error ( $\sigma_i$ ) as shown in equation (3.5), so that measurement with lower error have larger weight.

$$w_i = \frac{1}{\sigma_i^2} \quad (3.5)$$

The factorial design of the shelf-life was created and analysed with Minitab® Statistical Software (version 18.1, © 2017 Minitab, Inc., USA).

The Nano DSC thermograms were analysed using R 3.5.0 (R Core Team, 2018). First, the data were resampled to obtain alignment on a common temperature vector (as data were recorded as a function of time, and not temperature). This was done using the “resample” function and a “spline” interpolation method. Variation between samples was checked by Principal Component Analysis (PCA). The baseline was removed from thermograms of samples of interest between 20 and 110°C, using the fill peaks method and the following parameters: lambda of 4, half width of local window of 100, number of iterations in suppression loop of 50 and number of buckets to divide spectra into of 1500. Finally, peaks were obtained using the “uniroot.all” function applied to the first derivative of the thermogram, and inflexion points were found with the same function applied to the second derivative of the thermograms. The relevance of each peak and inflexion point was checked visually.

### 3.3 Results and discussion

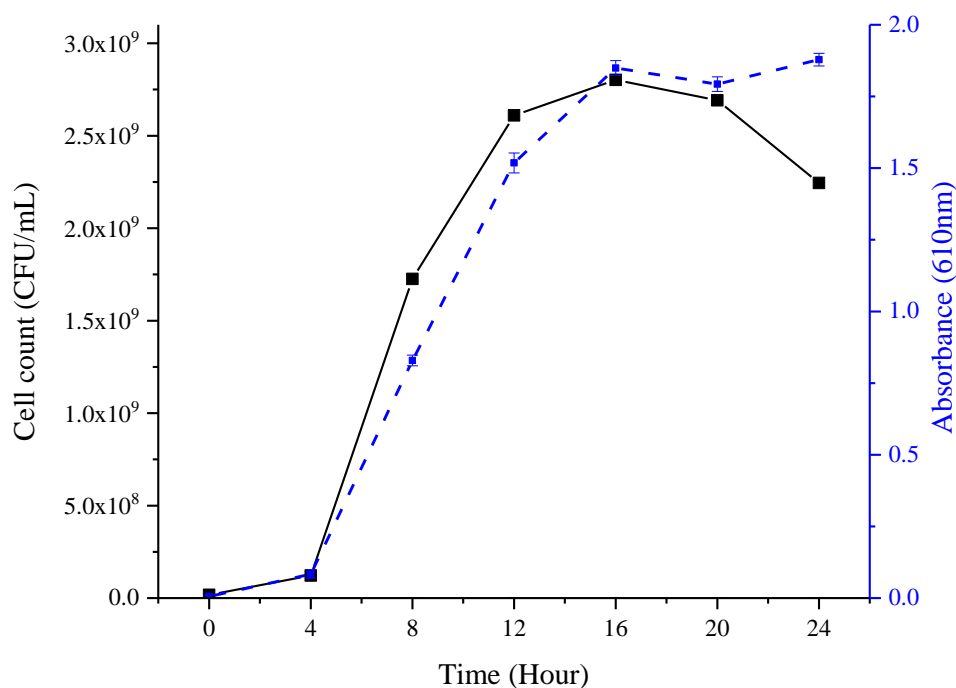
#### 3.3.1 Determination of the stationary phase

Prior to the start of the study, the growth curve of *Lb. rhamnosus* HN001 was established, in order to define the best harvesting time.

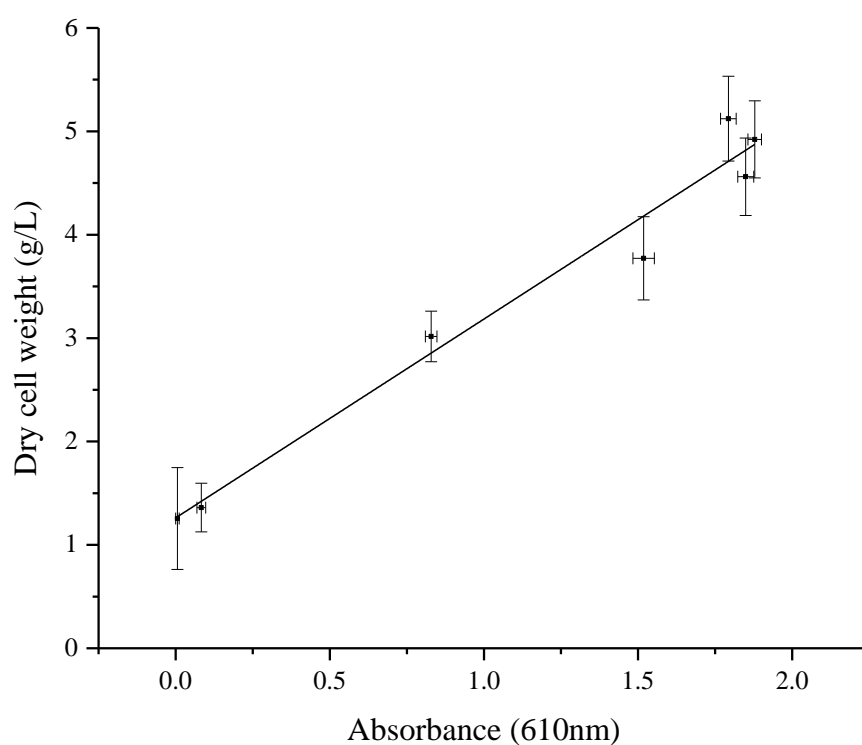
Figure 3.1 presents the growth curve with the bacteria count and absorbance values at 610 nm. Both absorbance and cell count number seems to reach a plateau at different times: i.e. 12 hours for the cell number and 16 hours for the absorbance.

The bacteria enters the stationary phase after about 16 hours of incubation where both the absorbance value and the cell count are reaching a plateau. The relationship between the absorbance and the dry cell weight is showed in Figure 3.2. The coefficient of determination of the linear regression ( $R^2$ ) is of 0.978 and the adjusted  $R^2$  is of 0.973, so the regression fits well the data. Thus, this relationship can be used later on to calculate the weight fraction of cell in the final powder, based on the absorbance values.





**Figure 3.1:** *Lb. rhamnosus* HN001 growth curve, incubated at 37°C in MRS media, followed by plate counting and absorbance reading at 610 nm. Data are shown as the mean of triplicates and the error bars represent the standard error.



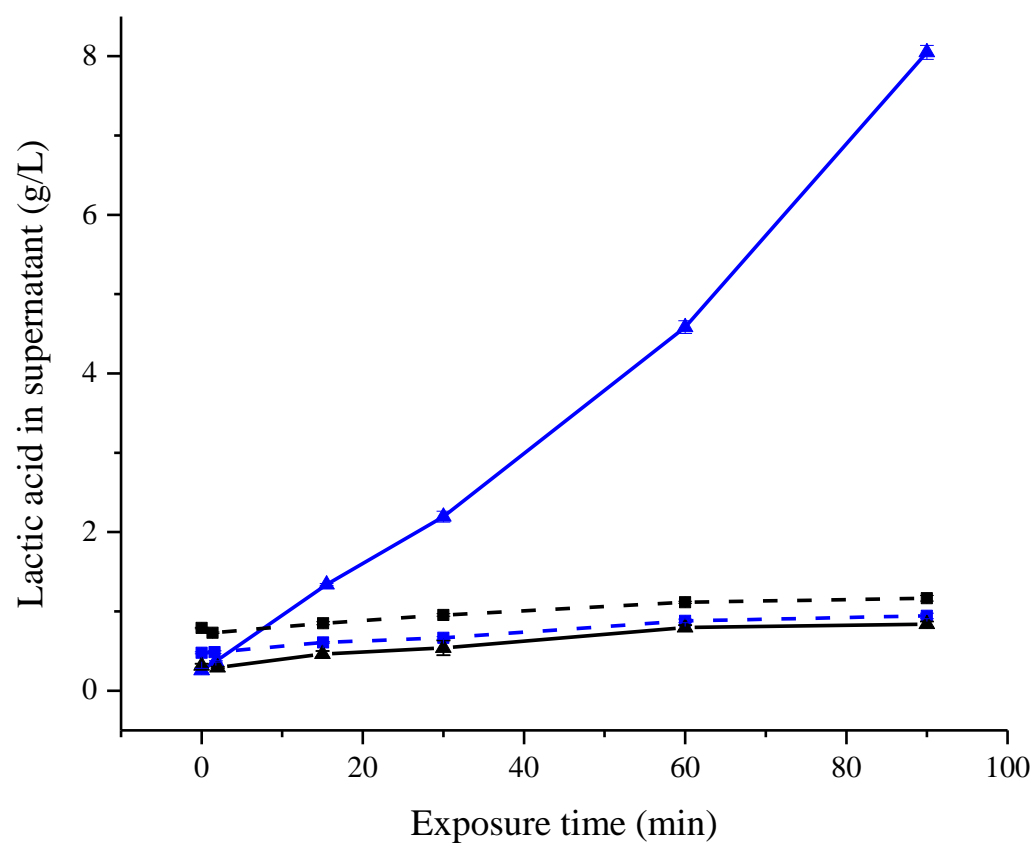
**Figure 3.2:** Relationship between the dry cell weight and the absorbance at 610 nm of *Lb. rhamnosus* HN001.  $y = 1.26 + 1.92x$  with  $R^2 = 0.978$ . Data are shown as the mean of triplicates and the error bars represent the standard error.

After 16 hours the cells growth is thus drastically lowered due to either acidification of the media or nutrient shortage. As outlined in section 2.2 the cells gain general stress resistance at this stage and will be thus harvested at this point for further experiments.

### **3.3.2 Uptake and metabolism of protectants prior to drying**

The second step of this study was to follow the uptake and catabolism of the glucose and sucrose at 4 and 20°C by HPLC.

From the monitoring of the solutes concentration in the supernatant, presented in Figure 3.3, a clear release, and thus production, of lactic acid could be noticed when the cells were exposed to glucose at 20°C. Production rate reached 1.3 mmol/min as shown in Table 3.1. Interestingly, this was not the case for sucrose where there was no clear release of lactic acid. Indeed, when cells were exposed to glucose at 4°C or to sucrose, the concentration of lactic acid in the supernatant increased only slightly. The metabolism appears to be slowed down at lower temperatures but not completely stopped. It has been previously showed that *Lb. rhamnosus* HN001 could utilise sucrose, but was not readily metabolising it, which explains the present results (Ceapa et al., 2015).

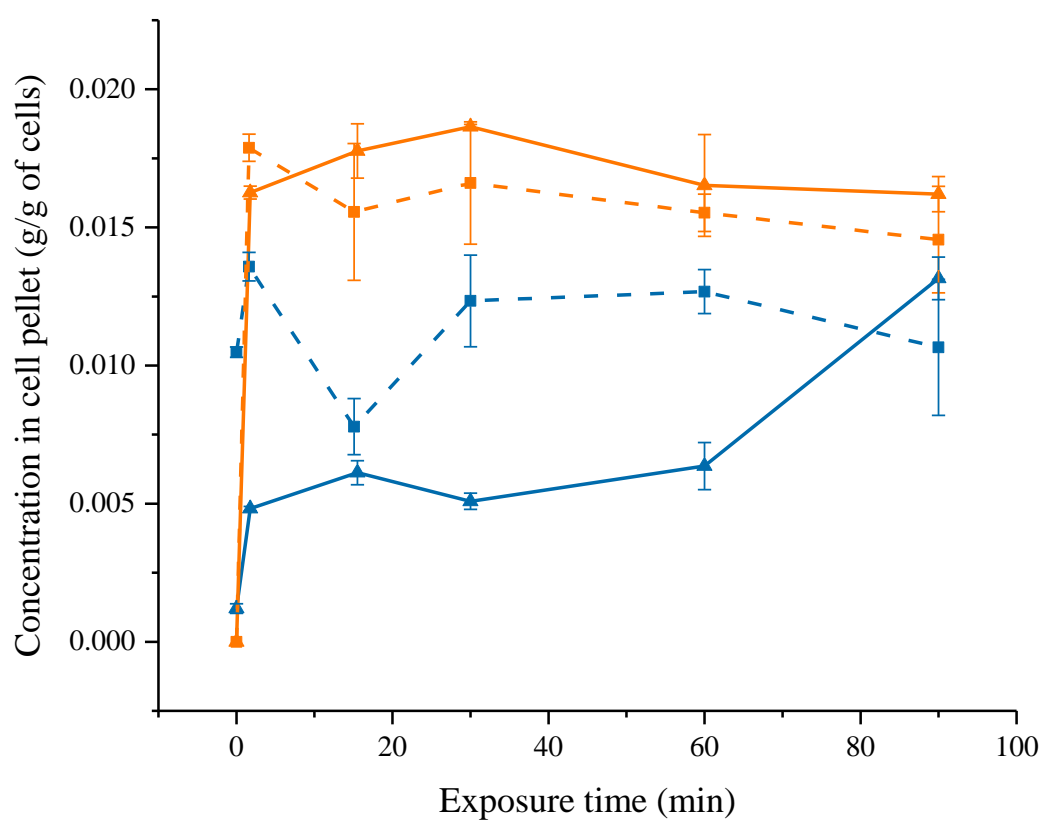


**Figure 3.3:** Comparison of lactic acid release in the supernatant from *Lb. rhamnosus* exposed to glucose (in blue) or sucrose (in black) solutions at 4°C (dashed line) or at 20°C (solid line). Data are shown as the mean of triplicates and the error bars represent the standard error.

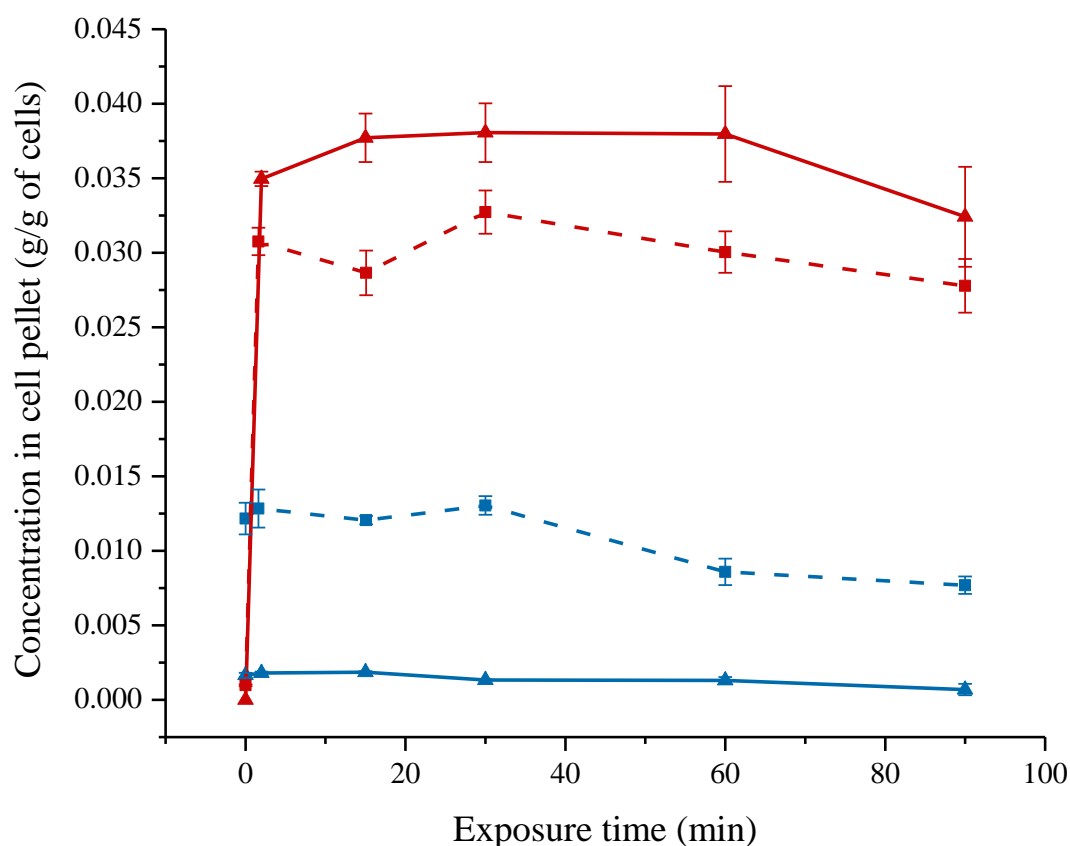
**Table 3.1:** Production of lactic acid in the cell supernatant after exposing *Lb. rhamnosus* to glucose or sucrose at 4 or 20°C. “Exp.” stands for exposure. Data are expressed as the mean of triplicates with their standard deviation.

Treatment		Lactic acid in supernatants					
Glucose 4°C	Exp. time (min)	0	1.62	15.08	30	60	90
	Concentration (g/L)	0.48 ± 0.02	0.49 ± 0.03	0.61 ± 0.02	0.67 ± 0.03	0.88 ± 0.04	0.94 ± 0.06
	Production rate (mmol/min)		0.05	0.1	0.04	0.08	0.02
Glucose 20°C	Exp. time (min)	0	1.75	15.5	30.25	60	90
	Concentration (g/L)	0.26 ± 0.05	0.37 ± 0.01	1.34 ± 0.02	2.19 ± 0.12	4.58 ± 0.14	8.05 ± 0.15
	Production rate (mmol/min)		0.72	0.78	0.64	0.89	1.28
Sucrose 4°C	Exp. time (min)	0	1.35	15.08	30	60	90
	Concentration (g/L)	0.79 ± 0.01	0.73 ± 0.01	0.85 ± 0.03	0.96 ± 0.03	1.11 ± 0.02	1.16 ± 0.06
	Production rate (mmol/min)		-0.48	0.1	0.08	0.06	0.02
Sucrose 20°C	Exp. time (min)	0	2	15	30.3	60.16	90
	Concentration (g/L)	0.32 ± 0.04	0.29 ± 0.02	0.46 ± 0.07	0.54 ± 0.16	0.8 ± 0.06	0.84 ± 0.06
	Production rate (mmol/min)		-0.13	0.15	0.06	0.1	0.02

Figure 3.4 and Figure 3.5 show the concentration of solutes in the cell extracts. It appeared that sugars were rapidly taken up by the cells, as in the first two minutes of exposure there was an increase from 0 g sugar taken up/g of to 0.018 and 0.016 g/g of cells for glucose at 4 and 20°C, and to 0.031 and 0.035 g/g of cells for sucrose at 4 and 20°C. For both sugars, there was no clear difference between the uptake at 4 and 20°C. Yet, it was expected that the entry at 4°C would be facilitated because at this temperature the lipid membrane partly crystallises and thus become more permeable (Leslie et al., 1995). In the case of *Lb. rhamnosus*, there are several transport systems for both sugars, and this strain has shown high affinity for mono and disaccharides (Gopal, Sullivan, et al., 2001). This could therefore, explain the similarities in term of solute uptake at both temperatures.



**Figure 3.4:** Glucose (orange) and lactic acid (blue) concentrations in cell pellet after exposure to glucose at 4°C (dashed line) or at 20°C (solid line). Data are shown as the mean of triplicates and the error bars represent the standard error.



**Figure 3.5:** Sucrose (red) and lactic acid (blue) concentrations in cell pellet after exposure to sucrose at 4°C (dashed line) or at 20°C (solid line). Data are shown as the mean of triplicates and the error bars represent the standard error.

### 3.3.3 Impact of the different exposure times on the stability of dried *Lb. rhamnosus*

The main purpose of this study was to find the ideal exposure time and temperature for the probiotic which would lead to better stability after drying. It was thought that the catabolism of the glucose could have a detrimental effect on the stability of *Lb. rhamnosus* as lactic acid is produced and as bacteria start a new growth phase. As previously shown, the amount of sugar interacting with the cells was constant during the 90 minutes of exposure. This means the sugars could potentially be interacting with the cells from the first minute of exposure. Thus, it was assumed that the time and temperature

of exposure would not have any positive effect on the cell viability. The time of exposure was increased to up to 4 hours in order to verify this assumption. Therefore as was done in the exposure study, the cells were exposed at 4 or 20°C to a sucrose or glucose solution and then freeze-dried. The solutions were made of an equal mix of the sugar and inulin to facilitate the freeze-drying. Inulin was also chosen as it has been shown to have protective properties which have been attributed to its random coil structure, allowing the molecule to interact with the cell membrane (Vereyken, Albert van Kuik, Evers, Rijken, & de Kruijff, 2003). The weight concentration had to be the same for glucose and sucrose solutions, to avoid difference in protection due to the difference in mass. The details of the treatments are presented in Table 3.2.

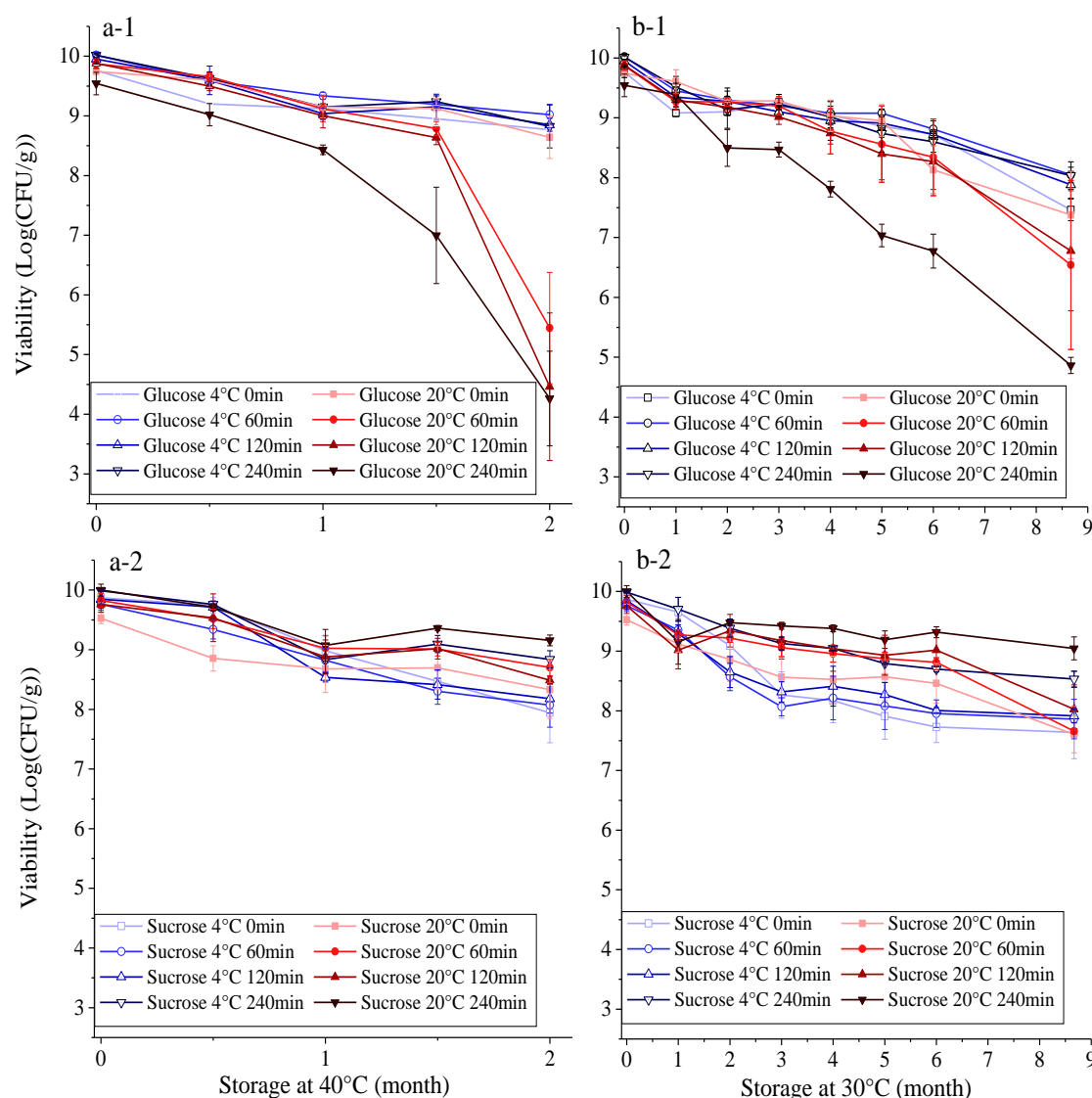
**Table 3.2:** Details of the protectant solution and the exposure settings for the shelf-life study of freeze-dried *Lb. rhamnosus*

Sample name	Protectant solution				Exposure settings	
	Glucose (g)	Sucrose (g)	Inulin (g)	Phosphate buffer (g)	Temperature (°C)	Time (min)
G-4-0	12.5	0	12.5	100	4	0
G-4-60	12.5	0	12.5	100	4	60
G-4-120	12.5	0	12.5	100	4	120
G-4-240	12.5	0	12.5	100	4	240
S-4-0	0	12.5	12.5	100	4	0
S-4-60	0	12.5	12.5	100	4	60
S-4-120	0	12.5	12.5	100	4	120
S-4-240	0	12.5	12.5	100	4	240
G-20-0	12.5	0	12.5	100	20	0
G-20-60	12.5	0	12.5	100	20	60
G-20-120	12.5	0	12.5	100	20	120
G-20-240	12.5	0	12.5	100	20	240
S-20-0	0	12.5	12.5	100	20	0
S-20-60	0	12.5	12.5	100	20	60
S-20-120	0	12.5	12.5	100	20	120
S-20-240	0	12.5	12.5	100	20	240

Cells exposed to sucrose at 20°C for 0 min, and to glucose at 20°C for 240 min, were the most impacted by the freeze-drying step, with a post drying viability of 9.53 and 9.56 log (CFU/g) respectively (Table 3.3 and Figure 3.6). Even though the cell count was not performed right before drying, each block of samples came from the same batch. The only difference between each sample would be the exposure to the solution. During the exposure time, cells may be exposed to acid stress (with a maximum reduction of pH from 7.2 to 6.7 for cell exposed to glucose at 20°C for 4 hours), cold stress (4°C and 20°C) and/or nutrient shortage. None of these stresses are known to be lethal, and it is thus assumed that the number of viable cell before drying is the same, or relatively close, for all samples. Cells exposed to sucrose for 240 min at 20°C presented a higher viability after drying, with a cell count of 10.0 log (CFU/g). Statistical analysis of cell viability after drying revealed a 3-way interaction between the sugar, the temperature and the time (see Table 3.4), highlighting that the exposure settings definitely had different impacts on the cells depending on the sugar used. This is most likely due to the catabolism of glucose.

When the samples where catabolism took place were stored, the viability of *Lb. rhamnosus* substantially decreased (cells exposed to glucose at 20°C for 240 min for both storage conditions). This was closely followed by cells exposed to glucose at 20°C for 120 and 60 min, when stored at 40°C. Cells exposed to glucose at 4°C had a similar trend, with death rate increasing with the increase in exposure time. However, this increment was not significant.





**Figure 3.6:** Shelf-life study conducted at 40°C (column a) and 30°C (column b) of *Lb. rhamnosus*

exposed to glucose (row 1) or sucrose (row 2), at 20°C (in red) and 4°C (in blue) for 0 min up to 240 min.

Data are shown as mean of triplicates and the error bars represent the standard error

On the other hand, cells exposed to sucrose, resulted in a lower death rate with increasing exposure time at either exposure temperature. This confirms that the optimal exposure settings for *Lb. rhamnosus* depend on the type of sugar. The statistical model showed significant 3-way interactions (sugar, temperature, time) explaining the death rate of cells stored at 40°C (Table 3.4). However, it was not the case for powders stored at 30°C, where only the interactions between sugar and temperature, and between sugar and

time were significant. Use of higher storage temperature may exacerbate differences between samples so weaker samples are more susceptible to the increase of temperature explaining the differences seen in the models.

The clear increase in death rate with the increase in exposure time to glucose at 20°C, confirms that the catabolism occurring during the exposure is detrimental for the cell stability. There are three possible explanations for this result. First, as the cells produce lactic acid, the pH of the protective solution decreases slightly (from 7.2 to 6.7), affecting the cells over time. This pH change was not observed when cells were exposed to sucrose. Second, when cells were exposed to the glucose solution at 20°C, the rate of use was about 6 g/L of glucose per hour. Thus, after 4 hours, the final concentration would be close to 7.6 % (w/w), instead of 10 % (w/w), and may not have been enough to protect the cells through the dehydration process and subsequent storage. Finally, as the cells use glucose over the time of the exposure, they start a new growth phase, thus becoming less resistant as the cells in early stationary phase are most stable. It appears that the variation in cell viability is bigger for cells exposed to glucose at 20°C, with standard deviation reaching up to 2.45 log (CFU/g) (see Table 3.3). As during the exposure cells are active, small differences in the harvesting could have led to wide differences in the use of glucose, hence in the stability of the cells. Strasser et al. (2009) found similar results for other strains. *Enterococcus faecium* and *Lactobacillus plantarum* were exposed to protectants at room temperature for 1 hour. The strains dried with glucose, had a shorter shelf-life than those dried with maltodextrin, trehalose or sucrose. As they did not compare different exposure settings, we cannot be certain that this effect was caused by the activity of the cells. However, the present results might shed some further light on their results as the low shelf-life of cells dried with glucose could have been due to its metabolism.

On the other hand, *Lb. rhamnosus* stability seemed to increase with increasing length of exposure time to sucrose, indicating that the sugar slowly entered or interacted with the cells, increasing its protective effect. To answer this hypothesis, the heat stability of the whole cells was assessed using calorimetry.

**Table 3.3:** Viability after drying and over storage of *Lb. rhamnosus* exposed to glucose or sucrose at 4 or 20°C for up to 4 hours prior to drying. Values are expressed in their arithmetic mean with their standard deviation.

Exposure treatment			Viability after drying	Shelf-life at 40°C		Shelf-life at 30°C	
				Viability after 2 months	Death rate at 40°C	Viability after 8.5 months	Death rate at 30°C
Glucose	4	0	9.76 ± 0.16	8.77±0.09	0.45 ± 0.07	7.46 ± 0.31	0.17 ± 0.07
Glucose	4	60	10.02 ± 0.09	9.02 ± 0.30	0.48 ± 0.08	8.05 ± 0.22	0.17 ± 0.03
Glucose	4	120	9.95 ± 0.14	8.85 ± 0.19	0.53 ± 0.13	7.88 ± 0.39	0.19 ± 0.03
Glucose	4	240	10.01 ± 0.06	8.82 ± 0.62	0.55 ± 0.20	8.03 ± 0.40	0.21 ± 0.06
Glucose	20	0	9.74 ± 0.07	8.64 ± 0.61	0.54 ± 0.29	7.38 ± 1.27	0.26 ± 0.18
Glucose	20	60	9.87 ± 0.14	5.44 ± 1.62	1.95 ± 0.57	6.54 ± 2.45	0.29 ± 0.32
Glucose	20	120	9.88 ± 0.13	4.46 ± 2.14	2.34 ± 0.80	6.78 ± 1.74	0.30 ± 0.22
Glucose	20	240	9.54 ± 0.33	4.26 ± 1.37	2.52 ± .60	4.86 ± 0.23	0.52 ± 0.08
Sucrose	4	0	9.87 ± 0.14	7.94 ± 0.87	1.02 ± 0.47	7.64 ± 0.76	0.36 ± 0.13
Sucrose	4	60	9.76 ± 0.17	8.07 ± 0.64	0.88 ± 0.41	7.86 ± 0.58	0.28 ± 0.13
Sucrose	4	120	9.85 ± 0.26	8.18 ± 0.42	0.93 ± 0.31	7.92 ± 0.21	0.27 ± 0.08
Sucrose	4	240	9.99 ± 0.01	8.84 ± 0.25	0.46 ± 0.29	8.53 ± 0.23	0.20 ± 0.03
Sucrose	20	0	9.53 ± 0.16	5.55 ± 0.84	0.51 ± 0.45	7.60 ± 0.54	0.16 ± 0.08
Sucrose	20	60	9.83 ± 0.20	8.70 ± 0.24	0.55 ± 0.15	7.66 ± 0.07	0.16 ± 0.03
Sucrose	20	120	9.76 ± 0.22	8.49 ± 0.10	0.44 ± 0.27	8.03 ± 0.71	0.09 ± 0.12
Sucrose	20	240	10.00 ± 0.17	9.16 ± 0.16	0.41 ± 0.11	9.05 ± 0.33	0.07 ± 0.01

**Table 3.4:** Statistical analysis of the factorial design for the stability of *Lb. rhamnosus* after freeze-drying and over storage.

Significance of the factors (p-value)	Viability after drying	Shelf-life at 40°C		Shelf-life at 30°C	
		Viability after 2 months	Death rate at 40°C	Viability after 8.5 months	Death rate at 30°C
Sugars (S)	NS	<0.0001	<0.0001	0.002	NS
Temperature (Temp)	0.013	<0.0001	<0.0001	0.019	NS
Time (T)	NS	NS	0.054	NS	NS
S*Temp	NS	<0.0001	<0.0001	0.008	<0.0001
S*T	0.057	0.002	0.005	0.042	-
Temp*T	NS	0.017	0.008	-	-
S*Temp*T	0.053	0.02	-	-	-
R <sup>2</sup> of the model	50.29%	83.17%	78.77%	48.4%	33.26%
Predicted R <sup>2</sup>	0%	61.26%	58.76	17.37%	8.04%

NS: Not significant (P&lt;0.05)

Factors excluding from the model are denoted with the “-“

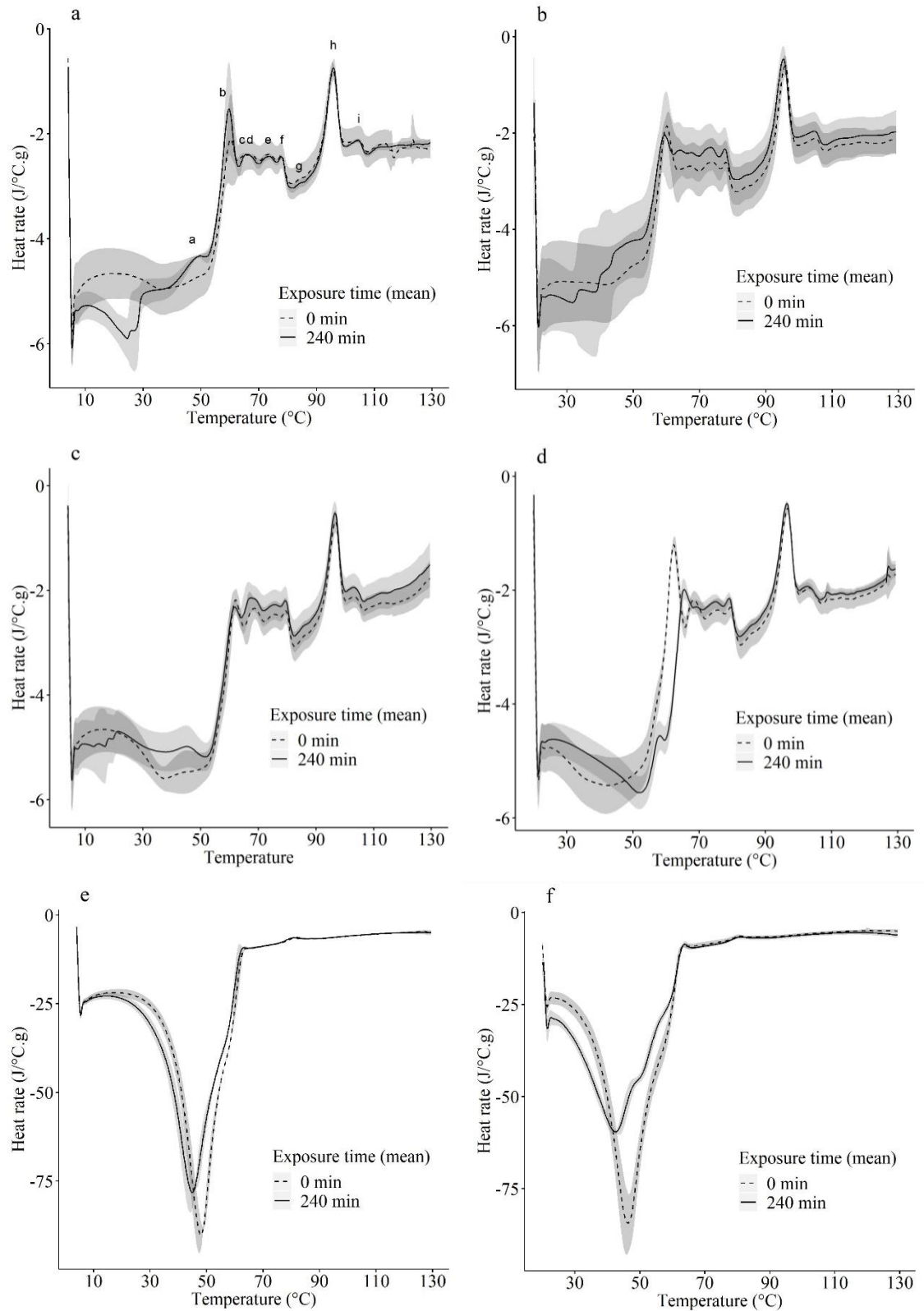
### 3.3.4 Understanding the interaction between the sugars and *Lb. rhamnosus*

In this study, *Lb. rhamnosus* cells were exposed to both sugar solutions and to phosphate buffer with four exposure conditions: 4°C for 0 and 4 hours, and 20°C for 0 and 4 hours, before being run on the Nano DSC. The averaged thermograms in Figure 3.7 show a clear difference between the cells exposed to glucose and the cells exposed to sucrose or to the control (buffer). Cells exposed to glucose presented a large exothermic peak, with a maximum between 40 and 50°C. The enthalpy of the peaks varied with the time and temperature of exposure. The smaller the peak, the less responsive the cells are to the glucose. The thermogram of cells that have been previously exposed 4 hours to the glucose, at 20°C, show a smaller exothermic peak meaning that less glucose have been used. During the 4 hours at 20°C, the cells had metabolised glucose and produced lactic acid. The pH drop (from 7.2 to 6.7) would have caused stress to the cells, resulting in

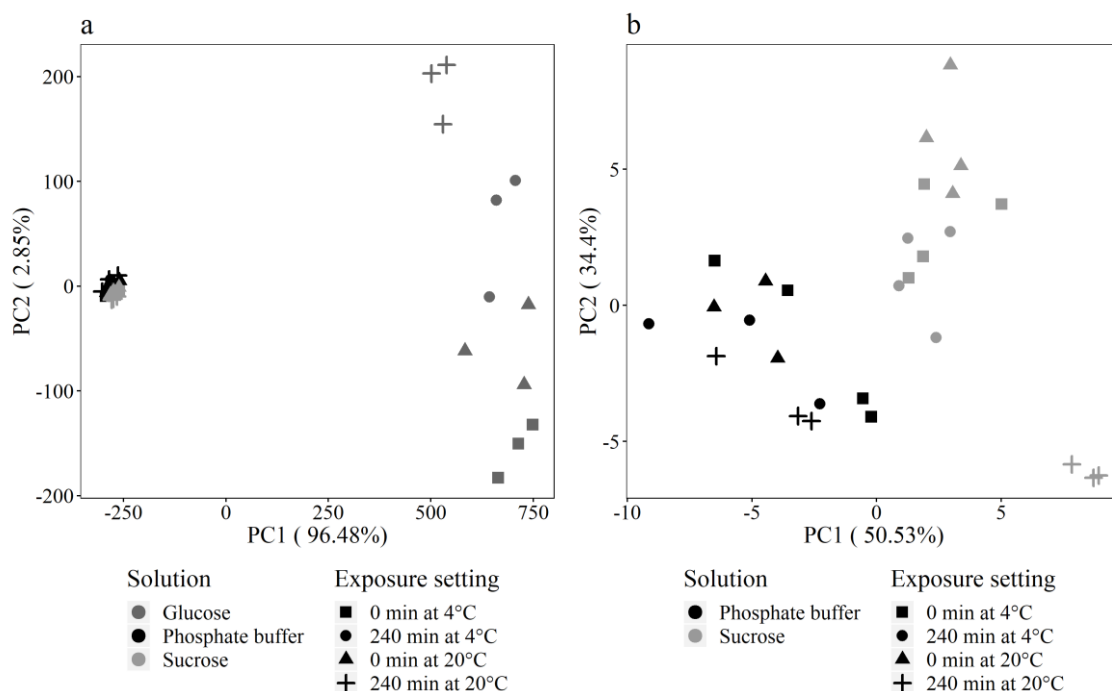
either a loss of viable cells or a lower ability to use the glucose present. As mentioned earlier, this self-imposed stress should not be lethal to the cells, thus it is more likely that the cell response to the stress decreased their metabolic response to glucose.

One to two shoulders were present on the exothermic peak: one at 49°C for cells exposed at 20°C for 4 hours, and one at 57°C for all cells exposed to glucose. It is most likely that an endothermic event occurred at the same time as the exothermic event. Even though there were no major endothermic events occurring at 49°C for the cells exposed to phosphate buffer only, or to the sucrose solution, as the cells metabolise the glucose, they were less stable to heat, and denaturation of biomolecules are most likely to occur at lower temperatures. This was confirmed by the overall instability to heat for the cells exposed to glucose. Indeed, from 63°C, the exothermic event ends and was followed by only three endothermic events: one directly after, between 63 and 63.5°C, one at 81°C and one around 85.5°C. From 92°C there were no more endothermic events, and the cells were thus completely denatured. This is a major difference from cells exposed to phosphate buffer and to sucrose, as their last events occurred around 108°C. This shows that glucose is not a good heat stabiliser for *Lb. rhamnosus*.

The PCA of the raw data (Figure 3.8) confirmed the grouping of samples exposed to phosphate buffer and sucrose compared to the cells exposed to glucose. These clusters were explained by the first principal component (PC). The second PC allows the separation of different exposure settings, following this order: cells exposed to glucose at 4 hours at 20°C, 4 hours at 4°C, 0 min at 20°C and 0 min at 4°C. Nano DSC is thus a technique which can potentially be used to measure the response of bacterial cells to a metabolisable sugar.



**Figure 3.7:** Thermograms of cells exposed to phosphate buffer (control, in graphs a and b), to sucrose (graphs c and d) or to glucose (graphs e and f) at 4°C (a,c and e) or 20°C (b,c and f) for 0 min (in dashed line) or 240 min (in solid line). The curve is the mean value of triplicates, and the standard deviation is denoted as the ribbon.



**Figure 3.8:** First and second principal components explaining the variance between all the thermograms of cells exposed to the different solutions. The thermograms of cells exposed to the phosphate buffer, glucose or sucrose solution, before baseline removal, are presented on the left (a). Thermograms of cells exposed to sucrose and phosphate buffer, after removal of the baseline are presented on the right (b).

The thermograms of the cells exposed to phosphate buffer and to sucrose were similar to each other. Between 10 to 50°C, and 110°C, the thermograms baseline follow a general increase. This corresponds to an increase in heat capacity ( $\Delta C_p$ ) which denotes the increase in energy required to increase the temperature of the solution. As the proteins unfold during the heating process, the non-polar moieties are being exposed, and the re-organisation of the water molecules around them cause the change in  $\Delta C_p$  (Bruylants, Wouters, & Michaux, 2005).

Overall, the effects of exposure on the samples were quite repeatable, with peaks location being maintained between replicate. However, the enthalpy of the peaks did present some variations (Figure 3.7). This meant that larger peaks could hide adjacent peak(s). The PCA of the thermogram of cells exposed to phosphate buffer and to sucrose,

after the removal of the baseline is presented in Figure 3.8 (b) and confirms the repeatability between samples. The samples are relatively well grouped together, with a clear clustering of cells occurring for samples exposed to the two solutions. Additionally, the cells exposed to sucrose for 240 min at 20°C were clearly clustered together aside from all the other samples.

Nine endothermic peaks were located on the thermograms of cells exposed to phosphate buffer. They were located between 45 and 110°C and were assigned a letter from “a” to “i” for ease of analysis (Figure 3.7 (a)). The main characteristics of the nine peaks, such as temperature at maximum and maximum heat flux (height of the peak) after removal of the baseline (Figure 3.9), are given in Table 3.5. It was not possible to fit the curve and calculate area of individual peaks, as the thermograms were too complex, so in order to avoid over-estimation of some of the peaks, only the melting temperature and the maximum heat flux of the peaks were reported.

An exothermic peak appeared between 20 and 45°C when the cells were exposed to the solution for 4 hours. The temperature of the peak extremes depended on the time of exposure – around 25°C for cells exposed at 4°C, and between 32 and 45°C when exposed at 20°C. There was more variation for the cells exposed at 20°C. Because the enthalpy of peak varied between samples, larger peaks could have hidden adjacent peak(s), and it was not always possible to find the 9 peaks on the thermograms.



**Table 3.5:** Mean value of peak maxima (T<sub>m</sub>) and maximal heat flux (C<sub>p</sub><sup>T<sub>m</sub></sup>) of the cells exposed to phosphate buffer or sucrose solution at 4 or 20°C for 0 min or 240 min.

Phosphate buffer at 4°C				Phosphate buffer at 20°C				Sucrose at 4°C				Sucrose at 20°C					
0 min		240 min		0 min		240 min		0 min		240 min		0 min		240 min			
T <sub>m</sub>	C <sub>p</sub> <sup>T<sub>m</sub></sup>	T <sub>m</sub>	C <sub>p</sub> <sup>T<sub>m</sub></sup>	T <sub>m</sub>	C <sub>p</sub> <sup>T<sub>m</sub></sup>	T <sub>m</sub>	C <sub>p</sub> <sup>T<sub>m</sub></sup>	T <sub>m</sub>	C <sub>p</sub> <sup>T<sub>m</sub></sup>	T <sub>m</sub>	C <sub>p</sub> <sup>T<sub>m</sub></sup>	T <sub>m</sub>	C <sub>p</sub> <sup>T<sub>m</sub></sup>	T <sub>m</sub>	C <sub>p</sub> <sup>T<sub>m</sub></sup>		
(°C)	(J/°C.g)	(°C)	(J/°C.g)	(°C)	(J/°C.g)	(°C)	(J/°C.g)	(°C)	(J/°C.g)	(°C)	(J/°C.g)	(°C)	(J/°C.g)	(°C)	(J/°C.g)		
a	48.9	0.0	48.6	0.1	49.9	0.1	50.0	0.1	51.0	0.0	48.1	0.0	51.5	0.0	49.4	0.0	
b'	NP	NP	NP	NP	NP	NP	NP	57.5	0.4	57.2	0.4	57.8	0.5	57.7	0.3		
b	59.7	1.6	59.6	2.0	60.1	2.0	59.2	1.5	61.7	1.9	61.6	1.6	62.3	2.5	65.4	1.9	
c	64.2	1.1	65.1	0.8	64.8	0.8	64.3	0.8	67.6	1.1	66.5	1.1	NP	NP	NP	NP	
d	67.0	0.7	68.0	0.6	67.3	0.6	67.4	0.6	70.2	0.8	68.6	15.5	68.0	1.0	68.9	1.2	
e	73.2	0.5	73.7	0.5	73.9	0.5	73.6	0.6	75.5	0.6	75.1	0.6	75.5	0.5	73.1	0.9	
f	78.0	0.5	78.0	0.5	78.1	0.6	77.8	0.6	79.7	0.6	79.6	0.6	79.7	0.6	79.1	0.7	
g	84.0	0.0	84.0	0.0	84.0	0.0	83.7	0.0	85.9	0.0	85.8	0.0	85.8	0.0	85.6	0.0	
h	95.8	1.7	95.9	1.8	95.9	2.0	95.4	2.0	96.9	1.8	96.7	1.8	96.8	1.8	96.6	1.8	
i	104.6	0.2	104.5	0.3	105.1	0.3	104.8	0.3	103.2	0.3	103.1	0.3	103.2	0.3	102.7	0.2	

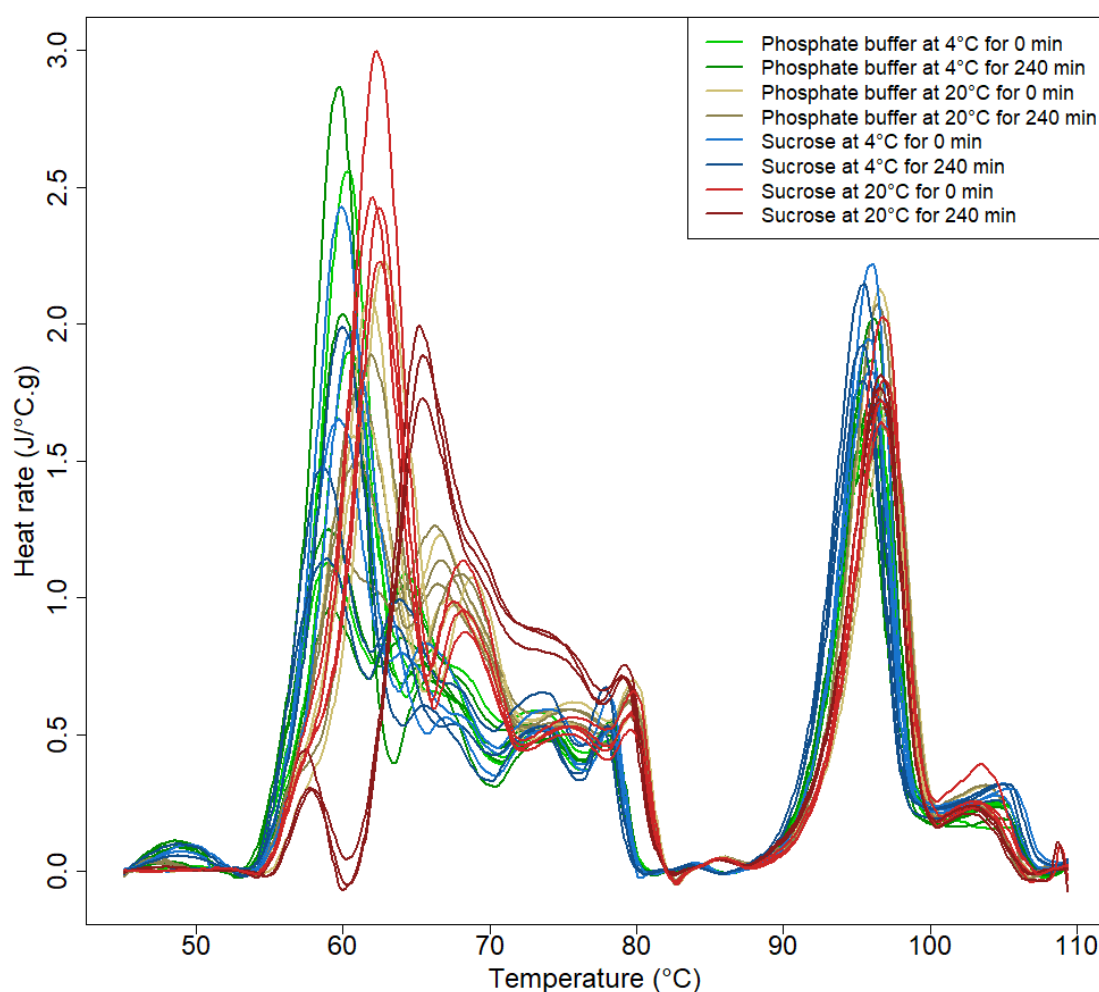
NP: not present

Cells exposed to sucrose at 4°C had a very similar pattern to cells exposed to phosphate buffer. However, there were three small differences. Firstly, the peak b was slightly smaller than for the cells exposed to phosphate buffer. Secondly, the exothermic peak occurred at a lower temperature: between 10 and 20°C. Finally, an additional peak appeared as shoulder around 57°C (which was called b') in some of the samples.

To compare the thermograms of the cells exposed to phosphate buffer and sucrose, the permanent part from 45 to 110°C was isolated. The baseline was then removed using the fill peaks method. When overlapping the thermographs (see Figure 3.9), a clear shift of seven peaks (b to h) toward higher temperatures could be distinguished, when cells were exposed to sucrose. Only the last endothermic peak (i) presented a maximum at a lower temperature when exposed to sucrose compared to phosphate buffer.

This shift to higher temperatures could be explained by two factors. Firstly, the stress induced by the increase in the osmotic pressure could lead to cells becoming more resistant to heat. Indeed, osmotically stressed cells produce general stress response proteins that can confer additional protection to the cells, including to heat stresses (Le Marrec, 2011; Xie et al., 2004; Zhang, Ji, Cheng, Xu, & Jin, 2018). Secondly, the presence of sucrose itself could protect the cells from heat by interacting with the different biomolecules e.g. by maintaining the proteins in their native form (Kilimann et al., 2006). This could explain why some biomolecules have high heat resistance and not others.

When exposing the cells to sucrose at 20°C, the peak b shifted to an even higher temperature (62.3°C when exposed 0 min and 65.4°C when exposed for 240 min). As a result, the peak b' was fully distinguishable when cells were exposed to sucrose at 20°C for 240 min. It is proposed that the shift is due to an interaction of the sucrose with the biomolecule. Over the 240 min at 20°C, the sucrose had the time to enter the cells, and interact with the biomolecules. This could explain why the cells exposed to sucrose at 20°C for 240 min had better stability during freeze-drying and over storage.



**Figure 3.9:** Thermograms of all samples exposed to phosphate buffer and to sucrose at 4 or 20°C for 0 min or 240 min after baseline removal.

The thermograms, shown in Figure 3.7 and Figure 3.9, were quite similar to what has been found in *Lb. plantarum* in the past (Lee & Kaletunç, 2002). The authors compared their results with a previous study on *E. coli* (Mackey et al., 1991), where they examined whole cells and cell components. They assigned the first major peak (peak b) to the biggest ribosomal unit. The denaturation temperature in *Lb. plantarum* was 63°C, which appeared to be close to the data from this study (between 59.6 and 60.2°C for cells exposed to phosphate buffer and 61 and 62.3°C when exposed to sucrose, with a maximum at 65.4°C for cells exposed to sucrose at 20°C for 240 min). The generally

lower denaturation temperature could be explained by the different heating rate: in their study they used 3°C/min with a standard DSC, while in this study, the rate was at 1°C/min, using a Nano DSC. With a faster heating rate, thermal events, such as denaturation, will occur at higher temperatures (Amani, Moosavi-Movahedi, & Kurganov, 2017). They found a smaller peak in *E.coli* at 56°C, that was associated with the 30S ribosomal unit but this peak was not visible on the *Lb. plantarum* thermogram. The b peak, which occurred around 57.5°C, and appeared when cells were exposed to sucrose, could correspond to this peak, obscured in the thermogram of cells exposed to phosphate buffer. Thus, sucrose would interact here with the bigger subunit of the ribosome when exposed to the solution for 240 min at 20°C. They also found a peak similar to the peak h in this study (around 95°C), occurring at 93°C in *Lb. plantarum* and associated to the DNA melting. *Lb. plantarum* genome has about 44.5% GC (guanine and cytosine nucleobases; Noda, Shiraga, Kumagai, Danshiitsoodol, & Sugiyama, 2018) compared to 46.7% for *Lb. rhamnosus* (Collett, Rand, Mason, & Stanton, 2008). This could explain this difference in melting temperature as a higher percentage of GC bases in the DNA lead to a higher melting temperature. The last peak (peak i, of about 105°C), was associated with cell wall components (Mackey et al., 1991). In order to confirm the identity of the peaks, extraction of cell components would be necessary as well as the analysis of their thermogram.

### 3.4 Conclusions

In this study, the nature of the interactions of cell components with protectants have been studied further, specifically looking at the effect of the exposure on the stability of *Lb. rhamnosus*, after drying and during storage. It was shown that, depending on the sugars used, the exposure might diminish or improve the viability of the bacterial cells after drying. It is believed that the effect would also be different depending on the strain

of bacteria. The main finding derived from this study was that the exposure of protectants should be done under conditions where the cells are not metabolising sugars.

The Nano DSC has proven to be a promising technique to examine the interactions between various solutes and cells. In the case of metabolisable sugars, the Nano DSC can give some information on how much energy the cells can use from a particular sugar source. In addition, this technique quickly showed interactions of the cells with protectants, i.e. sucrose. The shift of one peak toward higher melting temperatures could be related to the higher stability of the cells during storage. However, more studies comparing different solutes, their impact on the cell thermograms and the resulting stability of cells, are needed.

This first study allows the standardisation of the exposure settings for *Lb. rhamnosus* HN001 before drying. The exposure temperature was set at 4°C, to avoid any catabolism, and 1 hour was chosen as exposure time as it led to relatively good results for both sugar.

## Chapter 4 – Effect of different protectants on the viability of *Lactobacillus rhamnosus* during storage

---

### 4.1 Introduction

As mentioned previously, freeze-drying subjects bacterial cells to two different stresses: a freezing stress and a drying stress. Both stresses can cause cell damage, such as disruption of the membrane or protein denaturation, and can lead to cell death. Uptake of osmoprotectants and/or cryoprotectants by the cells could prevent the cell damage and protect intracellular biomolecules. As discussed previously (section 2.4.3), different strains respond differently to different protectants. Therefore, this study aims to find the most suitable protectant to enhance the stability of *Lb. rhamnosus* HN001 throughout the freeze-drying process and over storage.

In order to obtain optimal protection, protectants were selected according to three criteria. First, the potential protectant should be a small molecule, i.e. no bigger than a disaccharide so inferior to 350 g/mol. Second, the bacteria should be able to uptake or utilise this protectant. These two criteria would ensure the uptake of the solute, and thus the ability of the protectant to act, at first, as an osmoprotectant. Thirdly, protectant should have recognised effect on the bacteria genus, or have a potential protective effect. Six first protectants were selected based on these criteria, as they showed promising results on *Lb. rhamnosus*: sorbitol, MSG, fructose, glucose, lactose and sucrose (Carvalho et al., 2002; Jofré et al., 2015; Roos & Pehkonen, 2010; Saarela et al., 2006; Savini et al., 2010; Siaterlis et al., 2009; Sunny-Roberts & Knorr, 2009; Zhu et al., 2013). These protectants may as well protect the strain under study.

Galactoligosaccharides, containing a small amount of galactose, showed good results in the dried stability of *Lactobacillus* strains (Chen et al., 2014; Tymczyszyn, Gerbino, Illanes, & Gómez-Zavaglia, 2011). However, no study has investigated the effect of galactose itself on *Lb. rhamnosus*. In addition, trehalose is well recognised as a dehydration protectant that presents both a high glass transition temperature and the ability to interact with phospholipid headgroups (Crowe, Reid, & Crowe, 1996). These properties have been attributed to its unique clam shell conformation that allows the formation of more hydrogen bonds than other disaccharides (Albertorio et al., 2007). However, trehalose has not always been shown to be the best protectant during storage of freeze-dried *Lb. rhamnosus* (Carvalho et al., 2002) and therefore it would be interesting to compare it with other protectants. Finally, betaine is a promising osmoprotectant, which is naturally accumulated by bacteria when facing an osmotic stress (Glaasker et al., 1996; Glaasker et al., 1998; Hutkins et al., 1987; Sheehan et al., 2006; Zhao et al., 2014). However, no study looked at the potential impact of betaine on the storage stability of freeze-dried *Lb. rhamnosus*.

In this study, nine protectants namely, galactose, fructose, glucose, lactose, sucrose, trehalose, MSG, sorbitol and betaine, were compared for their effect on freeze-dried *Lb. rhamnosus* HN001 stability during storage at 30°C. To understand how interactions between protectants and cells affect the preservation of dried probiotics, Nano DSC was used to compare best performing protectants to less performing ones.

## 4.2 Material and methods

### 4.2.1 Materials

Inulin (Frutafit TEX, degree of polymerisation (DP)  $\geq 22$ ) was obtained from IMCD New Zealand Ltd., Auckland, New Zealand. Betaine, L-glutamic acid monosodium salt monohydrate (MSG), D-(+)-galactose and D-sorbitol were all bought

from Sigma Aldrich, Saint-Louis, MO. Analytical grade glucose and sucrose were obtained from Thermo Fisher Scientific, Waltham, MA. Trehalose was purchased from Med-Chem ingredients limited, Auckland, New-Zealand.

#### **4.2.2 Shelf-life study**

Cells were grown as described earlier (section 3.2.3), harvested at the start of the stationary phase, i.e. after 16 hours or when the absorbance reached 1.7, before being exposed to the protective solutions for 1 hour at 4°C and freeze-dried as detailed in section 3.2.6. Solution were made with 12.5% (w/v) of inulin and 12.5% (w/v) of one of the nine protectants (fructose, galactose, glucose, sucrose, lactose, trehalose, MSG, sorbitol and betaine). Freeze-dried powders were kept in a closed container and stored at 30°C for 6 months. The viability of the cells was monitored using the plate count method.

#### **4.2.3 Water activity measurement**

Water activity of the powders after freeze-drying was measured using a Decagon AquaLab 4TE water activity instrument (Decagon Devices Inc., WA, USA) at 20°C.

#### **4.2.4 Nano differential scanning calorimetry**

This study followed the same methods as presented in section 3.2.8, Nano DSC, with some modifications. Firstly, 15 mL of bacterial culture were centrifuged, washed twice with buffer and exposed to 15 mL of the protectant solutions maintained at 4°C. The bacterial cells were exposed to five different protectants: sorbitol, MSG, betaine, sucrose and galactose. Solutions were made up of 12.5% (w/v) of one of the protectant in phosphate buffer. Bacterial cells in phosphate buffer were used as controls. The cellular suspension was allowed to equilibrate for 1 hour at 4°C for equilibration, before spinning down the cells and re-suspending them in 1.5 mL of the same solution, to concentrate the cells 10 times. After degassing the slurry for 10 min, the samples were scanned from 4°C



to 130°C at 1°C/min, against the reference: phosphate buffer. The blank was subtracted from the sample thermogram and normalised to the weight concentration of the sample, before further analysis.

#### **4.2.5 Data analysis and statistics**

ANOVA was conducted on the shelf-life results using Minitab® 18.1. Thermograms from the Nano DSC were analysed by R 3.5.0 following the same process as described in section 3.2.9.

### **4.3 Results and discussion**

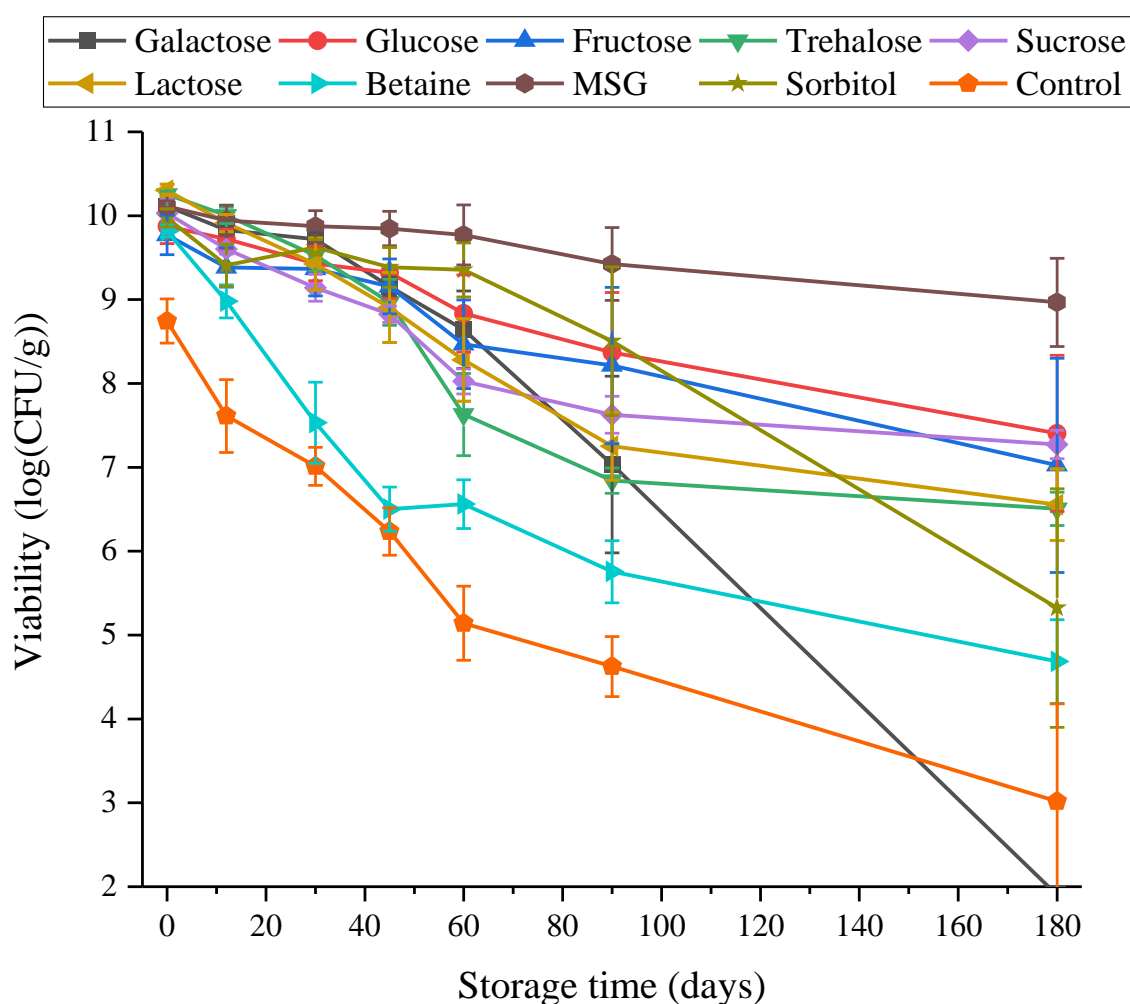
#### **4.3.1 Effect of different protectants on bacterial viability**

After finding the right exposure settings before drying (i.e. allowing the cells to equilibrate for one hour at 4°C, Chapter 3), the next step toward long-term survivability of *Lb. rhamnosus* HN001 in freeze-dried powders, was to find the protectants that best stabilise the bacteria over storage. For that purpose, nine desiccation protectants were compared for their impact on the bacterial stability – galactose, glucose, fructose, trehalose, sucrose, lactose, betaine, MSG and sorbitol. Each protectant needed to be tested and compared individually prior to exploring potential synergistic combinations. In this study, protectants were mixed with inulin (1:1 ratio), which was used as a carrier to improve drying efficiency.

The water activity of the powders following freeze-drying was mostly below 0.1 (Table 4.1) with the exception of the MSG samples which showed a higher water activity. Further drying of these samples, i.e. the samples were re-frozen and freeze-dried again, showed no change and so the samples were stored in their current state. The difficulty in drying the MSG samples could be due to the collapse or partial collapse of the powder during the drying process, preventing efficient drying. As each replicate was dried in a

new batch of freeze-drying, small variations in the drying process could have explain the variations in water activity values between replicates.

Samples dried with inulin alone (control) had the lowest viability after drying (8.74 log (CFU/g)) (Table 4.2). Mixing of the small molecular weight protectants with inulin significantly improved the survival to freeze-drying by up to 2.6 log (CFU/g), for samples dried with lactose. This confirmed that both penetrating and non-penetrating solutes are necessary for the protection of bacterial cells (Hubálek, 2003).



**Figure 4.1:** Stability of *Lb. rhamnosus* HN001 at 30°C. Each powder contained the protectant and inulin in a 1:1 ratio. Control consisted of inulin only. Each point represents the mean of triplicates, and the error bar represents the standard error.

**Table 4.1:** Water activity of the powders after freeze-drying prepared with a range of protectants  
(detailed values of the triplicates).

Water activity			
Sample	Replicate 1	Replicate 2	Replicate 3
Galactose	0.06	0.14	0.06
Glucose	0.11	0.08	0.10
Fructose	0.15	0.08	0.09
Trehalose	0.04	0.07	0.06
Sucrose	0.17	0.08	0.07
Lactose	0.05	0.06	0.05
Betaine	0.10	0.10	0.11
MSG	0.07	0.32	0.24
Sorbitol	0.07	0.17	0.05
Control (Inulin)	0.04	0.03	0.05

**Table 4.2:** Stability of *Lb. rhamnosus* HN001 in sugar powders after freeze-drying and over storage at 30°C. Data are expressed as the mean with the standard deviation of triplicates. Different superscript letters within the same column indicate significant differences (P<0.05)

Sugar	Viability after drying	Viability after 6 months	Death rate
	Log (CFU/g)	Log (CFU/g)	(/month)
Galactose	10.11 ± 0.08 <sup>a</sup>	≤ 2 <sup>b</sup>	1.24 ± 0.13 <sup>b</sup>
Glucose	9.88 ± 0.21 <sup>a</sup>	7.40 ± 0.93 <sup>a,b</sup>	0.43 ± 0.15 <sup>a,b</sup>
Fructose	9.87 ± 0.19 <sup>a</sup>	6.00 ± 1.37 <sup>a,b</sup>	0.65 ± 0.24 <sup>a,b</sup>
Trehalose	10.25 ± 0.04 <sup>a</sup>	6.50 ± 0.20 <sup>a,b</sup>	0.68 ± 0.02 <sup>a,b</sup>
Sucrose	10.03 ± 0.17 <sup>a</sup>	7.27 ± 0.17 <sup>a,b</sup>	0.46 ± 0.03 <sup>a,b</sup>
Lactose	10.30 ± 0.07 <sup>a</sup>	6.55 ± 0.43 <sup>a,b</sup>	0.65 ± 0.07 <sup>a,b</sup>
Betaine	9.82 ± 0.07 <sup>a</sup>	4.68 ± 0.50 <sup>a,b</sup>	0.79 ± 0.06 <sup>a,b</sup>
MSG	10.11 ± 0.07 <sup>a</sup>	8.97 ± 0.53 <sup>a</sup>	0.19 ± 0.08 <sup>a</sup>
Sorbitol	9.97 ± 0.11 <sup>a</sup>	5.32 ± 1.42 <sup>a,b</sup>	0.76 ± 0.24 <sup>a,b</sup>
Control	8.74 ± 0.26 <sup>b</sup>	3.02 ± 1.16 <sup>b</sup>	0.91 ± 0.27 <sup>a,b</sup>

Over the 6 months of the storage trial, there was a clear drop in *Lb. rhamnosus* viability when protectants betaine and galactose were present, and with the control (Figure 4.1). In contrast, cells dried with MSG presented a significantly better stability over the 6 months of storage (p-value = 0.007) with 1.1 log (CFU/g) and a final viability of about 9 log (CFU/g) (Table 4.2). In relation to cells dried with MSG, the performance of protectants followed the order: glucose, sucrose, fructose, lactose, trehalose and sorbitol.

Both sorbitol and galactose samples presented a relatively sudden drop from the second month of the shelf-life, but the cells dried with sorbitol were more stable, with a viability of 5.35 log (CFU/g) after 6 months. A rapid drop of the cell viability suggests that a detrimental event occurred to the freeze-dried powder, such as the crystallisation of the powder and/or an increase in water mobility. Galactose and glucose have a similar glass transition temperature of 30°C and 31°C respectively (Crowe, Hoekstra, et al., 1996; Roos, 1993). Thus, both powders should not have such different results if changes in the powder properties was the cause of bacterial loss. On the other hand, sorbitol has the lowest glass transition temperature of all samples at -3°C (Craig, Royall, Kett, & Hopton, 1999). Therefore, low glass transition temperature of the powder may not be sufficient to explain the rapid loss of bacterial cells. A weak interaction of galactose or sorbitol with the cells could also be behind this result. Overall, a deeper understanding of the cell and protectant interactions is needed to try and explain the drop in viability.

Interestingly, there was a positive correlation between the water activity and the viability after 6 months of the samples (with a Pearson correlation of 0.43 and p-value = 0.014) and a negative correlation between the water activity and the death rate (Pearson correlation of -0.42 and p-value = 0.015). Thus, the higher the water activity after drying, the better was the probiotic stability. For instance, the two MSG powders, which had the

highest water activities of 0.32 and 0.24 (replicate 2 and 3, Table 4.1), also showed the best viability after six months at 30°C with 9.1 and 9.8 log (CFU/g), respectively. In contrast, the last sample, which had a water activity of 0.07 after drying, resulted in a viability of 8 log (CFU/g) after six months. It was attempted to dry further the MSG samples, but this was unsuccessful. One possible reason is that the structure of the sample collapsed during the freeze-drying, thus preventing proper drying, and high water activity. As each replicates were dried in a different freeze-drying batch, small variation between the drying steps may have caused some powder to collapse (MSG powder replicate 2 and 3) and some to dry properly (replicate 1). It has been suggested that extreme desiccation is detrimental for the cells, and that there exists an optimum water activity for survival, which may depend upon the strain and would be between 0.1 and 0.2 (Castro et al., 1995; Scott, 1959). However, the positive correlation between the water activity and the viability of dried *Lb. rhamnosus* is in contrast to most previous studies (Albadran et al., 2015; Harel & Tang, 2014; Kurtmann, Carlsen, Risbo, et al., 2009; Kurtmann, Carlsen, Skibsted, et al., 2009; Tymczyszyn et al., 2012).

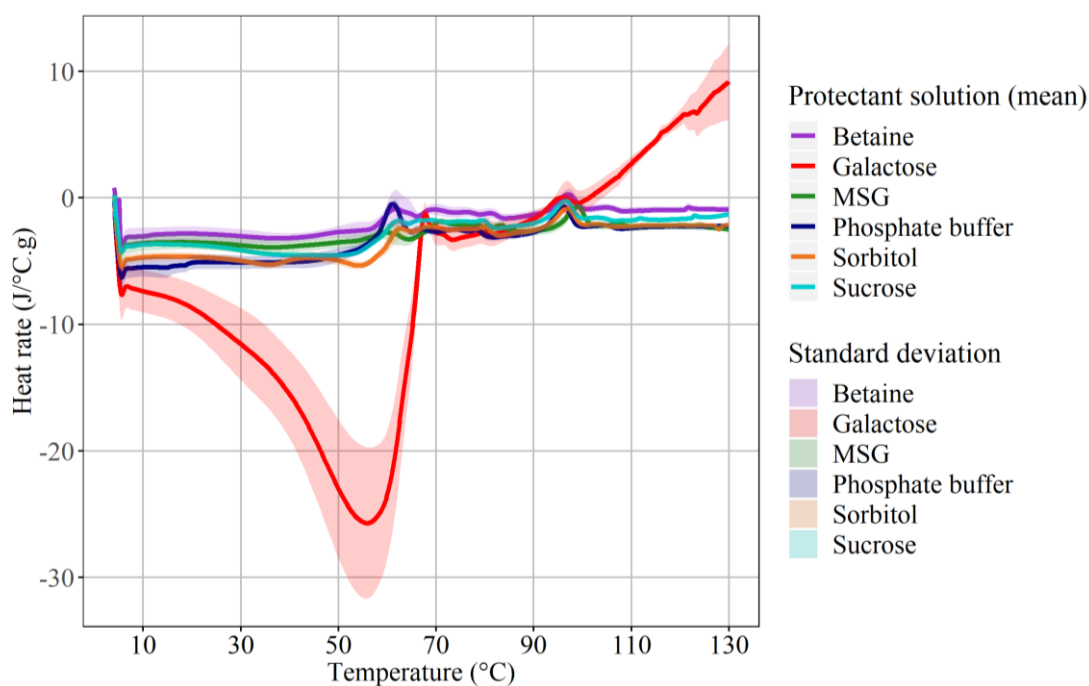
A better understanding of the powder structure and of the interactions of the protectant with the cells may help explaining the correlation between the water activity and the sample stability.

#### **4.3.2 Nano differential scanning calorimetry results**

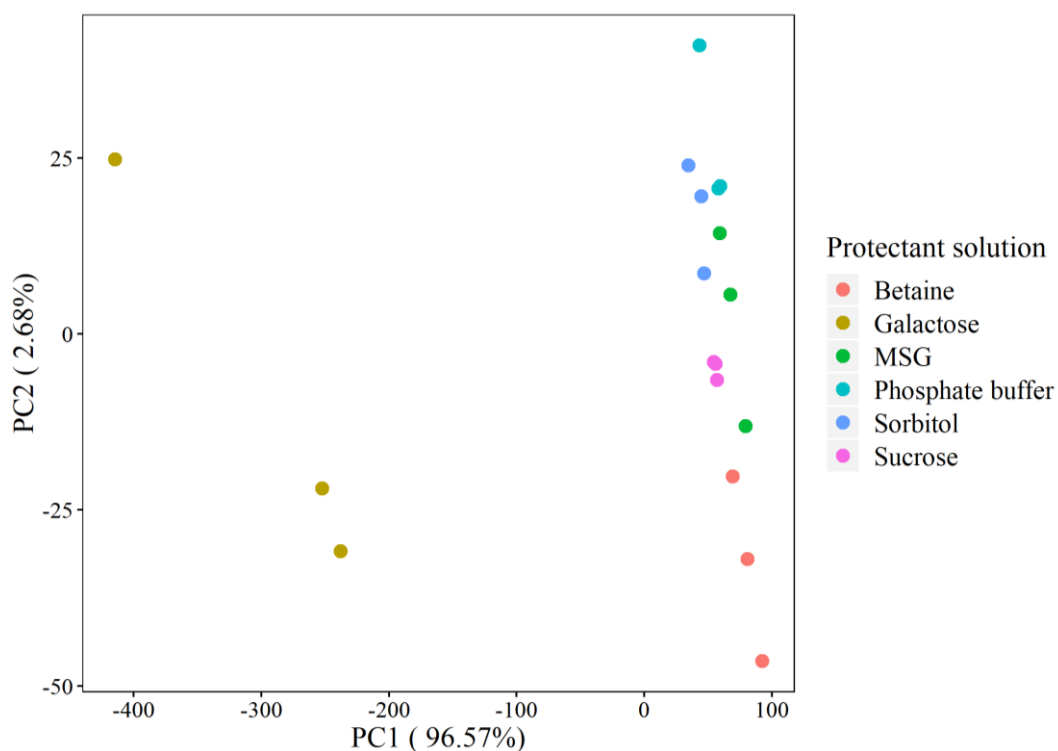
In order to explain the results from the shelf-life study the interaction of the protectants with *Lb. rhamnosus* was studied by Nano DSC. It was hypothesized that an increase in the stability of biomolecules against heat (i.e. a higher melting temperature or a higher enthalpy) would translate as an interaction between the protectant and the biomolecule and could be linked with a higher stability after drying, and over storage, as it was shown in the last chapter, when cells were exposed to sucrose at 20°C for 4 hours.

This technique might give an indication as to why galactose and sorbitol samples presented a sudden drop in viability after the second month of storage. These samples will be compared with the samples containing sucrose and MSG as they both led to good viability over the storage time. Finally, betaine has been discussed in the literature as a promising osmoprotectant. However, betaine gave very little protection to *Lb. rhamnosus* HN001. The use of Nano DSC might shed some light on why this might have been. Each protectant was prepared in phosphate buffer at 12.5% (w/v). A control sample, consisting only of phosphate buffer, was also prepared. Figure 4.2 presents the averaged thermograms for all samples.

The cells exposed to galactose showed a similar response to the one with glucose (see Chapter 3). There was a large exothermic peak with a maximum at 56°C, due to the metabolism of galactose. The height of the peak, however, was about half that of the exothermic peak found when cells were exposed to glucose. This means that the cells could not use as much energy from galactose as they did with glucose.

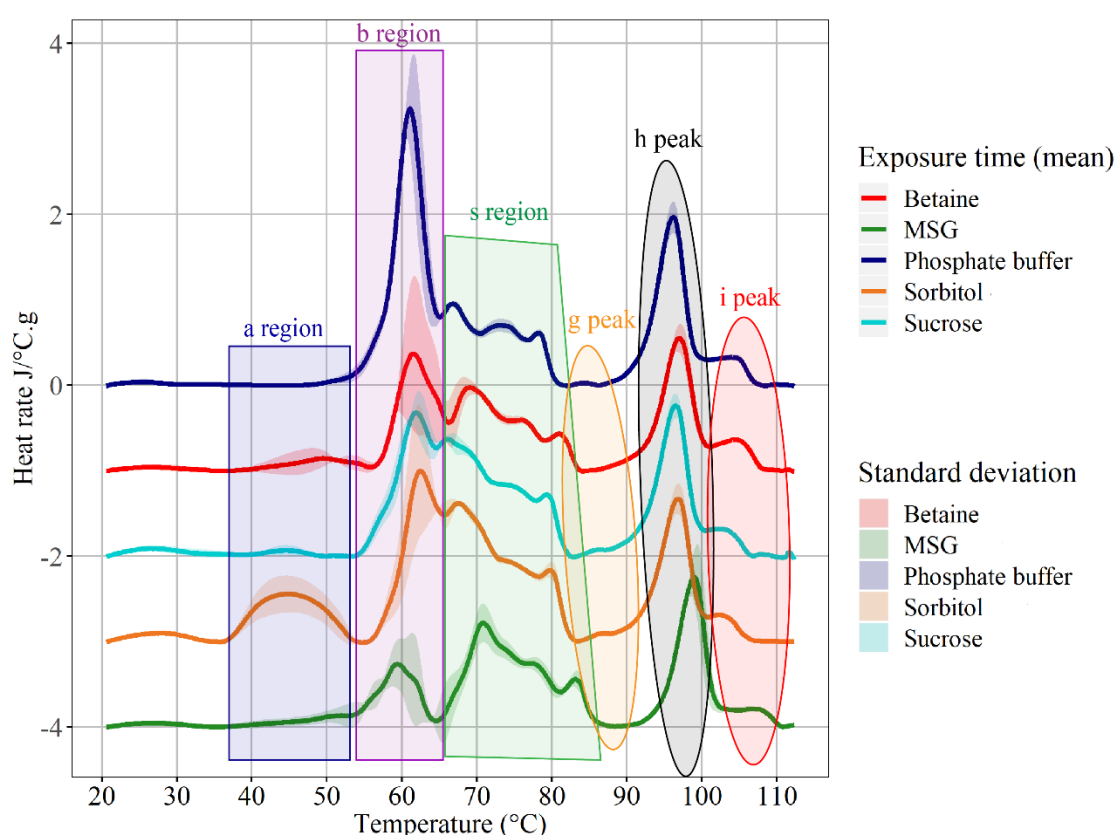


**Figure 4.2:** Thermograms of *Lb. rhamnosus* exposed to galactose, betaine, MSG, sorbitol or sucrose in phosphate buffer, or buffer alone. Data are shown as the mean of triplicates (in straight line) with their standard deviation (ribbon).



**Figure 4.3:** First two principal components of *Lb. rhamnosus* thermograms exposed to galactose, betaine, MSG, sorbitol or sucrose in phosphate buffer, or buffer alone.

Samples with sucrose and phosphate buffer showed good reproducibility, but more variations were found in scans of samples exposed to galactose, betaine, MSG and sorbitol variations, denoted by the standard deviation on Figure 4.2 and Figure 4.4. This is confirmed by PCA (Figure 4.3), where treatment types are clustered together but some variations persist. The main variations occurred between 40 and 70°C (see Figure 4.4). Phosphate buffer samples, however, presented the least variation, and thermograms were similar to that reported in Chapter 3.

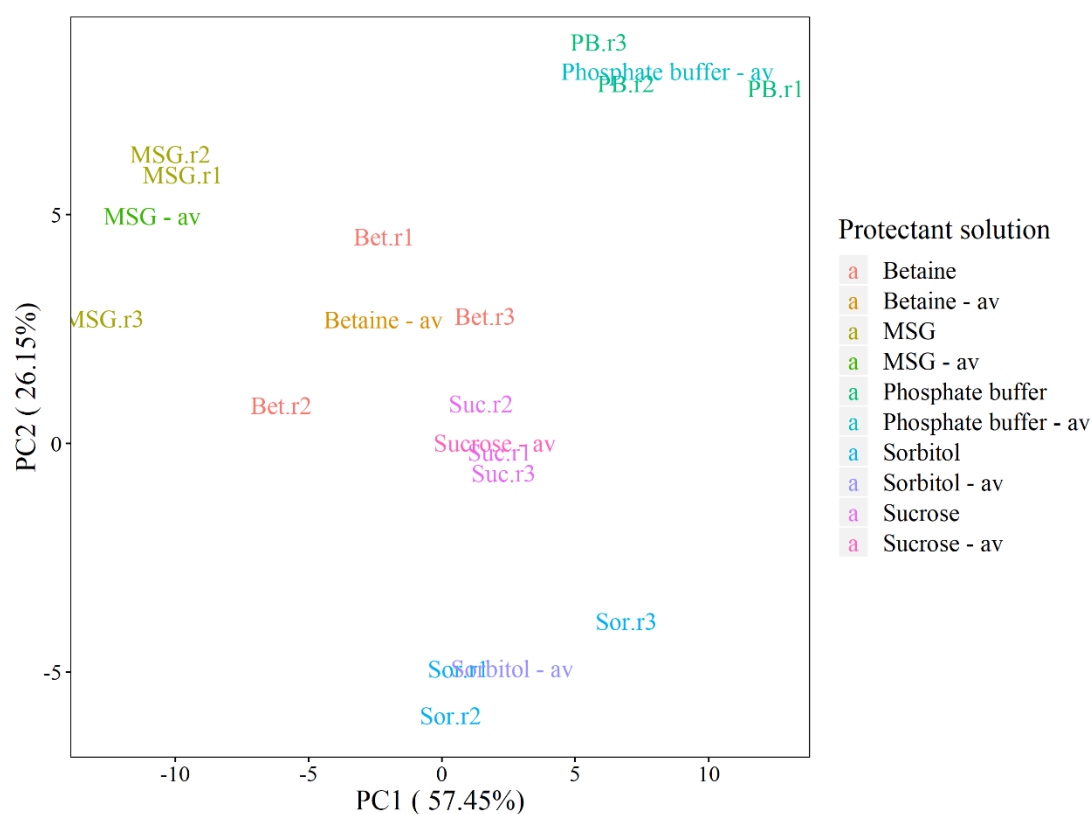


**Figure 4.4:** Baseline corrected thermograms of *Lb. rhamnosus* exposed to betaine, MSG, sorbitol, sucrose in phosphate buffer, or buffer alone. Mean value of triplicates are presented as the straight lines with their standard deviation (ribbon). Thermograms have been offset for clarity.

Each protectant led to a unique thermogram pattern, however the peaks were not always distinguishable (Figure 4.4). Thus, for ease of analysis, five main regions and



peaks were defined, grouping one or several endothermic events, as shown in Figure 4.4. The region a is situated between 35 and 54°C. The b region includes the first-major peak (T<sub>m</sub> around 61°C) which has been proposed to be due to the biggest ribosome subunit (see Chapter 3). This region was defined between 54 and 65°C and is followed by a series of 3 to 4 peaks with a characteristic staircase shape. This region was named the “s region” and starts around 65°C, finishing between 83°C and 87°C depending on the sample. Finally, the last three regions are defined as peaks g, h and i.



**Figure 4.5:** First two principal components of *Lb. rhamnosus* baseline corrected thermograms exposed to betaine, MSG, sorbitol, sucrose in phosphate buffer, or buffer alone. “av” stands for averaged thermogram, and “r” replicate.

The thermogram of cells exposed to MSG was the most different from the control (cells in phosphate buffer). This was confirmed by the PCA as both thermograms were separated on the first principal component, accounting for 57.45% of the variance between samples (Figure 4.5). The shape of the b region of cells exposed to MSG were relatively different from the other samples, and three peaks were identified, with  $T_m$  of 54.2, 58.8 and 60.3°C, and smaller enthalpy with a maximum heat flux of 0.2 J/°C.g for the first peak and 0.8 J/°C.g for the last two (see Table 4.3). Thus, the single peak seen on the control thermogram is not due to only one endothermic event, but several. As discussed in Chapter 3, this region includes the denaturation of both subunits of the ribosome, which would correspond to the 58.8 and 60.3°C peaks on the MSG thermogram, for the 30-S and 50-S subunits, respectively. From the s region onward, peaks presented a shift toward higher temperatures, compared to the control. The last two peaks of the s region, that are the most distinguishable, were compared between treatments by ANOVA. Both were significantly higher than compared to all other treatments ( $p$ -value<0.001). The second to last peak of the s region had a  $T_m$  of 4.1°C higher than the control and the  $T_m$  of the last peak was 5°C higher (Table 4.3). This set of biomolecules are, thus, significantly more stable when exposed to 12.5% (w/v) MSG solution. Peak g was not visible on all thermograms of cells exposed to MSG, most likely due to the shift of the s region toward higher temperatures. Peak h and i, were also easily distinguishable and were thus compared by ANOVA, they both presented a significantly higher  $T_m$  with MSG than for all other treatments ( $p$ -value<0.001), with a difference of 2.8°C and 3.4°C respectively, compared to the control. However, the maximal heat capacity of peak i was significantly smaller, even though the shape of this peak appeared to be broader. Thus, there might be other events occurring around the same temperature. As discussed earlier, these two peaks were previously identified as the DNA and the cell

wall components (Mackey et al., 1991). Therefore, it appears that these biomolecules were more stable in the presence of MSG.

Similar, yet smaller, shifts in the s region as well as h peak were also present in cells exposed to betaine. There was a shift of 2.7°C for the last two peaks of the s region compared to the control. In addition, peak h was significantly higher when cells were exposed to betaine, compared to the control, with a difference of 0.8°C. Finally, the b region presented two peaks ( $T_m$  of 60.6 and 63°C), with a unique shape, and smaller enthalpy compared to the control. This emphasises that this region is relatively sensitive to the sample treatment, and may cover about three endothermic peaks. Both MSG and betaine are charged amine salts, which could explain the similarities between the thermograms, as both compounds may have some similar interactions with the cell biomolecules. However, even though the thermograms of cells exposed to betaine had similarities with those exposed to MSG, they presented substantively different stability over storage. The powder obtained with betaine was very sticky and caked rapidly. This could be due to a higher hygroscopy and/or a rubbery powder and may have led to quicker loss of viability. It is thus assumed that the properties of the powder can be as important as the interactions of the protectants with the cells.

**Table 4.3:** Mean value of peak maxima (T<sub>m</sub>) and maximal heat capacity (C<sub>p</sub><sup>T<sub>m</sub></sup>) of *Lb. rhamnosus* exposed to solution of betaine, MSG, sorbitol or sucrose or buffer. n indicates the number of thermograms where the peaks were identified. Samples with different superscripts letters means statistical difference of their T<sub>m</sub> or their maximum heat capacity (C<sub>p</sub><sup>T<sub>m</sub></sup>) (p-value<0.05).

	Betaine			MSG			Phosphate buffer			Sorbitol			Sucrose		
	T <sub>m</sub>	C <sub>p</sub> <sup>T<sub>m</sub></sup>	n	T <sub>m</sub>	C <sub>p</sub> <sup>T<sub>m</sub></sup>	n	T <sub>m</sub>	C <sub>p</sub> <sup>T<sub>m</sub></sup>	n	T <sub>m</sub>	C <sub>p</sub> <sup>T<sub>m</sub></sup>	n	T <sub>m</sub>	C <sub>p</sub> <sup>T<sub>m</sub></sup>	n
	(°C)	(J/°C.g)		(°C)	(J/°C.g)		(°C)	(J/°C.g)		(°C)	(J/°C.g)		(°C)	(J/°C.g)	
<b>a region</b>	51.2	0.2	3	49.5	0.1	1				44.9	0.6	3	44.6	0.1	2
				54.2	0.2	2	54.0	0.4	2	58.5	0.4	1	57.5	0.5	3
<b>b region</b>	60.6	1.6	3	58.8	0.8	3	61.0	3.3	3	62.9	2.0	3	61.7	1.7	3
	63.0	1.1		60.4	0.8	3									
				67.4	0.5	3									
	69.0	1.0	3	70.9	1.2	3	66.8	1.0	3	67.4	1.6	3	66.3	1.4	3
<b>s region</b>				73.5	0.9	3			3	69.7	1.4	1	68.6	1.2	2
	75.8 <sup>b</sup>	0.6 <sup>c</sup>	3	77.2 <sup>a</sup>	0.8 <sup>b,c</sup>	3	73.1 <sup>c</sup>	0.7 <sup>b,c</sup>	3	73.7 <sup>c</sup>	1.0 <sup>b,c</sup>	3	73.5 <sup>c</sup>	0.8 <sup>a,b</sup>	3
	80.9 <sup>b</sup>	0.4 <sup>c</sup>	3	83.1 <sup>a</sup>	0.6 <sup>b,c</sup>	3	78.2 <sup>d</sup>	0.6 <sup>a,b,c</sup>	3	79.8 <sup>c</sup>	0.8 <sup>b,c</sup>	3	79.3 <sup>c</sup>	0.7 <sup>a,b</sup>	3
<b>g peak</b>	87.9 <sup>b</sup>	0.1 <sup>b</sup>	2	89.6 <sup>a</sup>	0.0 <sup>c</sup>	1	84.3 <sup>d</sup>	0.0 <sup>c</sup>	3	87.1 <sup>b</sup>	0.1 <sup>b,c</sup>	3	86.3 <sup>c</sup>	0.1 <sup>a,b</sup>	3
<b>h peak</b>	97.0 <sup>b</sup>	1.6 <sup>a</sup>	3	98.9 <sup>a</sup>	1.8 <sup>a</sup>	3	96.1 <sup>c</sup>	2.0 <sup>a</sup>	3	96.8 <sup>b,c</sup>	1.7 <sup>b,c</sup>	3	96.5 <sup>b,c</sup>	1.8 <sup>a</sup>	3
<b>i peak</b>	104.5 <sup>b</sup>	0.4 <sup>a</sup>	3	107.1 <sup>a</sup>	0.2 <sup>b</sup>	3	104.0 <sup>b</sup>	0.3 <sup>a</sup>	3	102.3 <sup>C</sup>	0.3 <sup>b,c</sup>	3	102.4 <sup>c</sup>	0.3 <sup>a</sup>	3

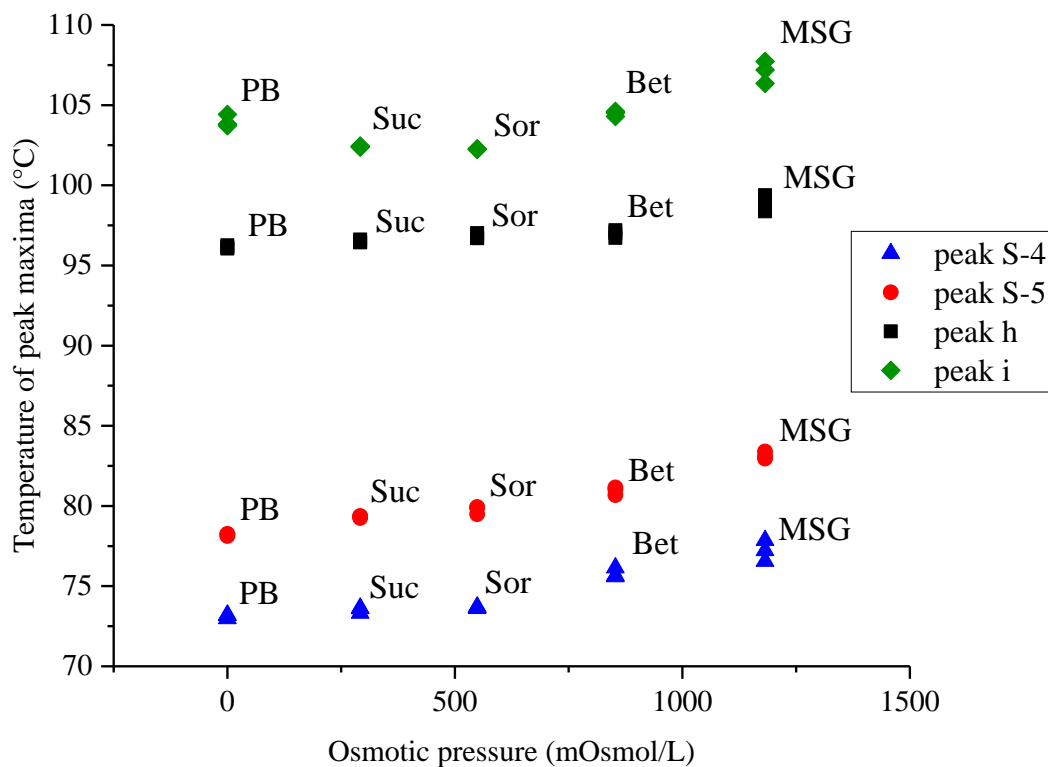
Thermograms of cells exposed to sorbitol and sucrose were very similar to each other, apart from region a. Both thermograms presented a peak at 44.9 and 44.6°C for sorbitol and sucrose respectively, however the peak in the sorbitol thermogram was much broader and with a higher maximal heat capacity. The other regions had the same number of peaks with a similar shape as well as close T<sub>m</sub> and maximum heat capacity values, even if sorbitol values were slightly higher (not significantly different). The similarities between both thermograms could be due to similar functional hydroxyl groups of both molecules and the fact that they have the potential to form hydrogen bonds with water or with the biomolecules. It has been previously found that osmotically stressed *Lb. rhamnosus* HN001 accumulated saccharides modified by glycerol and it was postulated that the increase in hydroxyl groups of osmoprotectants would protect macromolecules

when drying via hydrogen bonding (Prasad et al., 2003). However, similarities in thermograms did not translate into the same shelf-life results, as sucrose led to increased stability. This may be due to the powder characteristic, and more specifically to the higher glass transition temperature of sucrose (about 65°C; Craig et al., 1999) compared to sorbitol (around -3°C; Crowe, Hoekstra, et al., 1996). Indeed, it has been discussed before that a high glass transition temperature could help in stabilising the bacteria in the dried state (Crowe, Hoekstra, et al., 1996; Liu et al., 2016).

#### **4.3.3 Potential effect of the osmotic pressure on thermograms**

Studying the whole cell system, compared to studying the interaction of protectants with isolated biomolecules has the advantage of taking into account the osmotic pressure implied by the protective solutions. It is known that a sublethal osmotic treatment could improve heat stability as well as storage stability (Le Marrec, 2011; Nag & Das, 2013; Prasad et al., 2003). In this study, mass concentration of each solution was kept constant. Thus, the osmotic pressure varied between samples, and could have affected the results. The osmotic pressure was calculated and was plotted against the  $T_m$  of the four peaks identified (the last two peaks of the s region: peak S-4 and S-5; peak h and peak i) in Figure 4.6. Three out of four peaks showed an increase in their  $T_m$  with the increase in osmotic pressure. Peak i, however, did not show the same trend. If this peak was confirmed to be the cell wall components as proposed by Mackey et al. (1991), it could explain this result. Indeed, the protection mechanism of the solutes relies on their presence in the vicinity of the biomolecules. Thus, the stability of cytoplasmic biomolecules is affected by the uptake of the protectants, but not the cell wall components. The type of pressure is different as well. As mentioned previously an electrolyte stress is different from a non-electrolyte stress. MSG contains one mole of sodium salt per mole of glutamate, and the cells response would be somehow stronger to

that with non-electrolyte solutes. Additional studies are needed to know if the protective effect comes from the glutamate itself, or if it is helped by the presence of sodium.



**Figure 4.6:** Temperature of peak maxima of four peaks identified from the thermograms, as a function of osmotic pressure of the protectants concentration. Peak S-4 and S-5 are respectively, the second to last and last peak of the s region. PB stands for phosphate buffer, Suc for sucrose, Sor for sorbitol and Bet for betaine.

## 4.4 Conclusions

This study found that MSG was a promising protectant for *Lb. rhamnosus* HN001 and maintained good stability over storage at 30°C, even though the powder presented high water activity, suggesting that the structure collapsed during drying. Overall, the Nano DSC scans showed that MSG could interact with some of the cellular biomolecules, such as the DNA or the cell wall and could explain the good shelf-life results. However, the thermograms are not enough to explain all shelf-life results. It is most likely that the

structure of the powder altered the stability of some powders more than other in these standard conditions. More specifically, at the second month of the storage, sorbitol and galactose were both promising protectants, but this was followed by a sudden drop in stability of the cells. As the powders were stored in closed containers, they may have taken up some moisture, and this was confirmed by taking the water activity after 6 months, as samples were converging toward 0.22 of water activity.

It is worth noting that glutamate is a neurotransmitter, and the absorption of glutamate in a high dose (4mg/g) has caused neurodegeneration in infant rodents (Peñafiel, Cremades, Puelles, & Monserrat, 1985). In the formulation developed here, 1 g per day would be enough to deliver sufficient viable bacteria. This would lead to a consumption of about 0.5 g of MSG. A concentration of 100 mg/100 mL free glutamate in infant formulas is considered to be a high level, but not harmful to the infant (Ventura, Beauchamp, & Mennella, 2012). Thus, while the stabilisation matrix presented here might lead to a high concentration of glutamate for infants, it could be applied for other consumers, such as adults or the elderly.

Next step should thus compare MSG, sucrose, galactose and sorbitol on their interactions with the cell components and their structure, and how both parameters affect the cell viability. To lower the risk of variation between samples, water activity of the powders should be standardized, and samples should be stored in aliquots in air-tight containers.

## Chapter 5 – Optimising the stabilisation matrix for protection of *Lactobacillus rhamnosus*

---

### 5.1 Introduction

Numerous protectants have been used to dry and stabilise probiotics. Some studies have shown that complex matrices such as skim milk, or combinations of different protectants, e.g. trehalose and lactose, were more efficient in stabilising the bacteria than one protectant alone (Jofré et al., 2015; Roos & Pehkonen, 2010). The reason for this synergy between protectants is not well-understood. One proposed explanation could be that one protectant could interact with the cell biomolecules, while another maintains a high glass transition temperature of the powder. Another possible reason could be that some protectants enter the cells in an efficient way and can interact with the biomolecules in the cytoplasm, while others act from the outside of the cells (Hubálek, 2003). Thus, each protectant has its own location of action and a combination would therefore be best to the overall protection.

This study, therefore, aims to shed some light on the synergistic action of protectants on the stability of freeze-dried *Lb. rhamnosus* HN001 during storage. A thorough study of the powder characteristics and of the interaction of the cells with various combinations of the protectants will help develop a deeper understanding as to how they help to maintain the bacteria in a viable state during storage.

For that purpose, four protectants were mixed following a mixture design of experiment (DoE). One monosaccharide, one disaccharide, one sugar alcohol and one amino acid salt were chosen. In a prior study (Chapter 4), galactose conferred good protection over two months at 30°C but caused a sudden drop in stability from this time



point onwards. It was suspected that a destabilisation of the powder structure itself may have led to this result. Sucrose addition led to good viability over six months at 30°C, with a death rate of 0.46 /month. Similarly to galactose, sorbitol led to good stability of the bacteria over three months at 30°C, but a relatively rapid drop occurred over the subsequent three months of shelf-life. In addition, sorbitol interacts with the cell in a very similar pattern to that of sucrose, but has a very different glass transition temperature. The presence of both protectants in the design could help to improve our understanding of the importance of the glassy state of the powder and the protectant and cell interactions. Finally, the addition of MSG showed very promising results on *Lb. rhamnosus* with a death rate of 0.19 /month. Interestingly, the water activity after drying of this powder was relatively high and suggested that this protectant possesses a unique feature which allow good protection of the cells.

## **5.2 Materials and methods**

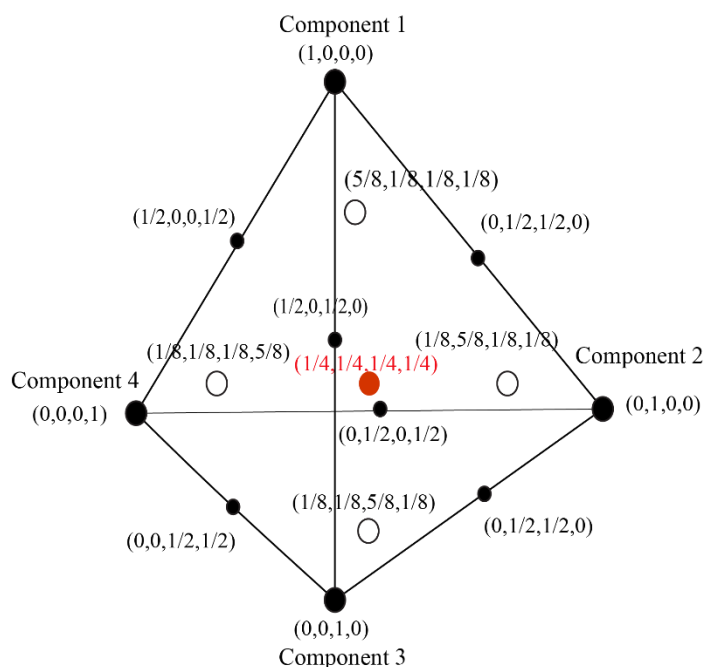
### **5.2.1 Materials**

Inulin (Frutafit TEX, DP  $\geq$  22) was obtained from IMCD New Zealand Ltd., Auckland, New Zealand. L-glutamic acid monosodium salt monohydrate (MSG), D-(+)-galactose and D-sorbitol were all bought from Sigma Aldrich, Saint-Louis, MO. Analytical grade sucrose was obtained from Thermo Fisher Scientific, Waltham, MA.

### **5.2.2 Design of experiments (DoE) – response surface methodology**

Four different protectants were chosen from the previous study (Chapter 4): galactose, sucrose, MSG and sorbitol. To determine the ideal ratio between these protectants, a mixture design of experiment (DoE) was followed.

Figure 5.1 presents the design followed in this study: a simplex lattice of degree 2 which is composed of the components alone and their binary mix, with an additional point as the centre point (in red) and the axial points (open circles).



**Figure 5.1:** Four-component mixture DoE followed in this study: augmented simplex-lattice of degree 2 with the centroid (in red) and axial points (open circles).

### 5.2.3 Shelf-life study

Cells were grown as described earlier (section 3.2.3), harvested at the start of the stationary phase, i.e. after 16 hours or when the absorbance reached 1.7, before being exposed to the protective solutions for 1 hour at 4°C and freeze-dried as detailed in section 3.2.6. Solution were made with 12.5% (w/v) of inulin and 12.5% (w/v) of a mix of the protectants previously selected, i.e. MSG, sorbitol, galactose and sucrose, following the mixture DoE presented above and described in Table 5.1. Samples were randomized and done in triplicates organised in three different blocks of experiments (i.e. each block being

freeze-dried in a different batch). Dried free cells were used as control later on the study and consisted in cells dried in phosphate buffer only.

Once freeze-dried, the powders were grounded using a pestle and a mortar. They were then mixed with skim milk powder ( $A_w=0.09$ ), at 10% (w/w) to standardise the  $a_w$ . The powder was split in individual three side seal foil pouches from Casp-Pak ©, and stored at 30°C for 8 months. The remaining probiotic powder was stored at -80°C until further use. The viability of the cells was monitored using the plate count method as outlined in section 3.2.6.

**Table 5.1:** Composition of the protectant solutions for optimising the stabilisation matrix following the mixture DoE presented in section 5.2.2.

MSG (g)	Sorbitol (g)	Galactose (g)	Sucrose (g)	Inulin (g)	Potassium Phosphate buffer (mL)
12.5	0	0	0	12.5	100
6.25	6.25	0	0	12.5	100
6.25	0	6.25	0	12.5	100
6.25	0	0	6.25	12.5	100
0	12.5	0	0	12.5	100
0	6.25	6.25	0	12.5	100
0	6.25	0	6.25	12.5	100
0	0	12.5	0	12.5	100
0	0	6.25	6.25	12.5	100
0	0	0	12.5	12.5	100
3.125	3.125	3.125	3.125	12.5	100
7.8125	1.5625	1.5625	1.5625	12.5	100
1.5625	7.8125	1.5625	1.5625	12.5	100
1.5625	1.5625	7.8125	1.5625	12.5	100
1.5625	1.5625	1.5625	7.8125	12.5	100

## **5.2.4 Characterisation of the powder**

### **5.2.4.1 Glass transition temperature**

Between 7 and 20 mg of powders were weighted into aluminium pans, before being sealed with hermetic lids and run on a DSC Q2000 (TA instruments, USA). Both pans were equilibrated at -30°C and heated to 100°C at a rate of 5°C/min, before being cooled at the same rate. The heating and cooling cycle was repeated once. The first cycle is referred as “scan” and the second as “rescan”. The glass transition value was taken on the rescan.

### **5.2.4.2 Scanning electron microscopy**

Small amounts of powdered sample were mounted on to aluminium stubs using double sided tape, sputter coated with approximately 100nm of gold (Baltec SCD 050 sputter coater) and viewed in the FEI Quanta 200 Environmental Scanning Electron Microscope at an accelerating voltage of 20kV.

### **5.2.4.3 Moisture content**

Prior to the measurement, aluminium pans were placed in a 105°C oven, for about 24 hours. They were then placed in a desiccator to cool down before weighing. Probiotic powders were allowed to reach ambient temperature, before placing about 2 g in the pans. The samples were dried for 24 h at 105°C. Each powder was prepared in duplicate

### **5.2.4.4 Water activity**

Water activity of the powders was monitored during the whole shelf-life, and measured at each counting point using a Decagon AquaLab 4TE water activity instrument (Decagon Devices Inc., WA, USA) at 20°C.

#### **5.2.4.5 Fourier-transform infra red (FTIR)**

The fifteen compositions from the mixture DoE were prepared without the bacteria, in triplicates and freeze-dried. Together with the samples containing *Lb. rhamnosus* HN001 the infrared spectra of the 90 samples were collected on a FTIR, Thermofisher Scientific Nicolet 5700 in at least triplicates. The FTIR was equipped with a germanium crystal plate and pressure tower Smart iTR™ Attenuated Total Reflectance (ATR). The dried powder was placed on the plate and pressed down with the pressure tower. The reflectance data were recorded from 675 cm<sup>-1</sup> to 4000 cm<sup>-1</sup> with 64 scans spectrum and a spectral resolution of 4 cm<sup>-1</sup>. Background was measured before each set of measurements, or every two hours and was directly subtracted from the spectrum. As a result, about 270 spectrum were obtained.

#### **5.2.5 Nano differential scanning calorimetry study of the synergy between MSG and sorbitol**

The Nano DSC study followed the same methodology as described in section 3.2.8. Cells were exposed to a solution of 10% (w/v) MSG and 2.5% (w/v) sorbitol in phosphate buffer. Results were then compared to previous results of cells exposed to 12.5% (w/v) MSG or 12.5% (w/v) sorbitol.

#### **5.2.6 Statistical analysis**

Statistical analysis, including the creation and analysis of the mixture DoE were performed with Minitab 18.1 software. R 3.5.0 were used to perform PCA and analyse thermograms as previously described in section 4.2.5. Similarly, the FTIR spectrum were pre-treated and analysed using R 3.5.0. Spectra were first centred and scaled before being smoothed using the Gaussian window method with a window of 10 points. Then, spectra were averaged before taking the first derivatives using a Savitsy-Golay smoothing filter,

with a filter order of 3 and a length of 11. This method gave the best separation between samples containing bacteria or only the protective matrix. Presence of outliers and consistency of the analysis was checked using PCA. Finally, the matrix spectra were removed from the samples spectra, with bacteria, using the non-subjective vector correction methodology followed by Hlaing et al. (2017) and detailed by (Berger et al., 1998). Briefly, the projection of the matrix vector was subtracted from the sample spectra (with the bacteria and the matrix), and is further described in Appendix A.

## 5.3 Results and discussion

### 5.3.1 Characteristics of the powder

The main powder characteristics, i.e. the glass transition temperature, of the powder, the moisture content and the water activity over storage are shown in Table 5.2. Even though the water activity of the powder was standardised by mixing with the skim milk powder, some variation persisted, and the overall water activity of the powders ranged between 0.14 and 0.18. As it could be expected, water activity was significantly correlated with moisture content (Pearson correlation = 0.61, p-value < 0.001). Similarly, the glass transition temperature was significantly correlated with both moisture content and water activity measured after drying, and before mixing with the skim milk powder (Pearson correlation of, respectively, -0.364, p-value < 0.05 and -0.533, p-value < 0.001).

Models of the T<sub>g</sub>, moisture content and water activity, taken after drying, are presented in Figure 5.2. For all three models, the block of sample was found to have a significant impact on the results. Each block of samples was dried in a different freeze-drying batch, thus some variations occurred between each drying. Even if correlations exist between these parameters, they all follow a different model. The water activity is linearly correlated with the amount of MSG in the powder. However, it is not the case for moisture content, which is more affected by the amount of galactose, or a mix of MSG

and galactose. Finally, the model representing Tg showed a clear plasticizing effect, i.e. a reduction of the Tg, of sorbitol. Similarly, a mix of MSG and galactose caused the decrease of the Tg, most likely due to the higher amount of water in the powder.

Interestingly, MSG samples, presented the higher water activity after drying (0.34), and over storage (0.18). This is a sign that the structure of the sample collapsed during freeze-drying, and would be verified by SEM micrographs (see section 5.2.4.2 and Figure 5.4).

Similarly, samples containing galactose led to relatively low water activities after drying, but to the highest moisture content reaching up to 16%. The sugar may have bonded with water, preventing an efficient drying, while maintaining the water activity down, i.e. less “free” water.

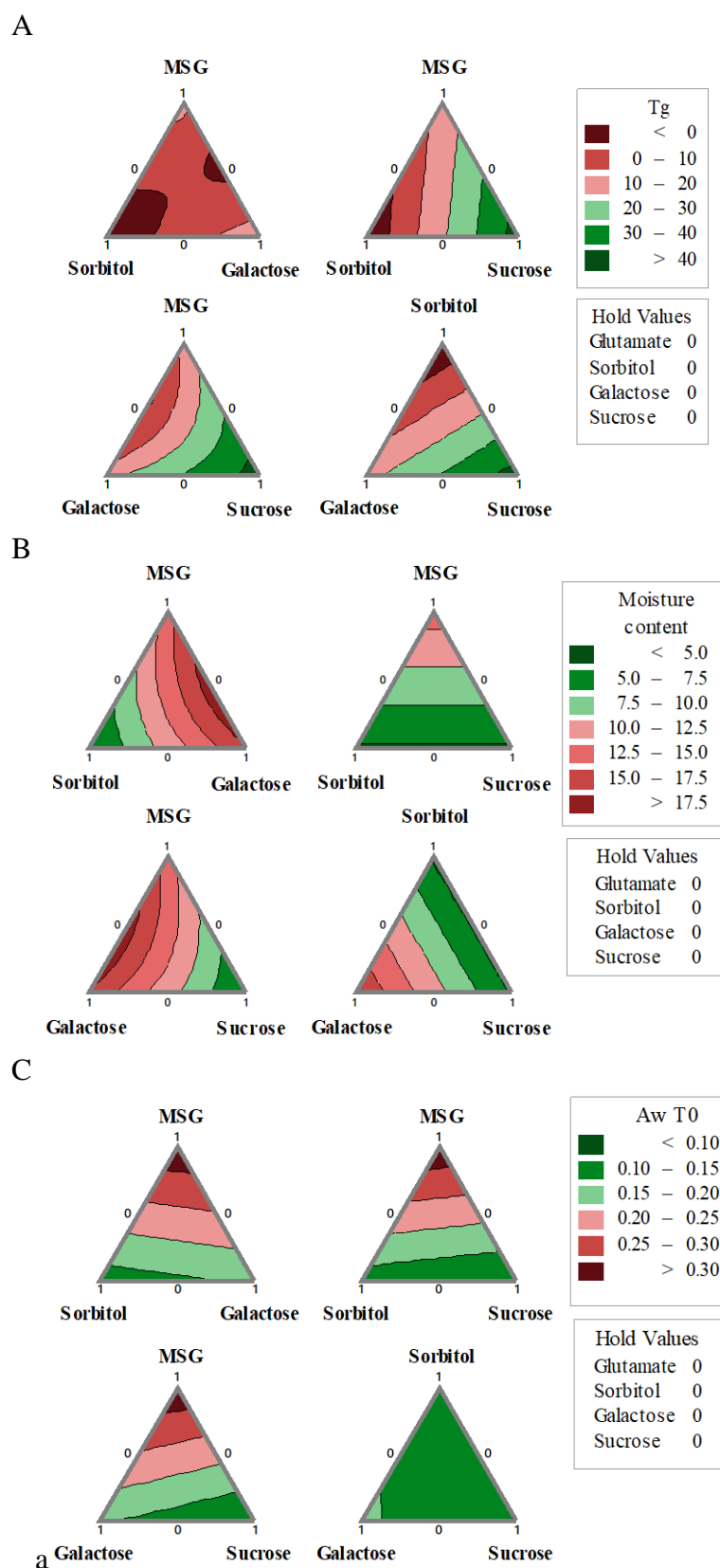
On the other hand, the presence of sorbitol or sucrose enabled efficient drying of the powder with a moisture content of about 4%. However, the presence of sorbitol depressed the glass transition temperature, while sucrose increased it. This was expected as sorbitol is a well-known plasticiser, with a glass transition temperature of -3°C (Craig et al., 1999) while sucrose has a glass transition temperature of 65°C (Crowe, Hoekstra, et al., 1996).

There is thus a clear impact of the composition of the powder on the physico-chemical properties of the samples, and the structure of the powder might help understanding some of those results.

**Table 5.2:** Powder characteristics of the samples – moisture content, water activity and glass transition temperature (T<sub>g</sub>). Moisture content and T<sub>g</sub> are the mean of three true replicates, measured three times with their standard deviation. Water activity is the mean value of the three replicates measured at least five times over the storage period with the standard deviation.

Sample	Powder composition				Glass transition temperature (°C)	Moisture content (%)	Water activity during storage
	MSG	Sorbitol	Galactose	Sucrose			
1	12.5	0	0	0	7.24 ± 3.27	13.87 ± 1.86	0.18 ± 0.01
2	6.25	6.25	0	0	4.62 ± 7.79	10.32 ± 1.14	0.17 ± 0.01
3	6.25	0	6.25	0	1.25 ± 11.90	17.98 ± 1.89	0.18 ± 0.02
4	6.25	0	0	6.25	31.49 ± 7.15	8.06 ± 1.39	0.16 ± 0.01
5	0	12.5	0	0	-8.49 ± 6.10	4.10 ± 2.15	0.16 ± 0.02
6	0	6.25	6.25	0	5.29 ± 0.33	10.25 ± 2.28	0.14 ± 0.01
7	0	6.25	0	6.25	12.43 ± 2.70	4.02 ± 1.26	0.14 ± 0.01
8	0	0	12.5	0	16.07 ± 3.76	16.13 ± 4.20	0.15 ± 0.01
9	0	0	6.25	6.25	25.17 ± 5.59	11.57 ± 4.62	0.15 ± 0.01
10	0	0	0	12.5	44.72 ± 1.47	4.22 ± 1.35	0.15 ± 0.01
11	3.125	3.125	3.125	3.125	8.95 ± 11.28	11.52 ± 0.67	0.16 ± 0.01
12	7.8125	1.5625	1.5625	1.5625	11.38 ± 11.44	11.63 ± 3.95	0.17 ± 0.02
13	1.5625	7.8125	1.5625	1.5625	-1.53 ± 7.67	8.05 ± 2.02	0.16 ± 0.02
14	1.5625	1.5625	7.8125	1.5625	-0.13 ± 9.11	16.29 ± 1.27	0.17 ± 0.02
15	1.5625	1.5625	1.5625	7.8125	20.23 ± 8.34	8.96 ± 2.22	0.15 ± 0.01





**Figure 5.2:** Mixture contour plots of the glass transition of powders (graph A), the moisture content after drying (graph B) and the water activity after drying (graph C). Blocks were included in the model, as they presented a significant impact on the variables.

### 5.3.2 Stability of *Lb. rhamnosus* HN001 at 30°C

The stability of *Lb. rhamnosus* was followed over 8 months of storage at 30°C. The death rate was calculated and the resulting model is presented in Figure 5.3 and explained by the Equation (5.1).

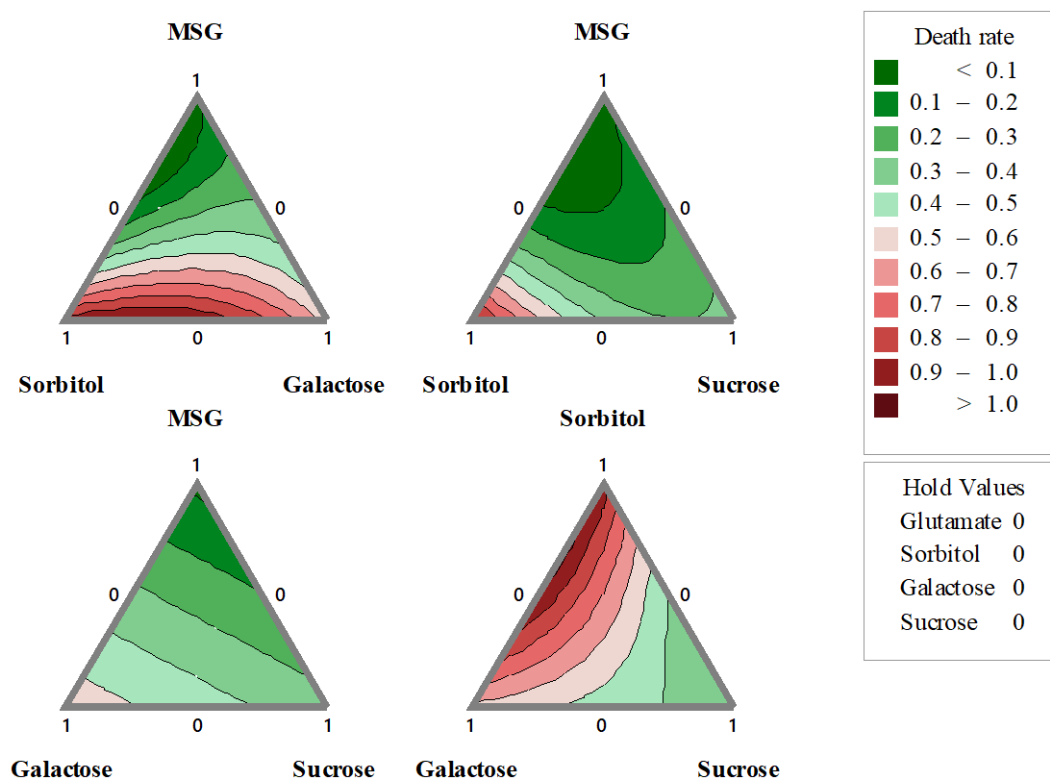
As previously found in last chapter, the mix of MSG and inulin led to the best stability over the 8 month period. After 8 months at 30°C there was a log reduction of only 0.59 log (CFU/g), and a death rate of 0.06 /month. This would lead to a total loss of 0.68 log (CFU/g) over a year when stored at 30°C.

The analysis of the model showed a synergy toward lower death rate between sucrose and sorbitol, as well as with MSG and sorbitol (Equation 5.1 and Figure 5.3). On the other hand, the combination of galactose and sorbitol increased the death rate of *Lb. rhamnosus* HN001.

The model predicted a positive death rate for a mixture of MSG and sorbitol between 72.3% MSG with 27.7% sorbitol, and 82.6% MSG with 17.4% of Sorbitol. Optimal value would be obtained with a mix of 77.8% of MSG and 22.2% of sorbitol.

$$\begin{aligned} \text{Death rate} = & 0.006 \times \text{MSG} + 0.077 \times \text{Sor} + 0.045 \times \text{gal} \\ & + 0.027 \times \text{Suc} - 0.01 \times \text{MSG} \times \text{Sor} \\ & + 0.006 \times \text{Sor} \times \text{Gal} - 0.006 \times \text{Sor} \times \text{Suc} \end{aligned} \quad (5.1)$$

$$R^2 = 78.2\% \text{ and predicted } R^2 = 68.5\%$$



**Figure 5.3:** Mixture contour plots of the death rate based on the component amounts, bacteria were stored 8 months at 30°C.

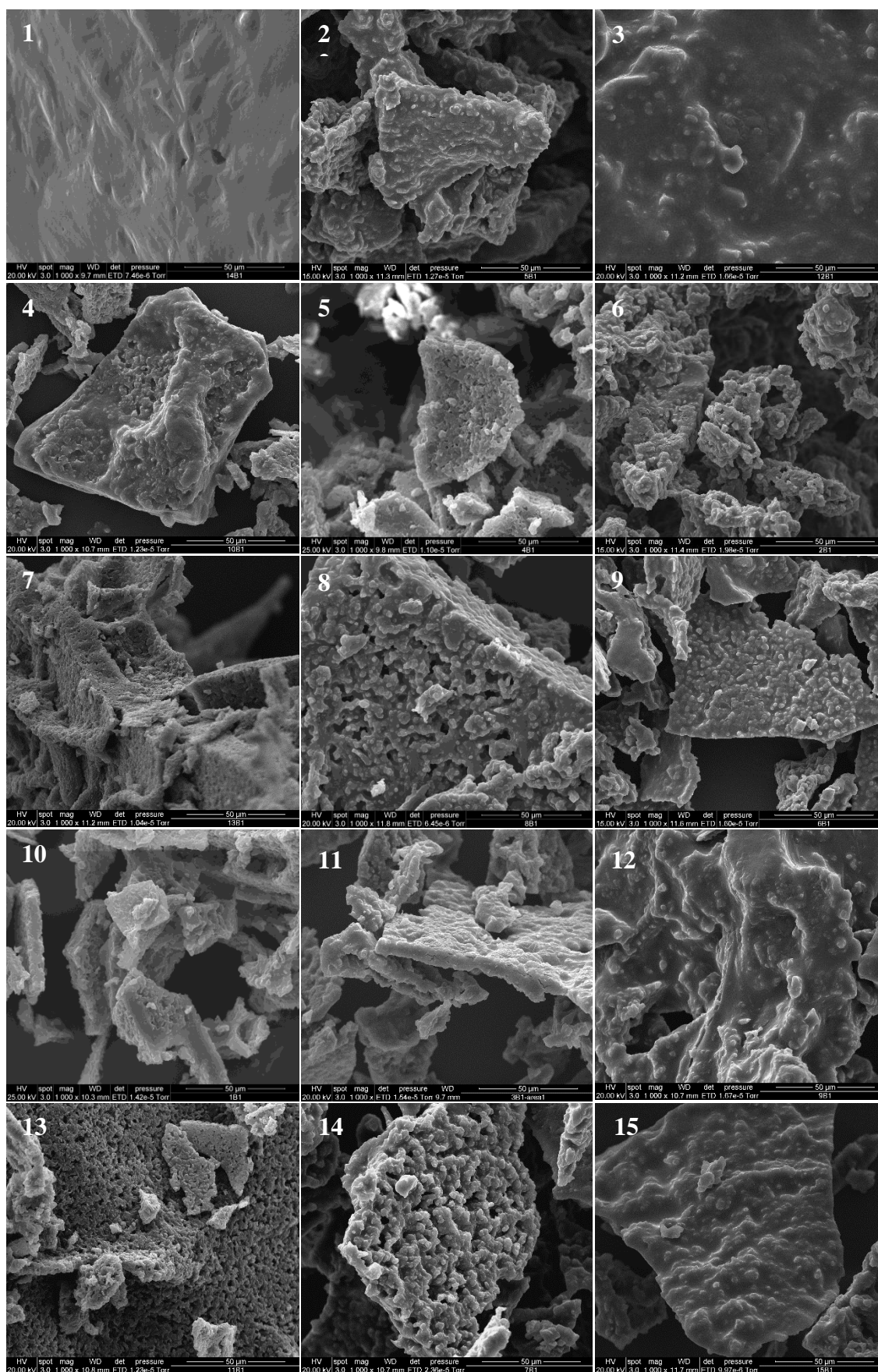
### 5.3.3 Powder structure

In order to better understand the viability results, it is essential to examine the structure of the powder. As mentioned previously, the structure might have impacted the stability of the bacteria. Thus, given the differences seen previously with the bacteria viability, differences are expected in the structure of the samples. The SEM micrographs are shown in Figure 5.4.

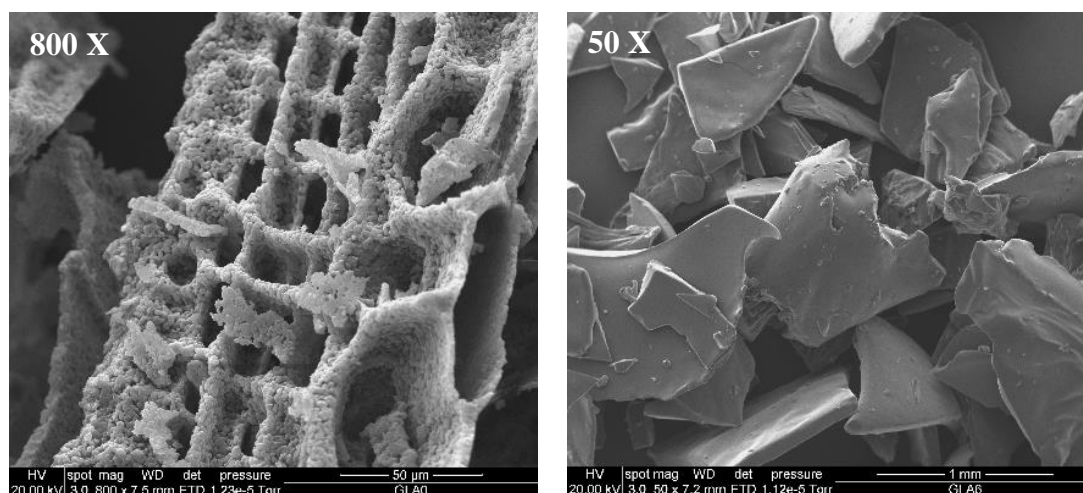
As observed, most of the samples presented a very rough and porous surface covered with small round structures. These structures are most likely the coil structure of the inulin forming during freeze-drying. This was confirmed with additional SEM pictures of samples without bacteria as presented in Figure 5.5 and Figure 5.6. Inulin

powder is very structured, porous and most likely crystalline. On the other hand, the mix MSG and inulin led to a very smooth structure and from the low magnification, the powder seemed very little porous.

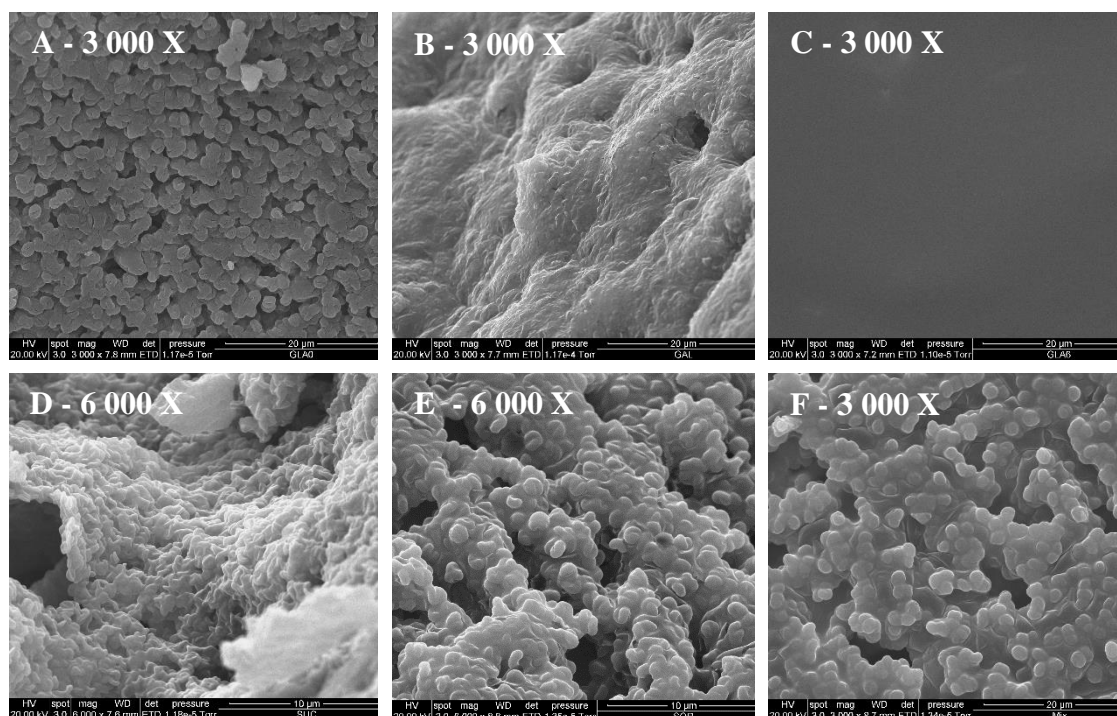
The higher magnification presented on Figure 5.6 confirmed that the surface was completely smooth. Inulin powder is covered with small coil structures, which has already been described in the literature (Vereyken et al., 2003). The addition of sucrose, sorbitol or a mix of the four protectants did not seem to alter this structure. However, addition of galactose led to a structure more similar to the MSG sample, but not as smooth. It seems thus, that MSG and galactose interacted somehow with inulin, preventing it to form coil structures. This confirms that the MSG and inulin powder collapsed during drying, as the cake shrank, and there is a clear loss of the porosity. This event occurs if the viscosity of the cake, during drying, decreases to a point where it cannot support itself. The galactose and inulin structure may have partially collapsed, explaining the high moisture content of this powder.



**Figure 5.4:** SEM micrographs of the first block of samples from the mixture DoE (magnification 1 000 X). Numbers indicate the sample number (composition detailed in Table 5.2).



**Figure 5.5:** SEM micrographs of freeze-dried powder of inulin in phosphate buffer without bacteria (on the left), and a mix of inulin and MSG (1:1) in phosphate buffer (on the right).



**Figure 5.6:** SEM micrographs of freeze-dried powder of mix of protectants without bacteria: 100% of inulin in buffer (A), inulin and galactose 1:1 (B), inulin and MSG (C), inulin and sucrose 1:1 (D), inulin and sorbitol 1:1 (E), and inulin with MSG, sorbitol galactose and sucrose 4:1:1:1:1 (F).

### 5.3.4 Multivariate analysis of the model

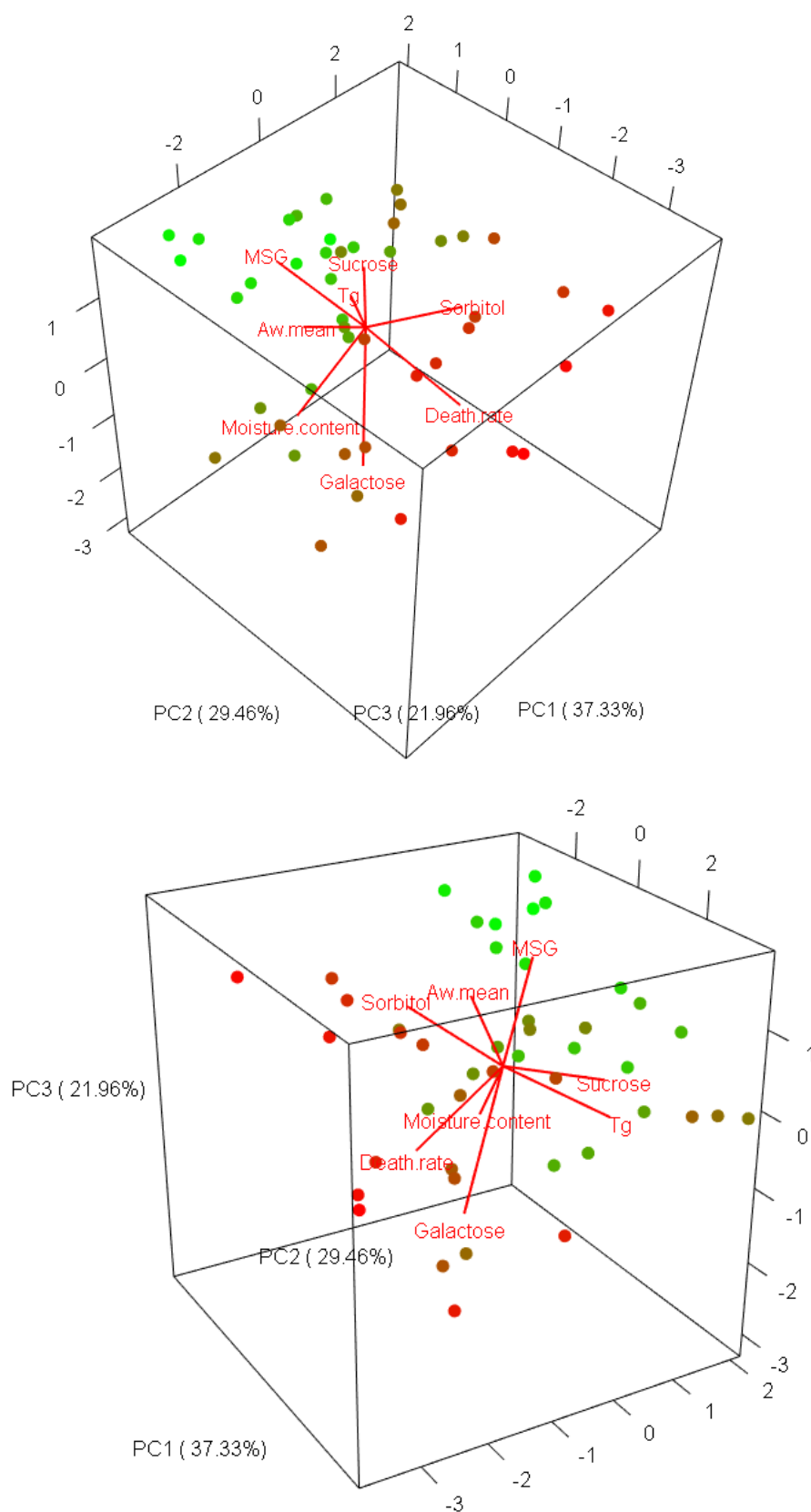
To understand how each factor interacts, PCA was performed. A three-dimensional representation is given in Figure 5.7. The PCA shows first, that the glass transition temperature is closely related to the sucrose. In addition, the death rate variable lies between galactose and sorbitol, meaning that a mix of galactose and sucrose lead to higher death rate. Water activity is closely related to MSG concentration, as are the samples with lower death rate (in green) which are located around the MSG variable on Figure 5.8. This was confirmed by Pearson correlations as water activity was significantly correlated with MSG – with a correlation of 0.57,  $p$ -value  $< 0.001$  – and negatively correlated with death rate – Pearson correlation of -0.36,  $p$ -value  $< 0.05$ . This negative correlation between the water activity and the death rate is in contrast to several studies (Albadran et al., 2015; Harel & Tang, 2014; Kurtmann, Carlsen, Risbo, et al., 2009; Kurtmann, Carlsen, Skibsted, et al., 2009; Tymczyszyn et al., 2012), but could be explained in two ways as introduced in Chapter 4. Firstly, the interaction of the MSG with the cells could be more beneficial than the water activity is detrimental to the cells (ranging from 0.13 and 0.2). Secondly, a slightly higher water activity could be, in fact, beneficial for the cells. As shown in previous studies, extreme desiccation is detrimental for the cells, and an optimum water activity was found between 0.1 and 0.2 depending potentially on the bacterial strain (Castro et al., 1995; Scott, 1959). It may be that for the *Lb. rhamnosus* HN001 strain, this optimum stands higher than 0.2.

There was no significant correlation between the glass transition temperature and the death rate. Values ranged from  $-15^{\circ}\text{C}$  to  $46^{\circ}\text{C}$  with most samples having a glass transition temperature below the storage temperature ( $30^{\circ}\text{C}$ ). Two out of the 15 samples presented a higher glass transition temperature, but this might not have been enough to confer protection to the cells, as it has been recommended to store products  $50^{\circ}\text{C}$  below

their glass transition temperature to significantly reduce molecular movement (Hancock et al., 1995).

A glassy state potentially protects the bacteria because it reduces various chemical and physical reactions such as oxidation, Maillard reactions or crystallisation. Crystallisation of the protectant has been shown to be detrimental to biomolecules during freeze-drying (Izutsu, Yoshioka, & Terao, 1993), and could have a negative impact on the viability of the cells over storage (Miao et al., 2008). Interestingly, Maillard reaction products have shown to possess antioxidant properties (Shi et al., 2019), and to protect from bacterial loss (Liu et al., 2017; Loyeau et al., 2018). It is likely that the powder with a high content of MSG did undergo a Maillard reaction over the storage period. This was confirmed by visual checking, as the powder went slightly brown. It is possible that the formation of Maillard reaction products together with the formation of the collapsed structure, i.e. the formation of an outer layer preventing interactions with the environment, protected the bacteria from oxidation, and could have improved their stability over storage.





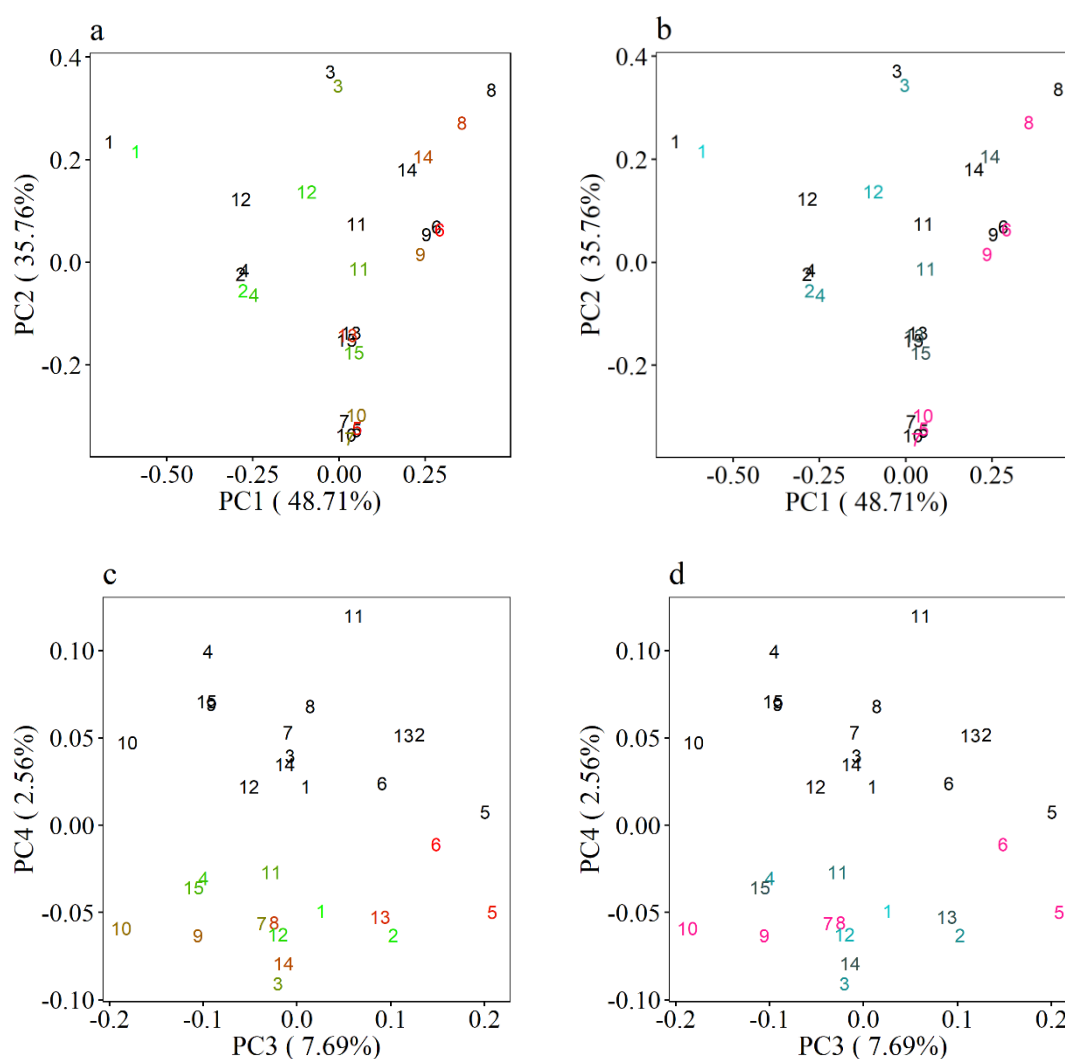
**Figure 5.7:** Three-dimensional representation of the three first principal components explaining the relationship between the death rate, the composition and the characteristics of the powder. Higher death rate is denoted with red dots, while low death rates are in green.

### 5.3.5 FTIR spectrum of the powders

The aim of the infrared study was to look at the effect of the stabilisation matrix on the bacterial cells after drying, and to correlate these results with the conclusions drawn from the Nano DSC study. Most of the studies using FTIR have dried the cells with little amount of protectants, in order to have a stronger signal of the bacteria (Linders et al., 1997; Meneghel et al., 2017; Oldenhof et al., 2005). However, this method is not representative of what is happening in normal conditions. A methodology presented by Hlaing et al. (2017) allows the spectra of the bacteria to be extracted from the powder. In their study, they were able to look at the effects of freeze-drying and spray-drying on the cellular components even though the amount of bacteria was of only 0.4% (w/w) in the powders. The first step involved finding adequate pre-treatments of the data to obtain separation of the matrices only (powders without bacteria) from the bacteria samples on the PCA. This should ensure a good subtraction of the matrices spectra from the samples spectra.

Figure 5.8 shows the first four principal components explaining all spectra (matrix spectra are in black and samples with bacteria in colours) after centre and scaling, smoothing, averaging and first derivation of the data. As it can be seen, the matrices and bacteria samples are well separated on the 4<sup>th</sup> principal component, which account for 2.56% of the variance between samples. This seems logical as the bacteria account for about 3.3% of the total weight of the samples. However, the subtraction of the matrices spectra did not show anything. It can be seen on the first two PC (graph a) that the samples which had a low death rate (in green) are clustered, however the clustering was driven by the composition of the powder only. On Figure 5.8 (part b) samples are similarly clustered as a function of the amount of MSG in the samples (in blue, light blue being the highest amount of MSG). On the PC3 and PC4, there is no clear clustering of the samples

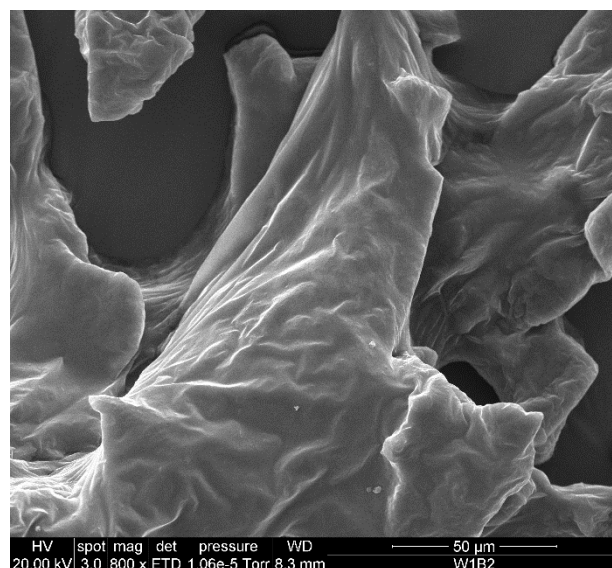
according to their death rate. This indicated that the FTIR spectra may not be able to give any additional information on why one sample is better protected than another. Indeed, the subtraction of the matrices spectra from the samples with bacteria did not lead to conclusive results. The details of the analysis are given in Appendix A.



**Figure 5.8:** First four PC of the powders spectra with and without bacteria, with first two PC in a and b, and second two PC in c and d. Matrices are in black, bacteria are coloured as a function of their death rate in graph a and c (green, lower death rate and red higher death rate). Bacteria samples are coloured as a function of their amount of MSG in graph b and d, with light blue higher amount of MSG, darker blue lower amount of MSG and pink, no MSG.

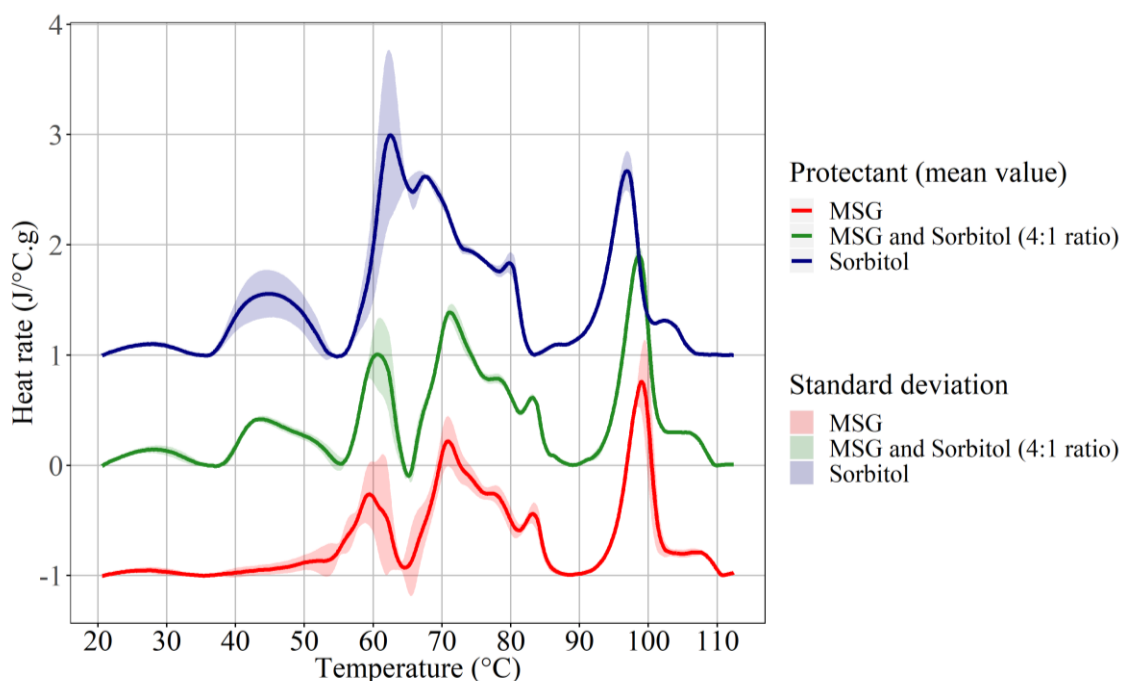
### 5.3.6 Synergy between sorbitol and MSG

The model obtained with the mixture DoE predicted an optimum death rate with a mix of MSG and sorbitol at a ratio of approximately 4:1. The PCA linking the properties of the powder and the death rate did not help explain the synergy between both protectants. Thus, we hypothesized that first, sorbitol did not impact the unique properties of the powder obtained with the MSG, and second, sorbitol could interact with additional biomolecules and stabilise them. In order to verify this hypothesis, the morphology of the new powder with MSG and sorbitol was studied with SEM, and the cells exposed to the MSG and sorbitol mix were run on the Nano DSC. Figure 5.9 confirms the first part of the hypothesis, as the structure obtained with MSG and sorbitol was very smooth, similarly to the one obtained with MSG only. Figure 5.10 shows the comparison of the cell thermograms exposed to the mix or to MSG and sorbitol alone. The resulting thermogram was very similar to the one from cells exposed to MSG only, apart from one detail: an additional peak was present at 43.6°C which was also seen on cells exposed to sorbitol with a relatively high enthalpy (see Chapter 4). This peak was attributed to the membrane lipid, as found in *E. coli* studied by conventional DSC (Brannan et al., 2015). The sorbitol could therefore interact with the phospholipids, which is consistent with the study by Santivarangkna et al. (2010) where sorbitol was found to interact with the membrane phospholipids.



**Figure 5.9:** SEM micrographs of the freeze-dried mix 4:1 MSG:Sorbitol with inulin and without bacteria.

Magnification 800 X.



**Figure 5.10:** Thermograms of *Lb. rhamnosus* HN001 run with a mix of MSG and sorbitol (4:1 ratio)

compared with the cells exposed to MSG and sorbitol alone, obtained from Chapter 4. The straight line

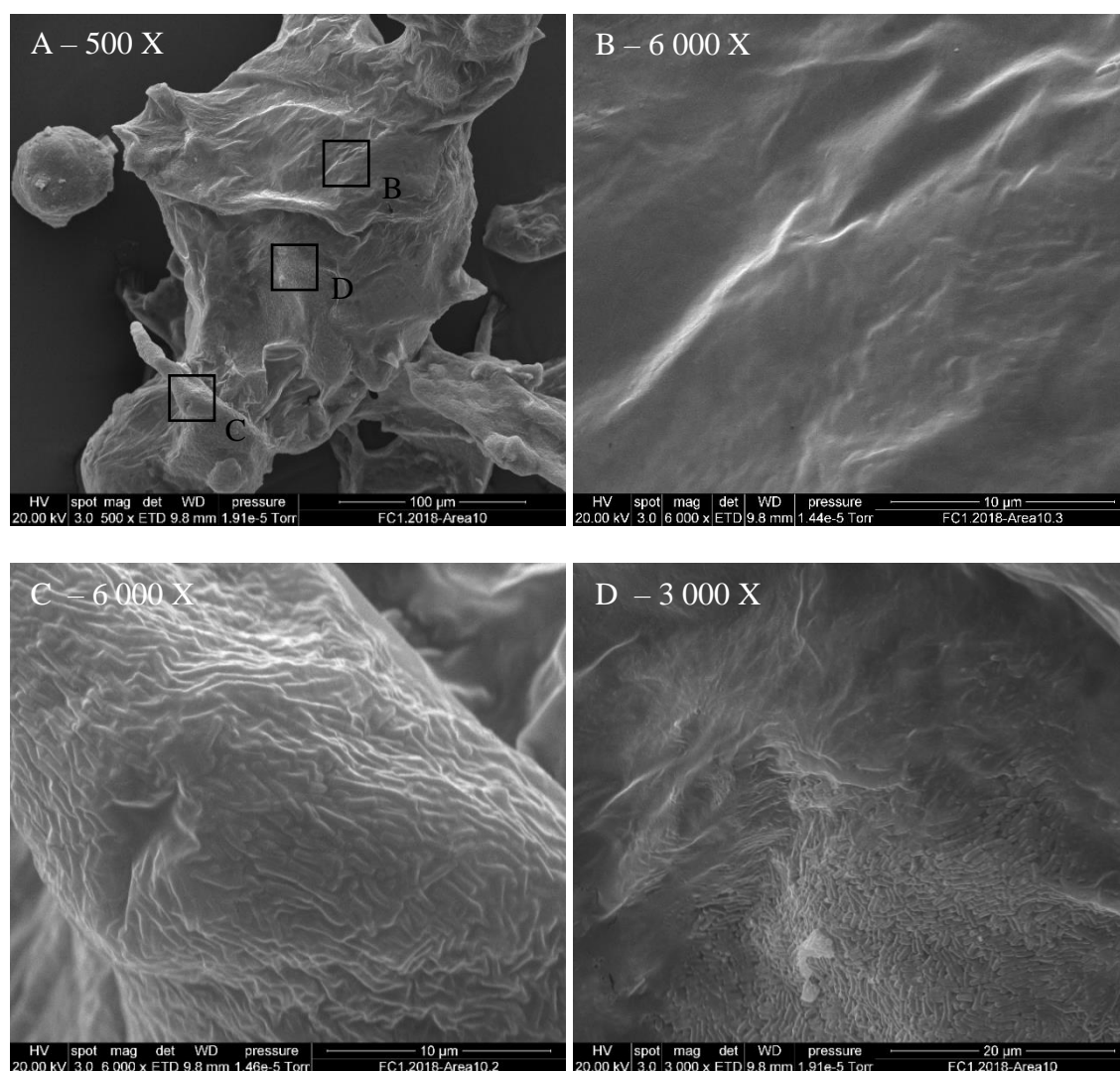
denotes the mean values of triplicates, and the ribbon shows the standard deviation.

It is thus believed, that both the collapsed structure of the powder, and the interactions of the protectant with the cell biomolecules helped stabilising *Lb. rhamnosus* HN001 during storage.

### **5.3.7 Cells dried in buffer**

To have a better understanding of the importance of the structure and of the interaction between cells and protectants, bacterial cells were dried with phosphate buffer only. The main interactions between protectants and cells are removed, as only potassium phosphate salts are presents. In addition, this matrix is relatively neutral as once dried the salts would not catalyse or scavenge oxidation and would not form Maillard reaction products.

The final powder consisted of 35% of bacterial cells and 65% potassium phosphate, i.e. about 10% more bacterial cells than in the above samples. The SEM pictures revealed a relatively heterogeneous powder with very smooth regions and bacteria well visible in other regions, as shown in Figure 5.11. The smooth regions are very similar to the structure seen in the MSG-inulin powder. Overall, the powder looked dense and compact. Characteristics of the powder are described in Table 5.3. It must be noted that this powder did not present any apparent glass transition temperature, even when running the sample from -30°C to 130°C.



**Figure 5.11:** SEM pictures of dried cells in phosphate buffer. Picture A shows the overall structure of the powder. Pictures B, C and D show characteristic details of the powder, location of these pictures are marked as black squares on picture A. Magnifications are indicated on the micrographs.

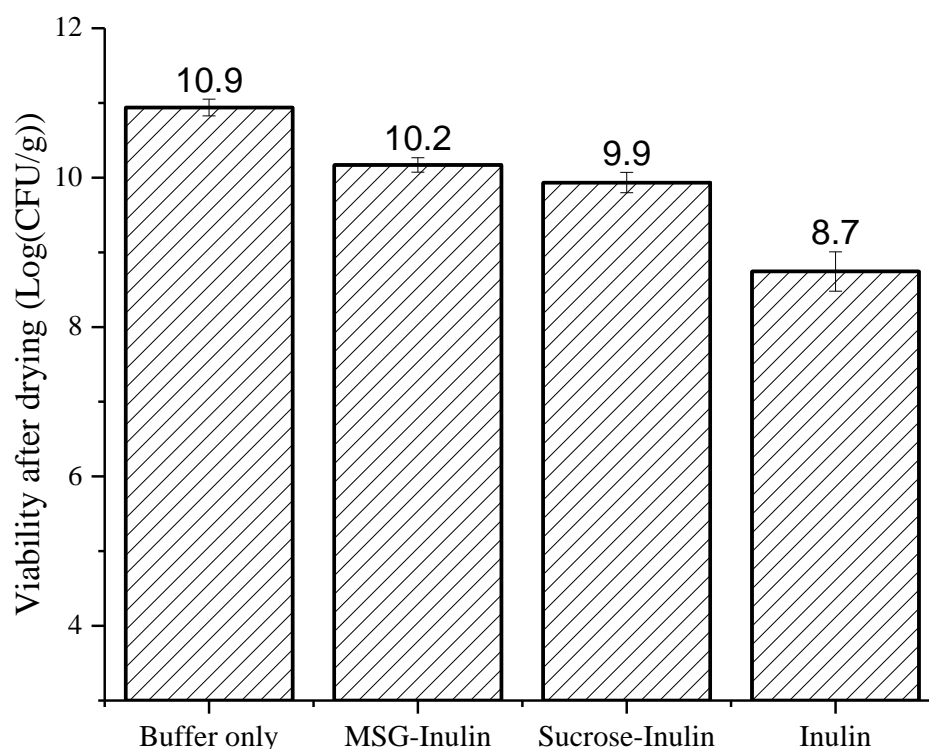
**Table 5.3:** Characteristics of freeze-dried *Lb. rhamnosus* HN001 dried in phosphate buffer. Data are expressed as the mean value with the standard deviation of triplicates.

Composition			Tg	Viability after drying Log (CFU/g)	Viability after 8 months at 30°C Log (CFU/g)	Death rate at 30°C /month
Cells	Potassium phosphate salts	Aw over storage				
34.90%	65.10%	0.15 ± 0.01	NP	10.94 ± 0.19	8.79 ± 0.50	0.21 R <sup>2</sup> =0.86

NP: not present

Cells survived freeze-drying relatively well as there were 10.9 log (CFU/g) which is about 6 times more than when dried with the mix MSG-inulin while there was 10.6 times more bacteria at the start (see Figure 5.12). Interestingly, there were 160 times (2.2 log) more viable cells present than in the inulin and buffer mix (results obtained from previous study, in Chapter 4). This indicates that inulin might disturb the cells during the freeze-drying. This could be due to its crystallisation. As mentioned earlier, crystallisation of water and of carriers can be detrimental to the biomolecules during drying (Izutsu et al., 1993). Thus, the addition of another protectant, such as MSG or sucrose, could protect the cells from the crystallisation-related damage. A study suggested that the key feature of inulin was its ability to interact with the phospholipids, and notably a more profound interaction with the membrane than other fructans (Vereyken et al., 2003). However, this could have caused disorganisation of the membrane instead of stabilisation, as it was found for *Lb. bulgaricus* CFL1 when freeze-dried with sucrose (Meneghel et al., 2017).





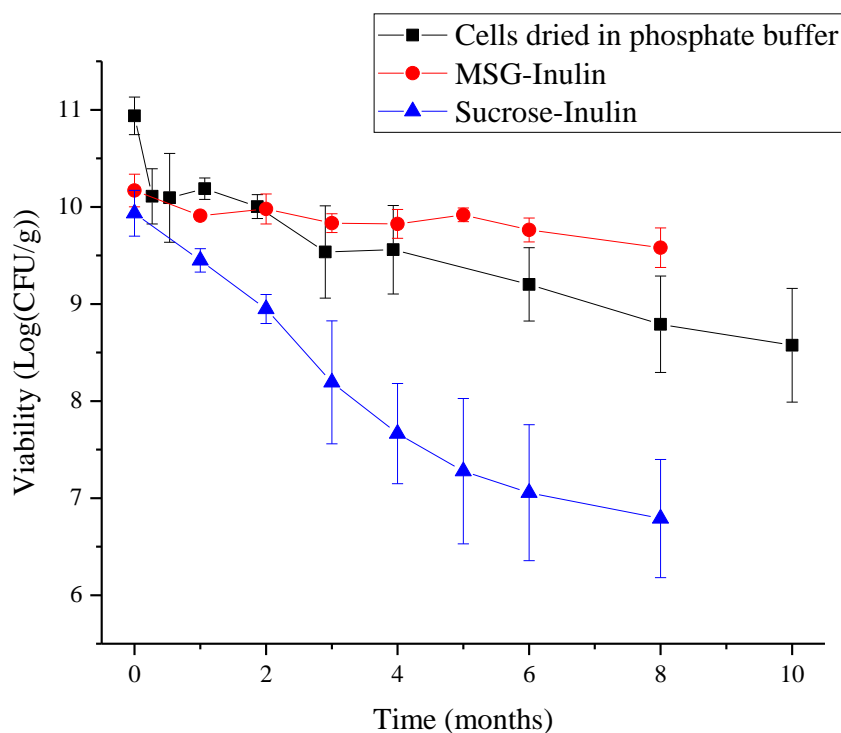
**Figure 5.12:** Comparison of the viability of cells dried in phosphate buffer only to cells dried with inulin, a mix of MSG and inulin and a mix of sucrose and inulin, all mixed with buffer. Results from cells mixed with inulin are from previous study in Chapter 4. The error bars denotes the standard error.

In the first week of storage of the cells dried in phosphate buffer, there was a drop of 0.8 log (CFU/g) followed by a slower loss of 1.3 log (CFU/g) over 8 months (Figure 5.13). The rapid drop during the first week can be due to either cells damaged by the freeze-drying dying off quickly, or cells present on the surface, which are directly in contact with the environment, and more inclined to degradation.

The overall death rate was of 0.21 /month of dried cells in buffer stored at 30°C. This result is better than from most of the formulations tested in the mixture DoE (see Figure 5.3). As a comparison point, the mix sucrose:inulin in a 1:1 ratio led to a death rate of 0.42 /month (Figure 5.13). There are two possible explanations. Firstly, the presence of some protectants such as sucrose can be detrimental to the cells, instead of stabilising them. As far as we know there is only one study that reported an adverse effect

from a “protectant” (sucrose) during freezing, on bacteria *Lb. bulgaricus* (Meneghel et al., 2017). As mentioned earlier, this study revealed that sucrose was causing disorganisation of the cell membrane. In the case of *Lb. rhamnosus* HN001, it was showed that sucrose and sorbitol interacted with the cell biomolecules and tended to stabilise them against heat denaturation. In addition, they had a protective effect during freeze-drying compared to cells dried with inulin (see Figure 5.12 and Chapter 4). However, stability during heat treatment or freeze-drying is different from the stability over storage. For instance, the solutes interacting with the cells could have crystallised during storage, thus damaging the biomolecules and leading to cell loss.

Secondly, the structure of the powders may protect cells dried in buffer only. Indeed, the morphology of the powder was relatively similar to the powder obtained with MSG-Inulin mix, which was very different to the others as they were very porous. It is believed that a compact and denser matrix can help the stabilisation of the bacteria by being more impermeable to the environment, i.e. moisture and oxygen. The benefits of a compact and dense matrix toward the stability of dried bacteria have been discussed in a number of studies (Alehosseini, Sarabi-Jamab, et al., 2019; Poddar et al., 2014).



**Figure 5.13:** Viability of cells dried in phosphate buffer, compared with cells dried with MSG and sucrose. Data are shown as the mean values of triplicates and error bars show the standard error.

## 5.4 Conclusions

In this study, dried *Lb. rhamnosus* HN001 was successfully stabilised over storage at 30°C with a final death rate of 0.06 /month and an expected cell loss of 0.68 log (CFU/g) over one year. The mixture DoE showed interaction of sorbitol with MSG with an ideal composition of about 80% of MSG and 20% of sorbitol. Thermograms of cells exposed to the mix of sorbitol and MSG showed interaction with most biomolecules, which could partially explain the stability. In addition, the unique structure of the powder could protect the cells from the environment. The results of cells dried with buffer only, also suggested that the structure of the powder is of importance in the stabilisation of dried probiotics. Conversely, neither low water activity nor high glass transition temperature led to stabilisation of the dried bacteria.

## Chapter 6 – Phase change materials for the stabilisation of *Lactobacillus rhamnosus*

---

### 6.1 Introduction

Studies on the stabilisation of probiotics focused on finding right protectants that stabilise the cells during drying and storage, and that often have a high glass transition temperature. However, as shown earlier, a high glass transition temperature is not always essential to protect bacteria over storage. Instead, a well-designed powder structure could confer high resistance to the cells. In addition, new types of materials have been found to give protection against heat treatment, i.e. Phase Change Materials (PCM) as discussed in section 2.5.2. A microcapsule containing this heat absorbing material, with a protective structure (e.g. a core and layer capsule with bacteria located in the inside) could potentially give additional resistance to the cells.

Additionally, because PCM can absorb heat from temperature fluctuation, they could potentially protect probiotics during transportation where temperatures can vary during the day. Transportation is the parameter of the probiotic's life cycle that has been neglected from the research to date. This parameter is of main importance for New Zealand's products as the country's economy principally relies on international trade. Export of New Zealand's good and services reached about \$80 billion in 2018 with primary destination being China, Australia and Europe ("Goods and services trade by country: Year ended June 2018 – corrected," 2018). Dairy products are the principal goods being exported and it is important to ensure the quality is maintained during transportation and until reaching the consumer. During transport in cargo ship, the temperature can fluctuate between 20 and 50°C in a day, and up to 60°C depending on

the zone (Rodríguez-Bermejo et al., 2007; Singh et al., 2012). However, all studies looking at the shelf-life of dried probiotic are taking place at constant temperature. How bacteria are affected by temperature fluctuation, and how to protect them from this stress is still unknown.

Witocan® 42/44, a triglyceride obtained by esterification of glycerine with selected fatty acids, is a PCM which has a melting temperature of 44°C, and a crystallisation occurring below 30°C. Therefore, heat would be absorbed around 44°C, when the lipid melts, and will be re-transferred to the system below 30°C, when the lipid crystallises. In theory the characteristics of this material make it ideal to protect bacterial cells under storage conditions mentioned previously.

Therefore, the first objective of the present study was to establish if the use of a PCM within an encapsulation matrix could help prolong the viability of bacterial cells, especially during transport where temperatures are likely to fluctuate. The second objective was to determine if the PCM needed to be surrounding the bacteria to protect from heat, or to be dispersed within a stabilisation matrix.

The PCM was emulsified into sodium caseinate as a carrier protein to avoid release of the lipid in the system upon melting. Sodium caseinate was chosen for its good encapsulation properties (Vega & Roos, 2006). In a second step, bacteria were suspended in a stabilisation matrix mix, as described previously. The first core-and-layer structure was obtained by spray drying both solutions through a three-fluid nozzle with the bacteria slurry sprayed in the inner-nozzle, and the emulsion system sprayed in the outer one. The second structure simply consisted of mixing both solutions just before freeze-drying. Two ratios of protein to PCM were compared: 1:1 and 1:3, to establish whether the amount of fat changing phase is correlated with the stability of the bacteria. This was compared to samples containing the stabilisation mix and the protein, as well as freeze-dried bacteria

in the stabilisation matrix only, obtained from last chapter (i.e. a mix of 80% of MSG and 20% of sorbitol, with inulin).

Samples were followed under two storage conditions: fluctuating temperature of 20 to 50°C in 24-hour cycles and under the mean temperature (35°C), to know how much the shelf-life of *Lb. rhamnosus* can be extended at high temperature, and to confirm if PCM protect from the temperature fluctuation itself.

## 6.2 Materials and methods

### 6.2.1 Materials

Witocan® 42/44 was generously given by IOI Oleo GmbH, Witten, Germany. Sodium caseinate was obtained from Fonterra, Auckland, New-Zealand. Inulin (Frutafit TEX, DP  $\geq$  22) was acquired from IMCD New Zealand Ltd., Auckland, New Zealand. Tween 20, Nile red, Fast green FCF, Acridine orange, L-glutamic acid monosodium salt monohydrate (MSG) and D-sorbitol were all bought from Sigma Aldrich, Saint-Louis, MO.

### 6.2.2 Sample Preparation

#### 6.2.2.1 Preparation of the stabilization matrix

The stabilisation matrix was prepared by firstly adding 12.5% (w/v) of inulin to sterile phosphate buffer (0.1 M, pH = 7.4) under stirring and low heat until complete dissolution (about 10 minutes). Then, 10% (w/v) of L-glutamate monosodium salt and 2.5% (w/v) of sorbitol were added to the solution. The solution was left to stir until all components were completely dissolved before being placed at 4°C until needed.

#### 6.2.2.2 Preparation of the coating

The coating solutions consisted of either an emulsion of Witocan® 42/44 with sodium caseinate and Tween 20, or the solution of sodium caseinate and Tween 20. 10%

(w/w) sodium caseinate was dissolved in water with stirring at low heat until complete dissolution of the protein. 1% (w/w) of Tween 20 was added to the final solution.

To prepare the emulsions, Witocan® 42/44 was added to the protein solution (two ratios of sodium caseinate to Witocan® were prepared: 1:1 and 3:1) and placed in a water bath at 65°C to melt the fat. A first coarse emulsion was formed by mixing with a hand held homogenizer (model D-130, LabServ, Ireland) at 90% of its maximum speed for 1 min. This coarse emulsion was then passed through a homogeniser at a pressure of 300 for the first pass, and 40 for the second, for 1 min.

Prior the drying, the moisture contents of the emulsions were measured in triplicate with a moisture analyser (model MB23, Ohaus, Australia) to ensure same concentration for all encapsulation solution (i.e. the protein solution and the emulsions). The emulsion was then diluted to obtain 10.9% of solids which correspond to the concentration of the protein solution (i.e. the more diluted).

#### **6.2.2.3 Particle size distribution of the emulsions**

The particle size distribution was measured using a Mastersizer 2000S (Malvern Panalytical Ltd., UK) before and after the dilution. All measurements used a refractive index of 1.33 for the water, and 1.47 for the oil droplet and an absorbance index of 0.01. Measurements were made in triplicates when the laser obscuration of 7 to 17% was reached

#### **6.2.2.4 Harvesting of the bacteria**

Bacteria were grown as previously described and harvested when entering the stationary phase by centrifugation at 4,000g for 5 min at 4°C. Cell pellets were washed twice with phosphate buffer before being re-suspended in the cold stabilisation matrix. Cellular suspensions were allowed to equilibrate for 1 hour at 4°C.

## 6.2.3 Drying

### 6.2.3.1 Freeze-drying






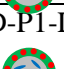

The coating solutions were added to the cellular suspension after the equilibration time. The true control consisted of the cells in the stabilisation matrix only and no coating solution was added to it. The suspensions were then freeze-dried as described in section 3.2.6.

### 6.2.3.2 Spray drying

Prior to spray drying, the coating solution and stabilisation matrix were not pre-mixed. The solutions were directly spray-dried after the equilibration time on a mini spray dryer B-290 from Buchi (Switzerland), mounted with a three-fluid nozzle, and coupled with a dehumidifier (B-296, Buchi, Switzerland). The stabilisation matrix was fed into the core of the nozzle, while the coating solution was fed into the outer chamber. The inlet temperature was set at 120°C and the aspiration at 100%. The outlet temperature was monitored over the drying period and varied between 66 and 76°C. The feeding rate was approximately 1.8 g/min for the core and 3.2 g/min for the coating. The aim was to obtain a 1:1 ratio between the core and the coating (dry basis) with about 3.3% of dried cells in the final powder as shown in Table 6.1.



**Table 6.1:** Composition of the seven samples with or without PCM. The little cartoons represent the desired structure, with the stabilisation matrix in grey, the bacteria in blue, the protein in green, and the lipid in red. All samples contained 3.3% (w/w) of dried cells.

Sample Name	Drying	Level of protein	Level of lipid	Step 1 - Stabilisation matrix				Step 2 - Coating		
				MSG	Sorbitol	Inulin	Phosphate salts	NaCas	Lipid	Tween 20
 FD-P0-L0	Freeze-drying	0	0	g	10.0	2.5	12.5	1.7	0.0	0.0
				%	36.3	9.1	45.4	6.0	0.0	0.0
 FD-P1-L0	Freeze-drying	1	0	g	5.0	1.3	6.3	0.8	12.0	0.0
				%	18.2	4.6	22.8	3.0	43.8	0.0
 FD-P1-L1	Freeze-drying	1	1	g	5.0	1.3	6.3	0.8	6.0	6.0
				%	18.2	4.6	22.8	3.0	21.9	21.9
 FD-P1-L3	Freeze-drying	1	3	g	5.0	1.3	6.3	0.8	3.0	9.0
				%	18.2	4.6	22.8	3.0	10.9	32.8
 SD-P1-L0	Spray-drying	1	0	g	5.0	1.3	6.3	0.8	12.0	0.0
				%	18.2	4.6	22.8	3.0	43.8	0.0
 SD-P1-L1	Spray-drying	1	1	g	5.0	1.3	6.3	0.8	6.0	6.0
				%	18.2	4.6	22.8	3.0	21.9	21.9
 SD-P1-L3	Spray-drying	1	3	g	5.0	1.3	6.3	0.8	3.0	9.0
				%	18.2	4.6	22.8	3.0	10.9	32.8

## 6.2.4 Shelf-life study

Once dried, the freeze-dried powders were ground using a mortar. Spray-dried powder did not need any grinding step. All samples were then mixed with skim milk powder ( $A_w=0.09$ ), at 10% (w/w). The powder was subsampled into three side seal foil pouches, and stored in two different incubators. The first incubator was set at a varying temperature between 20 and 50°C. The set up study was as follows: 6 hours at 20 °C, 6 hours going up to 50 °C, 6 hours at 50°C and 6 hours going back down at 20°C. The second incubator was set at a constant temperature of 35°C, which is the mean temperature of the first incubator. The shelf-life of the powder was followed for 6 months under fluctuated temperature, and for 12 months under constant temperature.

The remaining probiotic powder was stored at -80°C until further analysis.

#### **6.2.4.1 Enumeration of viable cell**

Samples from the 20-50°C study were enumerated every 15 days, while the samples from the 35°C incubator were tested every 30 days. The plating method was adapted from a method developed by Okuro, Thomazini, Balieiro, Liberal, and Fávaro-Trindade (2013) in order to melt the lipid in the samples and ensure release of all bacteria: 1 g of powder was rehydrated in 9 mL sterile salted peptone water which was pre-heated to 50°C. The bottle was shaken for at least 30 seconds at maximal speed before continuing with the serial dilution, at room temperature, following the methodology previously used, as described in section 3.2.6.

### **6.2.5 Characterisation of the powder**

#### **6.2.5.1 Differential scanning calorimetry**

DSC scans were performed as previously presented in section 5.2.4.1. Briefly, for samples containing the emulsion system, the measurement consisted of two first cycles from 0 to 50°C, in order to analyse the melting and crystallisation pattern of the powder, and one cycle from 0 to 100°C to look for any other events. The bulk lipid, Witocan® 42/44 was run from 10°C to 80°C, and emulsions were run after their dilution from 0°C to 65°C.

#### **6.2.5.2 Solid fat content nuclear magnetic resonance (SFC NMR)**

The powder was run on a Bruker Minispec NMR spectrometer, model Mq20 NMR Analyser (Bruker Analytische Messtechnik GmbH, Rheinstetten, Germany) to measure the solid fat content under cycles of temperatures. Measurements were done every minute over 48 hours. Two cycles of temperature were performed, following the same pattern as for the shelf-life (see section 6.2.4), starting with the step from 20 to

50°C. Temperature cycles were performed using a Haake F8 Circulator with refrigerated bath model C35 (Thermo Fisher Scientific Inc., USA).

#### **6.2.5.3 Scanning electron microscopy**

Samples were imaged as described in section 5.2.4.2.

#### **6.2.5.4 Confocal scanning laser microscopy (CSLM)**

In order to be visualised on the CSLM, additional samples were prepared, by staining them before drying, thus avoiding risk of powder dissolution and structural loss. Emulsions were stained with 2% (v/v) Nile red (1 mg/mL in acetone, for lipid staining) and 6% (v/v) Fast Green FCF (1 mg/mL in MilliQ water, for protein staining). Acridin orange was used for bacteria staining, and was directly added to the stabilisation matrix solution at 1mg/10mL of phosphate buffer. Bacteria were harvested as described above and mixed with the stained stabilisation matrix, before being dried with the emulsion

Powders were then dispersed into a droplet of canola oil to prevent dissolution while having good dispersion of the powder before placing a small amount on a cavity microslide. Microscopy imaging was performed using an LSM800 (Carl Zeiss Ltd., Germany) confocal microscope. Three laser lines were used: laser 405 for the Acridine Orange; 488 for the Nile Red and 640 for the Fast Green. Imaging was done using the 63x oil immersion objective lens (magnitude 1.8). Use of Airyscan and mosaic imaging was also done with the LSM 800 microscope. Laser excitation parameters were set at 405nm for the bacteria stained with Acridine Orange, 488 nm (argon laser – Nile Red) for the fat phase and 633 nm (helium-neon laser – Fast Green) for the protein phase. The micrographs produced were combined into images of the bacteria (in blue), lipid (in red) or protein (in green) phases.

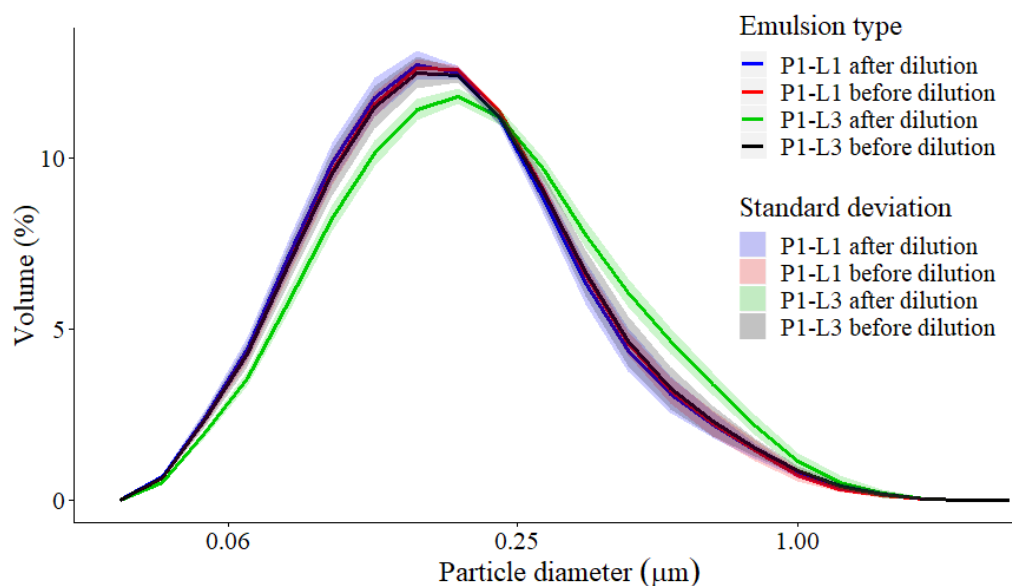
### 6.2.6 Statistical analysis

Statistical analysis were performed using ANOVA, followed by Tukey test. All statistical analysis were performed using Minitab 18.1.

## 6.3 Results and discussion

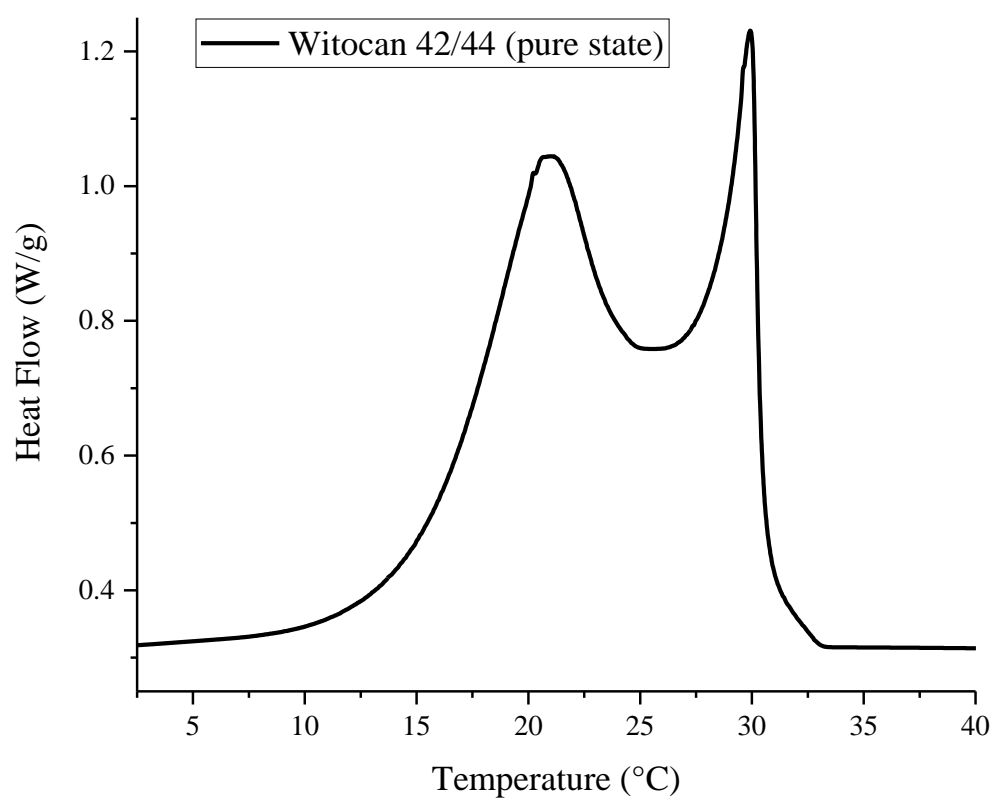
### 6.3.1 Emulsion characteristics

The particle size distribution of the emulsions was monitored before and after their dilutions to ensure consistency. Results are presented in Figure 6.1. The emulsion with higher amount of lipid (P1-L3) presented slightly higher particle size after dilution, but the difference was considered as negligible. The volume moment mean (De Brouckere Mean Diameter, i.e.  $D[4,3]$ , which is less impacted by small droplets) was of 0.20  $\mu\text{m}$  for P1-L1 and 0.23  $\mu\text{m}$  for P1-L3 after dilution. The median particle size was of 0.15  $\mu\text{m}$  for P1-L1 and 0.18  $\mu\text{m}$  for P1-L3 after dilution. A similar particle size distribution should ensure consistent melting and crystallisation pattern among all samples containing lipids.

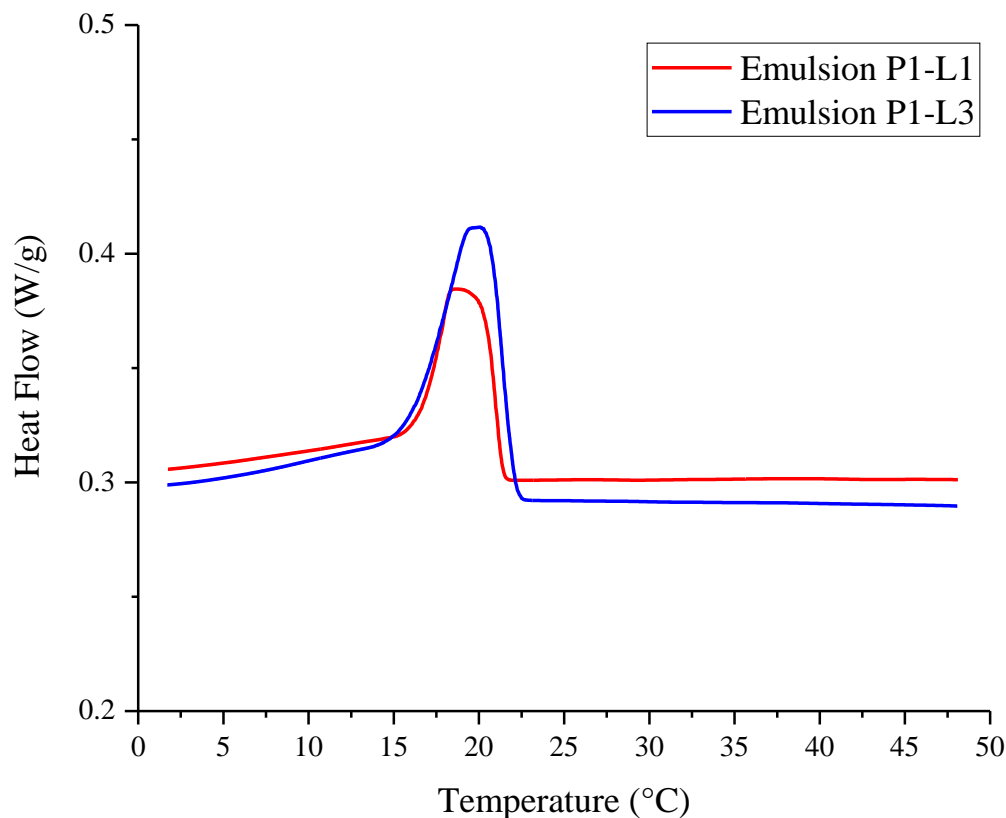


**Figure 6.1:** Particle size distribution of the emulsions before and after dilutions. The lines denote the mean value and the ribbon the standard deviation. Dilution was made before drying to match the concentration of the protein solution, i.e. 10.9% (w/w).

The resulting crystallisation pattern of the emulsions are presented in Figure 6.3 and the crystallisation of the bulk lipid is shown in Figure 6.2. Interestingly, when in the bulk state Witocan® 42/44, showed two peaks of crystallisation at 21°C and 30°C, there was only one peak of crystallisation present once the lipid was emulsified as shown in Figure 6.3 (with a maximum of crystallisation peak of about 18°C for P1-L1 and 20°C for P1-L3). The presence of two peaks on the crystallisation pattern of Witocan® 42/44 indicates that several crystallisation events are occurring. Even though the crystallisation peak for the emulsions are narrow (Figure 6.3), they are not sharp, suggesting that the two crystallisations events are still occurring. The lower crystallisation temperature of the emulsified lipid has already been reported by the literature, and was explained by the increase of inactive seed crystals caused by smaller particle size (Alba-Simionesco et al., 2006; Tang, Choi, & Ma, 2007; Zhang, Yuan, Zhang, & Cao, 2015).



**Figure 6.2:** Crystallisation pattern of Witocan® 42/44 in a pure state.



**Figure 6.3:** Crystallisation pattern of emulsions after dilution, which was made before drying to match the concentration of the protein solution, i.e. 10.9% (w/w).

### 6.3.2 Characteristics of the powders

#### 6.3.2.1 Internal structure of the powders (CSLM)

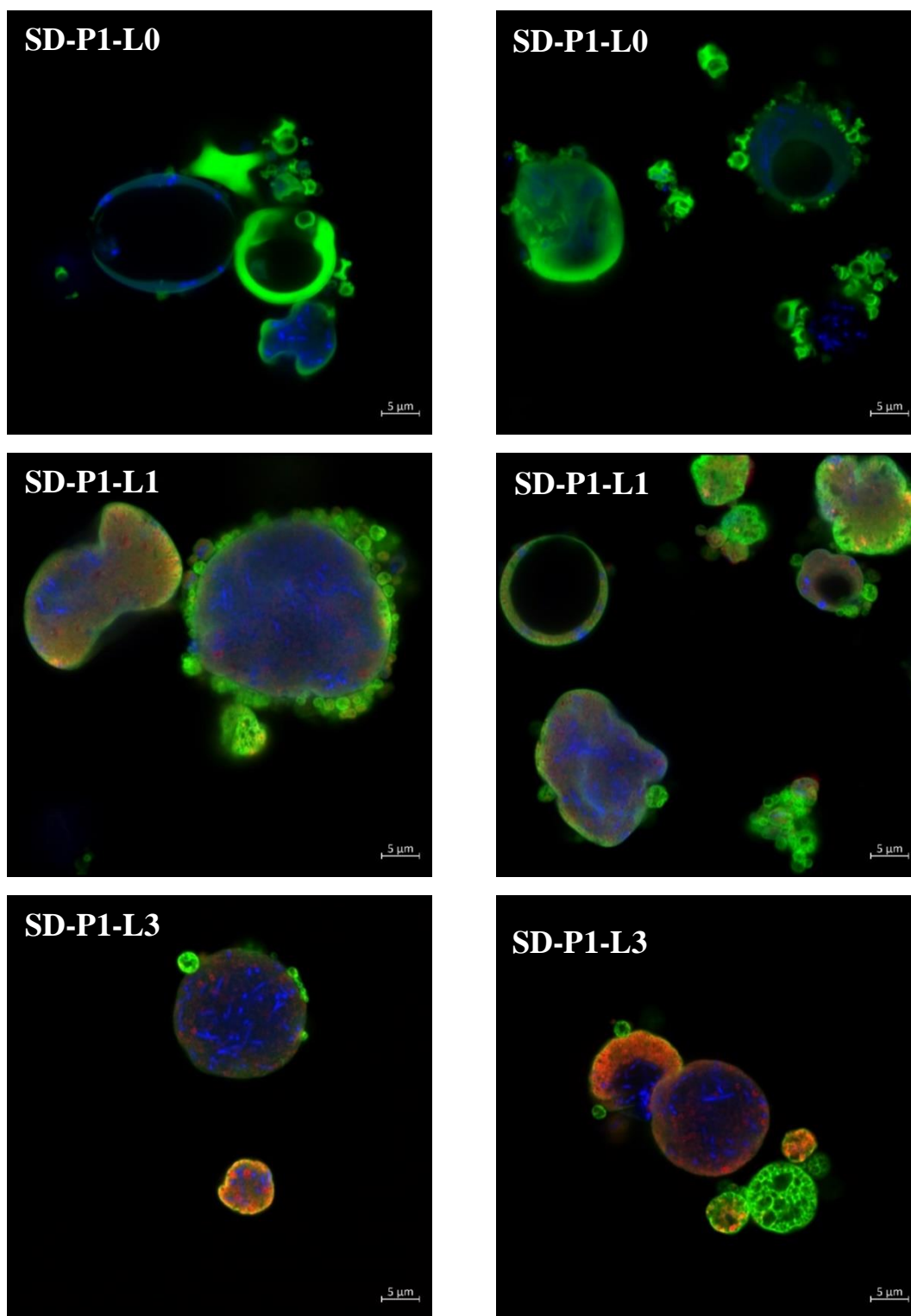
The next step was to prepare the spray-dried samples using the three-fluid nozzle. It was hypothesized that this nozzle configuration would give a powder with a core (bacteria) and layer structure. The internal structure was visualised by CSLM and images are shown in Figure 6.4. The images confirm that the bacteria are mostly present in the core of the particle, and the outer layer is denser in protein or lipid and protein. Some smaller particles, rich in proteins (mainly seen as green) are aggregating to the outside of the bigger particles where the bacteria are located. The signal for the lipid was stronger




on SD-P1-L3 compared to SD-P1-L1, confirming that more lipid was present in the powder. Interestingly, the lipid seemed to be relatively well dispersed around the bacteria, while the surface of the particles showed a higher density of protein. A possible explanation is that there was more protein present than needed to encapsulate the lipid droplets. As a result, the excess of protein migrated to the interface of the droplet when sprayed to lower the surface tension between the water and the air (Jayasundera et al., 2009). In addition, some particles appeared to be protein only, with no lipid but dark spots, so somehow, when the emulsion was sprayed, a separation occurred with droplets rich in lipids, and other richer in proteins. This could have been driven by a difference of density of the lipid droplets compared to the excess of protein dispersed in the system. Finally, in the absence of lipid, the particles presented a ring shape, while samples with lipid seemed to maintain a more spherical shape.

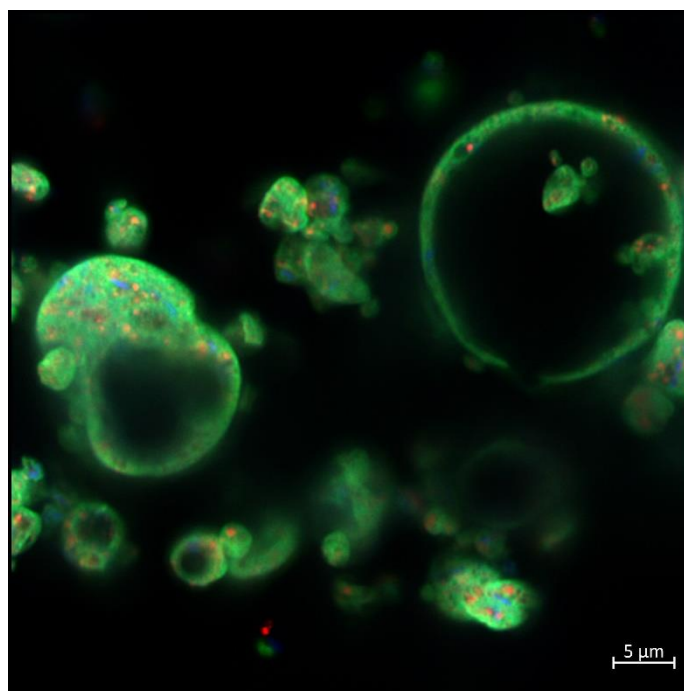
Figure 6.5 shows a spray-dried sample with bacteria, and lipid (P1-L1) sprayed with a two-fluid nozzle, so that both solutions were mixed before drying. On comparing the powders it can be said that the two-fluid nozzle produced a more homogenous powder as the protein, bacteria and lipids are dispersed throughout the particles contrary to the structure obtained with the three-fluid nozzle that show the core-and-layer structure, which may impart greater stability to the bacteria during storage.

It was not possible to visualise the structure of the freeze-dried sample using CSLM. The freeze-drying process affected the dyes which were added before the drying step as per the spray-dried samples. The most likely reason for this is because freeze-drying is a long process compared to spray drying. No differentiation between bacteria, lipid and protein could be seen on analysis. Thus, only SEM has been done on these powders, which will be presented in the next section. SEM pictures will help to further understand the overall structure.





**Figure 6.4:** Confocal microscopy of the spray-dried samples: SD-P1-L0 (  ) in first row, SD-P1-L1 (  ) in second row and SD-P1-L3 (  ) in third row. Bacteria are in blue, protein in green, and lipid in red. The bar indicates 5 μm.



**Figure 6.5:** Confocal microscopy of the spray-dried powder using a two-fluid nozzle. Bacteria in the stabilisation matrix was mixed with the emulsion system (P1-L1) before spraying. Bacteria are in blue, protein in green, and lipid in red. The bar indicates 5  $\mu\text{m}$ .

### 6.3.2.2 External structure of powders (*Scanning Electron Microscopy*)

Spray-dried powder with no PCM (SD-P1-L0), presented a deflated ballon-like shape (Figure 6.6). This is a common shape for spray-dried powders (Lapsiri, Bhandari, & Wanchaitanawong, 2012; Liu et al., 2018), and explains the ring shape seen in the confocal micrographs. As mentioned previously, the protein migrates quickly to the air and water interface. This layer dries first and as the rest of the moisture evaporates, the structure collapses, leading to this particular shape (Jayasundera et al., 2009).

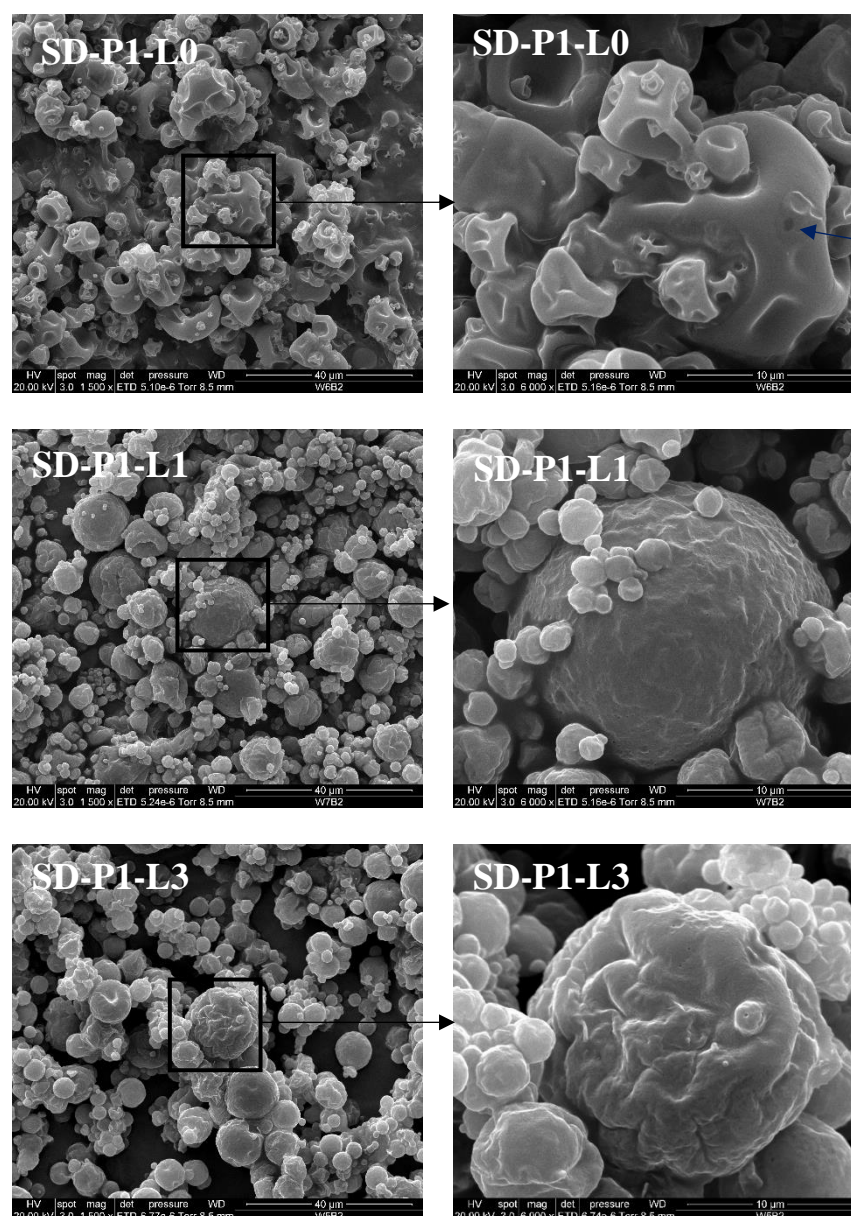
Spray-dried samples with PCM (SD-P1-L1 and SD-P1-L3), did not present the deflated shape (Figure 6.6). Instead, they had a coarse surface. This has already been noticed in the literature, and is characteristic of samples containing lipid (Vega & Roos,

2006). For all three spray-dried samples, no bacteria were found on the outside of the particles, confirming that bacteria are located in the core of the particles.

Figure 6.7 presents the SEM micrograph of freeze-dried samples. The control powder (FD-P0-L0) had a very smooth surface. In the left picture of Figure 6.7, the sample seems inflated, and as the microscope zoomed (in the right picture of Figure 6.7), the structure deflated. This suggests that a skin had formed on the outside of the sample. It was previously suggested (section 5.3.3) that the sample collapsed during freeze-drying, creating a layer on the outside which prevented the powders from drying completely. The presence of this skin on the sample reinforces this hypothesis.

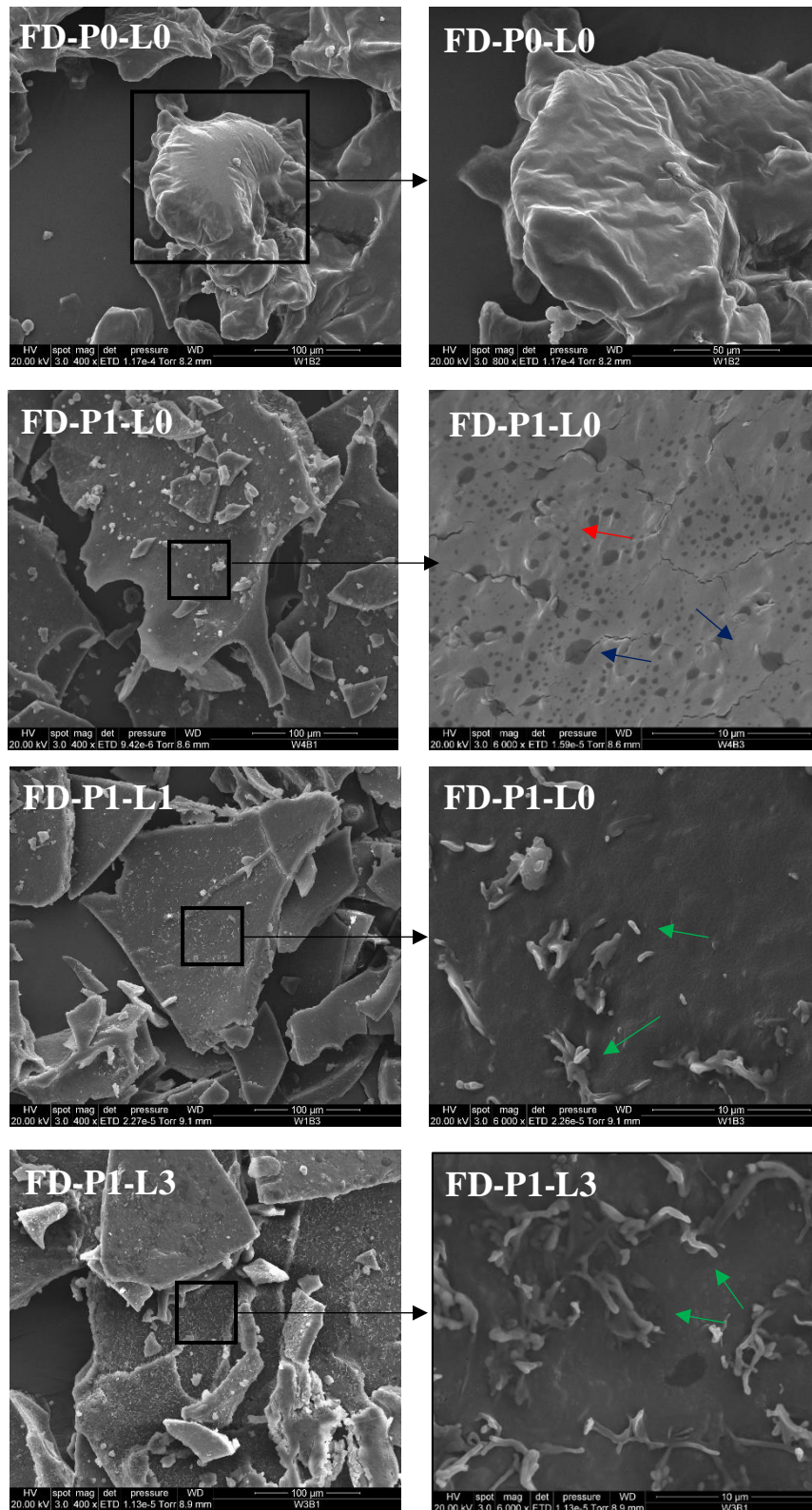
The addition of the sodium caseinate (FD-P1-L0) led to a slightly less smooth structure, suggesting that the powder did not collapse during the freeze-drying process. Some bacteria are visible on the surface as shown by the red arrow on the zoomed micrograph. In addition, the surface of the powder was covered with black stains. A similar black stain was also present on the spray-dried sample (Figure 6.6, blue arrow). Observations showed that these spots were not holes, but small black areas. No explanations on the cause of these stains were found in the literature. It is proposed that the sodium caseinate aggregated to itself or to other components of the protective matrix, and attracted the electron beam of the SEM, leading to these darker areas.

Both freeze-dried samples with PCM (FD-P1-L1 and FD-P1-L3) presented numerous rod-shape structures on the surface. It was initially thought that these structures were bacteria. However, examination of a control samples, of FD-P1-L3 without bacteria, showed in Figure 6.8 confirmed that they were not bacteria. As the density of these structures increased with the amount of PCM, they are most likely crystallised lipid on the surface.

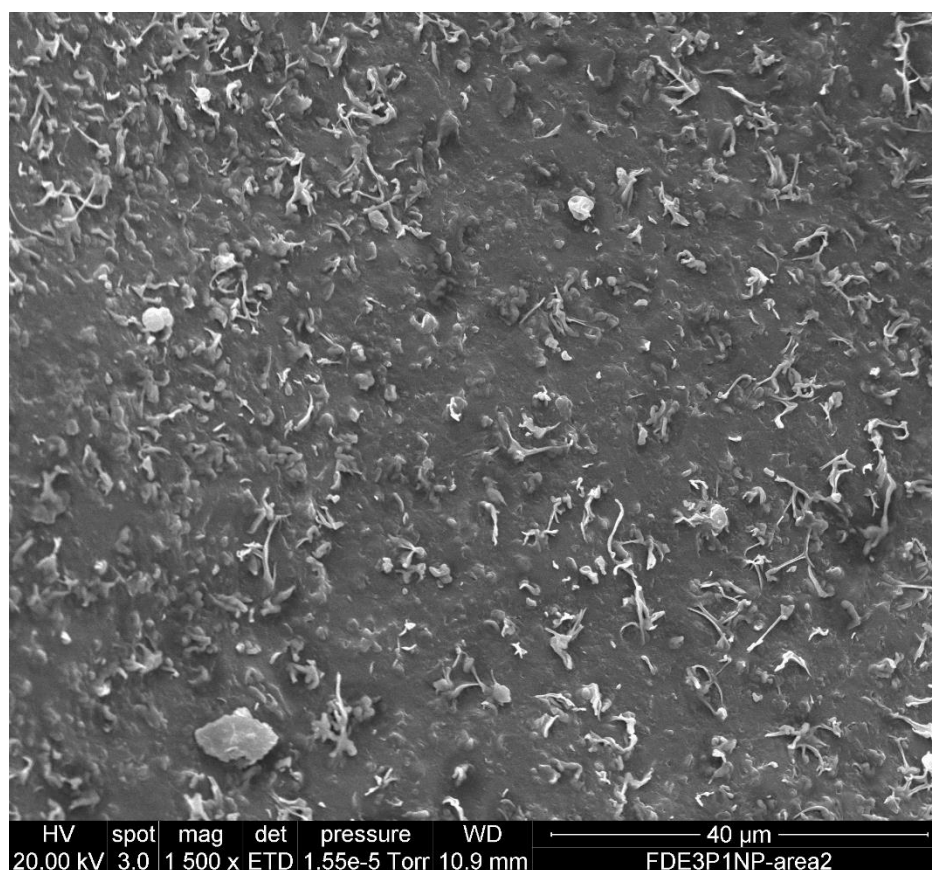


**Figure 6.6:** SEM micrographs of the spray-dried samples. SD-P1-L0 (🌀), SD-P1-L1 (🌀), and SD-P1-L3 (🌀). Micrographs on the right presents the enlargement (6 000 X) of the micrograph on the left (1 500 X). The blue arrow show a black stain.





**Figure 6.7:** SEM micrographs of the freeze-dried samples: FD-P0-L0 (🦠), FD-P1-L0 (🦠), FD-P1-L1 (🦠) and FD-P1-L3 (🦠). Micrographs on the right presents the enlargement (6 000 X, apart for FD-P0-L0, 800 X) of the micrograph on the left (400 X). Bacteria are denoted with a red arrow, crystallised fat with a green arrow and black stains with a blue arrow.



**Figure 6.8:** SEM micrograph of the FD-P1-L3 prepared without bacteria. Magnification 1500 X.

### 6.3.2.3 Thermal behaviour of the powder

The glass transition temperatures ( $T_g$ ) of the powder with no PCM is presented in Table 6.2, along with the water activity of all powders after drying.  $T_g$  values varied between 23.91°C and 37.64°C and it was significantly correlated with the water activity after drying, with a Pearson correlation of -0.79 ( $p$ -value < 0.05). Overall, freeze-drying led to a generally lower water activity, as the drying process might be more effective in terms of water removal from the sample, resulting in a higher glass transition temperature. Interestingly, the control sample (FD-P0-L0) presented a relatively low water activity, of about 0.17 with a high variation of 0.08. It was previously found (see section 5.3.1, Figure 5.2) that the increase in MSG led to an increase of water activity in the freeze-dried

powder. Here, the addition of the sorbitol helped obtaining a more efficient drying, but still led to the collapsed structure with the presence of an outer layer, as presented in the previous section. As a result, the  $T_g$  of the control powder was higher than expected, as the model obtained in last chapter predicted a  $T_g$  of about  $10^{\circ}\text{C}$  (Figure 5.2), and here it reached  $28.96^{\circ}\text{C}$ .

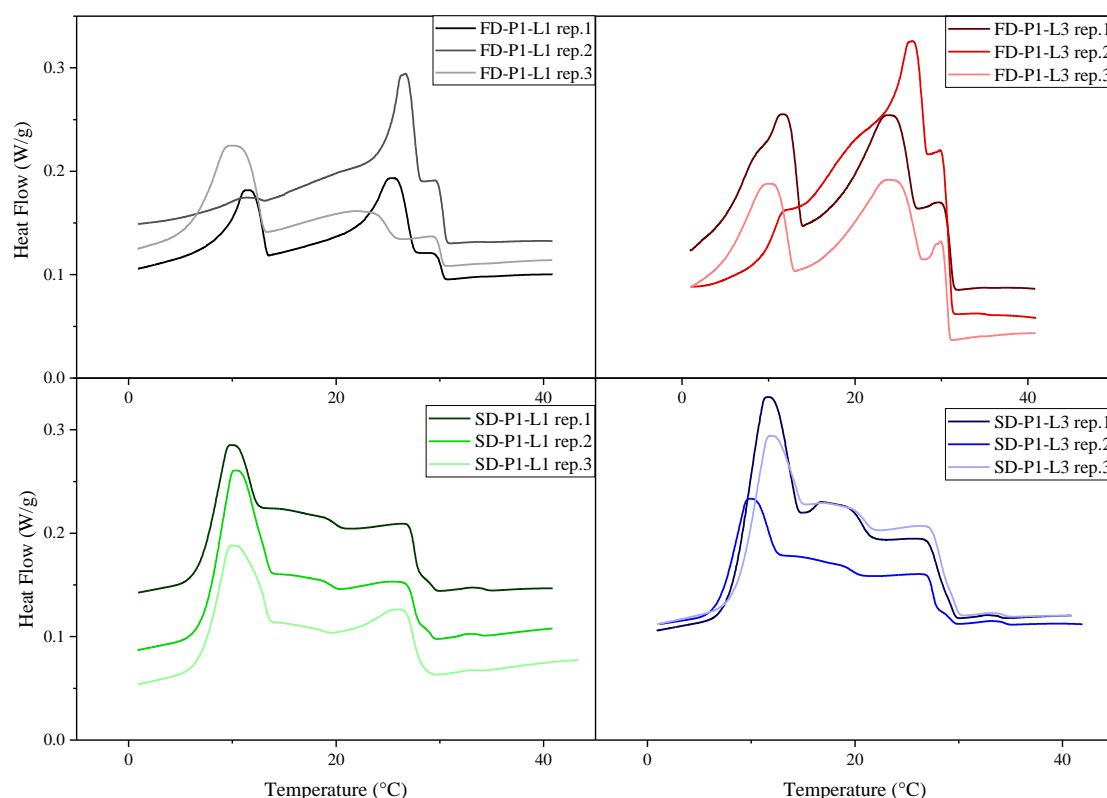
**Table 6.2:** Glass transition temperature and water activity of powders with and without PCM after drying.

Data are shown as the mean values of triplicates with their standard deviation.

Sample	water activity after drying	Glass transition temperature ( $^{\circ}\text{C}$ )
FD-P0-L0	$0.17 \pm 0.08$	$28.96 \pm 1.17$
FD-P0-L1	$0.06 \pm 0.02$	$37.64 \pm 3.83$
FD-P1-L1	$0.09 \pm 0.04$	ND
FD-P1-L3	$0.09 \pm 0.05$	ND
SD-P1-L0	$0.22 \pm 0.03$	$23.81 \pm 9.09$
SD-P1-L1	$0.15 \pm 0.04$	ND
SD-P1-L3	$0.16 \pm 0.03$	ND

The drying method also had an effect on the crystallisation pattern of the PCM as shown in Figure 6.9. Freeze-drying led to more variation between samples, with crystallisation generally occurring at higher temperatures. The crystallisation pattern depends on the lipid droplet size as well as the composition of the wall entrapping the droplets. The smaller the droplets, the lower the crystallisation occurs (Alba-Simionesco et al., 2006). In this experiment, the particle size distribution was controlled for all samples during the emulsification step (see Figure 6.1), therefore there was no correlation between the particle size distribution of the emulsions and the crystallisation pattern. Instead, the crystallisation pattern could be linked with the drying step. During the freezing step of the drying process, the growth of ice crystals can disrupt the structure of the emulsions. Similarly, the application of heat and pressure when going through the

spray dryer nozzle, may well affect the emulsion, and result in different crystallisation patterns. As PCM in the freeze-dried samples crystallised quicker than in the spray-dried samples, it is likely that freeze-dried samples had bigger PCM droplet size, compared to spray-dried samples.

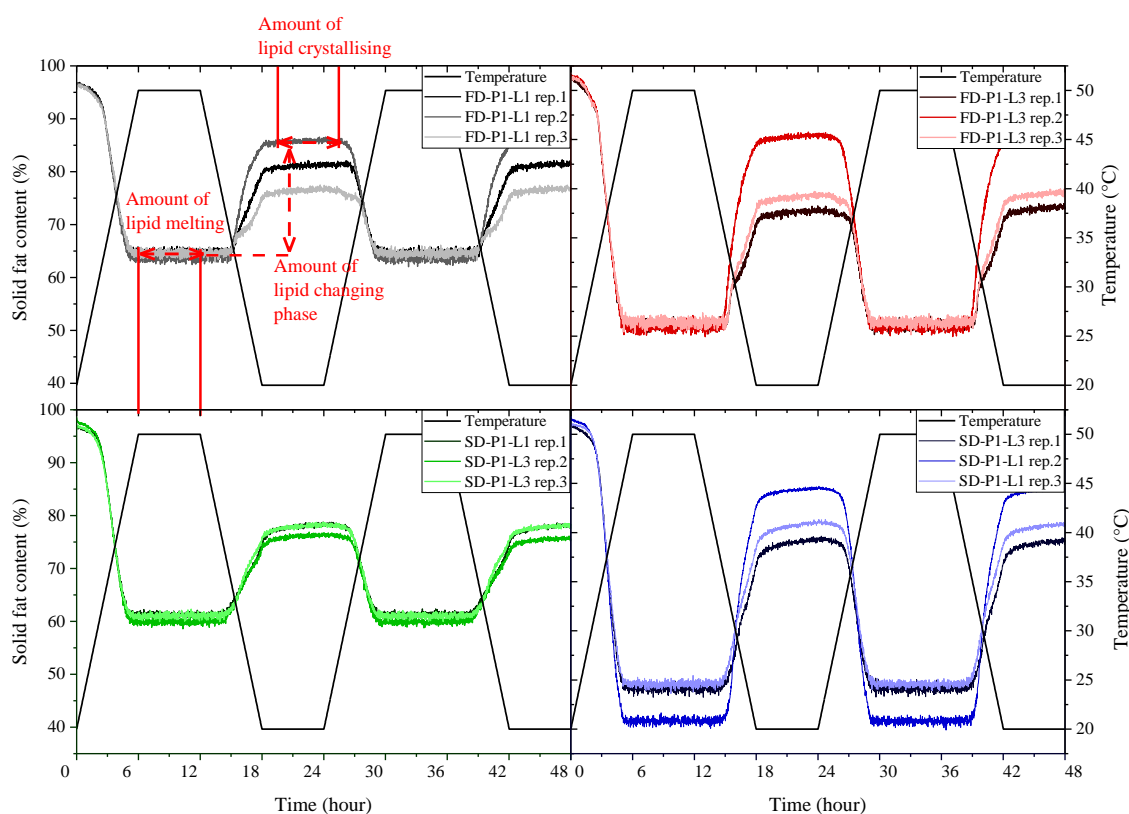


**Figure 6.9:** Crystallisation pattern of the 4 samples containing Witocan® 42/44, with the details of their replicate. Freeze-dried samples are presented at the top, and spray-dried samples at the bottom. Samples with 1:1 lipid to protein are on the left, and samples with 3:1 lipid to protein are on the right.

It was assumed that the enthalpy of the crystallisation between 20 and 50°C would be linked with the amount of phase changing lipid present in the samples during the cycles of temperature. To verify this assumption, the percentage of phase changing lipid was measured by SFC NMR over two cycles – 48 hours in total, showed in Figure 6.10. The measurements started at 20°C with the temperature being increased to 50°C over 6 hours,



then maintained at 50°C for 6 hours, and again lowered to 20°C over 6 hours where it was maintained there for a further 6 hours. This consisted of one cycle – 24 hours – and it was repeated once. From this measurement, the amount of lipid melting, of lipid crystallising and of lipid changing phase were calculated, as explained in Figure 6.10 and presented in Table 6.3.



**Figure 6.10:** Solid fat content change over two cycles of temperatures from 20 to 50°C of the 12 sample containing Witocan® 42/44. Freeze-dried samples are presented at the top, and spray-dried samples at the bottom. Samples with 1:1 lipid to protein are on the left, and samples with 3:1 lipid to protein are on the right.

It was observed that when the system was cooling back to 20°C, the amount of solid fat was not equal to the amount at time 0 and thus, some lipid was still in the liquid phase. Indeed, as seen on the DSC scans, crystallisation ended between 5 and 20°C.

However, the DSC scans were not representative of what happens in a 24-hour cycle of temperature, where temperature was changing at a much slower rate than occurs during a DSC run (with a rate of 5°C/min on the DSC and of about 0.08°C/min during the temperature cycles). During the DSC scan, the samples did not have time to crystallise properly, and the samples were supercooled due to the high cooling rate. In other words, the onset of the crystallisation occurs at a lower temperature when the cooling rate is high (e.g. on the DSC scans) than when the sample is cooled down slowly (e.g. in the storage conditions imposed here). As a result, the amount of lipid changing phase, as calculated on Figure 6.10, is correlated with both the total enthalpy of lipid crystallisation (Pearson correlation of 0.91, p-value < 0.001) and the enthalpy of crystallisation between 20 and 50°C (Pearson correlation of 0.95, p-value < 0.001) both calculated from the DSC measurement. Thus, the SFC NMR measurement represents the amount of lipid melting and crystallising during the cycles of temperatures, while the DSC gives additional information on the structure of the samples.

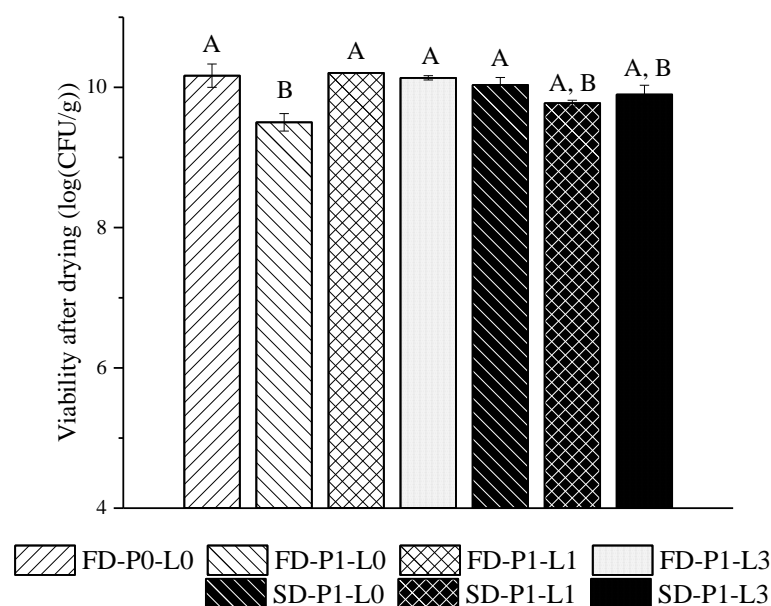
**Table 6.3:** Crystallisation behaviour of the samples with PCM. Data are expressed as the mean with the standard deviation of triplicates.

	DSC measurement		SFC NMR measurement		
	Total enthalpy of crystallisation (W/g)	Enthalpy of crystallisation from 20 to 50°C (W/g)	Amount of lipid melting (%)	Amount of lipid crystallising (%)	Amount of lipid changing phase (%)
FD-P1-L1	14.6 ± 1.8	7.2 ± 3.1	64.5 ± 0.7	81.4 ± 4.6	16.8 ± 5.1
FD-P1-L3	22.9 ± 3.9	12.8 ± 4.0	51.0 ± 0.3	78.1 ± 7.5	27.1 ± 7.7
SD-P1-L1	18.9 ± 0.9	5.4 ± 0.2	60.6 ± 0.7	77.3 ± 1.0	16.7 ± 0.4
SD-P1-L3	33.6 ± 4.3	13.0 ± 5.8	45.5 ± 3.8	79.3 ± 5.1	33.8 ± 8.7

### 6.3.3 Viability after drying

The viability of the samples after drying is shown in Figure 6.11. It can be first noted that the drying method did not seem to affect the viability of the bacteria, as it could be expected (Hlaing et al., 2017; Iaconelli et al., 2015). This was confirmed by ANOVA as no significant correlation was found between the drying method and the viability after drying.

Interestingly, the presence of PCM in the sample prior to drying (spray or freeze-drying) had no significant impact on bacteria viability. This was true for all levels of PCM used. As shown in the literature, phase change material has the potential to protect heat labile materials including bacteria from short heat treatment (Penhasi, 2013; Pitigraisorn et al., 2017). However, because of the spray drying set-up used, i.e. the three-fluid nozzle, the bacteria were not in contact with the emulsion system when the heat was implied. This method was chosen to obtain the layer of the microencapsulated lipid around the bacteria, with one drawback: the bacteria will be encapsulated by the emulsion system only outside the spraying nozzle where the lipid is already melted. The alternative is to spray-dry with a two-fluid nozzle, which doesn't lead to the core-and-layer structure as shown in Figure 6.5, but the bacteria would be in the vicinity of the lipid when sprayed, which could potentially protect them from temperature exposure in the spray-dryer.



**Figure 6.11:** Viability after drying of PCM samples. Data are the mean values of triplicates and the error bar denotes the standard error. Samples with different letter are significantly different ( $P < 0.05$ ).

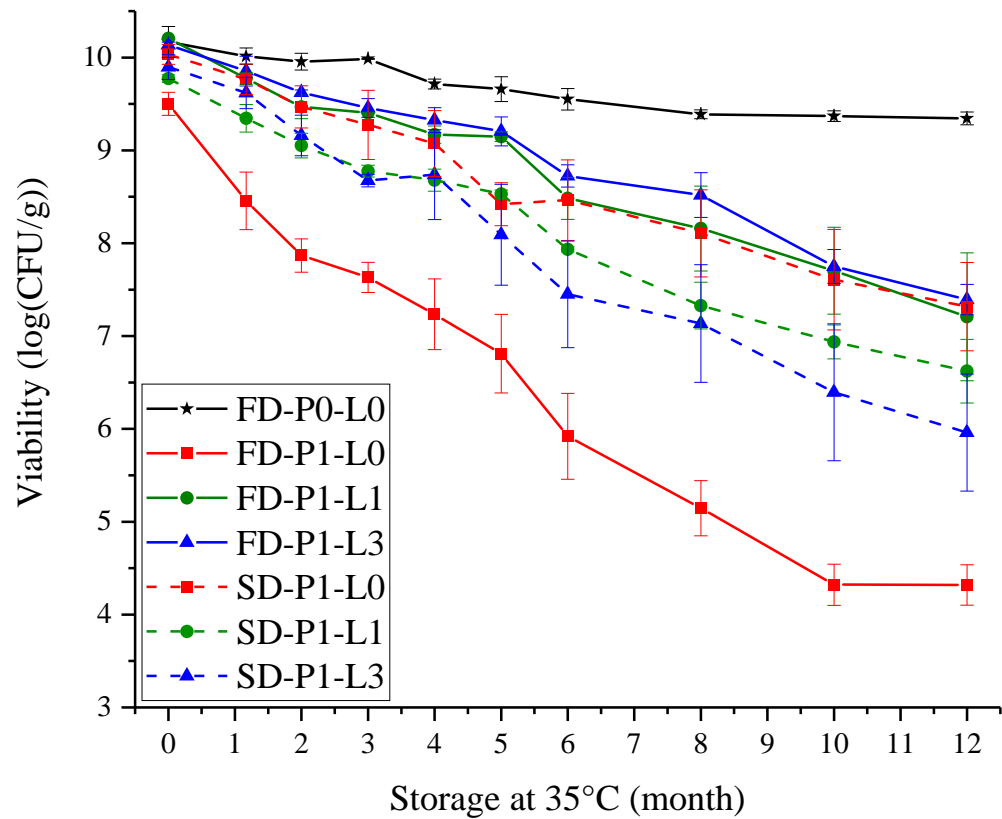
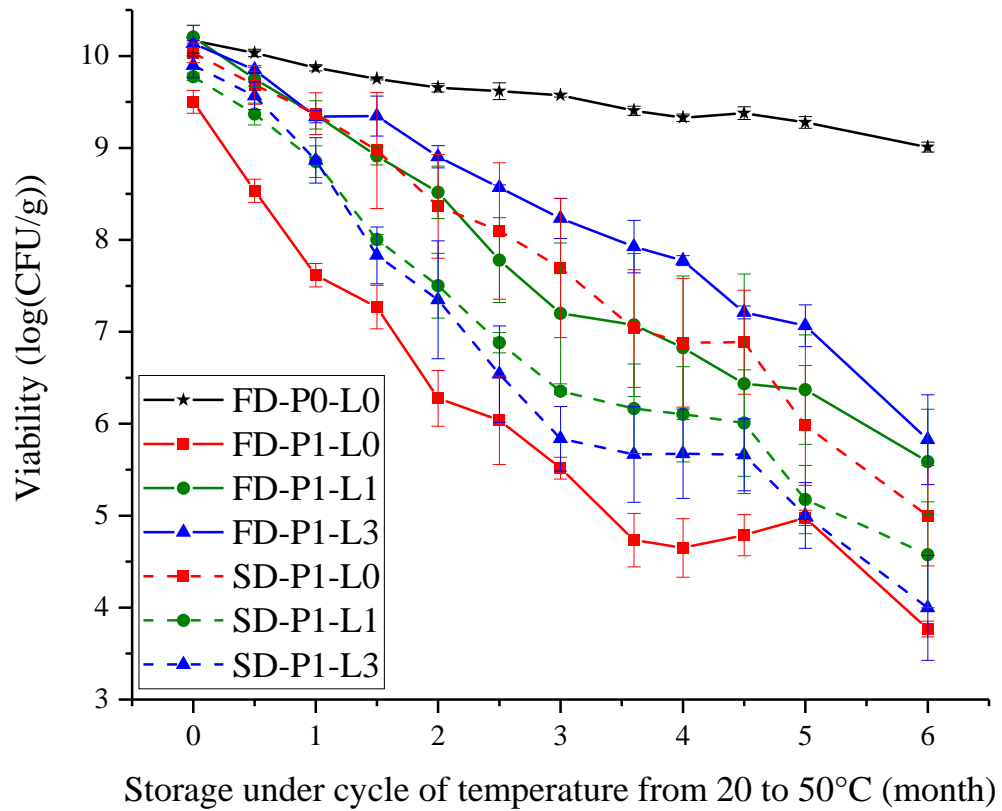
Nevertheless, one sample showed significantly lower viability compared to most samples: FD-P1-L0 with a cell count of 9.5 log (CFU/g). The spray-dried version of this sample, SD-P1-L0 presented a viability of 10.0 log (CFU/g). Thus, the presence of sodium caseinate was destabilising the bacteria during the freeze-drying but not during spray drying. When the sodium caseinate was mixed with the lipid, in the emulsion system (FD-P1-L1 and FD-P1-L3), the bacteria survived better than in the sample with no lipid. This could be due to the surfactant property of the sodium caseinate. In the absence of lipid, the protein may aggregate to itself, or to other components of the matrix, which could have caused the black stains seen on the SEM pictures. However, when adding the lipid to the mix or when spray-dried, the sodium caseinate will preferentially absorb to the oil and water interface, or to the air and water interface, thus preventing its aggregation. Presence of “free” proteins or protein aggregates in the system may thus be detrimental for the cells.

These results show that even if the drying method is not directly affecting the bacteria viability, the way the protectants behave during the drying does have an effect on the bacteria, and may as well affect the stability over time.

#### **6.3.4 Shelf-life studies**

For 6 months, samples were placed under fluctuating temperature between 20°C and 50°C. One cycle consisted of four steps of 6 hours: 6 hours at 20°C, 6 hours going up from 20°C to 50°C, 6 hours at 50°C and 6 hours going back down to 20°C, for a total of 24 hours. In parallel, samples were followed under a constant temperature of 35°C for 12 months.

Figure 6.12 shows both shelf-life studies. It was first obvious that the control sample, consisting of the freeze-dried stabilisation matrix only, resulted in the highest viability during storage. This sample was significantly better at protecting the bacteria compared to all other samples tested ( $p\text{-value} < 0.05$ ). The death rate was of 0.18 under fluctuating temperature, and 0.07 under constant temperature (Table 6.4). There are two potential explanations for this result. Firstly, there could be a minimal amount of the stabilisation matrix needed to protect the cells. For this study, it was decided to standardise the total amount of protection material. By doing that, the bias coming from different ratios between the bacteria and the protection material was avoided, but the amount of stabilisation matrix was higher in FD-P0-L0. Secondly, the composition of the stabilisation matrix (MSG, sorbitol and inulin) might be optimal, and the addition of other material could disrupt the structure of the final powder. As shown earlier, the structure of the powder seemed collapsed, with the formation of an outer layer. The replacement of part of the stabilisation matrix by sodium caseinate or by the emulsion system caused the structure to change and as discussed earlier, the structure of the powder may play an important role on the protection of the probiotic bacteria.



**Figure 6.12:** Shelf-life study of the PCM powders under fluctuating versus constant temperature. Data are the mean values of triplicates and the error bar denotes the standard error.

Results of FD-P1-L0 and SD-P1-L0 also suggested that the structure of the powder had a strong impact on the cell viability during storage. Indeed, both samples had the same composition but varied in the drying method, which caused different stresses to the cells and led to different structures. While freeze-drying is recognised as the gentlest drying method, the death rate of FD-P1-L0 was the worst with 0.89 /month under fluctuating temperature, and 0.49 /month under constant temperature. The spray-dried version of the sample presented a death rate of 0.84 /month under fluctuating temperature and 0.24 /month under constant temperature. The difference in death rate at constant temperature was significant ( $p\text{-value} < 0.05$ ), and showed that the structure obtained by spray drying was stabilising the bacteria. As shown on the SEM pictures (section 6.3.2), bacteria were seen on the surface of the freeze-dried powder and were thus, directly subjected to the environmental stresses. On the other hand, the spray-dried sample presented an outer layer of protein, seen on the confocal microscopy images (section 6.3.2). This layer created a barrier between the bacteria and the environment, similarly to the control sample, FD-P0-L0.

When the lipid was added to the protein mix, the death rate improved for the freeze-dried version (FD-P1-L1 and FD-P1-L3), but not for the spray-dried version (SD-P1-L1 and SD-P1-L3). Under fluctuating temperatures, the differences in death rate between samples were not significant, but in the same order as during the storage at constant temperature. This suggested that the lipid was not providing protection directly against the fluctuations of temperatures. This was confirmed by the SFC NMR results (see section 6.3.2), as there was no correlation between the death rate of the samples and the amount of lipid changing phase. It is believed that as the change of temperature is occurring over such a long period of time (6 hours), the energy absorbed by the phase changing of the lipid is not enough to protect the bacteria. Even though, the addition of

the lipid is still improving the viability of the cells in the freeze-dried sample. This could be due to the same reason proposed in previous paragraph: when adding the emulsion system, the protein is absorbed on the surface of the lipid droplets, and is not interacting with the bacteria, or with itself and aggregating.

Overall, the death rate was higher under fluctuating temperatures, compared to the storage at constant temperature (see Figure 6.12 and Table 6.4). For both storage condition, the order of best protection was as such: FD-P0-L0 >> FD-P1-L3 > FD-P1-L1 > SD-P1-L0 > SD-P1-L1 > SD-P1-L3 > FD-P1-L0.

**Table 6.4:** Details of the storage of samples with and without PCM. Data are expressed as the mean with their standard deviation of triplicates. Samples with different superscripts letter are significantly different ( $P < 0.05$ ).

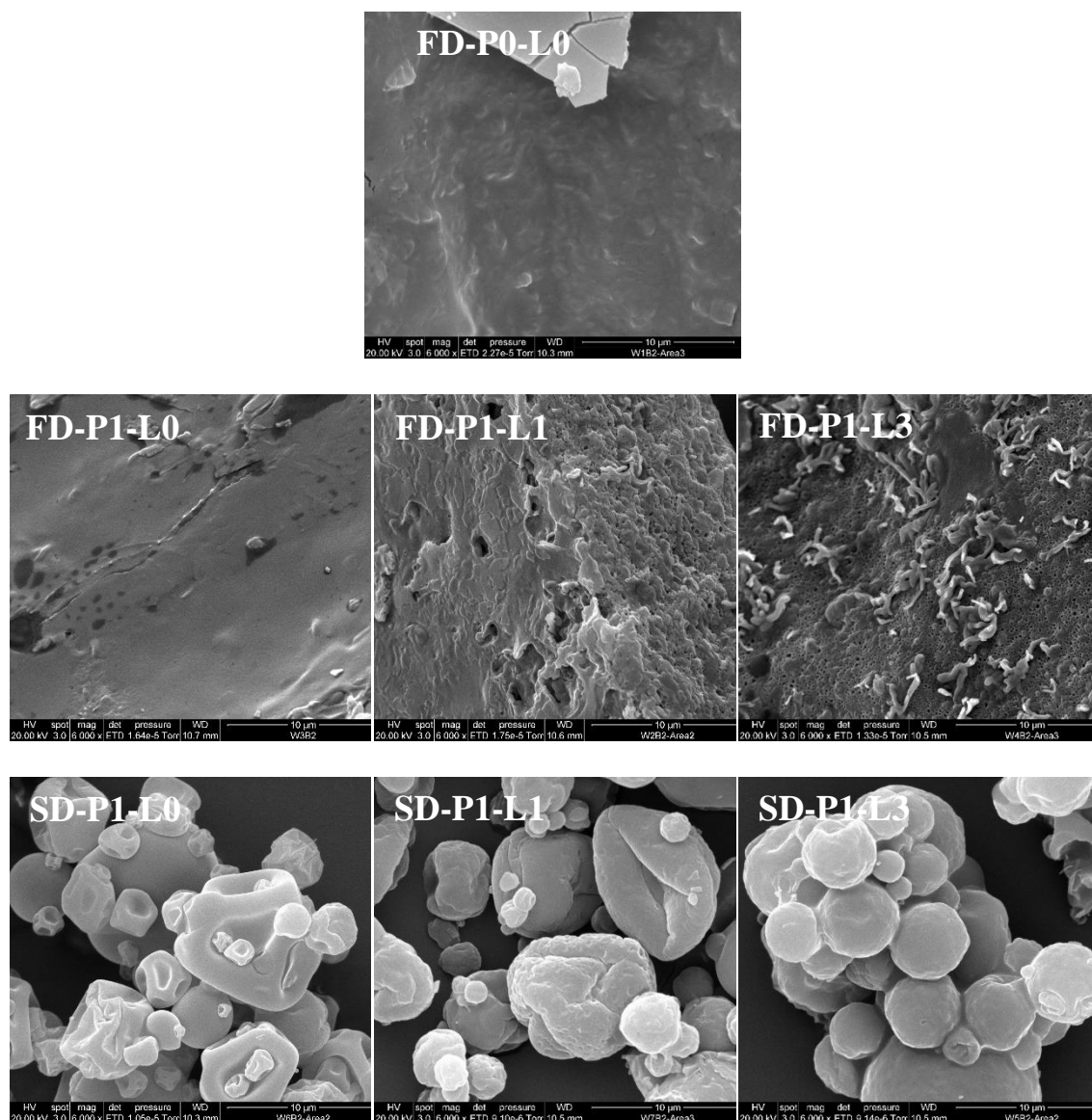
Sample name	Storage under fluctuating temperature		Storage at constant temperature	
	Death-rate /month	Water activity	Death-rate /month	Water activity
FD-P0-L0	$0.18 \pm 0.01^b$	$0.12 \pm 0.01$	$0.07 \pm 0.02^c$	$0.11 \pm 0.02$
FD-P1-L0	$0.89 \pm 0.05^a$	$0.10 \pm 0.01$	$0.44 \pm 0.03^a$	$0.09 \pm 0.01$
FD-P1-L1	$0.78 \pm 0.23^a$	$0.12 \pm 0.01$	$0.24 \pm 0.1^b$	$0.09 \pm 0.01$
FD-P1-L3	$0.66 \pm 0.14^a$	$0.11 \pm 0.01$	$0.23 \pm 0.02^{b,c}$	$0.09 \pm 0.01$
SD-P1-L0	$0.84 \pm 0.16^a$	$0.11 \pm 0.02$	$0.23 \pm 0.07^{b,c}$	$0.10 \pm 0.02$
SD-P1-L1	$0.89 \pm 0.15^a$	$0.12 \pm 0.03$	$0.27 \pm 0.02^b$	$0.11 \pm 0.03$
SD-P1-L3	$1.01 \pm 0.15^a$	$0.12 \pm 0.01$	$0.46 \pm 0.09^{a,b}$	$0.09 \pm 0.01$

Interestingly, there was a significant impact of the storage conditions on the water activity of the powder ( $p$ -value < 0.001). Powders stored under fluctuating temperature had, on average, a water activity of 0.018 higher than under constant temperature. A possible explanation is that with the increase of the temperature, crystallisation of the amorphous powder is accelerated and water bound with the amorphous solid is released and hence, increases in water activity (Jouppila, Lähdesmäki, Laine, Savolainen, & Talja,



2010; Jouppila & Roos, 1997). This higher water activity will then, increase chemical reaction rates, and ultimately, death rate of the probiotic bacteria.

The storage temperature had thus an effect on the physical and chemical state of the powders. SEM pictures after 3 months of storage under fluctuating temperature showed the formation of micropores in both freeze-dried samples containing the emulsion system (FD-P1-L1 and FD-P1-L3, see Figure 6.13). It has already been discussed that porous structure have a detrimental effect on the viability of probiotics (Poddar et al., 2014). Thus, the formation of pores in this samples could have accelerated the cell loss. However, no major structural changes were seen in the other samples and so did not bring further information on storage stability of the bacteria.



**Figure 6.13:** SEM micrographs of the freeze-dried and spray dried powder after 3 months under fluctuating temperature from 20 to 50°C. Magnification is of 6 000X for all micrographs.

### 6.3.5 Correlations between the death rates

Overall, it appeared that the death rate of the bacteria, when the samples had to endure fluctuating temperatures, was increased by up to two-fold compared to when the temperature remained constant. This correlation was confirmed by Figure 6.14 where each points of the plot represent a different sample. A linear correlation between both death rates could be expected, as explained below. Both death rates ( $k$ ) are following the Arrhenius equation:

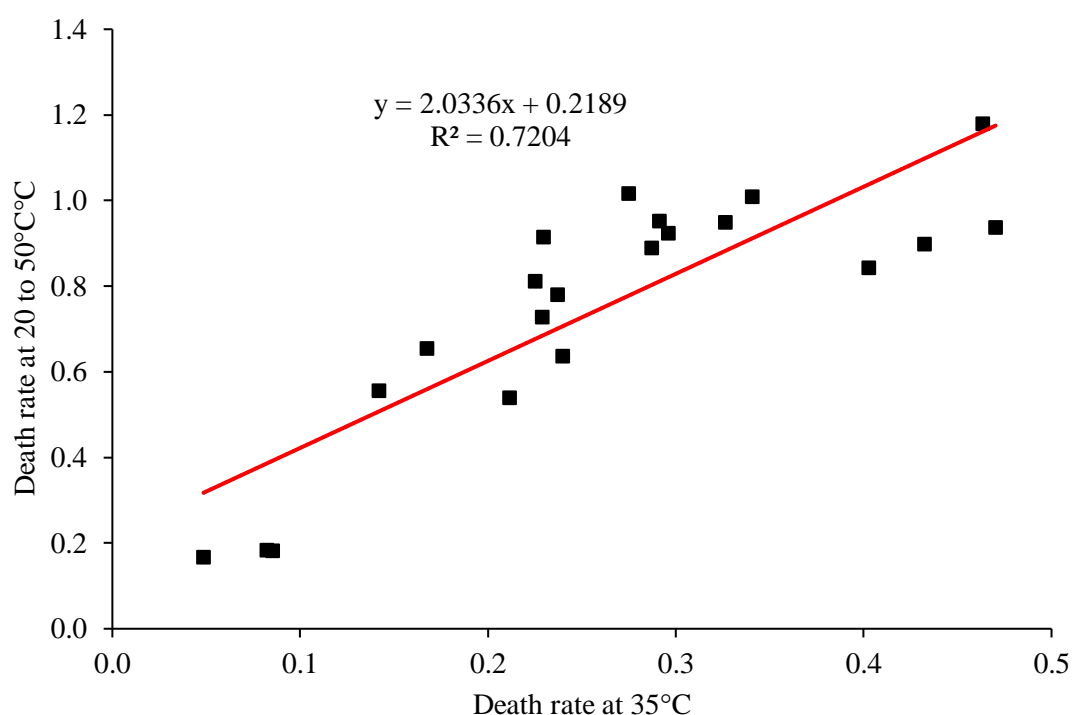
$$k = a \times e^{-\frac{E_a}{RT}} \quad (6.1)$$

Where  $a$  is the pre-exponential factor,  $E_a$  is the energy of activation,  $R$  the gas constant, and  $T$  the temperature. From it, the two death rates ( $k_1$  and  $k_2$ ) occurring at two different temperatures ( $T_1$  and  $T_2$ ) can be correlated:

$$\ln\left(\frac{k_1}{k_2}\right) = \frac{E_a}{R} \times \left(\frac{1}{T_2} - \frac{1}{T_1}\right) \quad (6.2)$$

Or

$$k_1 = k_2 \times e^{\frac{E_a}{R} \times \left(\frac{1}{T_2} - \frac{1}{T_1}\right)} \quad (6.3)$$



**Figure 6.14:** Correlation between the death rate under fluctuating temperature and under constant temperature.

A few models have been developed to model the kinetic of a reaction under fluctuating temperatures. They cover either square wave temperature fluctuation, or sinusoidal temperature fluctuation (Labuza, 1979; Nunes & Swartzel, 1990). These models allow the determination of the effective temperature, i.e. the constant temperature at which the same rate of reaction (or death rate here) would be obtained. However, to calculate the effective temperature the energy of activation is required, which would have needed an additional death rate value at another constant temperature.

## 6.4 Conclusions

In this chapter, PCM showed to be inefficient in protecting from temperature fluctuation occurring during transport. However, an effective way to extend the shelf-life of bacteria when facing fluctuating temperatures would be to reduce the amplitude of the

fluctuation, e.g. by insulation, as the death rate decreased by about two-folds when the temperature was maintained at the mean temperature. In addition, it was found that the structure of the powder is of main importance for the stability of the powder. The stabilisation matrix formula studied in this chapter is leading to very promising results. Further work should study this formula upon spray drying in order to lower the production cost of the probiotic powder. Finally, the present study hinted that the core and layer structure might have potential protection toward the probiotic as it creates a barrier between the bacteria and the environment. The development of new layer formulas could focus on the asset of an oxygen scavenger in this outer layer, which could decrease oxidation stresses.

## Chapter 7 – Overall discussion and conclusions

---

### 7.1 Summary and discussion

High temperature during storage leads to a dramatically high loss in the viability of dried probiotics. Nevertheless, being able to handle probiotic containing powder in every climate, and for a long period of time (i.e. from several months up to a couple of years) is of major economic interest for the industry. It is not completely understood how probiotics can be stabilised in the dried state. Three hypotheses have been proposed in the literature: (1) the protective matrix forms a glassy matrix, with a high glass transition temperature, and prevents any further chemical reactions (which could adversely affect the bacteria) from occurring; (2) protectants interact directly with the biomolecules present within the cell, maintaining them in their native structure (in other words preventing denaturation or other alterations); (3) protectants increase the free energy of water and are excluded from the vicinity of the biomolecules, thus keeping the biomolecules in a hydrated state while most of the water around them is removed from the system.

For all these protection mechanisms, it is important that the bacteria are exposed to protectants prior to drying so that these protectants could be both inside the cells and in the environment surrounding them. However, there was no consensus in the literature on the length of exposure to the protectants that needed to occur prior to drying, nor on the temperature that this exposure should be conducted at. Thus, the first part of the study (Chapter 3) was to investigate the effect of the time and temperature of exposure of two protective sugars (i.e. glucose and sucrose), on the stability of *Lb. rhamnosus* after drying. Differences in terms of optimal exposure between glucose and sucrose were observed. As

glucose was metabolised at 20°C, the longer the cells were exposed to the sugar, the quicker was the cell loss after drying. When cells were exposed to sucrose, at 4 or 20°C, 4 hours of exposure seemed to lead to higher stability after drying, while it was not the case for cells exposed to glucose at 4°C. Thus, it was difficult to choose one exposure setting that would fit most protectants. It was then decided to set the exposure to one hour at 4°C, as it was a good compromise between both sugars, and is relatively easy to manage by the industry. These exposure conditions were then used for the following studies. This study is the first that looked at the impact of exposure settings on stability of a probiotic bacteria in the dried state. Even though Hubálek (2003) reviewed different protectant for cryopreservation and highlighted the impact that exposure settings could have on the stability of micro-organisms, no such work has been done for drying stability, and focusing on probiotic bacteria. This might explain why some studies are still choosing exposure settings where the cells might metabolise the given protectants (Chen, Wang, Luo, & Shu, 2013; Strasser et al., 2009).

The other aspect that stood out from this initial study was the impact that the type of protectant could have on cell viability in the longer term. It was therefore essential to look to optimise the types of protectants best suited to the strain, but also possible combinations of these protectants.

Therefore, in Chapter 4, the interactions occurring between a range of protectants and cells were studied using a Nano DSC. Major differences were found between protectants. MSG was shown to be the protectant having the most positive effect on the stability of the biomolecules of *Lb. rhamnosus*, and this in turn seemed to be linked to the highest stability for powders stored at 30°C. Interestingly, powders containing MSG were the ones that presented with the highest water activity after drying. This tends to go against traditional thinking that higher water activity ( $\geq 0.15$ ) is detrimental to the cell

viability. It would seem that if suitable protectants have been used prior to drying, water activity may not be a limiting factor. Alternatively, the optimal water activity for *Lb. rhamnosus* HN001 may be higher than for other strains.

However, while for MSG, a high level of interaction with the cells led to a high viability during storage, this was not the case for all protectants assessed. For instance, sorbitol and sucrose presented similar interactions with cells biomolecules, but different stability results and could have been attributed to the difference in glass transition temperature. This led to the following study that aimed to look at various factors of the powder and their impact on the cell viability. Four protectants were chosen to look at synergistic mechanisms. MSG was first selected because it presented a good stability over storage despite its higher water activity. Sucrose and sorbitol were also chosen because they had similar molecular structure and interactions with the cells, but different glass transition temperature and different stability results. Therefore, their comparison allowed a better understanding of the impact of the glass transition temperature on the cell stability. Finally, galactose was integrated in the study as it presented a similar molecular structure compared to glucose, and similar glass transition temperature, but led a rapid drop of the cells viability. Thus, a closer study helped understanding why destabilisation of the cells occurred during storage, and if the storage conditions can improve the cells' stability. The four protectants, MSG, sorbitol, sucrose and galactose were then used in the following study (Chapter 5) to look for synergies between them and understand better the impact of the structure on the stability of the bacteria.

Interestingly, sample dried with MSG and inulin only were found to have a lower death rate than in Chapter 4 with 0.06 /month (see Table 7.1). This is most likely due to the improved storage conditions, i.e. mixing with skim milk powder and aliquoting (storing in individual pouches). Galactose also showed an improved death rate with a



reduction of two folds between Chapter 4 and Chapter 5. However, sorbitol and sucrose did not present much change in term of death rate, with even an increase in death rate for samples dried with sorbitol as shown below, in Table 7.1. Thus, different powder would react differently to the water activity depending on their composition.

**Table 7.1:** Death rate of bacteria dried in a 1:1 mix of protectant and inulin, comparison of results from Chapter 4 (samples were stored in closed container, but not aliquoted) and from Chapter 5 (where samples were mixed in skim milk powder and aliquoted in aluminium pouches).

<b>Protectant</b>	<b>Death rate without mixing with milk powder (no aliquoting, Chapter 4) (/month)</b>	<b>Death rate after mixing with milk powder (aliquoting, Chapter 5) (/month)</b>
MSG	0.19	0.06
Galactose	1.24	0.59
Sorbitol	0.76	0.92
Sucrose	0.46	0.42

Interestingly, samples dried with MSG and galactose had a smooth structure, while sorbitol and sucrose presented a very porous structure. It is proposed that the bacteria entrapped in a porous structure are more in contact with the environment, and thus with oxygen or moisture. It seems thus, that standardising the water activity was not beneficial for porous samples. It was actually found that the samples with better stability presented a higher water activity, and a relatively low glass transition temperature. An attempt was made to put the MSG powder, showing the highest water activity, in a second round of freeze-drying, to try to dry it further, but this was unsuccessful. Because of the smooth structure of the powder and the impossibility to dry it further, it was concluded that the powder collapsed during the first freeze-drying. As a result of the collapsing, a skin formed on the outside of the powder particles, leading to this smooth structure and preventing interactions between the core of the powder and the environment. This may have allowed keeping oxidation rates low. Similarly, the relatively high water activity of

the powder might have been optimal to keep oxidation rate low. As explained by Barbosa-Cánovas et al. (2008), the presence of just a monolayer of water molecules around components protects from oxidation, but when the amount of water decreases and the monolayer is no longer formed, contacts with oxygen increases. On the other hand, if there is more water present, mobility increases and so does oxidation. Further measurements of the oxidation of the bacteria are necessary to confirm this hypothesis.

It is possible to argue that if the powder had a collapsed structure, the water activity measurements, conducted using the dew point method, should be low. Indeed, the “free” water is entrapped below the skin formed during collapsing and cannot diffuse in the environment. However, when grinding the powder, trapped water from the collapsed powder would be released. The first water activity measurement was made after grinding the powder, which explained why it was still possible to measure the water activity of the powder even with a collapsed structure. The powder was then mixed with skim milk powder, so all samples were standardised. However, it is difficult to know if the mix was homogenous or not. Because of the collapsed structure of the powder, the water activity of the stabilisation matrix might have only changed a little after mixing with the skim milk powder.

The mixture DoE showed an improvement of the stability of the cells when a small quantity of sorbitol was added to the mix, even though sorbitol alone with inulin led to the lowest stability results. It was shown that sorbitol was interacting with an additional biomolecule, and thus protecting it, while the collapsed and smooth structure was maintained.

Conclusively, the mixture DoE conducted in Chapter 5 suggested that the structure had a major impact on the cell stability. The study of cells dried in pure potassium phosphate buffer partly confirmed this. These “free” cells sample also led to a

very smooth structure and relatively good stability. Apart from the potassium phosphate salts, which were present in all other formulations, there was no other protectants stabilising the biomolecules, but this sample led to better stability than when sucrose, sorbitol or galactose and inulin were added to the protective matrix. It is believed that the dense structure of the “free” cells led to the stabilisation of the bacteria. Only a few studies have suggested that the porosity of the powder can be detrimental to the cells (Alehosseini, Gomez del Pulgar, et al., 2019; Poddar et al., 2014). On the other hand, the good stability of “free” cells could also be due to the absence of “destabilising” solutes, i.e. “protectants” leading to cell loss. In Chapter 4, it was found that drying the bacteria with inulin in phosphate buffer led to a loss of approximately 2 more log than when dried in the buffer only. Only one study was found suggesting that some solutes used as protectants could actually lead to cell loss, by destabilising some of the cell components (Meneghel et al., 2017). In this study, sucrose was found to be interacting with the phospholipid membrane of a particular strain in a certain way that it would lead to cell loss during freezing. Inulin was also showed to interact with cells’ membrane, and this was proposed as a mechanism of action for stabilising them (Vereyken et al., 2003), but in the case of *Lb. rhamnosus* inulin could be destabilising the membrane, resulting in cell loss. As showed in Meneghel et al. (2017) study, every strain responds differently to different protectants.

A last explanation for the difference of stability would be that inulin crystallised during drying. This was shown on DSC scans, as melting peaks were present. It has been suggested that crystallisation of solutes can be detrimental to the cells (Foerst et al., 2012; Miao et al., 2008; Perdana, Fox, Siwei, Boom, & Schutyser, 2014). When a sufficient amount of MSG was added to the mix, the coil structure of the inulin was lost, as well as the crystallisation pattern and a collapsed and smooth structure was observed. Thus, for

the samples that did not contain MSG, is it the crystallisation, the porosity or the destabilisation of biomolecules that led to cell loss? In any case there is a clear interaction between protectants, which in turn impacted the cells in some ways. As discussed in the Chapter 2, interactions between protectants have not been studied for probiotic preservation, apart when used to form coacervates, while it is revealed here that these interactions have an impact on *Lb. rhamnosus*. This is a field that may be studied further.

The optimised stabilisation matrix obtained from Chapter 5, was used as a protection base for the last study, conducted in Chapter 6. This chapter aimed to answer the opening question: is there a material able to protect dried bacteria from heat? First of all, it is impossible to insulate bacteria from heat on the powder level, as particles are too small and heat transfer will happen quickly. To delay heat transfer, insulation needs to be located on the package. The other way to protect from heat, is to absorb it. This can be done with phase change materials (PCM), and has been shown to be efficient on short heat treatment. However, over storage, bacteria are not facing short heat treatment, but long waves of temperature fluctuation, occurring throughout the day. It was indeed found that the PCM had no protective effect on the bacteria even when located on the outer layer of the powder particles rather than dispersed in the matrix. However, it was showed, that decreasing the amplitude of the fluctuation would help stabilising bacteria, since the death rate was decreased by two-folds when the temperature was kept constant at the mean temperature. In addition, the study showed again that structure of the powder can protect the cells as the sample with stabilisation matrix, sodium caseinate and Tween 20, was significantly more stable when spray-dried than when freeze-dried. It was proposed that the core-and-layer structure obtained by the spray drying accounted for the improved stability. Nevertheless, such results were not found once the lipid was added to the system, as the freeze-dried version led to better stability results. It was proposed that in the

absence of lipids, and when freeze-dried, the protein would aggregate to itself or to other components of the stabilisation matrix, that would here lead to cell loss. So here again the interaction between protectants may affect the bacterial stability. On the other hand, when lipid was added to the spray-dried sample, the decrease of the stability could have been due to a different coverage of the particles, creating a more permeable layer as less protein were present.

One of the limitations of this study is that it focused only on one bacteria to protection matrix ratio, kept constant for all previous studies, with a concentration of 3.3% (w/w) of bacteria in the powder. As a result, the control sample, with bacteria dried in stabilisation matrix contained twice as much stabilisation mix compared to the other samples with protein or the emulsion system. It is thus difficult to say if the protection conferred by the stabilisation matrix is quantitative, or qualitative. To verify this, it would be necessary to repeat the study with the amount of stabilisation matrix doubled in all samples.

Finally, Chapter 5 and Chapter 6 showed that a high glass transition temperature was not necessary to achieve high stability of bacteria over storage (i.e. reduction of 0.8 log (CFU/g) over a year of storage at 35°C). In Chapter 5, multivariate analysis showed that T<sub>g</sub> was not correlated with lower death rate. Later, in Chapter 6, sorbitol was added to the stabilisation matrix and led to a more efficient drying with resulting powder having lower water activity. The glass transition temperature was thus improved, with a mean value of 29°C. However, this was not enough to confer a glassy matrix to the sample, as the storage temperature was of 35°C on average.

Conclusively, stabilisation of dried *Lb. rhamnosus* was achieved, with a final death rate of 0.07 /month at 35°C. This was of a major improvement compared with the previous study that stabilised *Lb. rhamnosus* HN001 in the dried state conducted by

Prasad et al. (2003), as they obtained a 2 log reduction over 14 weeks at 30°C, i.e. a death rate of about 0.6 /month. It was showed here that the mechanism of protection included, at least, interactions of protectants with biomolecules, as MSG led to outstanding cell stability to heat. However, a high glass transition temperature was not a necessary feature of the powder to achieve good stability. In addition, the stabilisation matrix presented a unique structure, and was thus proposed as a second mechanism of protection. Three hypothesis were raised to explain why such structure maintained bacteria viable for a longer time. First, the dense structure presented a layer, protecting the bacteria, in the core, from the environment, thus preventing from deteriorating compounds such as oxygen. Second, the presence of MSG prevented the inulin to interact with cells components and destabilise them, most likely by preventing the formation of coil structure. Finally, MSG hindered the crystallisation of inulin, hence, preventing damages to the cells.

## **7.2 Recommendations for future work**

Overall, three main mechanisms are potentially occurring together and stabilising the bacteria: (1) the interaction of protectants with cell components, (2) the interactions between protectants and (3) the formation of a unique structure of the powder. These mechanisms might as well destabilise the bacteria, and it is important to know in which context a certain mechanism can be beneficial or detrimental to the bacterial cell. The following point of research are proposed to further understand these mechanisms.

Firstly, the impact of the structure on the stability of the bacteria needs to be further investigated. A few studies have shown the importance of the structure on the stability of the bacteria, as discussed in section 2.5.1. However, powder structure is not yet recognised as a main protection mechanisms in stabilisation of dried probiotics. The present study showed that the structure of the powder was more important than a high

glass transition temperature for *Lb. rhamnosus* HN001. Thus, further studies need to come and complement this finding to look at different bacterial strains and maybe try to link the porosity of the powder with the stabilisation of the bacteria. Ideally study of the powder crystallisation, its porosity, the water activity and the oxidation rate of the bacteria need to be all put together to better explain the protection mechanisms of powder structure on bacterial stability during storage. Different structures of the powder can be achieved by using different drying technique such as freeze-drying versus spray-drying or spray-drying with different nozzles. Alternatively, freeze-drying process can be modulated to obtain collapsed and non-collapsed powder, and to study the resulting bacterial stability. Such work has been done on  $\beta$ -carotene stability by Harnkarnsujarit et al. (2012) but not yet on bacteria.

Secondly, the Nano DSC was showed to be a relatively easy technique to measure the response of the bacteria toward different protectants. It would be interesting to build a database with thermograms of different strains with different protectants, as well as identifying the denaturation peaks of each biomolecules. This would allow researchers to choose from different protectants having effects on certain biomolecules, and would help understanding better how thermal stability is related to storage stability of the bacteria. It would have been interesting here to look at the thermogram of cells with all the different samples prepared following the mixture DoE to be able to include thermogram data in the PCA, and see how much the protectant and cell interactions are impacting the final death rate of the bacteria. In addition, such Nano DSC analysis could be done after storing the bacteria for a time, to see what biomolecules are most affected during storage. This has been done by FTIR, but thermograms are easier to analyse compared to FTIR spectrum, which makes it less incline to interpretation errors. In addition FTIR is only giving

indications of the structural changes, and it does not directly tells if a biomolecule is more or less stable, while calorimetry allows to do that.

Thirdly, interaction between protectants could be further studied by using mixture DoE or other surface response methodology. It would be great to see, in the future, more research using these methodologies to understand synergistic effect of protectants. And as was done here in Chapter 5, use these methodology not only to measure the death rate, but also other factors of the powder. This would help understanding why protectants have synergistic effect. Similarly, more knowledge is needed on the potential destabilisation of certain “protectants”, rather than on their stabilisation of probiotics. Most studies looking at bacterial stability are not including a blank, i.e. bacteria dried without protectants, and when one blank is added to the study it often consists in bacteria dried in deionised water. However, deionised water will impose a hypoosmotic shock to the bacteria, thus destabilising it rather than having no effect. Here, phosphate buffer was used as a blank, as it was present in all samples and should not have major impact on the bacterial stability when used as itself. It was showed, however that it led to better storage stability than samples with added “protectants”. Such blanks should be used in further bacterial stability, to ensure that a “protective” solute is not detrimental to the bacterial strain studied.

Finally, even though PCM was not providing any additional protection to *Lb. rhamnosus* HN001 in the conditions tested here, it is believed that these types of materials can still have an impact on short heat treatments such as reconstitution of the powder, drying or pasteurisation. Potential studies may look further into these applications of PCM.



## References

---

- Accorsi, R., Manzini, R., & Ferrari, E. (2014). A comparison of shipping containers from technical, economic and environmental perspectives. *Transportation Research Part D: Transport and Environment*, 26, 52-59.
- Alba-Simionesco, C., Coasne, B., Dosseh, G., Dudziak, G., Gubbins, K., Radhakrishnan, R., & Sliwinska-Bartkowiak, M. (2006). Effects of confinement on freezing and melting. *Journal of Physics: Condensed Matter*, 18(6), R15.
- Albadran, H. A., Chatzifragkou, A., Khutoryanskiy, V. V., & Charalampopoulos, D. (2015). Stability of probiotic *Lactobacillus plantarum* in dry microcapsules under accelerated storage conditions. *Food Research International*, 74, 208-216.
- Albertorio, F., Chapa, V. A., Chen, X., Diaz, A. J., & Cremer, P. S. (2007). The  $\alpha, \alpha$ -(1 $\rightarrow$ 1) linkage of trehalose is key to anhydrobiotic preservation. *Journal of the American Chemical Society*, 129(34), 10567-10574.
- Alehosseini, A., Gomez del Pulgar, E.-M., Fabra, M. J., Gómez-Mascaraque, L. G., Benítez-Páez, A., Sarabi-Jamab, M., . . . Lopez-Rubio, A. (2019). Agarose-based freeze-dried capsules prepared by the oil-induced biphasic hydrogel particle formation approach for the protection of sensitive probiotic bacteria. *Food Hydrocolloids*, 87, 487-496.
- Alehosseini, A., Sarabi-Jamab, M., Ghorani, B., & Kadkhodae, R. (2019). Electro-encapsulation of *Lactobacillus casei* in high-resistant capsules of whey protein containing transglutaminase enzyme. *LWT*, 102, 150-158.
- Allonsius, C. N., van den Broek, M. F. L., De Boeck, I., Kiekens, S., Oerlemans, E. F. M., Kiekens, F., . . . Lebeer, S. (2017). Interplay between *Lactobacillus rhamnosus* GG and *Candida* and the involvement of exopolysaccharides. *Microbial Biotechnology*, 10(6), 1753-1763.
- Amani, M., Moosavi-Movahedi, A. A., & Kurganov, B. I. (2017). What can we get from varying scan rate in protein differential scanning calorimetry? *International Journal of Biological Macromolecules*, 99, 151-159.
- Ananta, E., Volkert, M., & Knorr, D. (2005). Cellular injuries and storage stability of spray-dried *Lactobacillus rhamnosus* GG. *International Dairy Journal*, 15(4), 399-409.
- Anderson, W. A., Hedges, N. D., Jones, M. V., & Cole, M. B. (1991). Thermal inactivation of *Listeria monocytogenes* studied by differential scanning calorimetry. *Microbiology*, 137(6), 1419-1424.
- Ann, E. Y., Kim, Y., Oh, S., Imm, J.-Y., Park, D.-J., Han, K. S., & Kim, S. H. (2007). Microencapsulation of *Lactobacillus acidophilus* ATCC 43121 with prebiotic substrates using a hybridisation system. *International journal of food science & technology*, 42(4), 411-419.
- Arakawa, T., & Timasheff, S. (1985). The stabilization of proteins by osmolytes. *Biophysical Journal*, 47(3), 411.
- Barbosa-Cánovas, G. V., Fontana, A. J., Schmidt, S. J., & Labuza, T. P. (2008). *Water Activity in Foods: Fundamentals and Applications*.
- Barbosa, J., Borges, S., Amorim, M., Pereira, M. J., Oliveira, A., Pintado, M. E., & Teixeira, P. (2015). Comparison of spray drying, freeze drying and convective hot air drying for the production of a probiotic orange powder. *Journal of Functional Foods*, 17, 340-351.

- Bereksi, N., Gavini, F., Bénézech, T., & Faille, C. (2002). Growth, morphology and surface properties of *Listeria monocytogenes* Scott A and LO28 under saline and acid environments. *Journal of Applied Microbiology*, 92(3), 556-565.
- Berger, A. J., Koo, T.-W., Itzkan, I., & Feld, M. S. (1998). An enhanced algorithm for linear multivariate calibration. *Analytical Chemistry*, 70(3), 623-627.
- Bolen, D. W., & Baskakov, I. V. (2001). The osmophobic effect: natural selection of a thermodynamic force in protein folding. *Journal of Molecular Biology*, 310(5), 955-963.
- Bolten, C. J., & Wittmann, C. (2008). Appropriate sampling for intracellular amino acid analysis in five phylogenetically different yeasts. *Biotechnology Letters*, 30(11), 1993-2000.
- Brannan, A. M., Whelan, W. A., Cole, E., & Booth, V. (2015). Differential scanning calorimetry of whole *Escherichia coli* treated with the antimicrobial peptide MSI-78 indicate a multi-hit mechanism with ribosomes as a novel target. *PeerJ*, 3, e1516.
- Broadbent, J. R., Larsen, R. L., Deibel, V., & Steele, J. L. (2010). Physiological and transcriptional response of *Lactobacillus casei* ATCC 334 to acid stress. *Journal of Bacteriology*, 192(9), 2445-2458.
- Broeckx, G., Vandenheuvel, D., Claes, I. J. J., Lebeer, S., & Kiekens, F. (2016). Drying techniques of probiotic bacteria as an important step towards the development of novel pharmabiotics. *International Journal of Pharmaceutics*, 505(1-2), 303-318.
- Broeckx, G., Vandenheuvel, D., Henkens, T., Kiekens, S., van den Broek, M. F. L., Lebeer, S., & Kiekens, F. (2017). Enhancing the viability of *Lactobacillus rhamnosus* GG after spray drying and during storage. *International Journal of Pharmaceutics*, 534(1), 35-41.
- Bruylants, G., Wouters, J., & Michaux, C. (2005). Differential scanning calorimetry in life science: Thermodynamics, stability, molecular recognition and application in drug design. *Current Medicinal Chemistry*, 12(17), 2011-2020.
- Bustamante, M., Villarroel, M., Rubilar, M., & Shene, C. (2015). *Lactobacillus acidophilus* La-05 encapsulated by spray drying: effect of mucilage and protein from flaxseed (*Linum usitatissimum* L.). *LWT - Food Science and Technology*, 62(2), 1162-1168.
- Capozzi, V., Weidmann, S., Fiocco, D., Rieu, A., Hols, P., Guzzo, J., & Spano, G. (2011). Inactivation of a small heat shock protein affects cell morphology and membrane fluidity in *Lactobacillus plantarum* WCFS1. *Research in Microbiology*, 162(4), 419-425.
- Cappa, F., Cattivelli, D., & Cocconcelli, P. S. (2005). The *uvrA* gene is involved in oxidative and acid stress responses in *Lactobacillus helveticus* CNBL1156. *Research in Microbiology*, 156(10), 1039-1047.
- Carvalho, A. S., Silva, J., Ho, P., Teixeira, P., Malcata, F. X., & Gibbs, P. (2002). Survival of freeze-dried *Lactobacillus plantarum* and *Lactobacillus rhamnosus* during storage in the presence of protectants. *Biotechnology Letters*, 24(19), 1587-1591.
- Carvalho, A. S., Silva, J., Ho, P., Teixeira, P., Malcata, F. X., & Gibbs, P. (2004). Effects of various sugars added to growth and drying media upon thermotolerance and survival throughout storage of freeze-dried *Lactobacillus delbrueckii* ssp. *Bulgaricus*. *Biotechnology Progress*, 20(1), 248-254.
- Castro, H. P., Teixeira, P. M., & Kirby, R. (1995). Storage of lyophilized cultures of *Lactobacillus bulgaricus* under different relative humidities and atmospheres. *Applied Microbiology and Biotechnology*, 44(1), 172-176.

- Ceapa, C., Lambert, J., van Limpt, K., Wels, M., Smokvina, T., Knol, J., & Kleerebezem, M. (2015). Correlation of *Lactobacillus rhamnosus* Genotypes and Carbohydrate Utilization Signatures Determined by Phenotype Profiling. *Applied and Environmental Microbiology*, 81(16), 5458-5470.
- Chen, H., Chen, S., Chen, H., Wu, Y., & Shu, G. (2014). Effects of carbon sources and prebiotics added to growth media on proliferation and survival of *Lactobacillus bulgaricus* LB6 during freeze-drying. *Journal of Chemical and Pharmaceutical Research*, 6(6), 894-899.
- Chen, H., Chen, S., Chen, H., Wu, Y., & Shu, G. (2015). Effects of sugar alcohol and proteins on the survival of *Lactobacillus bulgaricus* LB6 during freeze drying. *Acta Scientiarum Polonorum, Technologia Alimentaria*, 14(2), 117-124.
- Chen, H., Wang, J., Luo, Q., & Shu, G. (2013). Effect of NaH-CO<sub>3</sub>, MgSO<sub>4</sub>, sodium ascorbate, sodium glutamate, phosphate buffer on survival of *Lactobacillus bulgaricus* during freeze-drying. *Advance Journal of Food Science and Technology*, 5(6), 771-774.
- Chen, J. Y., Bohnsack, K., & Labuza, T. P. (1983). Kinetics of protein quality loss in enriched pasta stored in a sine wave temperature condition. *Journal of Food Science*, 48(2), 460-464.
- Chen, T., Wu, Q., Zhou, H., Deng, K., Wang, X., Meng, F., . . . Wei, H. (2017). Assessment of commercial probiotic products in China for labelling accuracy and probiotic characterisation of selected isolates. *International Journal of Dairy Technology*, 70(1), 119-126.
- Collett, M. A., Rand, C. J., Mason, C., & Stanton, J.-A. L. (2008). NZ\_ABWJ01000014 - *Lactobacillus rhamnosus* HN001 contig00040, whole genome shotgun sequence. from GenBank [http://www.ncbi.nlm.nih.gov/nuccore/NZ\\_ABWJ01000014.1](http://www.ncbi.nlm.nih.gov/nuccore/NZ_ABWJ01000014.1)
- Conrad, P. B., Miller, D. P., Cielenski, P. R., & de Pablo, J. J. (2000). Stabilization and preservation of *Lactobacillus acidophilus* in saccharide matrices. *Cryobiology*, 41(1), 17-24.
- Coulson, S. (2018, 5-6 March 2018). *Fermented foods: the missing food group in the Australian dietary guidelines*. Paper presented at the 3<sup>rd</sup> probiotics congress: Asia, Singapore.
- Craig, D. Q. M. (1990). Polyethylen glycols and drug release. *Drug Development and Industrial Pharmacy*, 16(17), 2501-2526.
- Craig, D. Q. M., Royall, P. G., Kett, V. L., & Hopton, M. L. (1999). The relevance of the amorphous state to pharmaceutical dosage forms: glassy drugs and freeze dried systems. *International Journal of Pharmaceutics*, 179(2), 179-207.
- Crowe, J. H., Carpenter, J. F., & Crowe, L. M. (1998). The role of vitrification in anhydrobiosis. *Annual Review of Physiology*, 60(1), 73-103.
- Crowe, J. H., Crowe, L. M., Carpenter, J. F., Rudolph, A. S., Wistrom, C. A., Spargo, B. J., & Anchordoguy, T. J. (1988). Interactions of sugars with membranes. *Biochimica et Biophysica Acta (BBA) - Reviews on Biomembranes*, 947(2), 367-384.
- Crowe, J. H., Crowe, L. M., Carpenter, J. F., & Wistrom, C. A. (1987). Stabilization of dry phospholipid bilayers and proteins by sugars. *Biochemical Journal*, 242(1), 1.
- Crowe, J. H., Hoekstra, F. A., & Crowe, L. M. (1989). Membrane phase transitions are responsible for imbibitional damage in dry pollen. *Proceedings of the National Academy of Sciences*, 86(2), 520-523.

- Crowe, J. H., Hoekstra, F. A., Nguyen, K. H. N., & Crowe, L. M. (1996). Is vitrification involved in depression of the phase transition temperature in dry phospholipids? *Biochimica et Biophysica Acta (BBA) - Biomembranes*, 1280(2), 187-196.
- Crowe, L. M., Reid, D. S., & Crowe, J. H. (1996). Is trehalose special for preserving dry biomaterials? *Biophysical Journal*, 71(4), 2087-2093.
- De Valdez, G. F., De Giori, G. S., De Ruiz Holgado, A. A. P., & Oliver, G. (1983). Protective effect of adonitol on lactic acid bacteria subjected to freeze-drying. *Applied and Environmental Microbiology*, 45(1), 302-304.
- Derzelle, S., Hallet, B., Francis, K. P., Ferain, T., Delcour, J., & Hols, P. (2000). Changes in cspL, cspP, and cspCmRNA abundance as a function of cold shock and growth phase in *Lactobacillus plantarum*. *Journal of Bacteriology*, 182(18), 5105-5113.
- Desmond, C., Ross, R. P., O'Callaghan, E., Fitzgerald, G., & Stanton, C. (2002). Improved survival of *Lactobacillus paracasei* NFBC 338 in spray-dried powders containing gum acacia. *Journal of Applied Microbiology*, 93(6), 1003-1011.
- Doherty, S. B., Gee, V. L., Ross, R. P., Stanton, C., Fitzgerald, G. F., & Brodkorb, A. (2011). Development and characterisation of whey protein micro-beads as potential matrices for probiotic protection. *Food Hydrocolloids*, 25(6), 1604-1617.
- Dormer, N. H., Berkland, C. J., & Singh, M. (2014). Chapter 11 - Monodispersed microencapsulation technology. In A. G. Gaonkar, N. Vasisht, A. R. Khare, & R. Sobel (Eds.), *Microencapsulation in the Food Industry* (pp. 111-123). San Diego: Academic Press.
- Drago, L., Rodighiero, V., Celeste, T., Rovetto, L., & de Vecchi, E. (2010). Microbiological evaluation of commercial probiotic products available in the USA in 2009. *Journal of Chemotherapy*, 22(6), 373-377.
- Duguid, J. G., Bloomfield, V. A., Benevides, J. M., & Thomas, G. J. (1996). DNA melting investigated by differential scanning calorimetry and Raman spectroscopy. *Biophysical Journal*, 71(6), 3350-3360.
- Dumont, F., Marechal, P. A., & Gervais, P. (2004). Cell size and water permeability as determining factors for cell viability after freezing at different cooling rates. *Applied and Environmental Microbiology*, 70(1), 268-272.
- Erlebach, C. E., Illmer, P., & Schinner, F. (2000). Changes of cell size distribution during the batch culture of *Arthrobacter* strain PI/1-95. *Antonie van Leeuwenhoek*, 77(4), 329-335.
- Espeau, P., Mondieig, D., Haget, Y., & Cuevas-Diarte, M. A. (1997). 'Active' package for thermal protection of food products. *Packaging Technology and Science*, 10(5), 253-260.
- Esposito, D., Del Vecchio, P., & Barone, G. (1997). Interactions with natural polyamines and thermal stability of DNA. A DSC study and a theoretical reconsideration. *Journal of the American Chemical Society*, 119(11), 2606-2613.
- Euromonitor International. (2019). Health and Wellness: Euromonitor from trade sources/national statistics. Retrieved from <https://www.euromonitor.com/>
- Faijes, M., Mars, A. E., & Smid, E. J. (2007). Comparison of quenching and extraction methodologies for metabolome analysis of *Lactobacillus plantarum*. *Microbial Cell Factories*, 6, 27-27.
- FAO/WHO. (2006). *Probiotics in food : health and nutritional properties and guidelines for evaluation : Report of a Joint FAO/WHO Expert Consultation on Evaluation of Health and Nutritional Properties of Probiotics in Food including Powder Milk with Live Lactic Acid Bacteria, Cordoba, Argentina, 1-4 October 2001 [and] Report of a Joint FAO/WHO Working Group on Drafting Guidelines for the*

- Evaluation of Probiotics in Food*, London, Ontario, Canada, 30 April -1 May 2002. Rome [Italy]: Food and Agriculture Organization of the United Nations, World Health Organization.
- Foerst, P., Kulozik, U., Schmitt, M., Bauer, S., & Santivarangkna, C. (2012). Storage stability of vacuum-dried probiotic bacterium *Lactobacillus paracasei* F19. *Food and Bioprocess Processing*, 90(2), 295-300.
- Fonseca, F., Béal, C., & Corrieu, G. (2000). Method of quantifying the loss of acidification activity of lactic acid starters during freezing and frozen storage. *Journal of Dairy Research*, 67(1), 83-90.
- Fonseca, F., Marin, M., & Morris, G. J. (2006). Stabilization of frozen *Lactobacillus delbrueckii* subsp. *bulgaricus* in glycerol suspensions: freezing kinetics and storage temperature effects. *Applied and Environmental Microbiology*, 72(10), 6474-6482.
- Fonseca, F., Meneghel, J., Cenard, S., Passot, S., & Morris, G. J. (2016). Determination of intracellular vitrification temperatures for unicellular micro organisms under conditions relevant for cryopreservation. *Plos One*, 11(4), e0152939.
- França, M. B., Panek, A. D., & Eleutherio, E. C. A. (2007). Oxidative stress and its effects during dehydration. *Comparative Biochemistry and Physiology Part A: Molecular & Integrative Physiology*, 146(4), 621-631.
- Frey, C. (2014). Chapter 7 - Fluid bed coating-based microencapsulation. In A. G. Gaonkar, N. Vasisht, A. R. Khare, & R. Sobel (Eds.), *Microencapsulation in the Food Industry* (pp. 65-79). San Diego: Academic Press.
- Gautier, J., Passot, S., Pénicaud, C., Guillemin, H., Cenard, S., Lieben, P., & Fonseca, F. (2013). A low membrane lipid phase transition temperature is associated with a high cryotolerance of *Lactobacillus delbrueckii* subspecies *bulgaricus* CFL1. *Journal of Dairy Science*, 96(9), 5591-5602.
- Giard, J.-C., Rince, A., Capiiaux, H., Auffray, Y., & Hartke, A. (2000). Inactivation of the stress- and starvation-inducible *gls24* operon has a pleiotrophic effect on cell morphology, stress sensitivity, and gene expression in *Enterococcus faecalis*. *Journal of Bacteriology*, 182(16), 4512-4520.
- Gill, H., Rutherford, K., & Cross, M. (2001). Dietary probiotic supplementation enhances natural killer cell activity in the elderly: an investigation of age-related immunological changes. *Journal of clinical immunology*, 21(4), 264-271.
- Giulio, B. D., Orlando, P., Barba, G., Coppola, R., Rosa, M. D., Sada, A., . . . Nazzaro, F. (2005). Use of alginate and cryo-protective sugars to improve the viability of lactic acid bacteria after freezing and freeze-drying. *World Journal of Microbiology and Biotechnology*, 21(5), 739-746.
- Glaasker, E., Konings, W. N., & Poolman, B. (1996). Osmotic regulation of intracellular solute pools in *Lactobacillus plantarum*. *Journal of Bacteriology*, 178(3), 575-582.
- Glaasker, E., Tjan, F. S. B., Ter Steeg, P. F., Konings, W. N., & Poolman, B. (1998). Physiological response of *Lactobacillus plantarum* to salt and nonelectrolyte stress. *Journal of Bacteriology*, 180(17), 4718-4723.
- Gomez-Mascaraque, L. G., Morfin, R. C., Pérez-Masiá, R., Sanchez, G., & Lopez-Rubio, A. (2016). Optimization of electrospraying conditions for the microencapsulation of probiotics and evaluation of their resistance during storage and in-vitro digestion. *LWT - Food Science and Technology*, 69, 438-446.
- Gong, X., Yu, H., Chen, J., & Han, B. (2012). Cell surface properties of *Lactobacillus salivarius* under osmotic stress. *European Food Research and Technology*, 234(4), 671-678.

- Goods and services trade by country: Year ended June 2018 – corrected. (2018). Retrieved from <https://www.stats.govt.nz/information-releases/goods-and-services-trade-by-country-year-ended-june-2018>
- Gopal, P. K., Prasad, J., Smart, J., & Gill, H. S. (2001). In vitro adherence properties of *Lactobacillus rhamnosus* DR20 and *Bifidobacterium lactis* DR10 strains and their antagonistic activity against an enterotoxigenic *Escherichia coli*. *International Journal of Food Microbiology*, 67(3), 207-216.
- Gopal, P. K., Sullivan, P. A., & Smart, J. B. (2001). Utilisation of galacto-oligosaccharides as selective substrates for growth by lactic acid bacteria including *Bifidobacterium lactis* DR10 and *Lactobacillus rhamnosus* DR20. *International Dairy Journal*, 11(1–2), 19-25.
- Guillot, A., Obis, D., & Mistou, M.-Y. (2000). Fatty acid membrane composition and activation of glycine-betaine transport in *Lactococcus lactis* subjected to osmotic stress. *International Journal of Food Microbiology*, 55(1), 47-51.
- Hancock, B. C., Shamblin, S. L., & Zografi, G. (1995). Molecular mobility of amorphous pharmaceutical solids below their glass transition temperatures. *Pharmaceutical Research*, 12(6), 799-806.
- Hanna, M. N., Ferguson, R. J., Li, Y. H., & Cvitkovitch, D. G. (2001). *uvrA* is an acid-inducible gene involved in the adaptive response to low pH in *Streptococcus mutans*. *Journal of Bacteriology*, 183(20), 5964-5973.
- Harel, M., & Tang, Q. (2014). Chapter 36 - Protection and delivery of probiotics for use in foods. In A. G. Gaonkar, N. Vasisht, A. R. Khare, & R. Sobel (Eds.), *Microencapsulation in the Food Industry* (pp. 469-484). San Diego: Academic Press.
- Harnkarnsujarit, N., Charoenrein, S., & Roos, Y. H. (2012). Porosity and water activity effects on stability of crystalline  $\beta$ -carotene in freeze-dried solids. *Journal of Food Science*, 77(11), E313-E320.
- Hartke, A., Giard, J.-C., Laplace, J.-M., & Auffray, Y. (1998). Survival of *Enterococcus faecalis* in an oligotrophic microcosm: Changes in morphology, development of general stress resistance, and analysis of protein synthesis. *Applied and Environmental Microbiology*, 64(11), 4238-4245.
- He, Q., Cao, C., Hui, W., Yu, J., Zhang, H., & Zhang, W. (2018). Genomic resequencing combined with quantitative proteomic analyses elucidate the survival mechanisms of *Lactobacillus plantarum* P-8 in a long-term glucose-limited experiment. *Journal of Proteomics*, 176, 37-45.
- Hernandez-Castro, R., Rodriguez, M. C., Seoane, A., & Garcia Lobo, J. M. (2003). The aquaporin gene *aqpX* of *Brucella abortus* is induced in hyperosmotic conditions. *Microbiology*, 149(Pt 11), 3185-3192.
- Hill, C., Guarner, F., Reid, G., Gibson, G. R., Merenstein, D. J., Pot, B., . . . Sanders, M. E. (2014). Expert consensus document. The International Scientific Association for Probiotics and Prebiotics consensus statement on the scope and appropriate use of the term probiotic. *Nature Reviews Gastroenterology & Hepatology*, 11(8), 506-514.
- Hlaing, M. M., Wood, B. R., McNaughton, D., Ying, D., Dumsday, G., & Augustin, M. A. (2017). Effect of drying methods on protein and DNA conformation changes in *Lactobacillus rhamnosus* gg cells by fourier transform infrared spectroscopy. *Journal of Agricultural and Food Chemistry*, 65(8), 1724-1731.
- Hong, S.-I., & Krochta, J. M. (2006). Oxygen barrier performance of whey-protein-coated plastic films as affected by temperature, relative humidity, base film and protein type. *Journal of Food Engineering*, 77(3), 739-745.

- Hubálek, Z. (2003). Protectants used in the cryopreservation of microorganisms. *Cryobiology*, 46(3), 205-229.
- Hutkins, R. W., Ellefson, W. L., & Kashket, E. R. (1987). Betaine transport imparts osmotolerance on a strain of *Lactobacillus acidophilus*. *Applied and Environmental Microbiology*, 53(10), 2275-2281.
- Iaconelli, C., Lemetais, G., Kechaou, N., Chain, F., Bermúdez-Humarán, L. G., Langella, P., . . . Beney, L. (2015). Drying process strongly affects probiotics viability and functionalities. *Journal of Biotechnology*, 214, 17-26.
- Ibarra, A., Acha, R., Calleja, M. T., Chiralt-Boix, A., & Wittig, E. (2012). Optimization and shelf-life of a low-lactose yogurt with *Lactobacillus rhamnosus* HN001. *Journal of Dairy Science*, 95(7), 3536-3548.
- Ibrahim, F., Ruvio, S., Granlund, L., Salminen, S., Viitanen, M., & Ouwehand, A. C. (2010). Probiotics and immunosenescence: cheese as a carrier. *FEMS Immunology & Medical Microbiology*, 59(1), 53-59.
- Izutsu, K., Yoshioka, S., & Terao, T. (1993). Decreased protein-stabilizing effects of cryoprotectants due to crystallization. *Pharmaceutical Research*, 10(8), 1232-1237.
- Jacobs, I. C. (2014). Chapter 5 - Atomization and spray-drying processes. In A. G. Gaonkar, N. Vasisht, A. R. Khare, & R. Sobel (Eds.), *Microencapsulation in the Food Industry* (pp. 47-56). San Diego: Academic Press.
- Jain, N. K., & Roy, I. (2009). Effect of trehalose on protein structure. *Protein Science : A Publication of the Protein Society*, 18(1), 24-36.
- Jang, S. E., Jeong, J. J., Choi, S. Y., Kim, H., Han, M. J., & Kim, D. H. (2017). *Lactobacillus rhamnosus* HN001 and *Lactobacillus acidophilus* La-14 attenuate *Gardnerella vaginalis*-infected bacterial vaginosis in mice. *Nutrients*, 9(6).
- Jayasundera, M., Adhikari, B., Aldred, P., & Ghandi, A. (2009). Surface modification of spray dried food and emulsion powders with surface-active proteins: A review. *Journal of Food Engineering*, 93(3), 266-277.
- Jiang, H., Zhang, M., McKnight, S., & Adhikari, B. (2013). Microencapsulation of  $\alpha$ -amylase by carrying out complex coacervation and drying in a single step using a novel three-fluid nozzle spray drying. *Drying Technology*, 31(16), 1901-1910.
- Jofré, A., Aymerich, T., & Garriga, M. (2015). Impact of different cryoprotectants on the survival of freeze-dried *Lactobacillus rhamnosus* and *Lactobacillus casei/paracasei* during long-term storage. *Beneficial Microbes*, 6(3), 381-386.
- Jouppila, K., Lähdesmäki, M., Laine, P., Savolainen, M., & Talja, R. A. (2010). Comparison of water sorption and crystallization behaviors of freeze-dried lactose, lactitol, maltose, and maltitol. In *Water Properties in Food, Health, Pharmaceutical and Biological Systems: ISOPOW 10* (pp. 477-482).
- Jouppila, K., & Roos, Y. H. (1997). Water sorption isotherms of freeze-dried milk products: Applicability of linear and non-linear regression analysis in modelling. *International Journal of Food Science and Technology*, 32(6), 459-471.
- Kajfasz, J. K., & Quivey, R. G. (2011). Responses of lactic acid bacteria to acid stress. In E. Tsakalidou & K. Papadimitriou (Eds.), *Stress Responses of Lactic Acid Bacteria* (pp. 23-53). Boston, MA: Springer US.
- Kalliomäki, M., Salminen, S., Arvilommi, H., Kero, P., Koskinen, P., & Isolauri, E. (2001). Probiotics in primary prevention of atopic disease: a randomised placebo-controlled trial. *The Lancet*, 357(9262), 1076-1079.
- Kankainen, M., Paulin, L., Tynkkynen, S., von Ossowski, I., Reunanen, J., Partanen, P., . . . de Vos, W. M. (2009). Comparative genomic analysis of *Lactobacillus*

- rhamnosus* GG reveals pili containing a human- mucus binding protein. *Proceedings of the National Academy of Sciences*, 106(40), 17193-17198.
- Kent, R. M., & Doherty, S. B. (2014). Probiotic bacteria in infant formula and follow-up formula: Microencapsulation using milk and pea proteins to improve microbiological quality. *Food Research International*, 64, 567-576.
- Khorasani, A. C., & Shojaosadati, S. A. (2017). Improvement of probiotic survival in fruit juice and under gastrointestinal conditions using pectin-nanochitin-nanolignocellulose as a novel prebiotic gastrointestinal-resistant matrix. *Applied Food Biotechnology*, 4(3), 179-191.
- Kilimann, K. V., Doster, W., Vogel, R. F., Hartmann, C., & Gänzle, M. G. (2006). Protection by sucrose against heat-induced lethal and sublethal injury of *Lactococcus lactis*: an FT-IR study. *Biochimica et Biophysica Acta (BBA)-Proteins and Proteomics*, 1764(7), 1188-1197.
- Klaenhammer, T., Altermann, E., Arigoni, F., Bolotin, A., Breidt, F., Broadbent, J., . . . Gasson, M. (2002). Discovering lactic acid bacteria by genomics. In *Lactic Acid Bacteria: Genetics, Metabolism and Applications* (pp. 29-58): Springer.
- Kolaček, S., Hojsak, I., Berni Canani, R., Guarino, A., Indrio, F., Orel, R., . . . Weizman, Z. (2017). Commercial probiotic products: A call for improved quality control. A position paper by the ESPGHAN working group for probiotics and prebiotics. *Journal of Pediatric Gastroenterology and Nutrition*, 65(1), 117-124.
- Kruger, M. C., Fear, A., Chua, W. H., Plimmer, G. G., & Schollum, L. M. (2009). The effect of *Lactobacillus rhamnosus* HN001 on mineral absorption and bone health in growing male and ovariectomised female rats. *Dairy Science and Technology*, 89(3-4), 219-231.
- Kurtmann, L., Carlsen, C. U., Risbo, J., & Skibsted, L. H. (2009). Storage stability of freeze-dried *Lactobacillus acidophilus* (La-5) in relation to water activity and presence of oxygen and ascorbate. *Cryobiology*, 58(2), 175-180.
- Kurtmann, L., Carlsen, C. U., Skibsted, L. H., & Risbo, J. (2009). Water activity - temperature state diagrams of freeze - dried *Lactobacillus acidophilus* (La - 5): Influence of physical state on bacterial survival during storage. *Biotechnology Progress*, 25(1), 265-270.
- Kurtmann, L., Skibsted, L. H., & Carlsen, C. U. (2009). Browning of freeze-dried probiotic bacteria cultures in relation to loss of viability during storage. *Journal of Agricultural and Food Chemistry*, 57(15), 6736-6741.
- Labuza, T. P. (1979). A theoretical comparison of losses in foods under fluctuating temperature sequences. *Journal of Food Science*, 44(4), 1162-1168.
- Labuza, T. P., & Saltmarch, M. (1982). Kinetics of browning and protein quality loss in whey powders during steady state and nonsteady state storage conditions. *Journal of Food Science*, 47(1), 92-96.
- Lahtinen, S. J., Forssten, S., Aakko, J., Granlund, L., Rautonen, N., Salminen, S., . . . Ouwehand, A. C. (2012). Probiotic cheese containing *Lactobacillus rhamnosus* HN001 and *Lactobacillus acidophilus* NCFM® modifies subpopulations of fecal lactobacilli and *Clostridium difficile* in the elderly. *AGE*, 34(1), 133-143.
- Lapsiri, W., Bhandari, B., & Wanchaitanawong, P. (2012). Viability of *Lactobacillus plantarum* TISTR 2075 in different protectants during spray drying and storage. *Drying Technology*, 30(13), 1407-1412.
- Le Marrec, C. (2011). Responses of lactic acid bacteria to osmotic stress. In E. Tsakalidou & K. Papadimitriou (Eds.), *Stress Responses of Lactic Acid Bacteria* (pp. 67-90). Boston, MA: Springer US.



- Lee, J., & Kaletunç, G. (2002). Evaluation of the heat inactivation of *Escherichia coli* and *Lactobacillus plantarum* by differential scanning calorimetry. *Applied and Environmental Microbiology*, 68(11), 5379-5386.
- Legako, J., & Dunford, N. T. (2010). Effect of spray nozzle design on fish oil–whey protein microcapsule properties. *Journal of Food Science*, 75(6), E394-E400.
- Leslie, S. B., Israeli, E., Lighthart, B., Crowe, J. H., & Crowe, L. M. (1995). Trehalose and sucrose protect both membranes and proteins in intact bacteria during drying. *Applied and Environmental Microbiology*, 61(10), 3592-3597.
- Li, C., Sun, J., Qi, X., & Liu, L. (2015). NaCl stress impact on the key enzymes in glycolysis from *Lactobacillus bulgaricus* during freeze-drying. *Brazilian Journal of Microbiology*, 46(4), 1193-1199.
- Lilly, D. M., & Stillwell, R. H. (1965). Probiotics: Growth-promoting factors produced by microorganisms. *Science*, 147(3659), 747-748.
- Lim, P. L., Toh, M., & Liu, S. Q. (2015). *Saccharomyces cerevisiae* EC-1118 enhances the survivability of probiotic *Lactobacillus rhamnosus* HN001 in an acidic environment. *Applied Microbiology and Biotechnology*, 99(16), 6803-6811.
- Linders, L. J. M., Wolkers, W. F., Hoekstra, F. A., & van 't Riet, K. (1997). Effect of added carbohydrates on membrane phase behavior and survival of dried *Lactobacillus plantarum*. *Cryobiology*, 35(1), 31-40.
- Lisboa, H. M., Duarte, M. E., & Cavalcanti-Mata, M. E. (2018). Modeling of food drying processes in industrial spray dryers. *Food and Bioproducts Processing*, 107, 49-60.
- Liu, H., Gong, J., Chabot, D., Miller, S. S., Cui, S. W., Ma, J., . . . Wang, Q. (2016). Incorporation of polysaccharides into sodium caseinate-low melting point fat microparticles improves probiotic bacterial survival during simulated gastrointestinal digestion and storage. *Food Hydrocolloids*, 54, 328-337.
- Liu, H., Gong, J., Chabot, D., Miller, S. S., Cui, S. W., Zhong, F., & Wang, Q. (2018). Improved survival of *Lactobacillus zeae* LB1 in a spray dried alginate-protein matrix. *Food Hydrocolloids*, 78, 100-108.
- Liu, L., Chen, P., Zhao, W., Li, X., Wang, H., & Qu, X. (2017). Effect of microencapsulation with the Maillard reaction products of whey proteins and isomaltooligosaccharide on the survival rate of *Lactobacillus rhamnosus* in white brined cheese. *Food Control*, 79, 44-49.
- Liu, X. T., Hou, C. L., Zhang, J., Zeng, X. F., & Qiao, S. Y. (2014). Fermentation conditions influence the fatty acid composition of the membranes of *Lactobacillus reuteri* I5007 and its survival following freeze-drying. *Letters in Applied Microbiology*, 59(4), 398-403.
- Liu, Y., & Bolen, D. (1995). The peptide backbone plays a dominant role in protein stabilization by naturally occurring osmolytes. *Biochemistry*, 34(39), 12884-12891.
- López-García, P., & Forterre, P. (2000). DNA topology and the thermal stress response, a tale from mesophiles and hyperthermophiles. *BioEssays*, 22(8), 738-746.
- López-Rubio, A., Sanchez, E., Wilkanowicz, S., Sanz, Y., & Lagaron, J. M. (2012). Electrospinning as a useful technique for the encapsulation of living bifidobacteria in food hydrocolloids. *Food Hydrocolloids*, 28(1), 159-167.
- Lorca, G. L., Barabote, R. D., Zlotopolski, V., Tran, C., Winnen, B., Hvorup, R. N., . . . Saier Jr, M. H. (2007). Transport capabilities of eleven gram-positive bacteria: Comparative genomic analyses. *Biochimica et Biophysica Acta (BBA) - Biomembranes*, 1768(6), 1342-1366.

- Loyeau, P. A., Spotti, M. J., Vanden Braber, N. L., Rossi, Y. E., Montenegro, M. A., Vinderola, G., & Carrara, C. R. (2018). Microencapsulation of *Bifidobacterium animalis* subsp. *lactis* INL1 using whey proteins and dextrans conjugates as wall materials. *Food Hydrocolloids*, 85, 129-135.
- Machado, M. C., López, C. S., Heras, H., & Rivas, E. A. (2004). Osmotic response in *Lactobacillus casei* ATCC 393: biochemical and biophysical characteristics of membrane. *Archives of Biochemistry and Biophysics*, 422(1), 61-70.
- Mackey, B., Miles, C., Parsons, S., & Seymour, D. (1991). Thermal denaturation of whole cells and cell components of *Escherichia coli* examined by differential scanning calorimetry. *Microbiology*, 137(10), 2361-2374.
- Marco, M. L., Heeney, D., Binda, S., Cifelli, C. J., Cotter, P. D., Foligné, B., . . . Hutkins, R. (2017). Health benefits of fermented foods: microbiota and beyond. *Current Opinion in Biotechnology*, 44, 94-102.
- Matalanis, A., Jones, O. G., & McClements, D. J. (2011). Structured biopolymer-based delivery systems for encapsulation, protection, and release of lipophilic compounds. *Food Hydrocolloids*, 25(8), 1865-1880.
- Mazeaud, I., Tse, K., Obert, J. P., Berger, C., Babin, G., Chaigneau, P., . . . Henri, E. (2014). Coated dehydrated microorganisms with enhanced stability and viability. In: Google Patents.
- Mazur, P. (1984). Freezing of living cells: mechanisms and implications. *American Journal of Physiology - Cell Physiology*, 247(3), C125-C142.
- Meneghel, J., Passot, S., Dupont, S., & Fonseca, F. (2017). Biophysical characterization of the *Lactobacillus delbrueckii* subsp. *bulgaricus* membrane during cold and osmotic stress and its relevance for cryopreservation. *Applied Microbiology and Biotechnology*, 101(4), 1427-1441.
- Meng, X. C., Stanton, C., Fitzgerald, G. F., Daly, C., & Ross, R. P. (2008). Anhydrobiotics: The challenges of drying probiotic cultures. *Food Chemistry*, 106(4), 1406-1416.
- Miao, S., Mills, S., Stanton, C., Fitzgerald, G. F., Roos, Y., & Ross, R. P. (2008). Effect of disaccharides on survival during storage of freeze dried probiotics. *Dairy Science and Technology*, 88(1), 19-30.
- Mika, J. T., & Poolman, B. (2011). Macromolecule diffusion and confinement in prokaryotic cells. *Current Opinion in Biotechnology*, 22(1), 117-126.
- Miles, C. A., Mackey, B. M., & Parsons, S. E. (1986). Differential scanning calorimetry of bacteria. *Microbiology*, 132(4), 939-952.
- Mitsuoka, T. (1992). Intestinal flora and aging. *Nutrition Reviews*, 50(12), 438-446.
- Moayyedi, M., Eskandari, M. H., Rad, A. H. E., Ziaee, E., Khodaparast, M. H. H., & Golmakani, M. T. (2018). Effect of drying methods (electrospraying, freeze drying and spray drying) on survival and viability of microencapsulated *Lactobacillus rhamnosus* ATCC 7469. *Journal of Functional Foods*, 40, 391-399.
- Mohácsi-Farkas, C., Farkas, J., Mészáros, L., Reichart, O., & Andrassy, É. (1999). Thermal denaturation of bacterial cells examined by differential scanning calorimetry. *Journal of Thermal Analysis and Calorimetry*, 57(2), 409-414.
- Molina-Höppner, A., Doster, W., Vogel, R. F., & Gänzle, M. G. (2004). Protective effect of sucrose and sodium chloride for *Lactococcus lactis* during sublethal and lethal high-pressure treatments. *Applied and Environmental Microbiology*, 70(4), 2013-2020.
- Montanari, C., Sado Kamdem, S. L., Serrazanetti, D. I., Etoa, F.-X., & Guerzoni, M. E. (2010). Synthesis of cyclopropane fatty acids in *Lactobacillus helveticus* and

- Lactobacillus sanfranciscensis* and their cellular fatty acids changes following short term acid and cold stresses. *Food Microbiology*, 27(4), 493-502.
- Nag, A., & Das, S. (2013). Improving ambient temperature stability of probiotics with stress adaptation and fluidized bed drying. *Journal of Functional Foods*, 5(1), 170-177.
- Noda, M., Shiraga, M., Kumagai, T., Danshiitsoodol, N., & Sugiyama, M. (2018). Characterization of the SN35N strain-specific exopolysaccharide encoded in the whole circular genome of a plant-derived *Lactobacillus plantarum*. *Biological and Pharmaceutical Bulletin*, 41(4), 536-545.
- Nunes, R. V., & Swartzel, K. R. (1990). Modeling chemical and biochemical changes under sinusoidal temperature fluctuations. *Journal of Food Engineering*, 11(2), 119-132.
- Oetjen, G.-W., & Haseley, P. (2004). *Freeze-drying*: John Wiley & Sons.
- Okuro, P. K., Thomazini, M., Balieiro, J. C. C., Liberal, R. D. C. O., & Fávaro-Trindade, C. S. (2013). Co encapsulation of *Lactobacillus acidophilus* with inulin or polydextrose in solid lipid microparticles provides protection and improves stability. *Food Research International*, 53(1), 96-103.
- Oldenhof, H., Wolkers, W. F., Fonseca, F., Passot, S., & Marin, M. (2005). Effect of sucrose and maltodextrin on the physical properties and survival of air-dried *Lactobacillus bulgaricus*: An in situ fourier transform infrared spectroscopy study. *Biotechnology Progress*, 21(3), 885-892.
- Oliveira, A., Moretti, T., Boschini, C., Baliero, J., Freitas, O., & Favaro-Trindade, C. (2007). Stability of microencapsulated *B. lactis* (BI 01) and *Lb. acidophilus* (LAC 4) by complex coacervation followed by spray drying. *Journal of microencapsulation*, 24(7), 685-693.
- Oster, M. (2018). *Probiotic supplements: theories on future growth*. Retrieved from <https://www.euromonitor.com/>
- Oxley, J. (2014). Chapter 4 - Overview of microencapsulation process technologies. In A. G. Gaonkar, N. Vasisht, A. R. Khare, & R. Sobel (Eds.), *Microencapsulation in the Food Industry* (pp. 35-46). San Diego: Academic Press.
- Pabari, R. M., Sunderland, T., & Ramtoola, Z. (2012). Investigation of a novel three-fluid nozzle spray drying technology for the engineering of multifunctional layered microparticles. *Expert opinion on drug delivery*, 9(12), 1463-1474.
- Palomino, M. M., Waehner, P. M., Fina Martin, J., Ojeda, P., Malone, L., Sanchez Rivas, C., . . . Ruzal, S. M. (2016). Influence of osmotic stress on the profile and gene expression of surface layer proteins in *Lactobacillus acidophilus* ATCC 4356. *Applied Microbiology and Biotechnology*, 100(19), 8475-8484.
- Papadimitriou, K., Alegría, Á., Bron, P. A., De Angelis, M., Gobbetti, M., Kleerebezem, M., . . . Kok, J. (2016). Stress physiology of lactic acid bacteria. *Microbiology and Molecular Biology Reviews*, 80(3), 837-890.
- Parlindungan, E., Dekiwadia, C., Tran, K. T. M., Jones, O. A. H., & May, B. K. (2018). Morphological and ultrastructural changes in *Lactobacillus plantarum* B21 as an indicator of nutrient stress. *LWT*, 92, 556-563.
- Passot, S., Gautier, J., Jamme, F., Cenard, S., Dumas, P., & Fonseca, F. (2015). Understanding the cryotolerance of lactic acid bacteria using combined synchrotron infrared and fluorescence microscopies. *Analyst*, 140(17), 5920-5928.
- Paul, A., Shi, L., & Bielawski, C. W. (2015). A eutectic mixture of galactitol and mannitol as a phase change material for latent heat storage. *Energy Conversion and Management*, 103, 139-146.

- Peñafiel, R., Cremades, A., Puellas, L., & Monserrat, F. (1985). Hyperthermia and the neurotoxicity of exogenous glutamate in infant rats. *Neurochemistry International*, 7(2), 237-242.
- Penhasi, A. (2013). US Patent No. US20150265662A1.
- Penhasi, A. (2015). Microencapsulation of probiotic bacteria using thermo-sensitive sol-gel polymers for powdered infant formula. *Journal of microencapsulation*, 32(4), 372-380.
- Pénicaud, C., Monclus, V., Perret, B., Passot, S., & Fonseca, F. (2018). Life cycle assessment of the production of stabilized lactic acid bacteria for the environmentally-friendly preservation of living cells. *Journal of Cleaner Production*, 184, 847-858.
- Perdana, J., Fox, M. B., Siwei, C., Boom, R. M., & Schutyser, M. A. I. (2014). Interactions between formulation and spray drying conditions related to survival of *Lactobacillus plantarum* WCFS1. *Food Research International*, 56, 9-17.
- Pielichowski, K., & Flejtuch, K. (2002). Differential scanning calorimetry studies on poly(ethylene glycol) with different molecular weights for thermal energy storage materials. *Polymers for Advanced Technologies*, 13(10-12), 690-696.
- Pieterse, B., Leer, R. J., Schuren, F. H. J., & van der Werf, M. J. (2005). Unravelling the multiple effects of lactic acid stress on *Lactobacillus plantarum* by transcription profiling. *Microbiology*, 151(12), 3881-3894.
- Pitigraisorn, P., Srichaisupakit, K., Wongpadungkiat, N., & Wongsasulak, S. (2017). Encapsulation of *Lactobacillus acidophilus* in moist-heat-resistant multilayered microcapsules. *Journal of Food Engineering*, 192, 11-18.
- Poddar, D., Das, S., Jones, G., Palmer, J., Jameson, G. B., Haverkamp, R. G., & Singh, H. (2014). Stability of probiotic *Lactobacillus paracasei* during storage as affected by the drying method. *International Dairy Journal*, 39(1), 1-7.
- Poolman, B., Spitzer, J. J., & Wood, J. M. (2004). Bacterial osmosensing: roles of membrane structure and electrostatics in lipid-protein and protein-protein interactions. *Biochimica et Biophysica Acta (BBA) - Biomembranes*, 1666(1-2), 88-104.
- Prasad, J., Gill, H., Smart, J., & Gopal, P. (1998). Selection and characterisation of *Lactobacillus* and *Bifidobacterium* strains for use as probiotics. *International Dairy Journal*, 8(12), 993-1002.
- Prasad, J., McJarrow, P., & Gopal, P. (2003). Heat and osmotic stress responses of probiotic *Lactobacillus rhamnosus* HN001 (DR20) in relation to viability after drying. *Applied and Environmental Microbiology*, 69(2), 917-925.
- Prasetia, K. D., & Kesetyaningsih, T. W. (2015). Effectiveness of growol to prevent diarrhea infected by enteropathogenic *Escherichia coli*. *International Journal of ChemTech Research*, 7(6), 2601-2611.
- Quintana, G., Gerbino, E., & Gómez-Zavaglia, A. (2017). Okara: A nutritionally valuable by-product able to stabilize *Lactobacillus plantarum* during freeze-drying, spray-drying, and storage. *Frontiers in Microbiology*, 8(APR).
- R Core Team. (2018). R: A language and environment for statistical computing. Retrieved from <https://www.R-project.org/>
- Ren, Y., & Zhang, Y. (2015). Numerical investigation of thermally triggered release kinetics of double emulsion for drug delivery using phase change material. *World Academy of Science, Engineering and Technology, International Journal of Medical, Health, Biomedical, Bioengineering and Pharmaceutical Engineering*, 9(6), 471-474.

- Rey, L., & May, J. C. (2004). Freeze-drying/lyophilization of pharmaceutical and biological products/edited by Louis Rey, Joan C. May. In.
- Rodríguez-Bermejo, J., Barreiro, P., Robla, J. I., & Ruiz-García, L. (2007). Thermal study of a transport container. *Journal of Food Engineering*, 80(2), 517-527.
- Roos, Y. (1993). Melting and glass transitions of low molecular weight carbohydrates. *Carbohydrate research*, 238, 39-48.
- Roos, Y. H., & Pehkonen, K. S. (2010). Entrapment of probiotic bacteria in frozen cryoprotectants and viability in freeze drying. In *Water Properties in Food, Health, Pharmaceutical and Biological Systems: ISOPOW 10* (pp. 283-290).
- Rosenberg, M., Kopelman, I., & Talmon, Y. (1990). Factors affecting retention in spray-drying microencapsulation of volatile materials. *Journal of Agricultural and Food Chemistry*, 38(5), 1288-1294.
- Rossi, R. M., & Bolli, W. P. (2005). Phase change materials for improvement of heat protection. *Advanced Engineering Materials*, 7(5), 368-373.
- Russo, R., Superti, F., Karadja, E., & De Seta, F. (2019). Randomised clinical trial in women with Recurrent Vulvovaginal Candidiasis: Efficacy of probiotics and lactoferrin as maintenance treatment. *Mycoses*.
- Saarela, M., Virkajärvi, I., Alakomi, H. L., Mattila-Sandholm, T., Vaari, A., Suomalainen, T., & Mättö, J. (2005). Influence of fermentation time, cryoprotectant and neutralization of cell concentrate on freeze-drying survival, storage stability, and acid and bile exposure of *Bifidobacterium animalis* ssp. *lactis* cells produced without milk-based ingredients. *Journal of Applied Microbiology*, 99(6), 1330-1339.
- Saarela, M., Virkajarvi, I., Nohynek, L., Vaari, A., & Matto, J. (2006). Fibres as carriers for *Lactobacillus rhamnosus* during freeze-drying and storage in apple juice and chocolate-coated breakfast cereals. *International Journal of Food Microbiology*, 112(2), 171-178.
- Santivarangkna, C., Aschenbrenner, M., Kulozik, U., & Foerst, P. (2011). Role of glassy state on stabilities of freeze-dried probiotics. *Journal of Food Science*, 76(8), R152-R156.
- Santivarangkna, C., Higl, B., & Foerst, P. (2008). Protection mechanisms of sugars during different stages of preparation process of dried lactic acid starter cultures. *Food Microbiology*, 25(3), 429-441.
- Santivarangkna, C., Naumann, D., Kulozik, U., & Foerst, P. (2010). Protective effects of sorbitol during the vacuum drying of *Lactobacillus helveticus*: An FT-IR study. *Annals of Microbiology*, 60(2), 235-242.
- Savini, M., Cecchini, C., Verdenelli, M. C., Silvi, S., Orpianesi, C., & Cresci, A. (2010). Pilot-scale production and viability analysis of freeze-dried probiotic bacteria using different protective agents. *Nutrients*, 2(3), 330-339.
- Scheffe, H. (1963). The simplex-centroid design for experiments with mixtures. *Journal of the Royal Statistical Society. Series B (Methodological)*, 25(2), 235-263.
- Schoug, Å., Olsson, J., Carlfors, J., Schnürer, J., & Håkansson, S. (2006). Freeze-drying of *Lactobacillus coryniformis* Si3—effects of sucrose concentration, cell density, and freezing rate on cell survival and thermophysical properties. *Cryobiology*, 53(1), 119-127.
- Scott, J. W. (1959). The effect of residual water on the survival of dried bacteria during storage. *Journal of general microbiology*, 19, 624-633.
- Sender, R., Fuchs, S., & Milo, R. (2016). Revised estimates for the number of human and bacteria cells in the body. *bioRxiv*.

- Senz, M., van Lengerich, B., Bader, J., & Stahl, U. (2015). Control of cell morphology of probiotic *Lactobacillus acidophilus* for enhanced cell stability during industrial processing. *International Journal of Food Microbiology*, 192, 34-42.
- Shah, N. P., Ding, W. K., Fallourd, M. J., & Leyer, G. (2010). Improving the stability of probiotic bacteria in model fruit juices using vitamins and antioxidants. *Journal of Food Science*, 75(5), M278-M282.
- Sharma, A., Sharma, S., & Buddhi, D. (2002). Accelerated thermal cycle test of acetamide, stearic acid and paraffin wax for solar thermal latent heat storage applications. *Energy Conversion and Management*, 43(14), 1923-1930.
- Sharma, A., Tyagi, V., Chen, C., & Buddhi, D. (2009). Review on thermal energy storage with phase change materials and applications. *Renewable and Sustainable energy reviews*, 13(2), 318-345.
- Sheehan, V. M., Sleator, R. D., Fitzgerald, G. F., & Hill, C. (2006). Heterologous expression of BetL, a betaine uptake system, enhances the stress tolerance of *Lactobacillus salivarius* UCC118. *Applied and Environmental Microbiology*, 72(3), 2170-2177.
- Shen, Z., Zhu, C., Quan, Y., Yuan, W., Wu, S., Yang, Z., . . . Wang, X. (2017). Update on intestinal microbiota in Crohn's disease 2017: Mechanisms, clinical application, adverse reactions, and outlook. *Journal of Gastroenterology and Hepatology (Australia)*, 32(11), 1804-1812.
- Shi, Y., Liang, R., Chen, L., Liu, H., Goff, H. D., Ma, J., & Zhong, F. (2019). The antioxidant mechanism of Maillard reaction products in oil-in-water emulsion system. *Food Hydrocolloids*, 87, 582-592.
- Siaterlis, A., Deepika, G., & Charalampopoulos, D. (2009). Effect of culture medium and cryoprotectants on the growth and survival of probiotic lactobacilli during freeze drying. *Letters in Applied Microbiology*, 48(3), 295-301.
- Singh, S. P., Saha, K., Singh, J., & Sandhu, A. P. S. (2012). Measurement and analysis of vibration and temperature levels in global intermodal container shipments on truck, rail and ship. *Packaging Technology and Science*, 25(3), 149-160.
- Smirnoff, N., & Cumbes, Q. J. (1989). Hydroxyl radical scavenging activity of compatible solutes. *Phytochemistry*, 28(4), 1057-1060.
- Song, S., Bae, D. W., Lim, K., Griffiths, M. W., & Oh, S. (2014). Cold stress improves the ability of *Lactobacillus plantarum* L67 to survive freezing. *International Journal of Food Microbiology*, 191, 135-143.
- Stefanello, R. F., Machado, A. A. R., Pasqualin Cavalheiro, C., Bartholomei Santos, M. L., Nabeshima, E. H., Copetti, M. V., & Fries, L. L. M. (2018). Trehalose as a cryoprotectant in freeze-dried wheat sourdough production. *LWT*, 89, 510-517.
- Strasser, S., Neureiter, M., Geppl, M., Braun, R., & Danner, H. (2009). Influence of lyophilization, fluidized bed drying, addition of protectants, and storage on the viability of lactic acid bacteria. *Journal of Applied Microbiology*, 107(1), 167-177.
- Streit, F., Delettre, J., Corrieu, G., & Béal, C. (2008). Acid adaptation of *Lactobacillus delbrueckii* subsp. *bulgaricus* induces physiological responses at membrane and cytosolic levels that improves cryotolerance. *Journal of Applied Microbiology*, 105(4), 1071-1080.
- Suharja, A. A., Henriksson, A., & Liu, S. Q. (2014). Impact of *Saccharomyces cerevisiae* on viability of probiotic *Lactobacillus rhamnosus* in fermented milk under ambient conditions. *Journal of Food Processing and Preservation*, 38(1), 326-337.

- Sunny-Roberts, E. O., & Knorr, D. (2009). The protective effect of monosodium glutamate on survival of *Lactobacillus rhamnosus* GG and *Lactobacillus rhamnosus* E-97800 (E800) strains during spray-drying and storage in trehalose-containing powders. *International Dairy Journal*, 19(4), 209-214.
- Sunny-Roberts, E. O., & Knorr, D. (2011). Cellular injuries on spray-dried *Lactobacillus rhamnosus* GG and its stability during food storage. *Nutrition and Food Science*, 41(3), 191-200.
- Tabanelli, G., Vernocchi, P., Patrignani, F., Del Chierico, F., Putignani, L., Vinderola, G., . . . Lanciotti, R. (2015). Effects of sub-lethal high-pressure homogenization treatment on the outermost cellular structures and the volatile-molecule profiles of two strains of probiotic lactobacilli. *Frontiers in Microbiology*, 6, 1006.
- Tamime, A. Y., Marshall, V. M., & Robinson, R. K. (1995). Microbiological and technological aspects of milks fermented by bifidobacteria. *Journal of Dairy Research*, 62(01), 151-187.
- Tang, C.-H., Choi, S.-M., & Ma, C.-Y. (2007). Study of thermal properties and heat-induced denaturation and aggregation of soy proteins by modulated differential scanning calorimetry. *International Journal of Biological Macromolecules*, 40(2), 96-104.
- Tannock, G. W., Munro, K., Harmsen, H. J. M., Welling, G. W., Smart, J., & Gopal, P. K. (2000). Analysis of the fecal microflora of human subjects consuming a probiotic product containing *Lactobacillus rhamnosus* DR20. *Applied and Environmental Microbiology*, 66(6), 2578-2588.
- Teixeira, P., Castro, H., & Kirby, R. (1996). Evidence of membrane lipid oxidation of spray-dried *Lactobacillus bulgaricus* during storage. *Letters in Applied Microbiology*, 22(1), 34-38.
- Teixeira, P., Castro, H., Mohácsi-Farkas, C., & Kirby, R. (1997). Identification of sites of injury in *Lactobacillus bulgaricus* during heat stress. *Journal of Applied Microbiology*, 83(2), 219-226.
- To, E. C., & Flink, J. M. (1978). 'Collapse', a structural transition in freeze dried carbohydrates. *International journal of food science & technology*, 13(6), 567-581.
- Toh, M., & Liu, S. Q. (2017). Influence of commercial inactivated yeast derivatives on the survival of probiotic bacterium *Lactobacillus rhamnosus* HN001 in an acidic environment. *AMB Express*, 7(1).
- Tsakalidou, E., & Papadimitriou, K. (2011). *Stress responses of lactic acid bacteria*: Springer Science & Business Media.
- Tunick, M. H., Novak, J. S., Bayles, D. O., Lee, J., & Kaletunç, G. (2009). Analysis of foodborne bacteria by differential scanning calorimetry. *Calorimetry in Food Processing: Analysis and Design of Food Systems*, 39, 147.
- Tymczyszyn, E. E., Gerbino, E., Illanes, A., & Gómez-Zavaglia, A. (2011). Galacto-oligosaccharides as protective molecules in the preservation of *Lactobacillus delbrueckii* subsp. *bulgaricus*. *Cryobiology*, 62(2), 123-129.
- Tymczyszyn, E. E., Gómez-Zavaglia, A., & Disalvo, E. A. (2005). Influence of the growth at high osmolality on the lipid composition, water permeability and osmotic response of *Lactobacillus bulgaricus*. *Archives of Biochemistry and Biophysics*, 443(1), 66-73.
- Tymczyszyn, E. E., Sosa, N., Gerbino, E., Hugo, A., Gómez-Zavaglia, A., & Schebor, C. (2012). Effect of physical properties on the stability of *Lactobacillus bulgaricus* in a freeze-dried galacto-oligosaccharides matrix. *International Journal of Food Microbiology*, 155(3), 217-221.

- van de Guchte, M., Serror, P., Chervaux, C., Smokvina, T., Ehrlich, S. D., & Maguin, E. (2002). Stress responses in lactic acid bacteria. *Antonie van Leeuwenhoek*, 82(1), 187-216.
- van der Waaij, D., Berghuis-de Vries, J. M., & Lekkerkerk, L.-v. (1971). Colonization resistance of the digestive tract in conventional and antibiotic-treated mice. *Journal of Hygiene*, 69(3), 405-411.
- Vega, C., & Roos, Y. H. (2006). Invited review: Spray-dried dairy and dairy-like emulsions—compositional considerations. *Journal of Dairy Science*, 89(2), 383-401.
- Venketesh, S., & Dayananda, C. (2008). Properties, potentials, and prospects of antifreeze proteins. *Critical Reviews in Biotechnology*, 28(1), 57-82.
- Ventura, A. K., Beauchamp, G. K., & Mennella, J. A. (2012). Infant regulation of intake: the effect of free glutamate content in infant formulas. *The American journal of clinical nutrition*, 95(4), 875-881.
- Vereyken, I. J., Albert van Kuik, J., Evers, T. H., Rijken, P. J., & de Kruijff, B. (2003). Structural requirements of the fructan-lipid interaction. *Biophysical Journal*, 84(5), 3147-3154.
- Vollaard, E. J., & Clasener, H. A. L. (1994). Colonization resistance. *Antimicrobial Agents and Chemotherapy*, 38(3), 409-414.
- Wang, S. M., Zhang, L. W., Xue, C. H., Li, H. B., Sun, Y., & Chi, Z. P. (2017). Research progress on the inhibitory effects of probiotics on N-nitroso compound-induced colon carcinoma. *Modern Food Science and Technology*, 33(4), 306-314.
- Wang, Y., Delettre, J., Corrieu, G., & Béal, C. (2011). Starvation induces physiological changes that act on the cryotolerance of *Lactobacillus acidophilus* RD758. *Biotechnology Progress*, 27(2), 342-350.
- Whelan, D. R., Hiscox, T. J., Rood, J. I., Bambery, K. R., McNaughton, D., & Wood, B. R. (2014). Detection of an en masse and reversible B- to A-DNA conformational transition in prokaryotes in response to desiccation. *Journal of the Royal Society Interface*, 11(97), 20140454.
- Wickens, K., Barthow, C., Mitchell, E. A., Kang, J., van Zyl, N., Purdie, G., . . . Crane, J. (2018). Effects of *Lactobacillus rhamnosus* HN001 in early life on the cumulative prevalence of allergic disease to 11 years. *Pediatric Allergy and Immunology*, 29(8), 808-814.
- Wickens, K., Black, P., Stanley, T. V., Mitchell, E., Barthow, C., Fitzharris, P., . . . Crane, J. (2012). A protective effect of *Lactobacillus rhamnosus* HN001 against eczema in the first 2 years of life persists to age 4 years. *Clinical & Experimental Allergy*, 42(7), 1071-1079.
- Wolfe, J. (1987). Lateral stresses in membranes at low water potential. *Functional Plant Biology*, 14(3), 311-318.
- Wolkers, W. F., & Oldenhof, H. (2015). Use of in situ Fourier transform infrared spectroscopy to study freezing and drying of cells. *Methods in molecular biology*, 1257, 147-161.
- Wood, J. M., Bremer, E., Csonka, L. N., Kraemer, R., Poolman, B., van der Heide, T., & Smith, L. T. (2001). Osmosensing and osmoregulatory compatible solute accumulation by bacteria. *Comparative Biochemistry and Physiology Part A: Molecular & Integrative Physiology*, 130(3), 437-460.
- Wu, C., Zhang, J., Wang, M., Du, G., & Chen, J. (2012). *Lactobacillus casei* combats acid stress by maintaining cell membrane functionality. *Journal of Industrial Microbiology & Biotechnology*, 39(7), 1031-1039.



- Xie, Y., Chou, L.-s., Cutler, A., & Weimer, B. (2004). DNA macroarray profiling of *Lactococcus lactis* subsp. *Lactis* IL1403 gene expression during environmental stresses. *Applied and Environmental Microbiology*, 70(11), 6738-6747.
- Ying, D. Y., Phoon, M. C., Sanguansri, L., Weerakkody, R., Burgar, I., & Augustin, M. A. (2010). Microencapsulated *Lactobacillus rhamnosus* gg powders: Relationship of powder physical properties to probiotic survival during storage. *Journal of Food Science*, 75(9), E588-E595.
- Yonekura, L., Sun, H., Soukoulis, C., & Fisk, I. (2014). Microencapsulation of *Lactobacillus acidophilus* NCIMB 701748 in matrices containing soluble fibre by spray drying: technological characterization, storage stability and survival after in vitro digestion. *Journal of Functional Foods*, 6, 205-214.
- Zawistowska-Rojek, A., Zareba, T., Mrowka, A., & Tyski, S. (2016). Assessment of the microbiological status of probiotic products. *Polish journal of microbiology*, 65(1), 97-104.
- Zhang, F., Li, X. Y., Park, H. J., & Zhao, M. (2013). Effect of microencapsulation methods on the survival of freeze-dried *Bifidobacterium bifidum*. *Journal of microencapsulation*, 30(6), 511-518.
- Zhang, Y., Lin, J., & Zhong, Q. (2015). The increased viability of probiotic *Lactobacillus salivarius* NRRL B-30514 encapsulated in emulsions with multiple lipid-protein-pectin layers. *Food Research International*, 71, 9-15.
- Zhang, Z., Yuan, Y., Zhang, N., & Cao, X. (2015). Thermophysical Properties of Some Fatty Acids/Surfactants as Phase Change Slurries for Thermal Energy Storage. *Journal of Chemical and Engineering Data*, 60(8), 2495-2501.
- Zhang, Z. Z., Ji, Y. X., Cheng, Y. F., Xu, L. Z. J., & Jin, R. C. (2018). Increased salinity improves the thermotolerance of mesophilic anammox consortia. *Science of the Total Environment*, 644, 710-716.
- Zhao, M., Wang, Y., Huang, X., Gaenzle, M., Wu, Z., Nishinari, K., . . . Fang, Y. (2018). Ambient storage of microencapsulated: *Lactobacillus plantarum* ST-III by complex coacervation of type-A gelatin and gum Arabic. *Food and Function*, 9(2), 1000-1008.
- Zhao, S., Zhang, Q., Hao, G., Liu, X., Zhao, J., Chen, Y., . . . Chen, W. (2014). The protective role of glycine betaine in *Lactobacillus plantarum* ST-III against salt stress. *Food Control*, 44, 208-213.
- Zhou, J. S., Gopal, P. K., & Gill, H. S. (2001). Potential probiotic lactic acid bacteria *Lactobacillus rhamnosus* (HN001), *Lactobacillus acidophilus* (HN017) and *Bifidobacterium lactis* (HN019) do not degrade gastric mucin in vitro. *International Journal of Food Microbiology*, 63(1-2), 81-90.
- Zhou, J. S., Shu, Q., Rutherford, K. J., Prasad, J., Birtles, M. J., Gopal, P. K., & Gill, H. S. (2000). Safety assessment of potential probiotic lactic acid bacterial strains *Lactobacillus rhamnosus* HN001, *Lb. acidophilus* HN017, and *Bifidobacterium lactis* HN019 in BALB/c mice. *International Journal of Food Microbiology*, 56(1), 87-96.
- Zhou, J. S., Shu, Q., Rutherford, K. J., Prasad, J., Gopal, P. K., & Gill, H. S. (2000). Acute oral toxicity and bacterial translocation studies on potentially probiotic strains of lactic acid bacteria. *Food and Chemical Toxicology*, 38(2-3), 153-161.
- Zhu, S. C., Ying, D. Y., Sanguansri, L., Tang, J. W., & Augustin, M. A. (2013). Both stereo-isomers of glucose enhance the survival rate of microencapsulated *Lactobacillus rhamnosus* GG during storage in the dry state. *Journal of Food Engineering*, 116(4), 809-813.

# Appendix A - FTIR study of the mixture powder

---

## A. 1 Introduction

FTIR method has been proposed to study the interaction of the protectants with the cells, in the dried state. However, most of the studies are looking at the dried cells with a small amount of protectants, so that the bacteria signal can be easily analysed. The limitation of this method is that the bacteria are not in their real conditions, where the amount of protectants is far higher than the amount of probiotics. A method, developed by Berger et al. (1998) aim to overcome this limitation by subtracting the spectra of a component (i.e. here, the protective matrix) from the overall spectra (i.e. the entrapped bacteria) to obtain the spectra of interests (i.e. the bacteria). This method, the non-subjective vector correction, was successfully used by Hlaing et al. (2017), who managed to look at the bacteria spectrum which were either spray-dried, or freeze-dried at a final percentage of 0.4% (w/w). The freeze-dried sample of this study contained about 3.3% (w/w) of bacteria, and was thus supposed to be adequate to apply the non-subjective vector correction methodology.

## A. 2 Methodology

The fifteen compositions from the mixture DoE were prepared without the bacteria, in triplicates and freeze-dried. Together with the samples containing *Lb. rhamnosus* HN001 the 90 samples were measured on the FTIR in at least triplicates, as described in section 5.2.4.5. Background was measured before each set of measurements, or every two hours and was directly subtracted from the spectrum. As a result, about 270 spectrum were obtained.

Spectra were analysed by R 3.5.0. They were first centred and scaled before being smoothed using the Gaussian window method with a window of 10 points. Then, spectra were averaged before taking the first derivative using a Savitsky-Golay smoothing filter, with a filter order of 3 and a length of 11. This method gave the best separation between samples containing bacteria or only the protective matrix. Presence of outliers and consistency of the analysis was checked using PCA.

Finally, the matrix spectra were removed from the samples spectra using the methodology followed by Hlaing et al. (2017). The R code was as following below. The “S.SNV.sm.SG.mean15” matrix contains the centred, scaled smoothed and averaged 30 spectra, with the 15 matrix-only spectra in the first 15 rows and the bacteria-and-matrix spectrum in the last 15 rows.

#1. Creation of an empty data frame to then store the Euclidian norm of each matrix-only spectrum (S.SNV.sm.SG2.mean15 is the corrected and averaged spectrum data with the protective matrices in the first 15 rows, and the whole samples in the last 15 rows)

```
MagnitudeBlank<-data.frame
```

```
MagnitudeBlank<-apply(X = S.SNV.sm.SG2.mean15[1:15,], MARGIN = 1, FUN = norm, '2')
```

#2. Calculation of the dot product between each matrix-only spectrum and its related bacteria-and matrix spectrum

```
Sdot=1
```

```
for (i in 1:15) {for(j in 16:30){
```

```
  Sdot[i]=pracma::dot(S.SNV.sm.SG.mean15[j,],S.SNV.sm.SG.mean15[i,]) }}
```

#3. Creation of the new data frame, and calculation of the vector corrected data (Final.cor.Data). The matrix-only spectra are normalised to their amount (96.3%)

```
Final.cor.Data<-data.frame
```

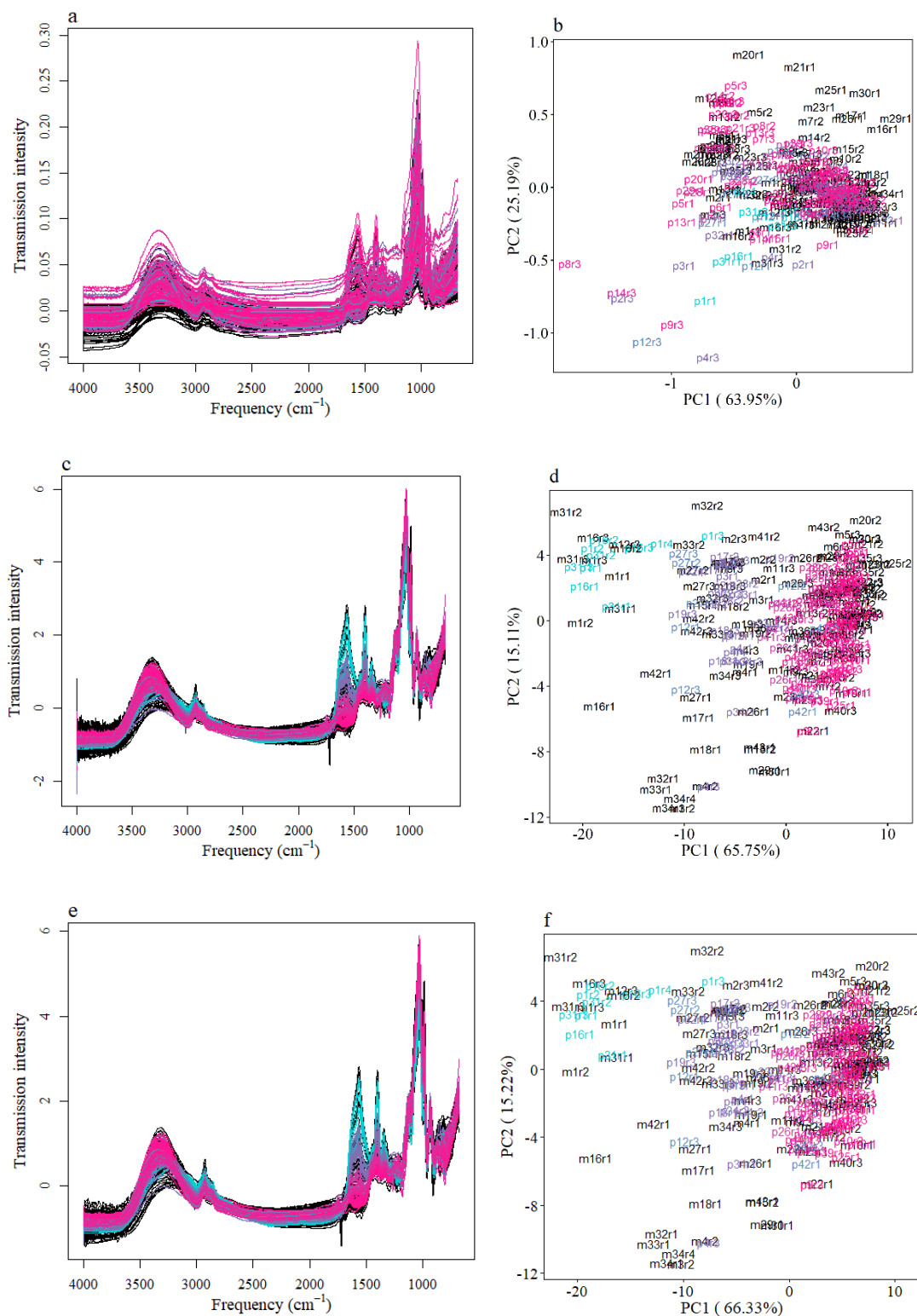
```
Final.cor.Data=S.SNV.sm.SG2.mean15[16:30,]-
```

```
((Sdot/(MagnitudeBlank^2))*0.963*S.SNV.sm.SG2.mean15[1:15,]) #corrected data
```

### **A. 3 Results**

The treatment process of the spectra, before averaging the data, is shown in Figure A.1. After centre and scaling, the samples with higher concentration of MSG are dissociating from the main cluster where most of the samples are located. This difference could be explained by the structure of the powders, which were not as brittle than the rest of the samples when the percentage of MSG was higher. The powders with higher amount of MSG were difficult to grind and were easily taking up moisture, either from the environment, or from the powder itself that had been trapped during the collapsing and was released during the grinding. As a result, the powder may not have covered the crystal plate as well as for the other samples. In addition, as it has been shown on the SEM micrographs, these samples are smoother than the others and they could have diffracted the light differently.

## Appendix A - FTIR study of the mixture powder

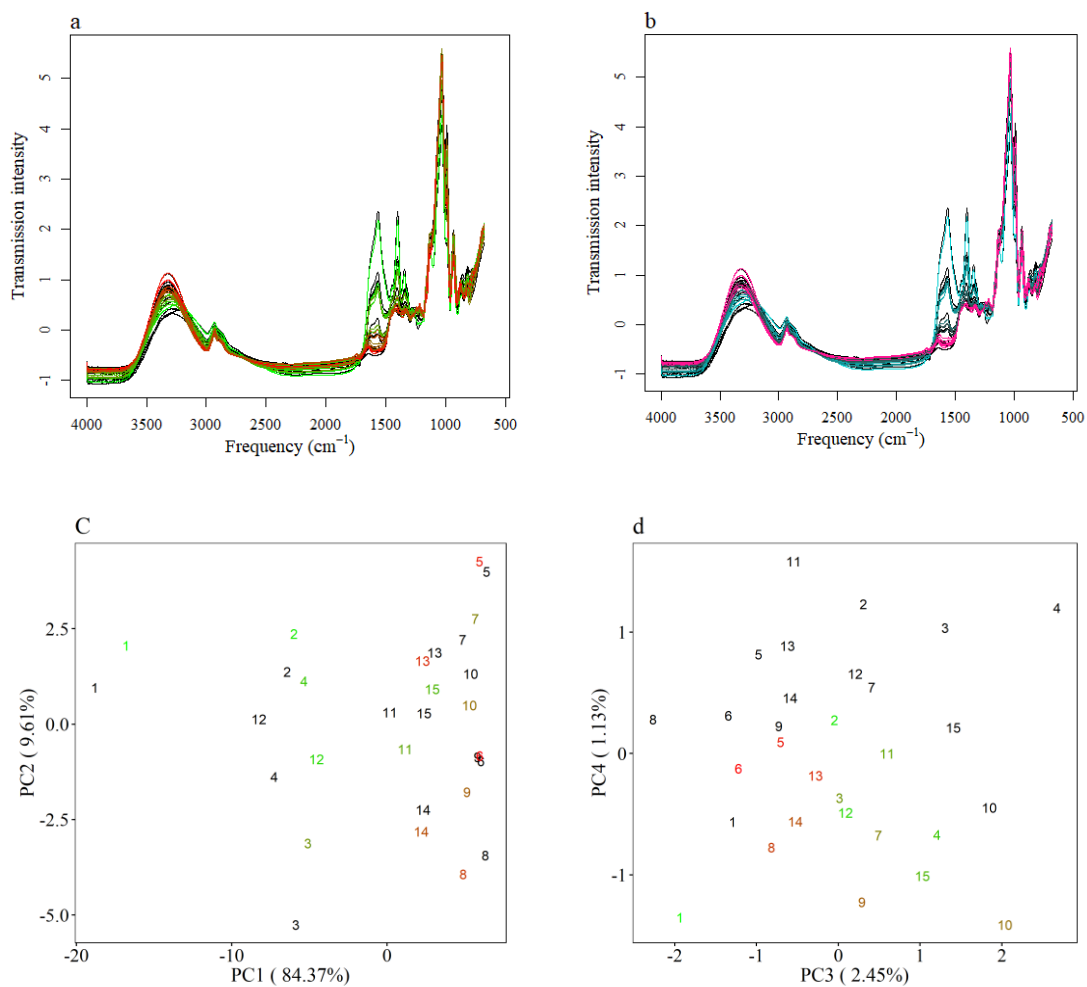


**Figure A.1:** Infra-Red spectra of the Mixture DoE samples (Chapter 5), with bacteria (in colour) or without bacteria (in black). Samples with bacteria are coloured as a function of their amount of MSG, with light blue being low amount of MSG, dark blue, lower amount of MSG and pink no MSG. After visualising the raw data (a, b), the treatment consisted in centre and scaling (c, d) and smoothing (e, f).

For each treatment the spectra are shown in a, c and e, and the first two PC in b, d and f.

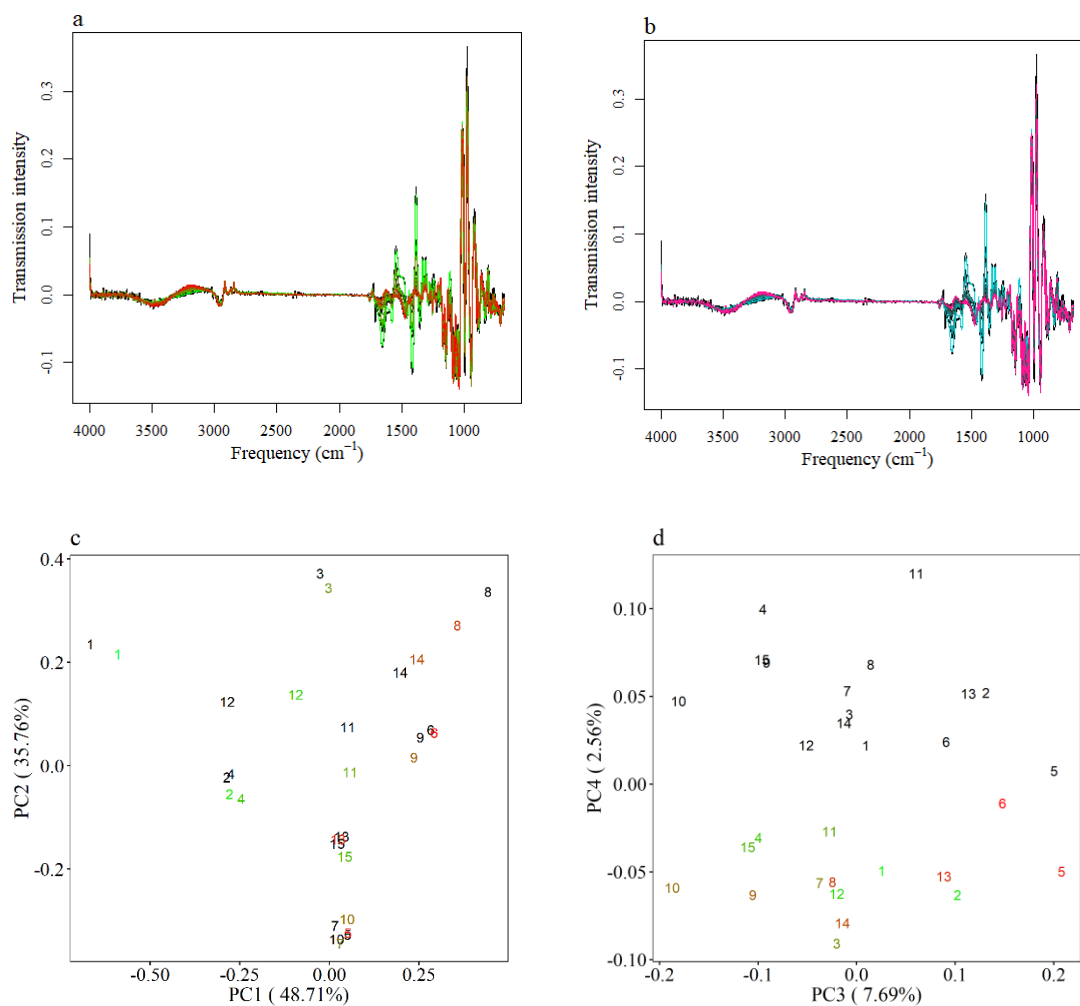
Averaged spectra, after the treatments, are shown in Figure A.2. Spectra are coloured as a function of their death rate (green to red), and as a function of their MSG content (light blue to pink). Samples with low death rate are clustering together on the PCA, and their variance is explained by the first PC. This results can be easily seen on the spectra as most of the variations are located in the  $1700 - 1300 \text{ cm}^{-1}$  region, where both samples with low death rate and high amount of MSG are distinguished by 4 main peaks. Because the low death rate are directly correlated to the amount of MSG in the powder, and because the FTIR measurement is also correlated to the composition of the samples, the study of the spectra will not bring any additional information than found in Chapter 5 until the protective matrix contribution is removed from the spectra. For this, the data need to be pre-treated so that the protective matrix and the samples with bacteria are separated on one of the PC. This was achieved after taking the first derivative of the averaged and corrected data, presented on Figure A.3. Indeed, the samples are separated along the 4<sup>th</sup> PC, accounting for 2.56 % of the variation in the samples.

## Appendix A - FTIR study of the mixture powder



**Figure A.2:** Averaged spectra of the mixture DoE after centring, scaling and smoothing. Spectra are shown in a and b, and the first four PC of the PCA are shown in c and d. Samples with no bacteria are shown in black. In a, c and d samples with bacteria coloured as a function of their death rate, green being lower death rate and red being higher. In figure b samples are coloured as a function of their MSG content, in light blue higher amount of MSG, dark blue lower amount and pink no MSG.

## Appendix A - FTIR study of the mixture powder



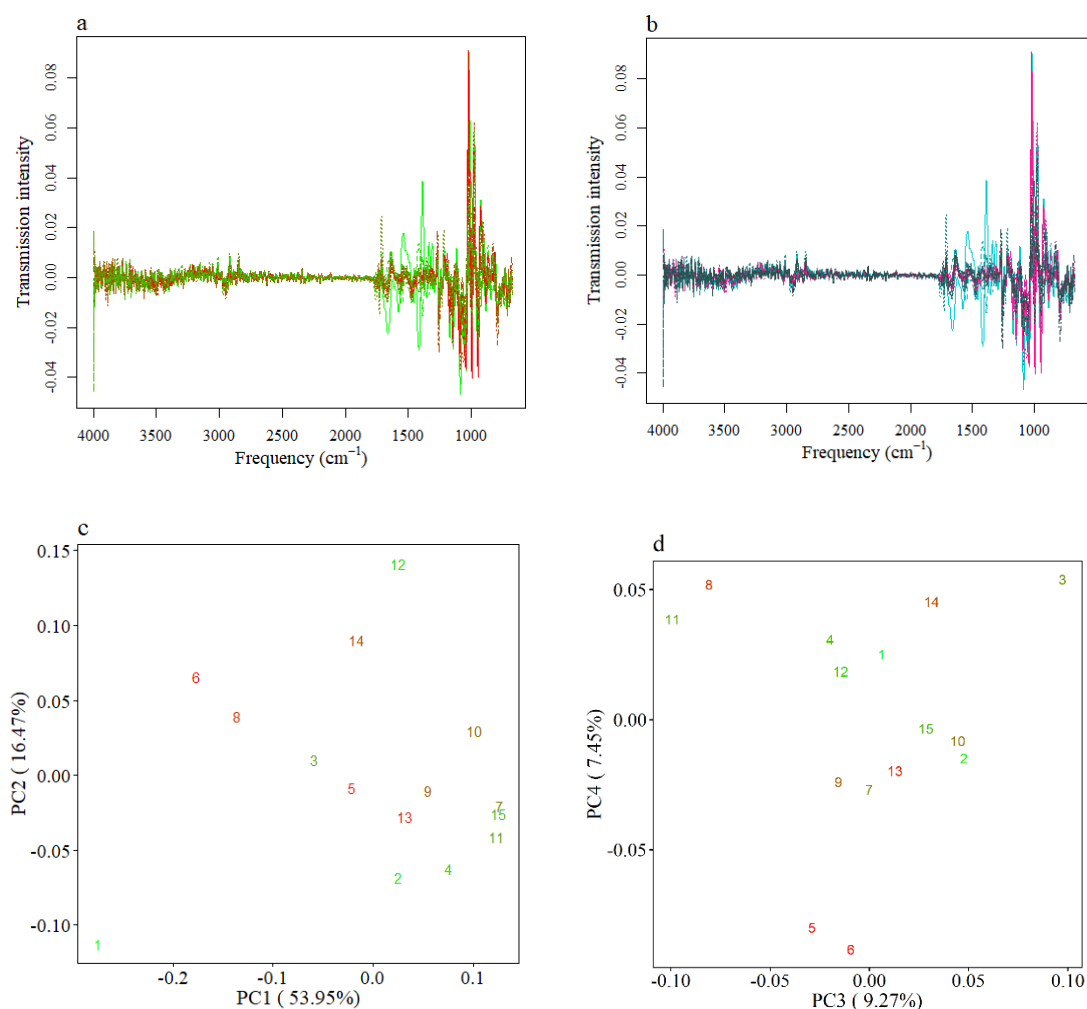
**Figure A.3:** First derivative of the averaged and corrected spectra of the mixture DoE (a,b). The four first PC of the PCA are shown in c and d. Samples are shown as a function of their death rate in a, c and d (green low death rate, red high death rate) and as a function of the MSG amount in b (light blue higher amount of MSG, dark blue lower amount and pink no MSG).

As the first derivative of the averaged data after centring, scaling, and smoothing, led to separation of the samples with and without probiotics on the 4<sup>th</sup> PC, the vector correction was conducted on these corrected data.

The vector corrected data are presented on Figure A.4. Interestingly, the spectra are similar to the 1<sup>st</sup> derivative, before the vector correction (Figure A.3) and it seems that the correction only led to a reduction of the signal, but not a proper subtraction. The main difference on the spectra for samples with low death rate is still located in the 1700 -1300



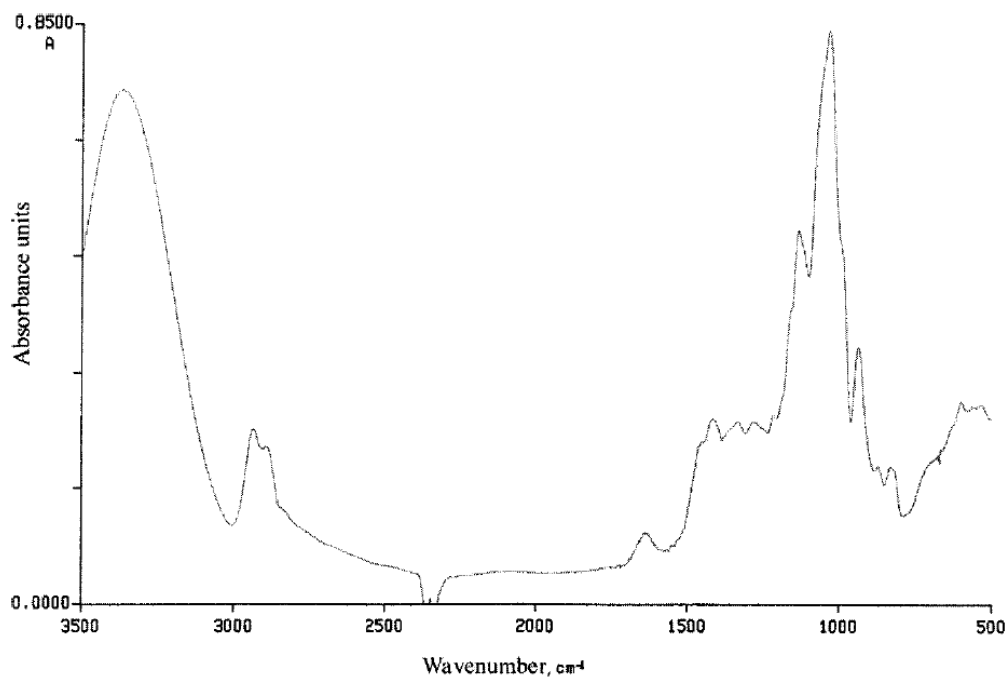
cm<sup>-1</sup> region, which is linked to the amount of MSG in the powder as shown in the graph b. The PCA did not show clear clustering of the low and high death rates. Thus, it appeared that the non-subjective vector correction was not an adequate method for these freeze-dried samples.



**Figure A.4:** Vector corrected spectra of the mixture DoE (a,b). The four first PC of the PCA are shown in c and d. Samples are shown as a function of their death rate in a, c and d (green low death rate, red high death rate) and as a function of the MSG amount in b (light blue higher amount of MSG, dark blue lower amount and pink no MSG).

Another use of these spectra is to look at the signal of the inulin, to verify if MSG-inulin interactions seen on the powder structure (Section 5.3.3) can be seen on the inulin

spectra. The inulin spectra, retrieved from Grube, Bekers, Upite, and Kaminska (2002) is presented in Figure A.5. Three major peaks and one shoulder are easily identified in the region  $1200 - 900 \text{ cm}^{-1}$ .

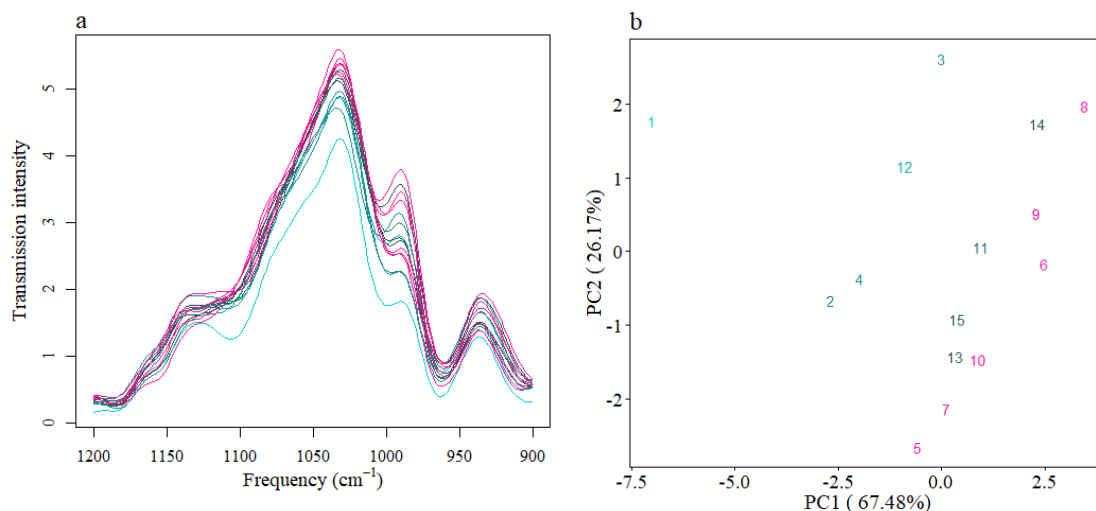


**Figure A.5:** IR spectra of Inulin, retrieved from Grube et al. (2002)

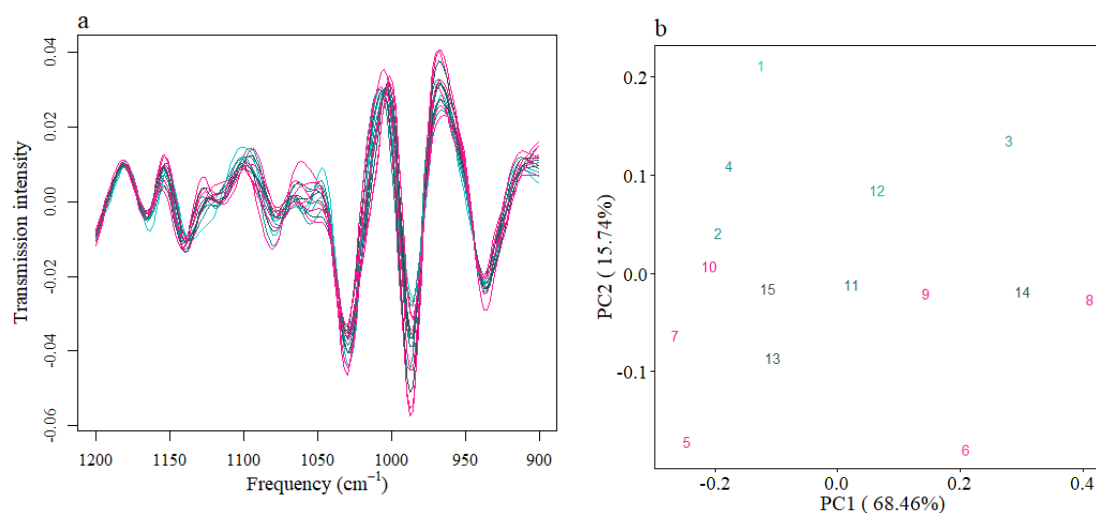
These four peaks and shoulder were also seen on the samples spectra. This region was isolated and showed on Figure A.6. The spectra show that the intensity of the inulin signal is decreasing with the increase of the amount of MSG, and the PCA show a clear hierarchical organisation of the samples with increasing amount of MSG, along the first PC.

In order to remove this bias, caused by the difference of intensity, the second derivative was used for further analysis (Figure A.7), and the peak location was determined from it. As it can be seen on Figure A.7, the bias created by the amount of

MSG in the powder was removed, and the samples are not organised as function of their MSG amount on the PCA anymore.

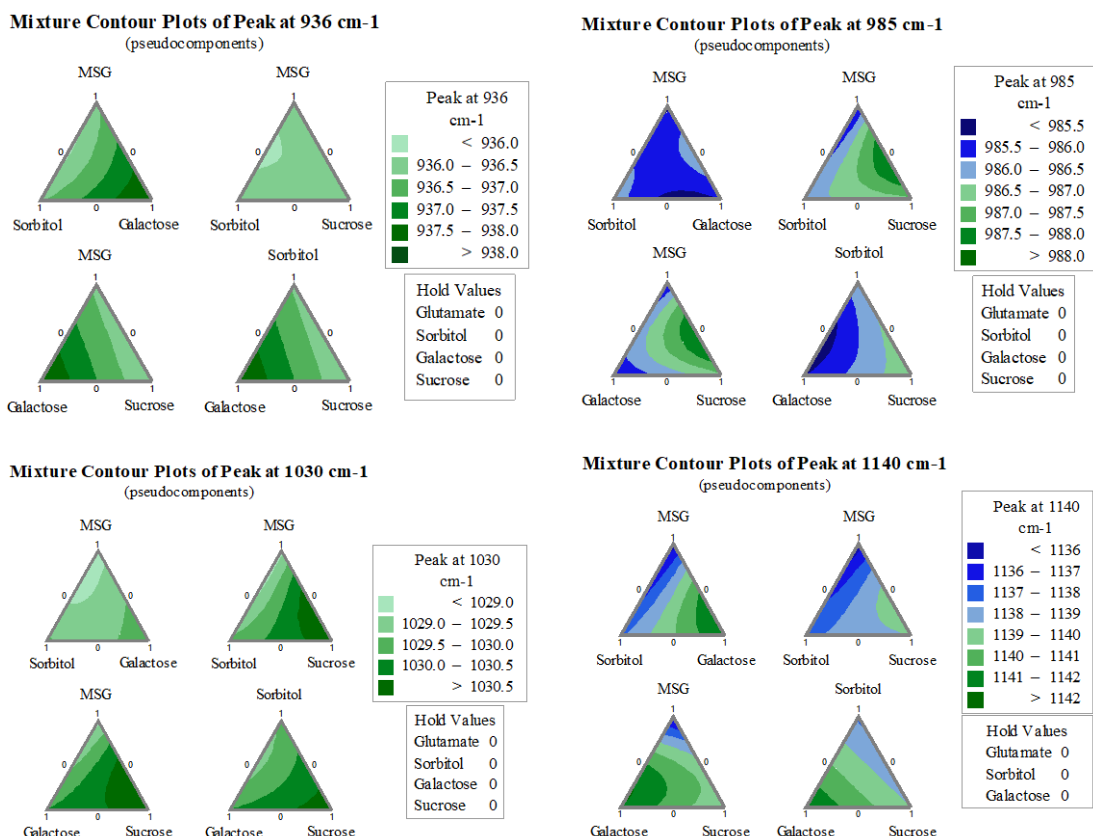


**Figure A.6:** Centred, scaled, smoothed and averaged spectra of the 15 mixes (a), isolation of the 900 – 1200  $\text{cm}^{-1}$  region, corresponding to the inulin signal. The PCA of this region is showed in b, and samples are coloured as a function of the MSG amount (light blue higher amount of MSG, dark blue lower amount and pink no MSG).



**Figure A.7:** Second derivative of centred, scaled, smoothed and averaged spectra of the 15 mixes (a), isolation of the 900 – 1200  $\text{cm}^{-1}$  region, corresponding to the inulin signal. The PCA of this region is showed in b, and samples are coloured as a function of the MSG amount (light blue higher amount of MSG, dark blue lower amount and pink no MSG).

The four peaks locations were taken from the second derivative and the impact of the composition on their location was determined following the mixture DoE analysis as shown on Figure A.8. The SEM micrographs from Chapter 5, section 5.2.4.2 showed a different structure for powder containing MSG compared to sorbitol and sucrose, with an in-between structure for galactose. It was thus, hypothesized that MSG and galactose interacted somehow with inulin, but galactose to a lesser extent, contrary to sucrose or sorbitol that should not show any interaction with inulin. Variations of the peak location were of the order of  $2\text{ cm}^{-1}$ , up to  $6\text{ cm}^{-1}$ . The resolution of the measurements was of  $4\text{ cm}^{-1}$  it is, hence, difficult to be ascertain that these shifts are due to interactions of the inulin with one of the other compounds, or if it is caused by the low resolution. Indeed, the analysis of the composition impact on the peak location shown on Figure A.8 do not show the trend expected, as for instance, sorbitol and sucrose do not have the same effects on the peak locations. In addition, MSG and galactose often have opposite results. As a conclusion, the FTIR spectra is not bringing any additional information on the potential interaction of inulin with MSG leading to a very smooth structure.



**Figure A.8:** Mixture contour plots of the four peaks associated with the signal of inulin.

## A.4 Conclusion

The present work conducted of the FTIR measurement of the mixture DoE samples aimed to complement Chapter 5 by first, looking if the interactions of the protectants with the cells components in the dried state could be identified and second, if the FTIR analysis could give additional information on why inulin was not forming coil structures in the presence of MSG. For the first aim, the non-subjective vector correction proposed by Hlaing et al. (2017) was followed. Even if a good separation of the samples with and without bacteria was obtained after pre-treatment of the data, the subtraction of the protective matrix spectra did not give the spectra of the bacteria only. Conversely, Hlaing et al. (2017) found a separation of the samples with and without bacteria on the first principal component accounting for 96.5% of the variation even though the amount

of bacteria was only 0.4 % (w/w) in the final powder. Thus, their method of preparation might have implied an additional step that would increase the amount of bacteria in the measured sample or the bacteria signal, but which is not mentioned in the publication. For the second aim of this work, the shift in peak location of the inulin were either below the resolution of the measurement, or not aligned with our first hypothesis.

To conclude, the FTIR measurements of the Mixture DoE samples did not give additional information than what is already given in Chapter 5.

## A. 5 References

- Berger, A. J., Koo, T.-W., Itzkan, I., & Feld, M. S. (1998). An enhanced algorithm for linear multivariate calibration. *Analytical Chemistry*, 70(3), 623-627.
- Grube, M., Bekers, M., Upton, D., & Kaminska, E. (2002). Infrared spectra of some fructans. *Journal of Spectroscopy*, 16(3-4), 289-296.
- Hlaing, M. M., Wood, B. R., McNaughton, D., Ying, D., Dumsday, G., & Augustin, M. A. (2017). Effect of drying methods on protein and DNA conformation changes in *Lactobacillus rhamnosus* gg cells by fourier transform infrared spectroscopy. *Journal of Agricultural and Food Chemistry*, 65(8), 1724-1731.



**MASSEY UNIVERSITY**  
GRADUATE RESEARCH SCHOOL

## STATEMENT OF CONTRIBUTION DOCTORATE WITH PUBLICATIONS/MANUSCRIPTS

We, the candidate and the candidate's Primary Supervisor, certify that all co-authors have consented to their work being included in the thesis and they have accepted the candidate's contribution as indicated below in the *Statement of Originality*.

Name of candidate:	Sarah Priour	
Name/title of Primary Supervisor:	Dr. Ashling Ellis	
Name of Research Output and full reference:		
Sugar uptake by <i>Lactobacillus rhamnosus</i> and its impact on shelf-life		
In which Chapter is the Manuscript /Published work:	Chapter 3	
Please indicate:		
<ul style="list-style-type: none"> <li>The percentage of the manuscript/Published Work that was contributed by the candidate:</li> </ul>	85%	
and		
<ul style="list-style-type: none"> <li>Describe the contribution that the candidate has made to the Manuscript/Published Work:</li> </ul>		
The candidate conducted the laboratory work and wrote the manuscript		
For manuscripts intended for publication please indicate target journal:		
International Journal of Food Microbiology		
Candidate's Signature:	sarah priour	Digitally signed by sarah priour Date: 2019.07.25 16:30:34 +12'00'
Date:		
Primary Supervisor's Signature:	Ashling Ellis	Digitally signed by Ashling Ellis Date: 2019.07.25 19:53:29 +12'00'
Date:		

(This form should appear at the end of each thesis chapter/section/appendix submitted as a manuscript/ publication or collected as an appendix at the end of the thesis)



**MASSEY UNIVERSITY**  
GRADUATE RESEARCH SCHOOL

## STATEMENT OF CONTRIBUTION DOCTORATE WITH PUBLICATIONS/MANUSCRIPTS

We, the candidate and the candidate's Primary Supervisor, certify that all co-authors have consented to their work being included in the thesis and they have accepted the candidate's contribution as indicated below in the *Statement of Originality*.

Name of candidate:	Sarah Priour	
Name/title of Primary Supervisor:	Dr. Ashling Ellis	
Name of Research Output and full reference:		
Effect of phase change materials and powder structure on the shelf-life stability of Lactobacillus rhamnosus HN001		
In which Chapter is the Manuscript /Published work:	Chapter 6	
Please indicate:		
<ul style="list-style-type: none"> <li>The percentage of the manuscript/Published Work that was contributed by the candidate:</li> </ul>	85%	
and		
<ul style="list-style-type: none"> <li>Describe the contribution that the candidate has made to the Manuscript/Published Work:</li> </ul>		
The candidate conducted the laboratory work and wrote the manuscript.		
For manuscripts intended for publication please indicate target journal:		
Journal of Food Engineering		
Candidate's Signature:	sarah priour	Digitally signed by sarah priour Date: 2019.07.25 16:33:53 +12'00'
Date:		
Primary Supervisor's Signature:	Ashling Ellis	Digitally signed by Ashling Ellis Date: 2019.07.25 19:54:37 +12'00'
Date:		

(This form should appear at the end of each thesis chapter/section/appendix submitted as a manuscript/ publication or collected as an appendix at the end of the thesis)